APPLICATION OF ENVIRONMENTAL-FRIENDLY REACTIONS IN HIGH VALUE COMPOUND SYNTHESIS: SYNTHETIC STUDIES TOWARDS THE TOTAL SYNTHESIS OF DACTYLOLIDE

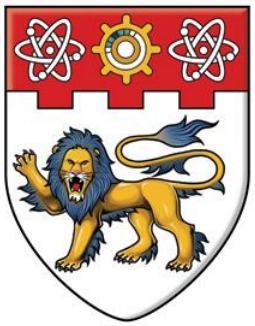

NANYANG TECHNOLOGICAL UNIVERSITY

APPLICATION OF ENVIRONMENTAL-FRIENDLY REACTIONS IN HIGH VALUE COMPOUND SYNTHESIS: SYNTHETIC STUDIES TOWARDS THE TOTAL SYNTHESIS OF DACTYLOLIDE

WONG ZHEN ZHOU

Interdisciplinary Graduate School

Nanyang Environment & Water Research Institute

2016

WONG ZHEN ZHOU

2016

APPLICATION OF ENVIRONMENTAL-FRIENDLY REACTIONS IN HIGH VALUE COMPOUND SYNTHESIS: SYNTHETIC STUDIES TOWARDS THE TOTAL SYNTHESIS OF DACTYLOLIDE

WONG ZHEN ZHOU

Interdisciplinary Graduate School
Nanyang Environment & Water Research Institute

A thesis submitted to the Nanyang Technological University in partial fulfillment
of the requirement for the degree of
Doctor of Philosophy

2016

Acknowledgement

I would like to express my gratitude towards following parties for their support and assistance in my PhD studies.

1. Financial support from **Interdisciplinary Graduate School (IGS)** and **Nanyang Environment and Water Research Institute (NEWRI)** of **Nanyang Technological Universities (NTU)**. The scholarship awarded allowed me to focus on my research study without concerning on financial burden. Besides, the programme also allowed me to not only further explore in my main expertise of organic chemistry, but also had a glance in biological sciences.
2. My supervisor, **Prof. Loh Teck Peng** (School of Physical and Mathematical Sciences), who provided me opportunity to pursue my research study in his laboratory. His trust and advices allowed me to not only work in research, but also had a chance to involve in laboratory management.
3. My co-supervisor, **Assoc. Prof. Liu Chuan Fa** (School of Biological Sciences), and my ex-mentor, **Prof. Huang Jingmei** (South China University of Technology), who provided me advices throughout my study.
4. My current mentor, **Dr. Sreekumar Pankajakshan** (School of Physical and Mathematical Sciences), who provided me great assistance in my thesis writing. Besides, he also provided me the opportunity to be tutor in his teaching subject. Being a tutor in undergraduate modules was the most important and impactful experience in my research study.
5. Administrative support from **Interdisciplinary Graduate School (IGS)** and **Nanyang Environmental and Water Research Institute (NEWRI)**, who provided support in academic matters and organized various activities, such as recreational activities, seminars, etc, which made my research study more vibrant and interesting. They are Mr. Khoo Soon Sheng, Jacky and Ms. Hera Catharina Adam from NEWRI, Ms. Ellen Heng Yuxuan, Mr. Lee Wai Onn and other members from IGS Team.
6. Administrative and laboratory support from **School of Physical and Mathematical Sciences**, who efficiently handled my academic and research requests. They are Ms. Chen Xiaoping, Ms. Florence Ng Pei Fan, Mdm. Goh Ee Ling (NMR) and Mdm. Zhu Wen Wei (mass spectrometry).

7. **My students, colleagues and seniors** in Prof. Loh's Laboratory, who supported me from various aspects, including research work, laboratory management and mental support throughout my research study. They are my students, Mr. Chng Zhi Guang, Ms. Yip Ee Shin, Ms. Deng Xiaozhou, Ms. Tan Yi Ping, Ms. Chew Ye Qiu and Ms. Sripriya Jayakody, my colleagues and seniors, Ms. Cheng Jun Kee, Dr. Koh Peng Fei Jackson, Dr. Nicole Loy Shen Yen, Dr. Chua Sin Siu, Dr. Chok Yew Keong, Dr. Wong Mun Yee, Dr. Chen Yuchen, Mr. Shen Liang and Mr. Wang Wee Jian.
8. **My family**, especially my parents, who gave me fully support and trust in the direction that I pursued, **my uncle and his family** in Singapore for providing support during my unstable life time and **my housemates and high school friends** who endured my hard times and shared my enjoyment during the study.

Lastly, the journey of this research study in these four years provided me a new insight regarding my life. No matter how this journey ends, I have already known myself more in the aspect of quality life, spiritual context and self realization. This journey was not easy to walk through but served as an important experience for my future.

Table of Contents

Index of Abbreviations

Å	Angstrom
℃	Degree centigrade
*L	Chiral ligand
[H]	Hydrogenation
[O]	Oxidation
2D	Two-dimensional
Ac	Acetyl
AIBN	Azobisisobutyronitrile
Ar	Aryl
Asn	Asparagine
atm	Atmospheric pressure
BASF	Badische Anilin und Soda Fabrik (Baden Aniline and Soda Factory)
BINAP	2,2'-Bis(diphenylphosphino)-1,1'-binaphthyl
BINOL	1,1’-Bi-2-naphthol
Biphep	2,2’-Bis(diphenylphosphino)-1,1'-biphenyl
BITIP	BINOL titanium tetraisopropoxide
Bn	Benzyl
Boc	*t*-Butyloxycarbonyl
BOM	Benzyloxy methyl
Bu	Butyl
*i*Bu	*i*-Butyl
*n*Bu	*n*-Butyl
*t*Bu	*t*-Butyl
Bz	Benzoyl
CAN	Ceric ammonium nitrate
cat.	Catalyst
Cp	Cyclopentadienyl
Cp*	Pentamethylcyclopentadienyl
CSA	Camphorsulfonic acid
dba	Dibenzylideneacetone
DBMP	2,6-Di-*t*-butyl-4-methylpyridine
DBU	1,8-Diazabicyclo[5.4.0]undec-7-ene

DCC	*N*,*N*'-Dicyclohexylcarbodiimide
DCE	1,2-Dichloroethane
DDQ	2,3-Dichloro-5,6-dicyano-1,4-benzoquinone
de	Diastereomeric excess
DEAD	Diethyl azodicarboxylate
DET	Diethyltartrate
DETA	Diethylenetriamine
DHP	Dihydropyran
DIAD	Diisopropyl azodicarboxylate
DIBAL-H	Diisobutylaluminum hydride
DIC	*N,N*′-Diisopropylcarbodiimide
DIEA *or* DIPEA	Diisopropylethylamine (Hunig's base)
DIPA	Diisopropylamine
DIPT	Diisopropyl tartrate
DMA	Dimethylacetamide
DMAD	Dimethyl acetylenedicarboxylate
DMAP	4-*N*,*N*-Dimethylaminopyridine
DMB	3,4-Dimethoxybenzyl
DMF	*N*,*N*-Dimethylformamide
DMP	Dess-Martin periodinane
DMSO	Dimethyl sulfoxide
DPPBA	Diphenylphosphino benzoic acid
dppf	1,1′-Bis(diphenylphosphino)ferrocene
dppp	1,3-Bis(diphenylphosphino)propane
d.r.	Diastereomer ratio
DTBP	2,6-Di-*t*-butylpyridine
EDC	1-Ethyl-3-(3-dimethylaminopropyl)carbodiimide
ee	Enantiomeric excess
ent-	Enantiomer
EPHP	1-Ethylpiperidine hypophosphite
epi-	Epimer
Eq	Equation
eq *or* equiv	equivalent
ESI	Electron spray ionization

Et	Ethyl
FGI	Functional group interconversion
g	gram
G2/M	Gap 2 (of interphase)/Mitosis of cell cycle
Gen.	Generation
GI_{50}	50% Growth inhibition
h	hour
H-G	Hoveyda-Grubbs
His	Histidine
HMDS	Hexamethyldisilazane
HRMS	High resolution mass spectrometry
HWE	Horner-Wadsworth-Emmons
Hz	Hertz
i-	*iso*-
IBX	2-Iodoxybenzoic acid
IC_{50}	50% Inhibition concentration
Ile	Isoleucine
Imid.	Imidazole
Ipc_2B	Diisopinocamphenylborane
L	Ligand
LA	Lewis acid
LAH	Lithium aluminium hydride
LDA	Lithium diisopropylamide
LDBB	Lithium 4,4’-di-*tert*-butylbiphenylide
Me	Methyl
mg	milligram
MHz	Megahertz
min	minute
mmHg	millimeter of mercury
mol	mole
MOM	Methoxymethyl
MS	Molecular sieves
MW	Microwave
NBS	*N*-Bromosuccinimide

NHC	*N*-Heterocyclic carbene
NHK	Nozaki-Hiyama-Kishi
NIS	*N*-Iodosuccinimide
nM	nanomolar
NME	*N*-Methylephedrine
NMO	*N*-Methylmorpholine-*N*-oxide
NMP	*N*-Methylpyrrolidone
NMR	Nuclear magnetic resonance
NOESY	Nuclear Overhauser effect spectroscopy
Nuc.	Nucleophilic
OP or OPG	Protected alcohol
OTf	Trifluoromethanesulfonate or Triflate
p-	*para*-
PBB	*p*-Bromobenzyl
PCC	Pyridinium chlorochromate
PG	Protecting group
Ph	Phenyl
Piv or Pv	Pivolyl
PMB	*p*-Methoxybenzyl
ppm	part per million
PPTS	Pyridinium *p*-toluenesulfonate
*i*Pr	*i*-Propyl
PS	Polystyrene
PTSA	*p*-Toluenesulfonic acid
py	Pyridine
pybox	Pyridine bis(oxazoline)
R	Side chain
Red-Al	Sodium bis(2-methoxyethoxy)aluminumhydride
r.t.	Room temperature
sec	second
Sia	Siamyl
t-	*tert*-
TA	Tartaric acid
TBAF	Tetrabutylammonium fluoride

TBDPS	*t*-Butyldiphenylsilyl
TBHP	*t*-Butyl hydroperoxide
TBS	*t*-Butyldimethylsilyl
TEMPO	(2,2,6,6-Tetramethylpiperidin-1-yl)oxyl
Teoc	2-(trimethylsilyl)ethoxycarbonyl
TES	Triethylsilyl
TFA	Trifluoroacetic acid
(Th)CuCNLi	Lithium(2-thienyl)cyanocuprate
THF	Tetrahydrofuran
THP	Tetrahydropyran or tetrahydropyranyl
Thr	Threonine
TIPS	Triisopropylsilyl
TMEDA	Tetramethylethylenediamine
TMS	Trimethylsilyl
TPAP	Tetrapropylammonium perruthenate
TRIP	3,3′-Bis(2,4,6-triisopropylphenyl)-1,1′-binaphthyl-2,2′-diyl hydrogenphosphate
Ts	Tosyl
v/v	Volumn/volumn
X	Halide or pseudohalide

Preface

This dissertation was prepared as a comprehensive research progress report during four-year study on application of environmental-friendly reactions in the synthesis of high value compound, specifically dactylolide, with the best of author's knowledge.

This dissertation consists of four chapters. **Chapter One** provides the general idea of Green Chemistry and natural products, followed by an overview of synthetic methodologies that have been developed for the synthesis of 2,6-*syn*-4-exomethylene tetrahydropyran ring and conjugated diene. This overview includes methodologies that developed by others as well as Loh's research group, which are $In(OTf)_3$-catalyzed intramolecular (2,5)-oxonium-ene cyclization and metal-catalyzed direct cross coupling reaction, together with a comparison of these methodologies from the perspective of Green Chemistry.

In order to show the feasibility of our group's methodologies in high value compound synthesis, dactylolide, a natural product extracted from marine sponge was chosen as target molecule due to its featured southern 2,6-*syn*-4-exomethylene tetrahydropyran ring and northern conjugated diene motifs. In **Chapter Two**, the discovery of dactylolide and zampanolide, another marine natural product which shared similar macrolide core with dactylolide, was introduced. Furthermore, the biological activity of these two natural products, which showed their potential to become anticancer drug candidate, was also discussed. Until the date that this dissertation was prepared, the interesting structure and bioactivity of dactylolide and zampanolide have attracted 16 research groups worldwide to synthesize these two compounds. A brief overview of each reported synthesis was provided in this chapter, together with a summary on the synthetic strategies that employed by each research group.

Chapter Three focuses on the author's effort in the synthetic studies towards the total synthesis of dactylolide. In order to establish the synthetic route which featured our group's methodologies, synthesis of racemic dactylolide was targeted in this study. This chapter was started with retrosynthetic analysis, followed by synthetic efforts made on the designated fragments under two different synthetic routes and finally concluded with the established syntheses of C1-C8 fragment and C9-C19 fragment of dactylolide.

General method, experimental procedures and supporting information in this project were provided in **last chapter**.

It would be author's honour if this dissertation could serve as a guide and stepping stone for those who work in the synthesis of dactylolide or any related research.

CHAPTER ONE

INTRODUCTION

1.1 Introduction to Green Chemistry[1] and examples in high value compound synthesis

Since industrial revolution sparked in late 18th century, chemical industry had been evolved exponentially in order to meet the need from increasing world population as well as the profit of the chemical business. However, the chemical waste generated from the process becomes an unavoidable threat towards the Mother Nature and also the entire ecological system. Awareness on the pollution from chemical industry was raised among public, policy-makers as well as scientific community since mid of 20th century.

In 1998, Paul Anastas and John C. Warner proposed 12 Principles of Green Chemistry, which are outlined in their groundbreaking book, *Green Chemistry: Theory and Practice*.[2] These principles have been treated as an important guideline in the search of reactions which are environmentally sustainable. Moreover, to answer whether a chemical reaction is greener than others, 'Green Metrics', which measures 'greenness' of a reaction or synthetic plan quantitatively *via* holistic approach, is proposed and now widely accepted by scientific community. Such examples of 'Green Metrics' include atom economy (AE, Eq 1) and reaction mass efficiency (RME, Eq 2), which showed below.[3]

$$Atom\ Economy\ (AE) = \frac{MW_{product}}{\sum MW_{reactant}} \qquad \text{(Eq 1)}$$

MW = Molecular Weight

$$Reaction\ Mass\ Efficiency\ (RME) = (\varepsilon)(AE)\left(\frac{1}{SF}\right)(MRP) \qquad \text{(Eq 2)}$$

ε = yield; SF = Stoichiometric Factor; MRP = Material Recovery Parameter

Equation 1, which addresses one of the Green Chemistry Principles, *i.e.* atom economy, considers the greenness of a reaction from the perspective of molecular weight (MW). This metric show that multi-component reactions, bond-forming reactions and condensations are mostly highly atom economical if compared with eliminations, conventional oxidations or reductions and substitutions. Therefore, significant

[1] History of Green Chemistry. http://www.acs.org/content/acs/en/greenchemistry/what-is-green-chemistry/history-of-green-chemistry.html (accessed May 31, 2016).
[2] Anastas, P. T.; Warner, J. C. *Green Chemistry: Theory and Practice*; Oxford University Press: New York, 1998.
[3] Andraos, J. Application of Green Metrics Analysis to Chemical Reactions and Synthesis Plans. In *Green Chemistry Metrics: Measuring and Monitoring Sustainable Processes*; Lapkin, A., Constable, D. J. C., Eds.; John Wiley and Sons: United Kingdom, 2008; pp 69-199.

development in searching for highly atom economical reactions is flourishing since the concept of atom economy is proposed. Two of the Nobel-prize-awarded reactions, which are catalytic asymmetric synthesis (awarded to William S. Knowles, Ryoji Noyori and K. Barry Sharpless in 2001) and olefin metathesis (awarded to Yves Chauvin, Robert H. Grubbs and Richard R. Schrock in 2005), are impactful examples of highly atom economical reactions.

These awarded methodologies not only exhibit the applicability in lab bench synthesis, but are also able to be applied in industrial application. Noyori's asymmetric hydrogenation was used for industrial synthesis of levofloxacin, an antibiotic sold under trade names such as Levaquin® to treat bacterial infections.[4] Sharpless's epoxidation was also reported as an efficient asymmetric synthesis in the precursor towards antibacterial erythromycin.[5] Not only in pharmaceutical production, these *green* reactions are also utilized in petrochemical production. One of the famous olefin productions, namely Shell Higher Olefin Process (SHOP), uses Molybdate catalyst in the third step of the process to yield linear internal olefin. A worldwide production capacity of over 1 million tonne per year of higher olefin was sold by Shell under trade name of Neodene®.[6] (Scheme 1.1.1)

On the other hand, reaction mass efficiency (RME, Eq 2) provides more holistic quantitative analysis for a chemical reaction and synthetic plan. This metric, which investigates from the perspective of reaction yield, atom economy, stoichiometric factor and material recovery, is a more practical and comprehensive analysis on typical chemical reactions by evaluating the materials used (and the economical cost associated with) in its reaction stage, work-up stage and purification stage. With this holistic green metric, 'Reduce Derivatives', one of the 12 Principles of Green Chemistry, could be addressed and verified quantitatively.

[4] Noyori, R. *Angew. Chem. Int. Ed.* **2002**, *41*, 2008-2022.
[5] Rossiter, B. E.; Katsuki, T.; Sharpless, K. B. *J. Am. Chem. Soc.* **1981**, *103*, 464-465.
[6] Mol, J. C. *J. Mol. Catal. A: Chem.* **2004**, *213*, 39-45.

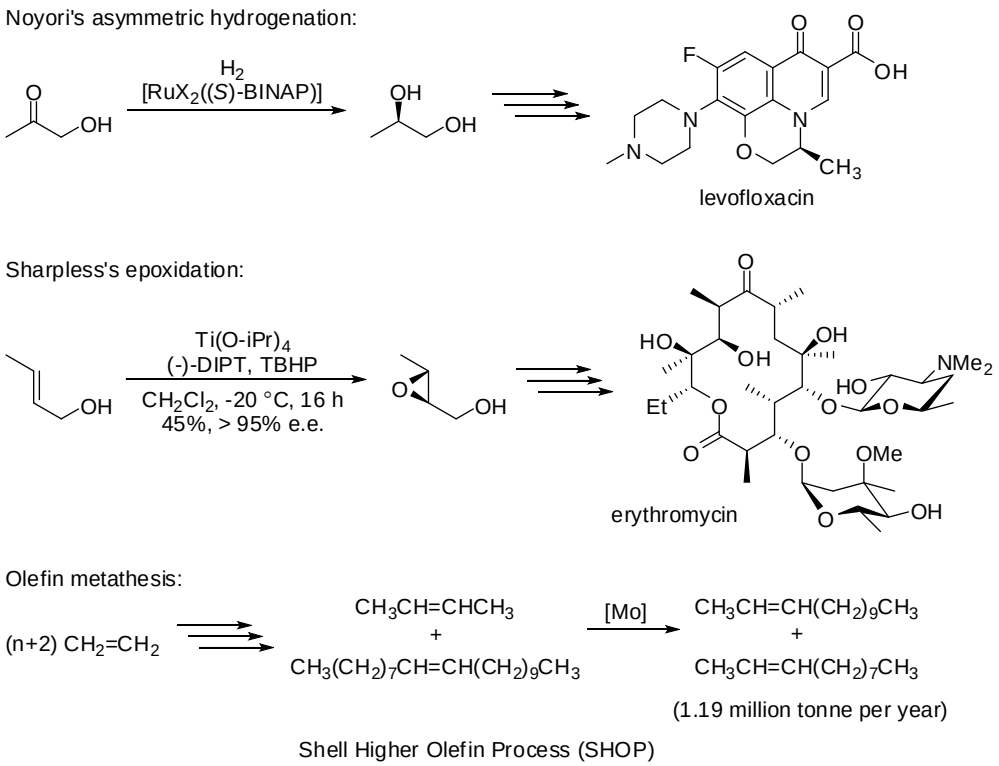

Scheme 1.1.1 Application examples of Nobel Prize awarded *green* reactions.

Not limited with maximizing atom economy and reaction yield in each step, RME also suggests that minimizing overall reaction steps, maximizing parallel synthesis routes and degree of convergence would increase the degree of 'greenness' of a synthetic plan of complex molecules. These green strategies would become the underlying concepts when we drafted the blueprint of our synthetic studies of high value compound.

1.2 Natural products as sources of high value compound synthesis

Pharmaceutical compound is one of the so called "high value compounds" in research area. It does not only provide therapeutic treatment towards diseases, but also generates monetary profit and employment in research sector. One of the main sources of pharmaceutical compounds could be derived from our Mother Nature. Since the Bronze Age, humans utilize plants and herbs to cure various diseases. With the fast development in organic and analytical chemistry, chemists are able to isolate the active ingredients in plants, herbs and marine sponges. However, direct isolation of active ingredient from organism sometimes is not feasible due to the minute quantity obtained from a relatively huge amount of crude materials. Therefore, scientists tend to synthesize the active ingredient artificially to meet the demanding market of therapeutic natural products.

With the four major classes of biomolecules, namely carbohydrates, proteins, lipids and nucleic acids, the nature assembles these therapeutic natural products with the assistance of various enzymes participated in complex biological pathways. These natural products have elegant and highly specific structure which is beyond imagination and the synthesis of these complex natural products becomes highly challenging.

Despite of the complex molecular structure, the current state of the art in organic chemistry enables the synthesis of natural products. Since the synthesis of urea by Wöhler in 1828,[7] the organic chemistry community started to explore the possibilities to synthesize natural organic compounds from simple molecules. Among the early efforts in this area, E. Fisher (1902) and H. Fischer (1930) were awarded with Nobel Prize for their pioneering work in syntheses of purine and sugars (E. Fischer) and hemin (H. Fischer) respectively. With advanced chromatographic and spectroscopic technique developed after World War II, natural product synthesis has been burgeoning.[8]

One of the most impactful natural product syntheses is the synthesis of paclitaxel or Taxol®, which served as an anticancer drug in ovarian, breast and lung cancers. Paclitaxel, which isolated from Pacific yew trees in 1960s, was commercialized in 1993 and hit its peak annual sales of nearly US$ 1.6 billion in 2000. Other examples of natural products, such as digoxin (cardiac drug isolated from Foxglove), aspirin (analgesic

[7] Wöhler, F. *Annalen der Physik* **1828**, *88*, 253-256.
[8] Nicolaou, K. C.; Sorensen, E. J.; Winssinger, N. *J. Chem. Edu.* **1998**, *75*, 1226-1258.

isolated from willow) and L-DOPA (Antiparkinsonian drug isolated from seedings of *Vicia faba*), also plays significant roles in treating minor diseases such as fever or inflammation to serious diseases such as cardiovascular diseases or Parkinson's disease.[9] The recent example in this synthetic area is antimalaria drug Artemisinin (isolated from *Artemisia annua* or qinghao in Chinese), which its discovery was awarded with Nobel Prize in Medicine in 2015. (Scheme 1.2.1)

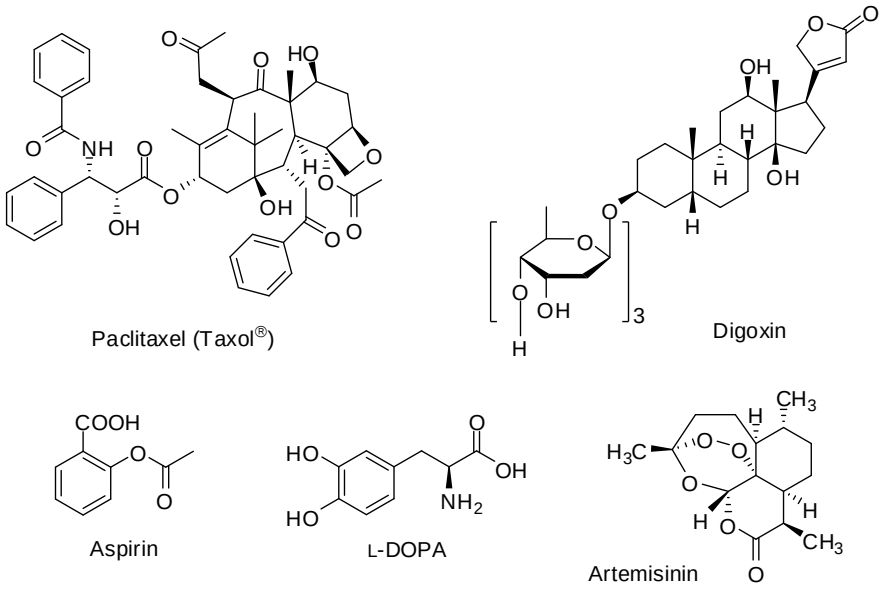

Scheme 1.2.1 Examples of natural products commercialized as therapeutic drugs.

[9] The Top Pharmaceuticals That Changed The World, *Chem. Eng. News* **2005**, *83*.

1.3 Structural motifs of natural products and the synthetic examples

1.3.1 Classification of natural products based on structural motifs

Almost every entity in our universe could be categorized according to their similar properties, the wide range of natural products could also be classified based on molecular structure, taxonomy, physiological activity and biogenesis.[10] From synthetic viewpoint, molecular structure is the most common classification to be used by synthetic chemists. In 2005, Max Planck Institute of Molecular Physiology charted a structural classification of natural products (SCONP).[11] They revealed that 90% of their investigating natural products are ring-containing compounds, which could be categorized into three major types, namely carbocycles, *N*-heterocycles and *O*-heterocycles. Carbocycles, such as cholesterol and prostaglandin, are those with a ring formed by carbon atoms. *N*-Heterocycles, on the other hand, have at least one nitrogen atom incorporated in the ring structure. Examples of *N*-heterocycles include morphine and thiamine (vitamin B_1). *O*-Heterocycles, as the name suggested, is a cyclic compound that comprised of at least one oxygen atom. Examples include α-maltose and (+)-centrolobine. Another important structural motif is polyene, a conjugated system that made up by alternating carbon-carbon double bond and single bond. Examples of natural products that contained polyene motifs are α-carotene and natamycin. (Scheme 1.3.1)

[10] Natori, S. Classification of Natural Products. In *Natural Products Chemistry* [Online]; Nakanishi, K.; Goto, T.; Itô, S.; Natori, S.; Nozoe, S., Eds; Kodansha Ltd: Japan, 1974; Volume 1, Chapter 1, pp 1-10. http://www.sciencedirect.com.ezlibproxy1.ntu.edu.sg/science/article/pii/B9780125139014500068 (accessed April 28, 2016).

[11] Koch, M. A.; Schuffenhauer, A.; Scheck, M.; Wetzel, S.; Casaulta, M.; Odermatt, A.; Ertl, P.; Waldmann, H. *Proc. Natl. Acad. Sci. U.S.A.* **2005**, *102*, 17272-17277.

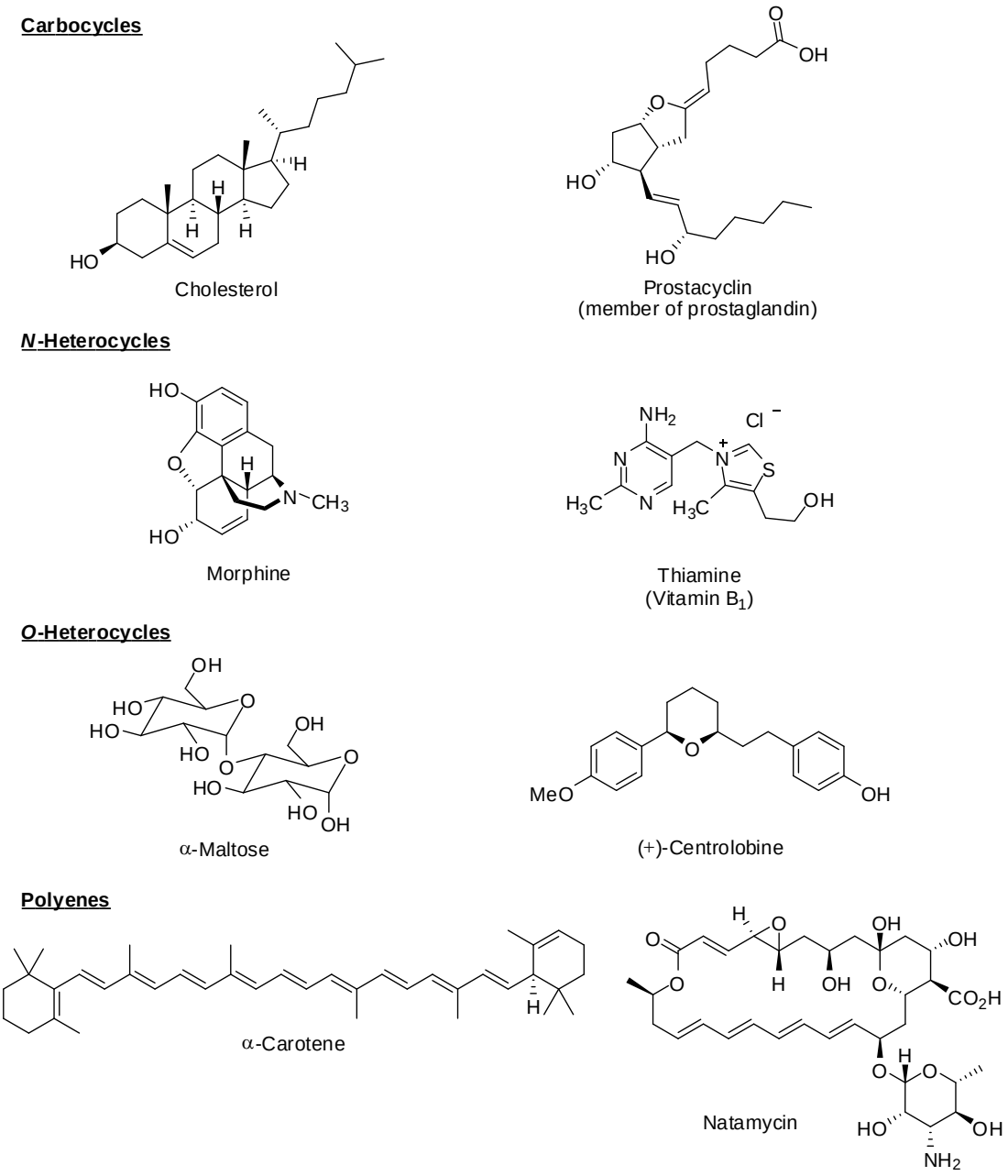

Scheme 1.3.1 Structural Classification of Natural Products (SCONP) and their examples.

In this dissertation, synthesis of *O*-heterocycles, or more specifically, 2,6-*syn*-4-exomethylene tetrahydropyran and polyenes, or more specifically, conjugated diene system with environmental-friendly reactions were our main focus. Therefore, a series of synthetic examples of these two motifs, either developed by our group or others, will be introduced in following sections.

1.3.2 2,6-*syn*-4-exomethylene tetrahydropyran ring as structural motifs and its synthetic examples

O-Heterocycles, as introduced in Structural Classification of Natural Products (SCONP), have different ring sizes and number of oxygen atoms. (Scheme 1.3.2) These ring structures could be further categorized into 4 different types. The smallest *O*-heterocycle is oxirane, which is a 3-membered ring with an oxygen atom. Increasing the ring size will result in more variable structures, mainly furan-type (5-membered ring) and pyran-type (6-membered ring). Furan or pyran with 2 oxygen atoms within the ring is called dioxalane or dioxane respectively. In this dissertation, synthesis of tetrahydropyran (THP) is one of our main interests.

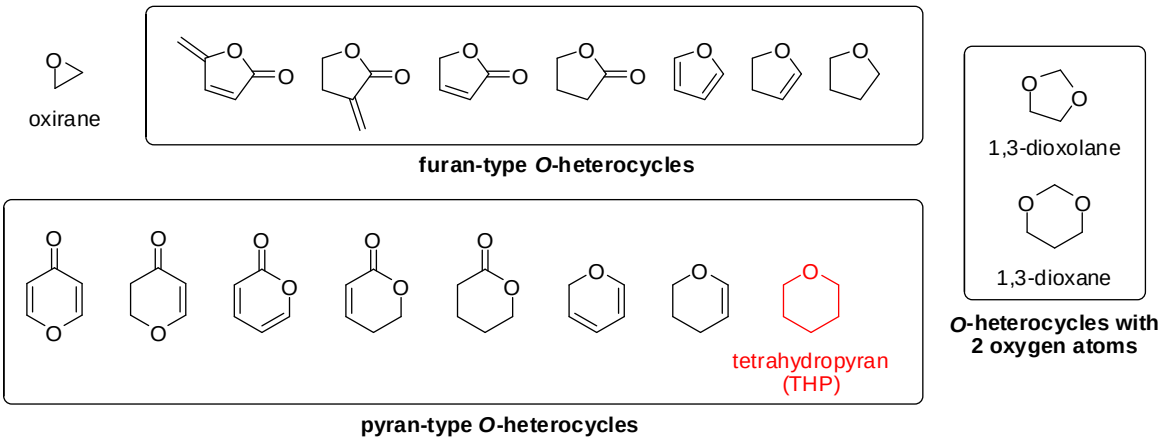

Scheme 1.3.2 Different types of *O*-heterocycles based on SCONP.

Nature is a sophiscated designer. As a result, tetrahydropyran rings found in natural products always have different substituents on its carbon atoms. The restriction of bond rotation within the ring results in various stereochemistry of this cyclic structure. By convention, *syn* isomers are those with two highest priority substituents at the same side, while *anti* isomers have them at opposite side of the molecule. In our particular interest, 2,6-*syn*-4-exomethylene tetrahydropyran will be discussed extensively. Examples of the presence of such scaffold in natural products are shown in Scheme 1.3.3.

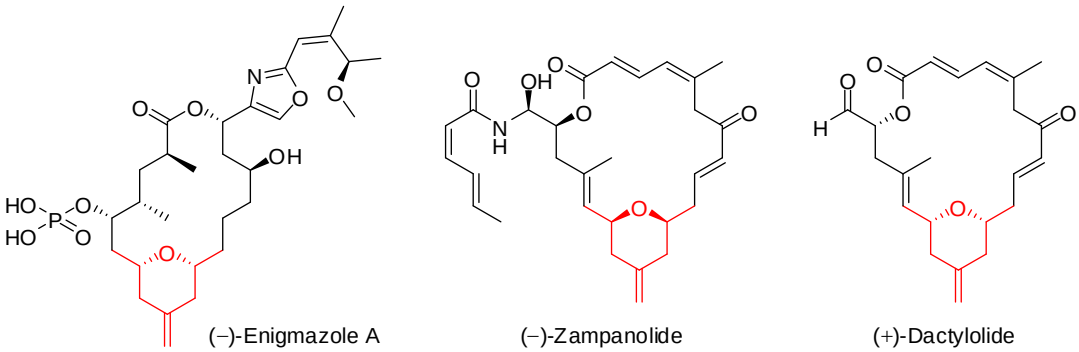

Scheme 1.3.3 Natural products containing 2,6-*syn*-4-exomethylene tetrahydropyran.

(–)-Enigmazole A, an 18-membered macrolide ring extracted from the sponge *Cinachyrella enigmatica*, is also an example of natural products that containing 2,6-*syn*-4-exomethylene tetrahydropyran. This marine-derived macrolide selectively targets aberrant c-Kit tyrosine kinase, which is a very rare phenotypic effect.[12,13] The first synthesis of Enigmazole A was completed by Molinski and co-workers in 2010,[14] followed by Smith and co-workers' work in 2015[15] and Fürstner and co-workers' work in 2016.[16]

(–)-Zampanolide and (+)-Dactylolide, natural products extracted from marine sponge, have similar macrolide core structure, which also consists of a 2,6-*syn*-4-exomethylene tetrahydropyran. Synthesis of such tetrahydropyran in the total or formal syntheses of two natural products will be extensively discussed in Chapter 2, while model study of tetrahydropyran synthesis will be discussed in following sections of this chapter.

[12] Oku, N.; Takada, K.; Fuller, R. W.; Wilson, J. A.; Peach, M. L.; Pannell, L. K.; McMahon, J. B.; Gustafson, K. R. *J. Am. Chem. Soc.* **2010**, *132*, 10278-10285.
[13] Henrich, C. J.; Goncharova, E. I.; Wilson, J. A.; Gardella, R. S.; Johnson, T. R.; McMahon, J. B.; Takada, K.; Bokesch, H. R.; Gustafson, K. R. *Chem. Biol. Drug. Des.* **2007**, *69*, 321–330.
[14] Skepper, C. K.; Quach, T.; Molinski, T. F. *J. Am. Chem. Soc.* **2010**, *132*, 10286-10292.
[15] Ai, Y; Kozytska, M. V.; Zou, Y.; Khartulyari, A. S.; Smith, A. B. *J. Am. Chem. Soc.* **2015**, *137*, 15426-15429.
[16] Ahlers, A.; Haro, T, Gabor, B., Fürstner, A. *Angew. Chem. Int. Ed.* **2016**, *55*, 1406-1411.

1.3.2.1 Construction of 2,6-syn-4-exomethylene tetrahydropyran ring in Enigmazole A

1.3.2.1.1 Molinski's approach[14]

Molinski and co-workers began their synthesis of 2,6-*syn*-4-exomethylene tetrahydropyran ring with hetero-Diels-Alder (HDA) cycloaddition between aldehyde and diene. (Scheme 1.3.4) With multiple attempts, they finally synthesized the pyran ring by treating the mixture of aldehyde and diene with BF_3 OEt_2, which led to a separable mixture of diasteroisomers. The desired pyran product was then coupled with oxazole fragment to complete the macrolide core of Enigmazole A. The exomethylene on tetrahydropyran ring was then converted from ketal to ketone, followed by treating with nonbasic Lombardo's reagent (Zn, $TiCl_4$, CH_2Br_2).

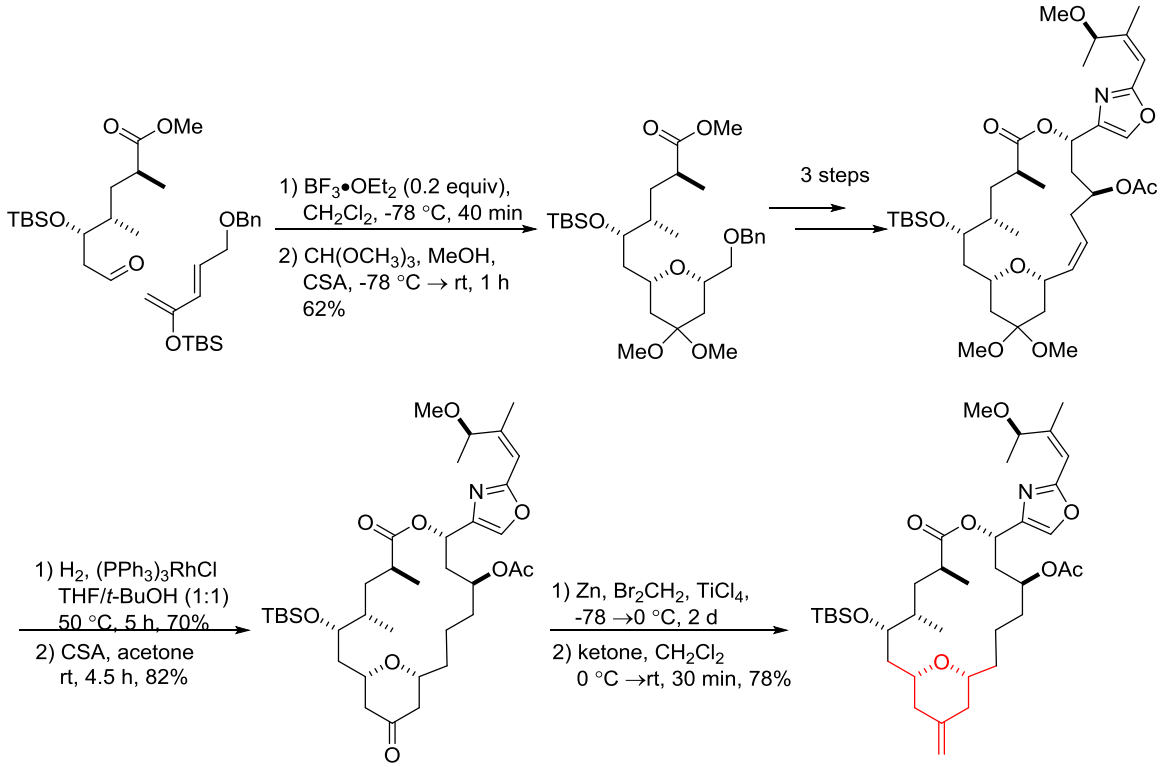

Scheme 1.3.4 Molinski's approach towards the construction of 2,6-*syn*-4-exomethylene tetrahydropyran ring in Enigmazole A.

1.3.2.1.2 Smith's approach[15]

Smith and co-workers prepare 2,6-*syn*-4-exomethylene tetrahydropyran ring by employing a Three-Stage Petasis-Ferrier Union/Rearrangement. (Scheme 1.3.5) The synthesis started from union (stage 1) between carboxylic acid and aldehyde. Addition of trace amount of water into the standard conditions of HMDS/TMSOTf provided dioxanone in a high yield of 95%. Petasis olefination (Stage 2) with microwave irradiation yielded enol acetal in 87%, followed by rearrangement, which treated with Me_2AlCl and methylene ylide ($Ph_3P{=}CH_2$), furnished the target 2,6-*syn*-4-exomethylene tetrahydropyran ring.

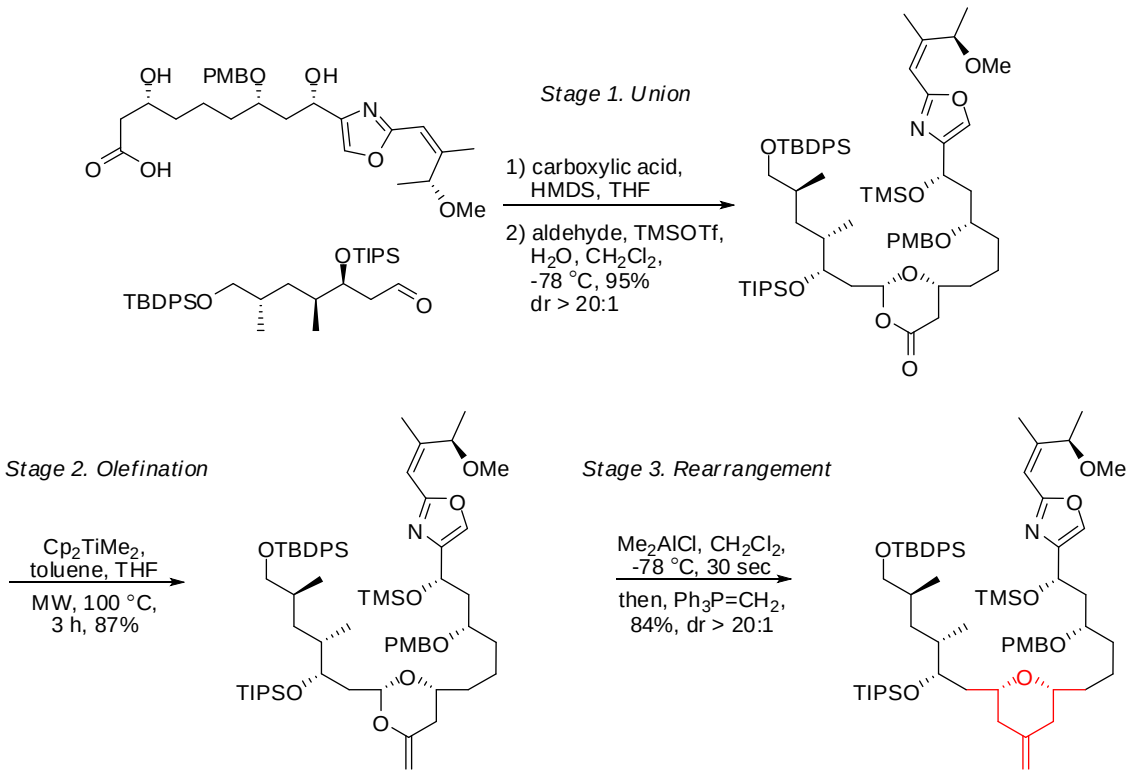

Scheme 1.3.5 Smith's approach towards the construction of 2,6-*syn*-4-exomethylene tetrahydropyran ring in Enigmazole A.

1.3.2.1.3 Fürstner's approach[16]

In Fürstner and co-workers' work in the synthesis of Enigmazole A, 2,6-*syn*-4-exomethylene tetrahydropyran ring was constructed *via* stereoselective gold catalyzed [3,3]-sigmatropic rearrangement. Started from (*R*)-3-bromo-2-methylpropan-1-ol, the macrolide core was formed after 12 steps of transformation, then treatment with gold precatalyst, which is a complex of Biphep and AuCl, and $AgSbF_6$ resulted in the desired 2,6-*syn*-4-exomethylene tetrahydropyran ring through transannular hydroalkoxylation of transient allenyl acetate.

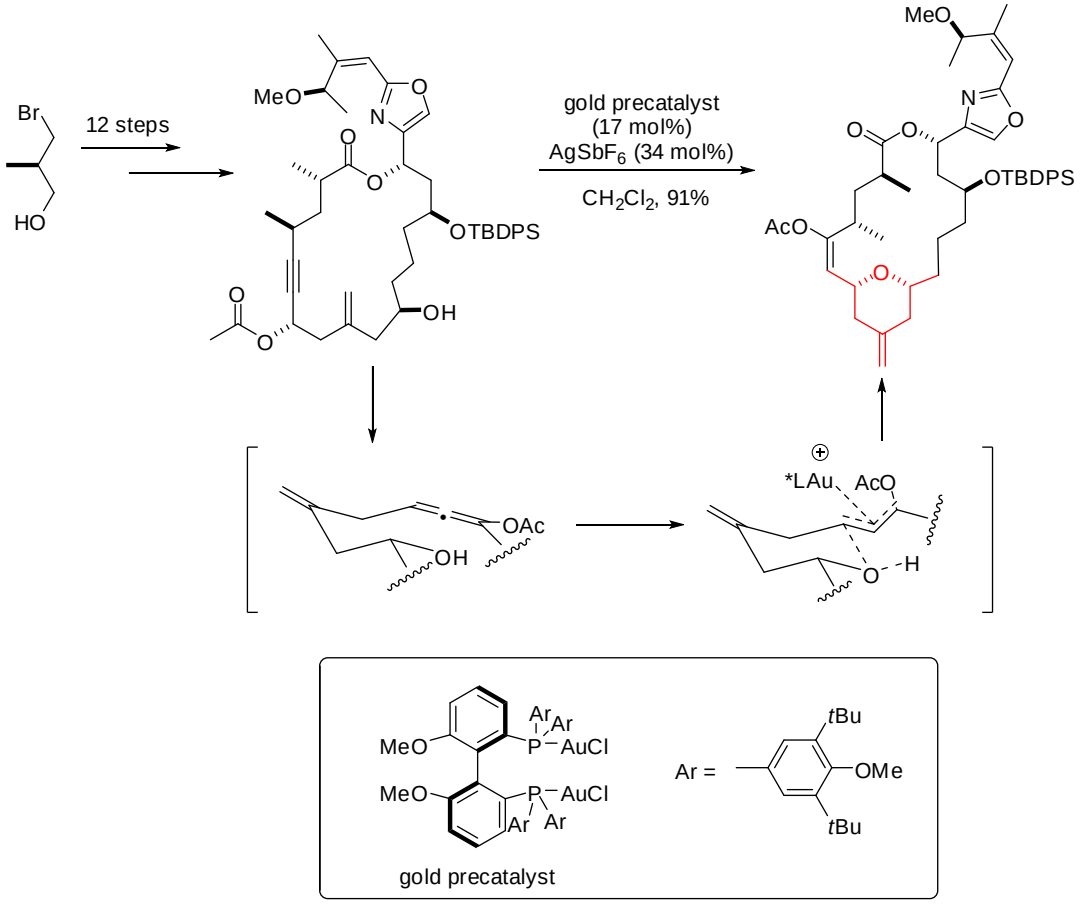

Scheme 1.3.6 Fürstner's approach towards the construction of 2,6-*syn*-4-exomethylene tetrahydropyran ring in Enigmazole A.

1.3.2.2 Development of tetrahydropyran ring synthesis in Loh's research group

Indium and organoindium compounds are studied extensively in our research group for decades. One of the major synthetic areas in the indium-related study is the formation of cyclic ether catalyzed by indium salts.[17] In this section, a brief summary on the chronological development of study towards the synthesis of 2,6-*syn*-4-exomethylene tetrahydropyran, which is our intended target in this dissertation, is provided.

1.3.2.2.1 Discovery on cyclic ether formation from homoallylic alcohol catalyzed by $In(OTf)_3$[18]

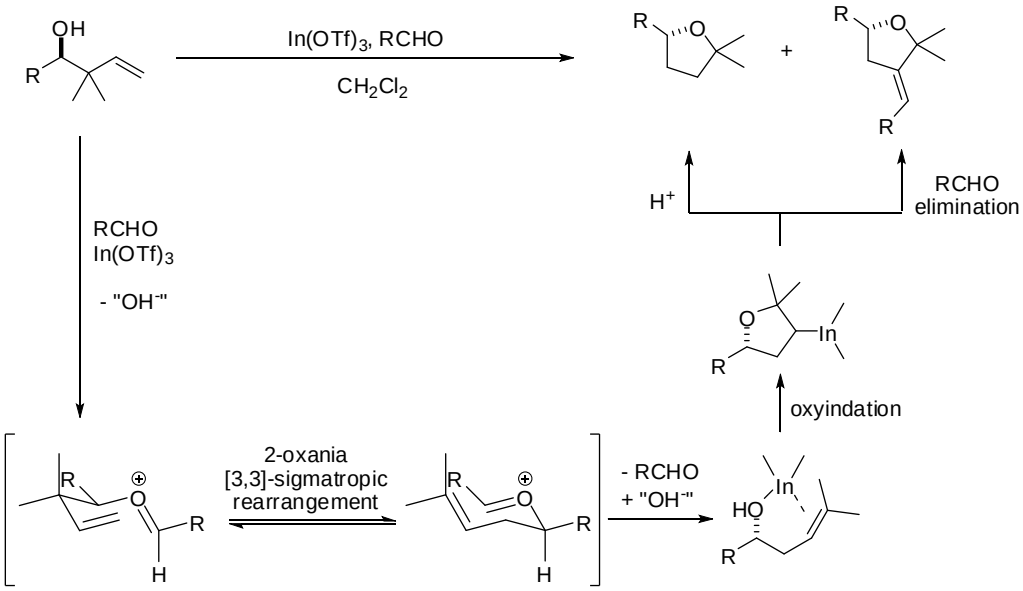

Scheme 1.3.7 2-Oxonia [3,3]-Sigmatropic Rearrangement/Cyclization catalyzed by $In(OTf)_3$ and its plausible mechanism.

[17] Other studies that are not introduced in this disseratation include: (a) Chan, K.-P.; Loh, T.-P. *Tetrahedron Lett.* **2004**, *45*, 8387-8390. (b) Chan, K.-P.; Loh, T.-P. *Org. Lett.* **2005**, *7*, 4491-4494. (c) Chan, K.-P.; Seow, A.-H.; Loh, T.-P. *Tetrahedron Lett.* **2007**, *48*, 37-41. (d) Chan, K.-P.; Ling, Y. H.; Loh, T.-P. *Chem. Commun.* **2007**, 939-941. (e) Liu, F.; Loh, T.-P. *Org. Lett.* **2007**, *9*, 2063-2066. (f) Hu, X.-H.; Liu, F.; Loh, T.-P. *Org. Lett.* **2009**, *11*, 1741-1743. (g) Zhou, H.; Loh, T.-P. *Tetrahedron Lett.* **2009**, *50*, 4368-4371. (h) Chua, S.-S.; Alni, A.; Chan, L.-T. J.; Yamane, M.; Loh, T.-P. *Tetrahedron* **2011**, *67*, 5079-5082. (i) Li, B.; Lai, Y.-C.; Zhao, Y.; Wong, Y.-H.; Shen, Z.-L.; Loh, T.-P. *Angew. Chem. Int. Ed.* **2012**, *51*, 10619-10623.

[18] Loh, T.-P.; Hu, Q.-Y.; Ma, L.-T. *J. Am. Chem. Soc.* **2001**, *123*, 2450-2451.

With the extensive findings on indium(III) salt-catalyzed aldol reactions in our research group,[19] Loh and co-workers started to explore the possibility to synthesize cyclic ether with catalytic indium(III) salt. A tandem sequence of 2-oxania [3,3]-sigmatropic rearrangement and cyclization was reported in 2001. This $In(OTf)_3$-catalyzed reaction provide accessibility towards tetrahydrofuran ring from homoallylic alcohol and aldehyde as precursors. (Scheme 1.3.7) The mechanism of this reaction was further solidified with its successful application in the synthesis of the steroid side chain. (Scheme 1.3.8)

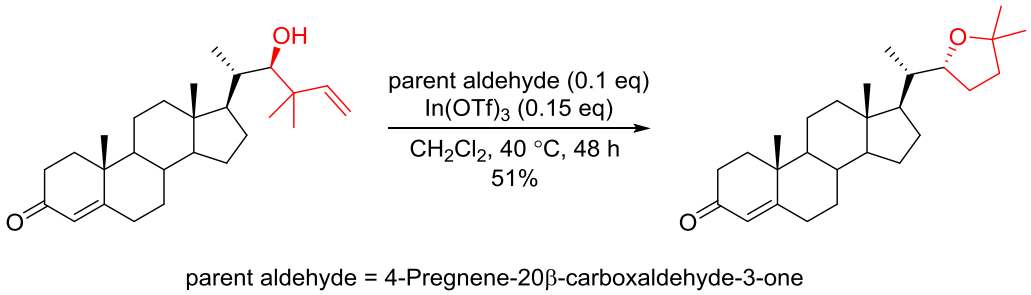

Scheme 1.3.8 Application to the synthesis of steroid side chain.

1.3.2.2.2 In(OTf)$_3$-catalyzed (3,5)-oxonium-ene cyclization in construction of substituted cyclic ether[20]

Encouraged by the above findings, the oxonium formed in the reaction could be redesigned structurally to promote intramolecular oxonium-ene reaction, which will lead to the formation of various cyclic ethers, including tetrehydrofuran and tetrahydropyran. Intramolecular oxonium-ene reaction could be classified into three subtypes according to Mikami's terminology, namely (1,5), (2,5) and (3,5).[21] The first two subtypes are well studied at that time, except (3,5)-oxonium-ene reaction.

[19] (a) Loh, T.-P.; Pei, J.; Cao, G.-Q. *J. Chem. Soc., Chem. Commun.* **1996**, 1819. (b) Loh, T.-P.; Pei, J.; Lin, M. *J. Chem. Soc., Chem. Commun.* **1996**, 2315. (c) Loh, T.-P.; Chua, G.-L.; Vittal, J. J.; Wong, M.-W. *J. Chem. Soc., Chem. Commun.* **1998**, 861. (d) Loh, T.-P.; Wei, L.-L. *Tetrahedron Lett.* **1998**, *39*, 323. (e) Loh, T.-P.; Huang, J.-M.; Goh, S. H.; Vittal, J. J. *Org. Lett*. **2000**, *2*, 1291.

[20] Loh, T.-P.; Hu, Q.-Y.; Tan, K.-T.; Cheng, H.-S. *Org. Lett.* **2001**, *3*, 2669-2672.

[21] For a review, please refer: Mikami, K.; Shimizu, M. *Chem. Rev.* **1992**, *92*, 1021-1050.

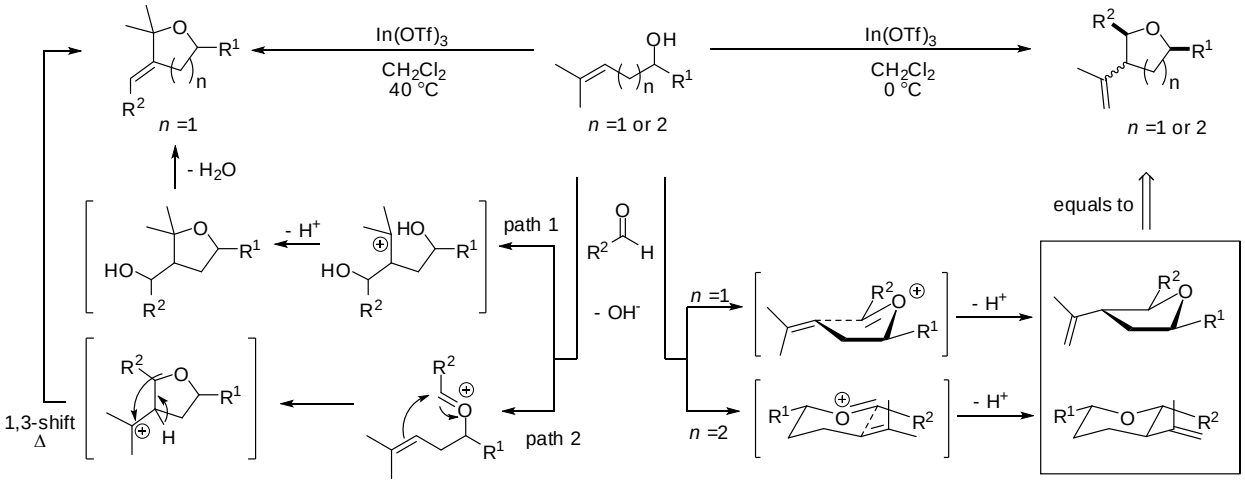

Scheme 1.3.9 In(OTf)$_3$-catalyzed (3,5)-oxonium-ene cyclization in construction of substituted cyclic ether.

As shown in Scheme 1.3.9, Loh and co-workers employed In(OTf)$_3$ to catalyze the reaction between aldehyde and homoallylic alcohol or its elongated homologue. Depending on the reaction temperature, different substituted cyclic ethers were obtained. When the reaction was conducted at 40 ℃, alkylidene tetrahydrofuran was obtained in the case of homoallylic alcohol as precursor. Two plausible mechanisms were deduced in the paper, however, it was later proved that path 2, which involves (3,5)-oxonium-ene cyclization and thermodynamically controlled 1,3-shift, is the reasonable mechanism.

On the other hand, exo-vinyl tetrahydrofuran or tetrahydropyran could be synthesized at 0 ℃ from homoallylic alcohol or its elongated homologue respectively. As shown in Scheme 1.3.9, the mechanism of the formation of these two cyclic ethers involves intramolecular (3,5)-oxonium-ene cyclization on the five- or six-membered transition states.

1.3.2.2.3 In(OTf)$_3$-catalyzed tandem carbonyl-ene/intramolecular (2,5)-oxonium-ene cyclization[22]

Later in 2002, Loh and co-workers reported a tandem reaction, which involved carbonyl-ene reaction and intramolecular (2,5)-oxonium-ene cyclization. This In(OTf)$_3$-catalyzed reaction provided an access to 2,3-*anti*, 2,6-*syn*-4-exo-alkylidene tetrahydrofuran from alkene and two aldehydes (R group could be different). (Scheme 1.3.10) Carbonyl-ene reaction forms homoallylic alcohol in the first place. Addition of second aldehyde will form 6-membered oxonium transition state, which two R groups positioned themselves at equatorial position to minimize 1,3-diaxial interaction. Finally, oxonium-ene cyclization leads to the formation of major tetrahydropyran product. It is to take note that stereochemistry of minor product obtained in this reaction was not determined by authors.

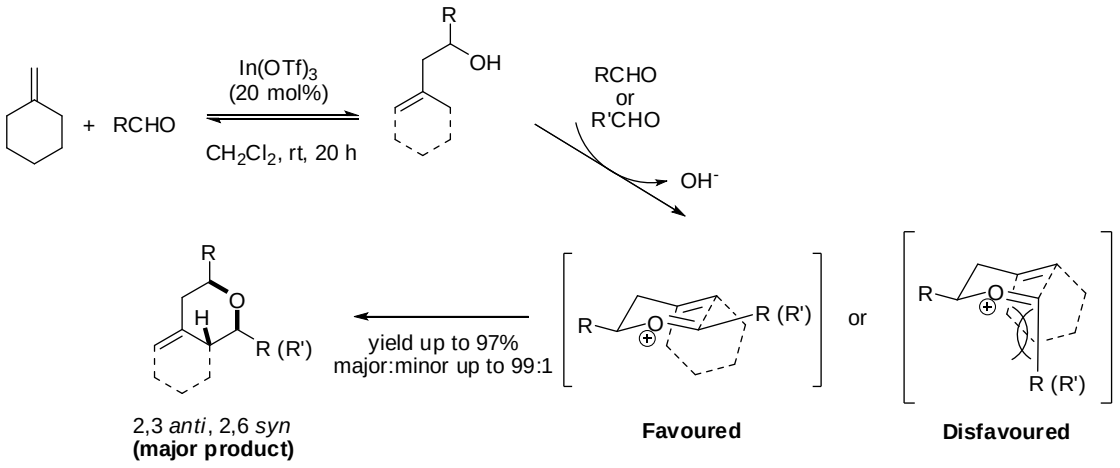

Scheme 1.3.10 In(OTf)$_3$-catalyzed tandem carbonyl-ene/intramolecular (2,5)-oxonium-ene cyclization.

[22] Loh, T.-P.; Feng, L.-C.; Yang, J.-Y. *Synthesis* **2002**, *7*, 937-940.

1.3.2.2.4 Synthesis of 2,6-syn-4-exomethylene tetrahydropyran via In(OTf)$_3$-catalyzed intramolecular (2,5)-oxonium-ene cyclization[23]

As part of the effort in exploring indium-salt catalyzed oxonium-ene cyclization, Loh and co-workers synthesized 2,6-*syn*-4-exomethylene tetrahydropyran, which is the target scaffold in the synthesis of dactylolide, *via* In(OTf)$_3$-catalyzed intramolecular (2,5)-oxonium-ene cyclization. Starting from aldehyde and homoallylic alcohol, oxonium transition state was formed under catalytic activity from In(OTf)$_3$. Similar as previous tandem reaction, the favoured oxonium transition state is the one that the two R groups are positioned at equatorial position. This will lead to the formation of 2,6-*syn*-tetrahydropyran product under (2,5)-oxonium-ene cyclization. On the other hand, the disfavoured transition state will lead to 2,6-*anti*-tetrahydropyran product. According to the authors, various type of 4-exomethylene tetrahydropyran (R^1 = alkyl, aryl, vinyl, R = alkyl, aryl, vinyl, ester) could be obtained at a yield ranged from 50% to 90% and *syn*/*anti* selectivity from 58:42 to 95:5. (Scheme 1.3.11)

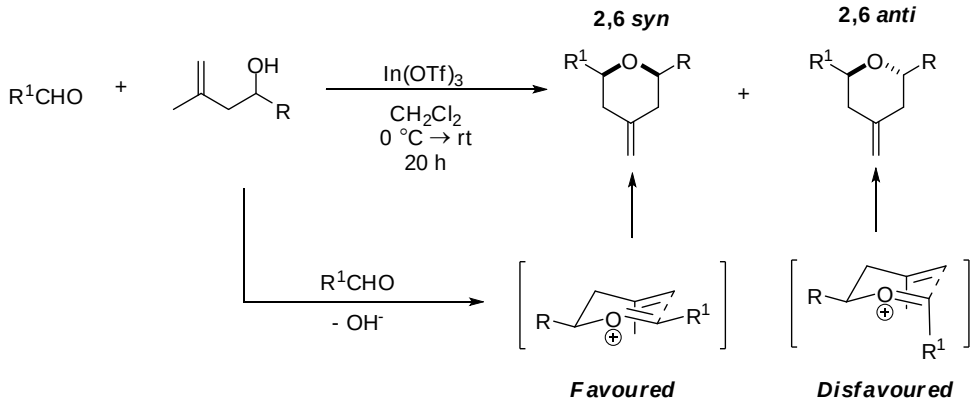

Scheme 1.3.11 In(OTf)$_3$-catalyzed intramolecular (2,5)-oxonium-ene cyclization in the synthesis of 2,6-*syn*-4-exomethylene tetrahydropyran.

Inspired by Smith's work on total synthesis of (+)-dactylolide and (+)-zampanolide, this oxonium-ene strategy was employed in the synthesis of common tetrahydrofuran scaffold of zampanolide and dactylolide. (Scheme 1.3.12) Starting from (2*E*)-3-bromobut-2-enal, indium-mediated allylation with allylic bromide resulted in bromoheptadienol, a homoallylic alcohol which was subjected to (2,5)-oxonium-ene cyclization with alkyl aldehyde. Under the standard conditions, the 2,6-disubstituted-4-exomethylene

[23] Loh, T.-P.; Yang, J.-Y.; Feng, L.-C.; Zhou, Y. *Tetrahedron Lett.* **2002**, *43*, 7193.

tetrahydropyran, which served as a precursor to access the synthesis of dactylolide and zampanolide, was obtained at a yield of 70% and *syn*/*anti* selectivity of 75:25.

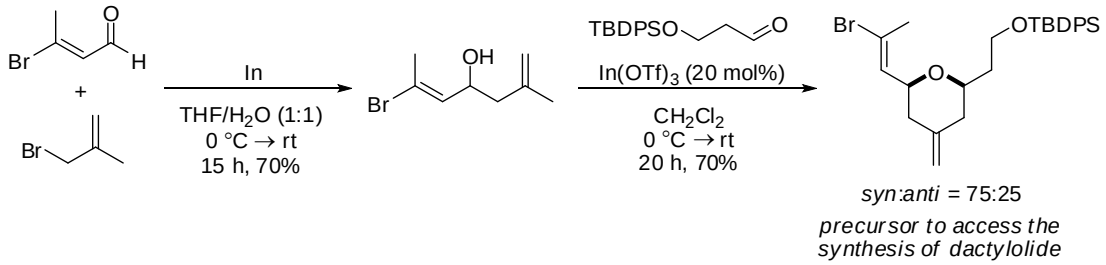

Scheme 1.3.12 Synthesis of tetrahydropyran scaffold of dactylolide *via* $In(OTf)_3$-catalyzed intramolecular (2,5)-oxonium-ene cyclization.

1.3.2.3 Synthetic studies of 2,6-syn-4-exomethylene tetrahydropyran by other group

Saikia and co-workers reported synthesis of dihydropyran (DHP) and tetrahydropyran (THP) *via* oxonium-ene cyclization reaction,[24] which is similar to our report in 2002. Instead of $In(OTf)_3$, they discovered that BF_3 OEt_2 is efficient Lewis acid in their model study. They employed aryl or vinyl aryl aldehyde and homoallylic alcohol as coupling partners. Depend on R'' group on homoallyic alcohol, different pyran product could be obtained. If R'' group is hydrogen (H), dihydropyran **I** was obtained predominantly, while R'' group is aryl group, 2,6-*syn*-4-exomethylene tetrahydropyran **III** was obtained predominantly. Besides, the products obtained are *syn*-isomer. No *anti*-isomer was observed by the authors. (Scheme 1.3.13)

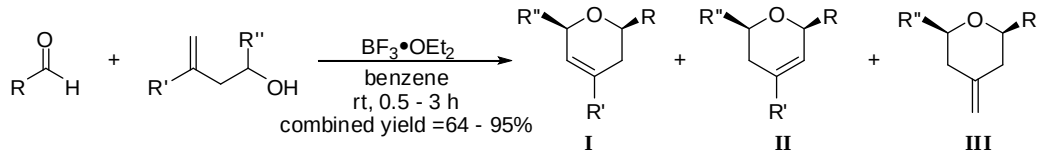

(a) R = Aryl or Aryl vinyl, R' = Ph or Me, **R" = H**, **I** (DHP) is predominant
(b) R = Aryl, R' = Me, **R" = Aryl**, **III** (THP) is predominant

Scheme 1.3.13 Saikia's synthesis of dihydropyran (DHP) and tetrahydropyran (THP) *via* oxonium-ene cyclization.

The mechanism proposed by Saikia and co-workers were similar to that proposed by our group. Coordination of Lewis acid on carbonyl group of aldehyde promotes nucleophilic attack by homoallylic alcohol. Followed by formation of oxonium, which resulted in a more favourable six membered chair transition state, the oxonium-ene reaction leads to three different pyrans depend on the position where the proton is removed. (Scheme 1.3.14)

[24] Bondalapati, S.; Reddy, U. C.; Saha, P.; Saikia, A. K. *Org. Biomol. Chem.* **2011**, *9*, 3428-3438.

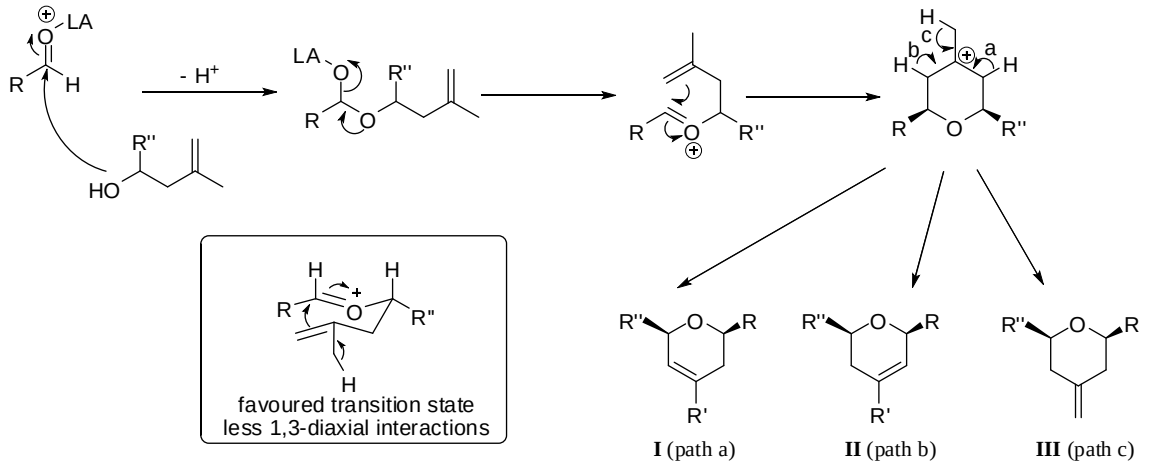

Scheme 1.3.14 Saikia's proposed mechanism of dihydropyran and tetrahydropyran synthesis *via* oxonium-ene cyclization.

Hoveyda and co-workers, on the other hand, reported an operationally simple, efficient and diastereoselective synthesis of 2,6-*syn*-4-exomethylene tetrahydropyrans catalyzed by triflic acid,[25] which is a Brønsted acid. Inspired by their inadvertent observation in Mo-catalyzed asymmetric ring-closing metathesis from enol ether, they found that catalytic amount, which only 0.01 mol%, of triflic acid provided a mixture of tetrahydropyran **I** and dihydropyrans **II** and **III**, which tetrahydropyran **I** is the most predominant product. Instead of obtaining pure *syn*-isomer, the catalytic protocol achieved diastereomeric excess of more than 98% for the cyclic ethers formed. (Scheme 1.3.15)

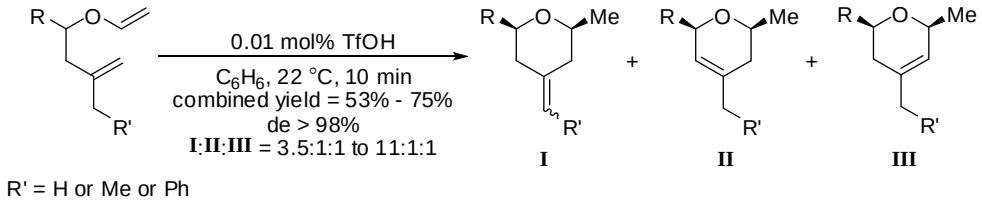

Scheme 1.3.15 Hoveyda's synthesis of 2,6-*syn*-4-exomethylene tetrahydropyrans catalyzed by triflic acid.

Apart from the main results above, they also observed a few of interesting points, including (a) the reaction could be undergone in various types of solvents but resulted in lower product selectivity; (b) the reaction could be conducted at -78 ℃; (c) prolonged reaction, for example, after 5 days, tetrahydropyran **I** is converted into dihydropyrans **II**

[25] Puglisi, A.; Lee, A.-L.; Schrock R. R.; Hoveyda, A. H. *Org. Lett.* **2006**, *8*, 1871-1874.

and **III**. Pure tetrahydropyran **I** is highly sensitive to TfOH and converted to dihydropyrans **II** and **III** at room temperature in 1 hour; (d) Conversion is extremely low (< 2%) if terminal alkene acts as substrate.

1.3.2.4 Comparison between Loh's and Saikia's strategy on synthesis of 2,6-syn-4-exomethylene tetrahydropyrans

Comparison is made between Loh's strategy and Saikia's strategy on synthesis of 2,6-*syn*-4-exomethylene tetrahydropyrans and shown in Table 1.3.1. It is obvious that Loh's strategy is better than Saikia's in some aspects. Loh's strategy could be employed in a larger scope of substrate, while Saikia's strategy is only limited to aryl substituted cyclic ether. From the viewpoint of Lewis acid, Loh's strategy requires catalytic amount of $In(OTf)_3$, while stoichiometric amount of $BF_3 \cdot OEt_2$ is required in Saikia's strategy. This implies that Loh's strategy is more advantageous than Saikia's in terms of green chemistry. Although Loh's strategy has its limitation in steroselectivity, it provides tetrahydropyran as sole product. On the contrary, Saikia's strategy is excellent in its stereochemistry despite that mixture of tetrahydropyran (THP) and dihydropyran (DHP) was obtained and could not be separated in some cases. As the substituents on 2- and 6-position of tetrahydropyran scaffold in dactylolide are vinyl and alkyl, therefore, Loh's strategy will be employed in our synthetic plan.

	Loh's (2002)	**Saikia's (2011)**
Scope of reaction (R group at 2- and 6-position of THP)	Alkyl, aryl, vinyl, ester	Aryl only
Lewis acid	$In(OTf)_3$ (catalytic, 20 mol%)	$BF_3 \cdot OEt_2$ (stoichiometric, 1 equiv.)
Solvent	CH_2Cl_2 (dichloromethane)	C_6H_6 (benzene)
THP/DHP	Only THP product	THP is predominant than DHP
syn*/*anti	*syn* and *anti*-product observed	Only *syn*-product

Table 1.3.1 Comparison between Loh's strategy and Saikia's strategy on synthesis of 2,6-*syn*-4-exomethylene tetrahydropyrans.

1.3.3 Conjugated diene as structural motifs and its synthetic examples

Conjugated polyene structure is also a common structural motif could be found in large variety of natural products.[26] By convention, there are two types of alkene conformation, namely *cis* and *trans*. *cis*-Isomer has two relatively higher priority groups at the same side across carbon-carbon double bond, while *trans*-isomer has them on the opposite side of each other. However, *cis* and *trans* notation is not a suitable naming system for all kind of alkene, especially tri- and tetrasubstituted alkene are considered. Therefore, the most suitable and unambiguous naming system is *E*/*Z* notation, which determined by the Cahn-Ingold-Prelog (CIP) priority rules. By determine the priority of substituent linked to each carbon atom of alkene firstly, the alkene with higher priority groups at the same side is notated as (*Z*)-alkene, while higher priority groups at opposite side is notated as (*E*)-alkene.

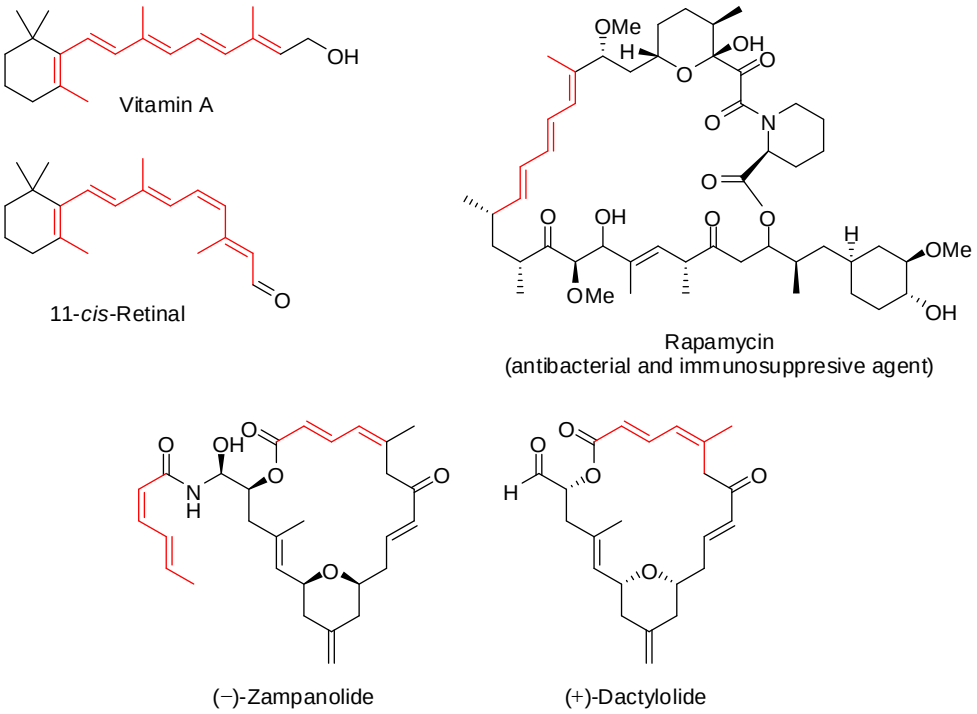

Scheme 1.3.16 Examples of polyene natural products.

Some examples of conjugated polyene are shown in Scheme 1.3.16. Vitamin A and 11-*cis*-Retinal, one of components forming rhodopsin, are important polyene natural products involved in visual phototransduction. Rapamycin, on another hand, is a

[26] A comprehensive review of polyene natural products: Thirsk, C.; Whiting, A. *J. Chem. Soc., Perkin Trans. 1* **2002**, 999-1023.

macrolide structure containing conjugated triene. It is discovered as metabolites from bacteria *Streptomyces* and is an antibacterial and immunosuppressive agent.[27] Marine-derived macrolides, such as (–)-zampanolide and (+)-dactylolide, are macrolides containing conjugated diene. These two natural products will be further discussed in Chapter 2.

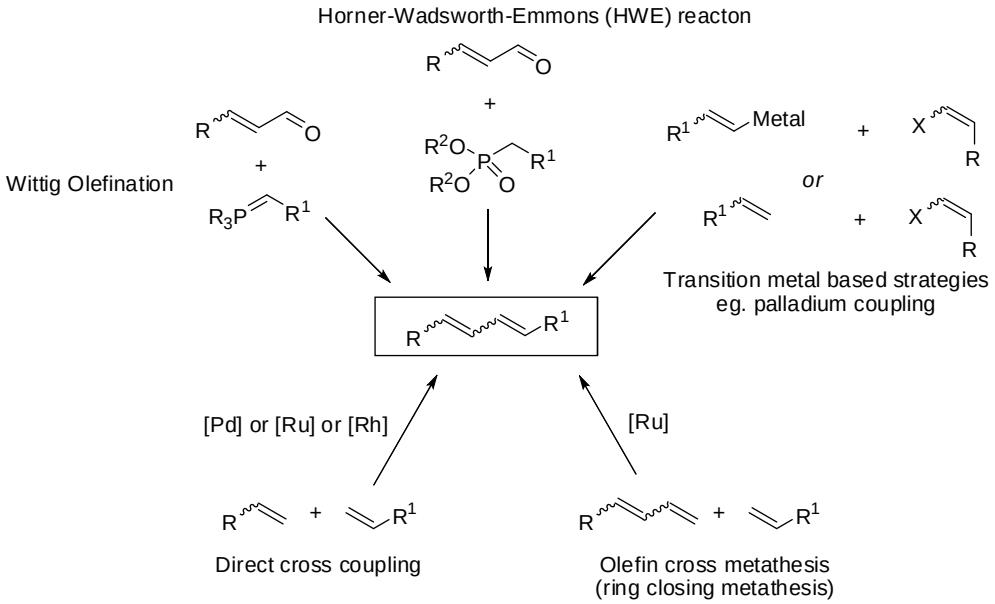

Scheme 1.3.17 Synthetic strategies to construct polyene motif.

Due to the rich existence of polyene motifs in natural product, synthesis of such structural motif has been studied extensively since 20th century. (Scheme 1.3.17) Up to date, common synthetic strategies taken to construct polyene motif include Wittig olefination, Horner-Wadsworth-Emmons (HWE) reaction (Section 1.3.3.1), transition metal based strategies, such as palladium coupling (Section 1.3.3.2) and olefin metathesis (Section 1.3.3.3). Recently, extensive studies on direct cross coupling between two olefins *via* alkenyl C-H activation have been reported by Loh's group and others. This synthetic strategy, which will be discussed in Section 1.3.3.4, becomes an emerged *green* reaction in the synthesis of conjugated diene.

[27] (a) Isolation: Vtzina, C.; Kudelski, A.; Sehgal, S. N. *J. Anribiot.* **1975**, *28*, 721; Sehgal, S. N.; Baker, H.; Vtzina, C. *J. Anribiot.* **1975**, *28*, 727. (b) Structure: Swindells, D. C. N.; White, P. S.; Findlay, J. A. *Can. J. Chem.* **1978**, *56*, 2491; Findlay, J. A.; Radics, L. *Can. J. Chem.* **1980**, *58*, 579.

1.3.3.1 Wittig olefination and Horner-Wadsworth-Emmons reaction

Wittig olefination is first discovered by Georg Wittig in 1954.[28] This strategy allows chemists to synthesize olefin from aldehyde or ketone with phosphonium ylide. By using stabilized or non-stabilized ylide, (*E*)- or (*Z*)-alkene could be obtained as major product respectively. With this revolutionary strategy, Georg Wittig was then awarded with Nobel Prize in Chemistry in 1979 for his contribution on alkene preparation.

However, the need to prepare appropriate ylide beforehand, mixture of isomeric olefin product requiring further separation and the removal of solid phosphine oxide by-product makes Wittig olefination become less popular in natural product synthesis, especially its analogue strategy, Horner-Wadsworth-Emmons reaction,[29] was revealed in a later time.

Horner-Wadsworth-Emmons reaction employed stabilized phosphonate carbanions instead of phosphonium ylide as its synthetic counterpart. This strategy produces (*E*)-alkene prominently, and generated water-soluble dialkylphosphate salt by-product, which could be removed by aqueous extraction easily.

Synthetic examples of Wittig olefination and Horner-Wadsworth-Emmons reaction are shown in Scheme 1.3.18 and 1.3.19. In the synthesis of Vitamin A, BASF constructs the tetraene carbon chain by utilizing Wittig olefination.[30] On the other hand, one of the significant synthetic applications of Horner-Wadsworth-Emmons reaction is Nicoloau's synthesis of amphotericin B. A total of three HWE reactions were performed in this total synthesis, whereas two of them constructs the hexaene component, while the last HWE reaction induces the ring closing, which lead to completion of amphotericin B.[31]

---

28 (a) Wittig, G.; Schöllkopf, U. *Chemische Berichte* **1954**, *87*, 1318. (b) Wittig, G.; Haag, W. *Chemische Berichte* **1955**, *88*, 1654-1666.

29 (a) Horner, L.; Hoffmann, H. M. R.; Wippel, H. G. *Ber.* **1958**, *91*, 61–63. (b) Horner, L.; Hoffmann, H. M. R.; Wippel, H. G.; Klahre, G. *Ber.* **1959**, *92*, 2499–2505. (c) Wadsworth, W. S., Jr.; Emmons, W. D. *J. Am. Chem. Soc.* **1961**, *83*, 1733. (d) Wadsworth, W. S., Jr.; Emmons, W. D. *Org. Synth.* **1965**, *45*, 44.

30 Exner, K. M.; Massonne, K.; Laas, H.; Glas, D.; Szarvas, L. Method for producing vitamin A acetate using the Wittig reaction, WO 2005058811, Jun 30, 2005.

31 Nicolaou, K. C.; Daines, R. A.; Chakraborty T. K.; Ogawa, Y. *J. Am. Chem. Soc.* **1988**, *110*, 4685-4696.

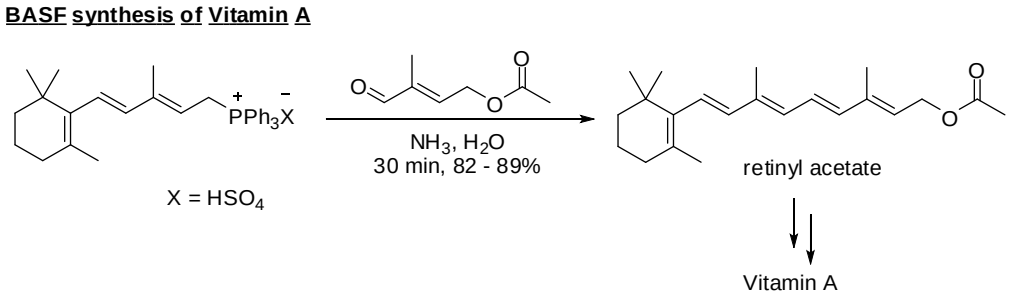

Scheme 1.3.18 BASF synthesis of Vitamin A, a synthetic application example of Wittig olefination

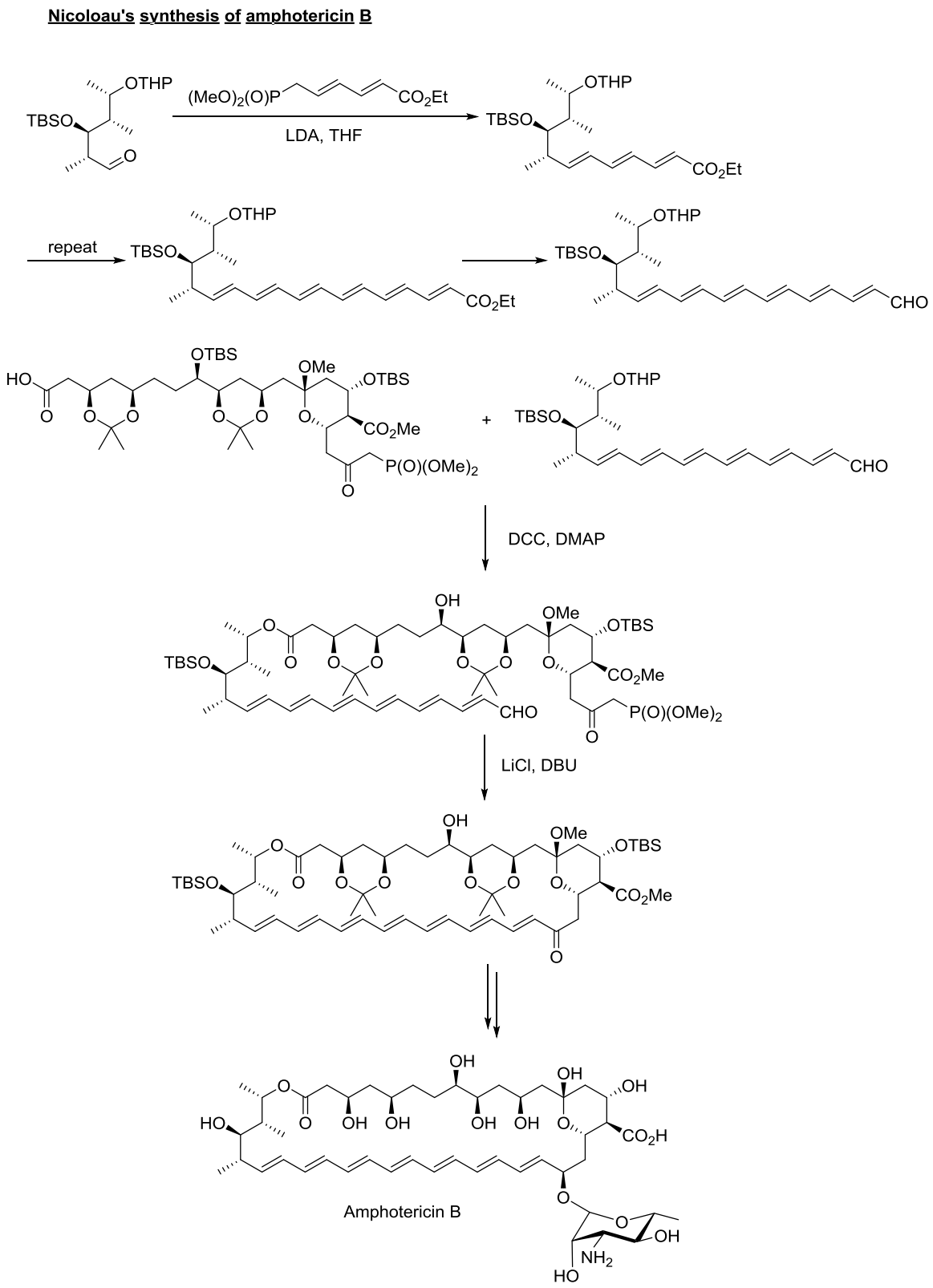

Scheme 1.3.19 Nicoloau's synthesis of Amphotericin A, a synthetic application example of HWE reaction.

1.3.3.2 Palladium coupling in polyene synthesis

As the organic chemistry flourishes, a number of different types of palladium-catalyzed cross coupling appear in the arena of olefin synthesis. These reactions include Stille reaction,[32] Suzuki reaction,[33] Heck reaction[34] and Negishi reaction.[35] (Scheme 1.3.20) These synthetic strategies use palladium salt as catalysts to form carbon-carbon bond between two sp^2 carbon atoms, which one of them is always recruited from halide compound. In 2010, Richard F. Heck, Ei-ichi Negishi and Akira Suzuki received Nobel Prize in Chemistry on their contribution on this area.

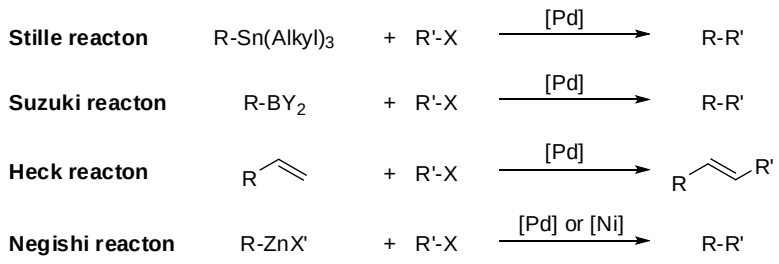

Scheme 1.3.20 Summary of palladium coupling reaction. R,R' = alkenyl or aryl, X,X' = halide or pseudohalide (eg. OTf), Y = alkyl or alkoxyl.

Selected synthetic examples of palladium coupling to construct polyene structure are shown as followed. Panek and Masse employed Stille reaction in their synthesis of mycotrienol, a potent antifungal natural product. (Scheme 1.3.21) The triene scaffold in mycotrienol was constructed from dialkenyl halide and tributylstannylethene, catalyzed by $Pd(MeCN)_2Cl_2$.[36]

[32] Review: Stille, J. K. *Angew. Chem. Int. Ed. Engl.* **1986**, *25*, 508–524.
[33] (a) Miyaura, N.; Yamada, K.; Suzuki, A. *Tetrahedron Lett.* **1979**, *20*, 3437-3440. (b) Miyaura, N.; Suzuki, A. *J. Chem. Soc., Chem. Commun.* **1979**, 866-867. (c) Miyaura, N.; Suzuki, A. *Chem. Rev.* **1995**, *95*, 2457-2483.
[34] (a) Heck, R. F.; Nolley, Jr., J. P. *J. Org. Chem.* **1972**, *37*, 2320-2322. (b) Mizoroki, T.; Mori, K.; Ozaki, A. *Bull. Chem. Soc. Jap.* **1971**, *44*, 581.
[35] (a) King, A. O.; Okukado, N.; Negishi, E. *J. Chem. Soc., Chem. Commun.* **1977**, 683-684. (b) Negishi, E.; King, A. O.; Okukado, N. *J. Org. Chem.* **1977**, *42*, 1821-1823.
[36] Panek, J. S.; Masse, C. E. *J. Org. Chem.* **1997**, *62*, 8290.

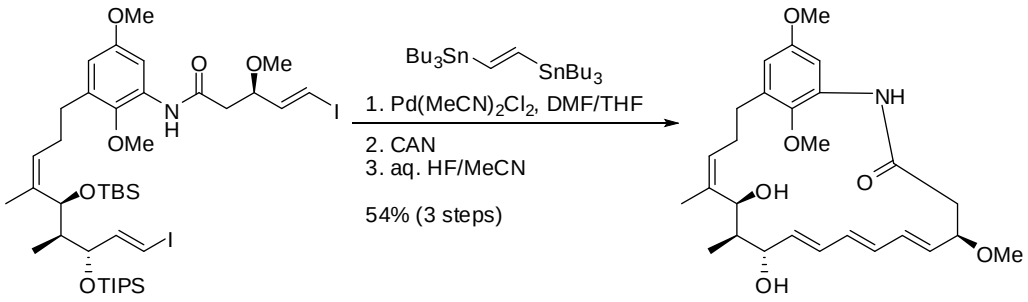

Scheme 1.3.21 Panek and Masse's synthesis of mycotrienol, a synthetic application example of Stille reaction.

On the other hand, de Lera and co-workers synthesized retinol, one of the forms of Vitamin A, by employing thallium-accelerated Suzuki reaction. With the participation of 10% aqueous thallium hydroxide solution, retinol was furnished at a yield of 83% at ambient temperature from alkenyl halide and alkenylboronic acid counterparts.[37] (Scheme 1.3.22)

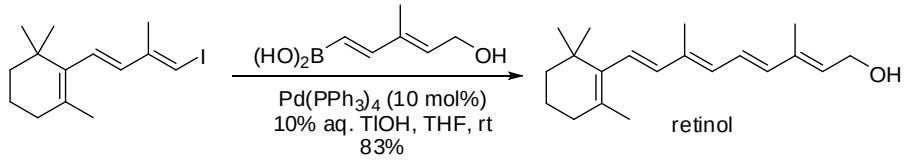

Scheme 1.3.22 de Lera's synthesis of retinol, a synthetic application example of Suzuki reaction.

Negishi reaction is also always utilized in natural product synthesis. One of the examples is Lipshutz's synthesis of hexaenoate scaffold of dermostatin A, which possesses antifungal bioactivity against human pathogens. Dienylzinc reagent, formed from alkenyl iodide, reacted with alkenyl bromide, followed by desilylation to yield conjugated pentaene. Pentaene was then hydrozirconated, transmetalated to aluminium and exposed to ethyl chloroformate to furnish the haxaenoate scaffold.[38] (Scheme 1.3.23)

[37] Torrado, A.; Iglesias, B.; Lopez, S.; de Lera, A. R. *Tetrahedron* **1995**, *51*, 2453-2454.
[38] Lipshutz, B. H.; Ullman, B.; Lindsley, C.; Pecchi, S.; Buzard, D. J.; Dickson, D. *J. Org. Chem.* **1998**, *63*, 6092-6093.

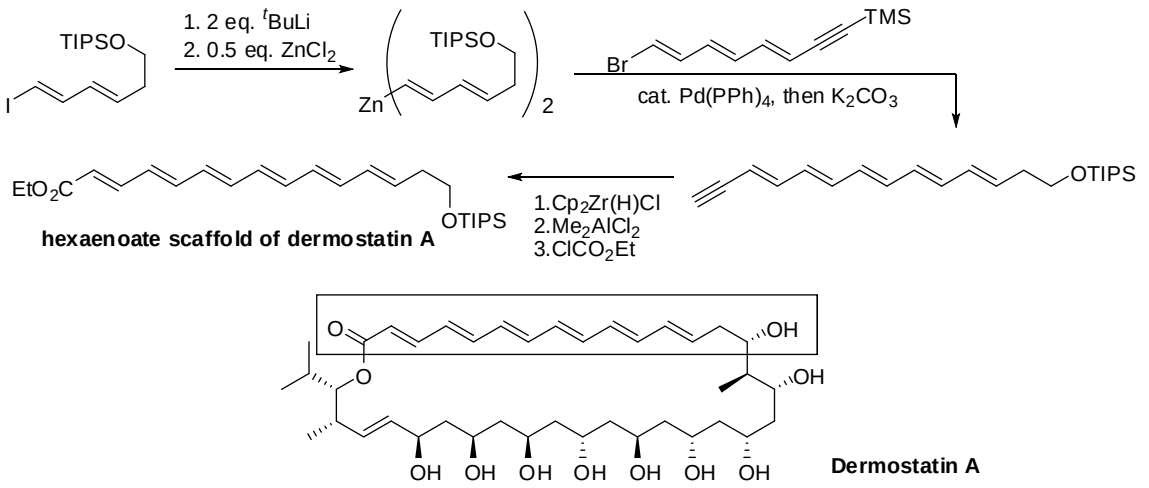

Scheme 1.3.23 Lipshutz's synthesis of hexaenoate scaffold of demostatin A, a synthetic application example of Negishi reaction.

1.3.3.3 Olefin metathesis in diene synthesis

Olefin metathesis[39] is another popular strategy in the olefin synthesis. The feature of this reaction is its intermolecular exchange of alkylidene (R_2=C) from two alkene functional groups, promoted by metal-carbene complexes. Common types of olefin metathesis include cross-metathesis (CM), ring-opening cross-metathesis (ROM), ring-closing metathesis (RCM) and intermolecular enyne metathesis.

Among these olefin metatheses, intermolecular enyne metathesis, or ring-closing enyne metathesis (RCEM), is the most common strategy to construct diene structure. However, instead as final product, the diene structures are always subjected to subsequent Diels-Alder reaction to yield target products. (Scheme 1.3.24) One of the examples of this synthetic strategy is Kashinath and Reddy's synthesis of isofregenedadiol, a bicyclic terpene. [40] Started from enyne, a conjugated diene was formed *via* RCEM. The diene was then subjected to second cross methatesis and Diels-alder/aromatization to furnish the core skeleton of isofregenedadiol. (Scheme 1.3.25) This synthesis was also demonstrated as one-pot reaction in toluene, which allow the chemist avoid tedious purification and reduce environment impact by reducing the solvent used.

[39] Comprehensive articles on olefin metathesis, please see: (a) Chatterjee, A. K.; Choi, T.-L.; Sanders, D. P.; Grubbs, R. H. *J. Am. Chem. Soc.* **2003**, *125*, 11360-11370.(b) Connon, S. J.; Blechert, S. *Angew. Chem. Int. Ed.* **2003**, *42*, 1900-1923.

[40] Kashinath, K.; Reddy, D. S. *Org. Biomol. Chem.*, **2015**, *13*, 970-973.

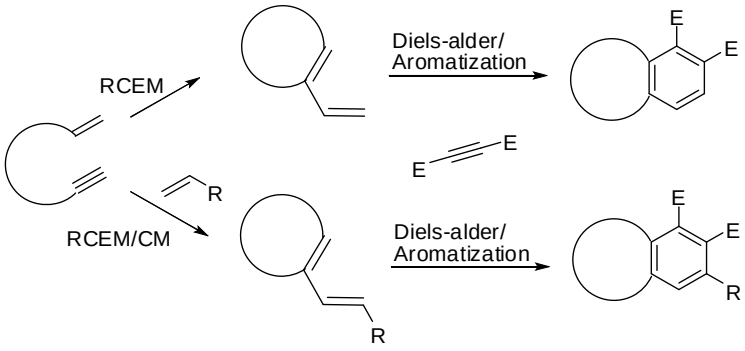

Scheme 1.3.24 Enyne metathesis/Diels-alder/Aromatization strategy to access core skeleton of natural products.

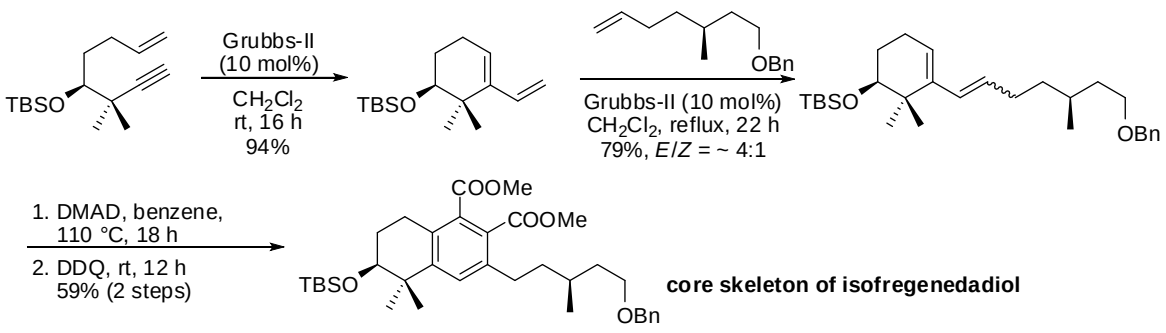

Scheme 1.3.25 Enyne metathesis/Diels-alder/Aromatization strategy in synthesis of core skeleton of isofregenedadiol.

1.3.3.4 Direct cross coupling developed in Loh's research group

Although aforementioned strategies provide feasible access to conjugated diene motif, limitations still persist in the chemical transformation. From the viewpoint of *green* chemistry, Wittig reaction and HWE reaction do not perform well in terms of atom economy as phosphorus salts are produced as side products. Palladium-catalyzed cross coupling reactions require pre-formed halide and highly toxic metal catalyst in some cases. Olefin metathesis, despite of its highly efficient catalytic properties, requires multi-step to install olefin one at each time to construct polyene structure. In order to solve the limitations above, a straightforward strategy, such as coupling two single olefins into a conjugated diene catalytically without pre-installation of activating group on the olefins, would serve as a more powerful strategy in conjugated diene synthesis.

The first of such strategy was reported by Ishii and co-workers in 2004. They demonstrated synthesis of muconate derivatives from acrylates and vinyl carboxylates *via* oxidative cross-coupling catalyzed by complex $Pd(OAc)_2$/HPMoV/O_2 system.[41] However, cross coupling between acrylates and simple alkenes was only revealed in 2009 by Loh and co-workers. The direct cross coupling was catalyzed by a single metal catalyst, $Pd(OAc)_2$ and used oxygen as oxidant. This methodology works excellent when aromatic alkene or cycloalkene was used as coupling partner. Aliphatic alkene only provides moderate yield and *E*/*Z* selectivity. [42] Later in 2010, Loh and co-workers reported another palladium-catalyzed direct cross coupling reaction, which coupled indenes, a rigid trisubstituted alkenes, and electron-deficient alkenes, including acrylates into a conjugated diene.[43] (Scheme 1.3.26)

[41] Hatamoto, Y.; Sakaguchi, S.; Ishii, Y. *Org. Lett.* **2004**, *6*, 4623-4625.
[42] Xu, Y.-H.; Lu, J.; Loh, T.-P. *J. Am. Chem. Soc.* **2009**, *131*, 1372-1373.
[43] Xu, Y.-H.; Wang, W.-J.; Wen, Z.-K.; Hartley, J. J.; Loh, T.-P. *Tetrahedron Lett.* **2010**, *51*, 3504-3507.

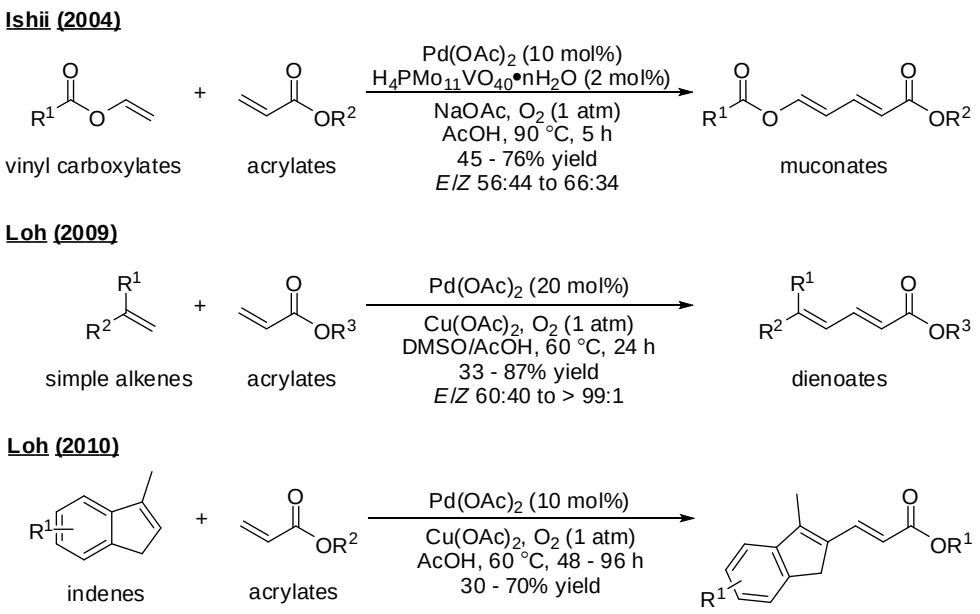

Scheme 1.3.26 First three examples of direct cross couplings of two olefins by Ishii and Loh.

These groundbreaking discoveries then inspired subsequent cross coupling of different combination of olefins, reported by not only Loh's group (examples will be introduced later in this section), but also the groups of Yu, Glorius and Liu. (Scheme 1.3.27) Yu and co-workers synthesized diene from α–oxoketene dithioacetals and terminal olefins with palladium-catalyzed cross coupling. The 1,2-dithiane group was served as an activation group for internal alkenyl C-H bond in the reaction. The resulted diene product was used as a precursor in the synthesis of bicylic pyridiones.[44] Instead of palladium catalyst, Glorius's group is the first research group using rhodium catalyst to synthesize α,β-γ,δ-unsaturated amino acids, which alkene configuration prefers as (*Z*,*E*)-isomer. Amide group was designed as directing group in this stereoselective reaction.[45] Liu, on the other hand, synthesized conjugated diene from allyl esters and allyl acrylates and able to achieved *E*,*E*:*Z*,*E* ratio up to 99:1.[46]

[44] Yu, H.; Jin, W; Sun, C.; Chen, J.; Du, W.; He, S.; Yu, Z. *Angew. Chem. Int. Ed.* **2010**, *49*, 5792-5797.
[45] Besset, T.; Kuhl, N.; Patureau, F. W.; Glorius, F. *Chem. Eur. J.* **2011**, *17*, 7167-7171.
[46] Zhang, Y.; Cui, Z.; Li, Z.; Liu, Z.-Q. *Org. Lett.* **2012**, *14*, 1838-1841.

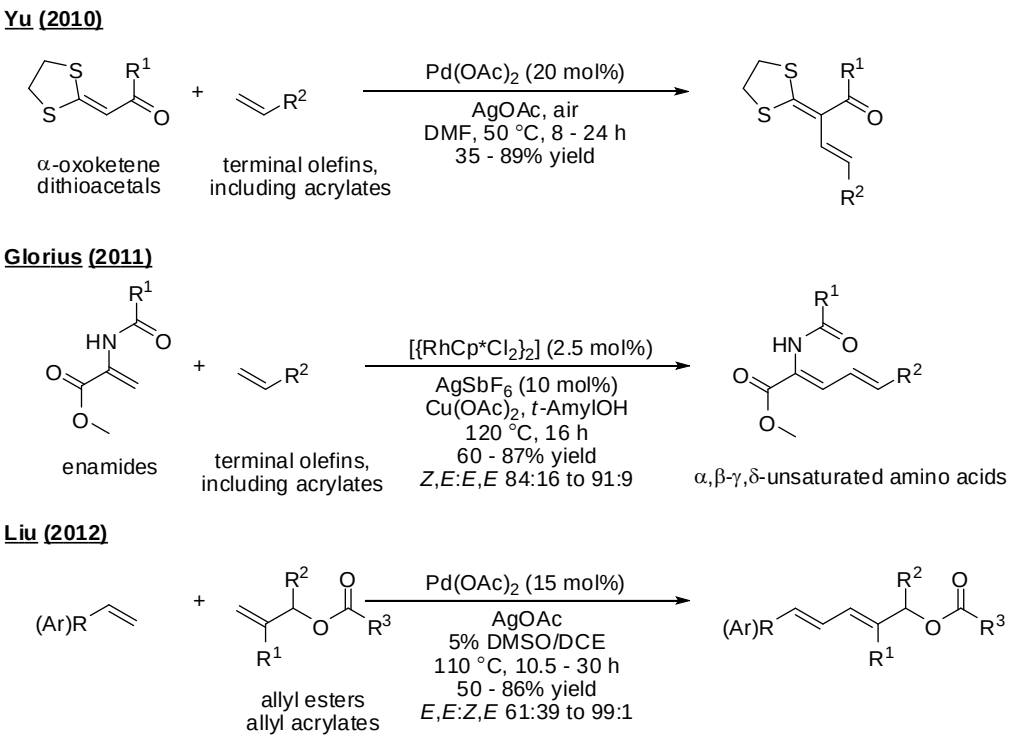

Scheme 1.3.27 Selected examples of direct cross coupling developed by Yu, Glorius and Liu.

The discovery of palladium-catalyzed direct cross coupling in our group encourages us to further explore direct cross coupling of different types of alkenes, especially relatively less reactive aliphatic alkenes. Moreover, we also focus on the application of these methodologies, such as natural product synthesis.

In 2011, Xu *et al.* reported cross-coupling between enamide and acrylate. An X-ray crystallography analysis on the intermediate was performed in this study and showed that cyclic vinylpalladium complex was formed when palladium acetate coordinated to the enamide in dimethyl sulfoxide as solvent. This coupling reaction is catalyzed by palladium acetate and used oxygen as sole oxidant, which potentially to be applied in industry in view of environmental and economical advantages.[47] (Scheme 1.3.28)

[47] Xu, Y.-H.; Chok, Y. K.; Loh, T.-P. *Chem. Sci.* **2011**, *2*, 1822-1825.

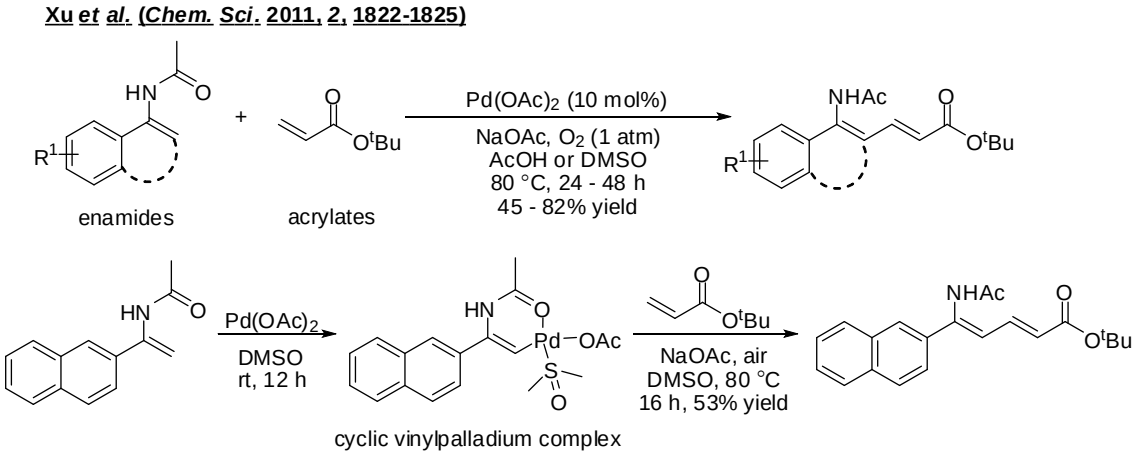

Scheme 1.3.28 Direct cross coupling between enamide and acrylate. Cyclic vinylpalladium complex was proved to be formed during the reaction.

In the earlier findings of direct cross coupling reaction, aliphatic alkenes provided lower yield and selectivity if compared with aromatic alkenes. However, this limitation was resolved later by Wen *et al.* in their report on direct cross coupling between unactivated alkenes and acrylates. Homoallylic alcohol and allylic alcohol were successfully coupled with acrylates and the final products, dienoates, could be obtained at a yield up to 82% and *E*/*Z* selectivity up to 95:5. In this direct cross coupling reaction, not only $Pd(OAc)_2$ acted as catalyst, catalytically amount of 1,10-phenanthroline (ligand) and $AgSbF_6$ (additive) are necessary to facilitate the reaction. From the viewpoint of application, this synthetic strategy was applied in a formal synthesis of C13 – C21 diene fragment of palmerolide A, a cytotoxic marine macrolide.[48] (Scheme 1.3.29)

[48] Wen, Z.-K.; Xu, Y.-H.; Loh, T.-P. *Chem. Eur. J.* **2012**, *18*, 13284-13287.

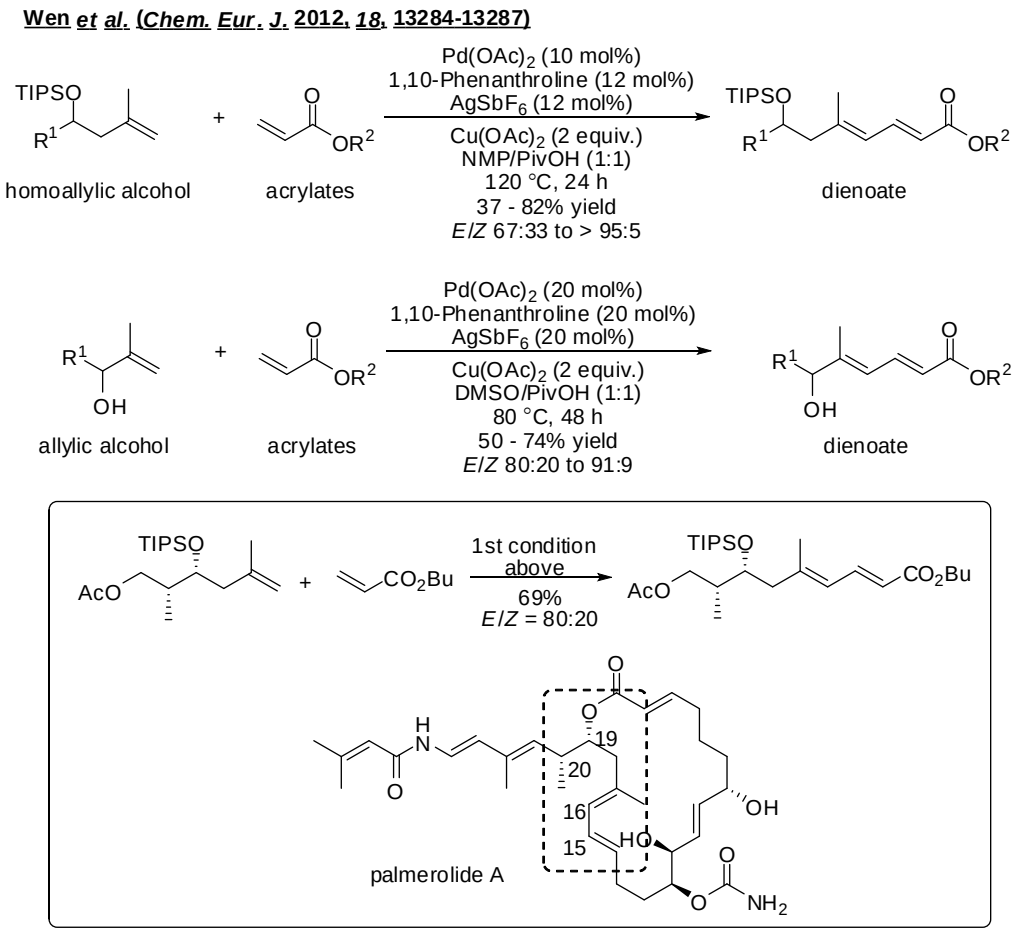

Scheme 1.3.29 Direct cross coupling between homoallylic alcohol or allylic alcohol and acrylates. This synthetic strategy was applied in formal synthesis of C13 – C21 fragment of palmerolide A.

Contrast with previous reported palladium-catalyzed direct cross coupling reactions, Zhang and Loh demonstrated ruthenium- and rhodium-catalyzed direct cross coupling reactions. This new methodology synthesized (*Z*,*E*)-dienamides by coupling acrylamides with a wide range of terminal olefins, including acrylates (R^5 = COOR), vinylsulfonylbenzene (R^5 = SO_2Ph), styrene (R^5 = Ar), acrylamide (R^5 = $CONR_2$), acrylonitrile (R^5 = CN), phosphonate (R^5 = $PO(OR)_2$)and Weinreb amide (R^5 = CONROR).[49] (Scheme 1.3.30)

[49] Zhang, J.; Loh, T.-P. *Chem. Commun.* **2012**, *48*, 11232-11234.

Inspired by Yu's work using monoprotected amino acid as effective ligands in arene C-H activation,[50] Wen *et al.* able to synthesize 1,3-dienes from simple alkenes by using Ac-Ile-OH as ligand in palladium-catalyzed direct cross coupling reaction. This methodology demonstrated a straightforward access to aliphatic conjugated diene, without preinstall any activating group on the starting olefin. However, the coupling partner must be an electron-deficient alkene, such as acrylates, acrylamide, phosphonate and Weinreb amide. Another improvement made in this study is the effectiveness in synthesizing (*E*,*E*)-diene, whereby *E*/*Z* selectivity could be up to > 99:1.[51] (Scheme 1.3.30)

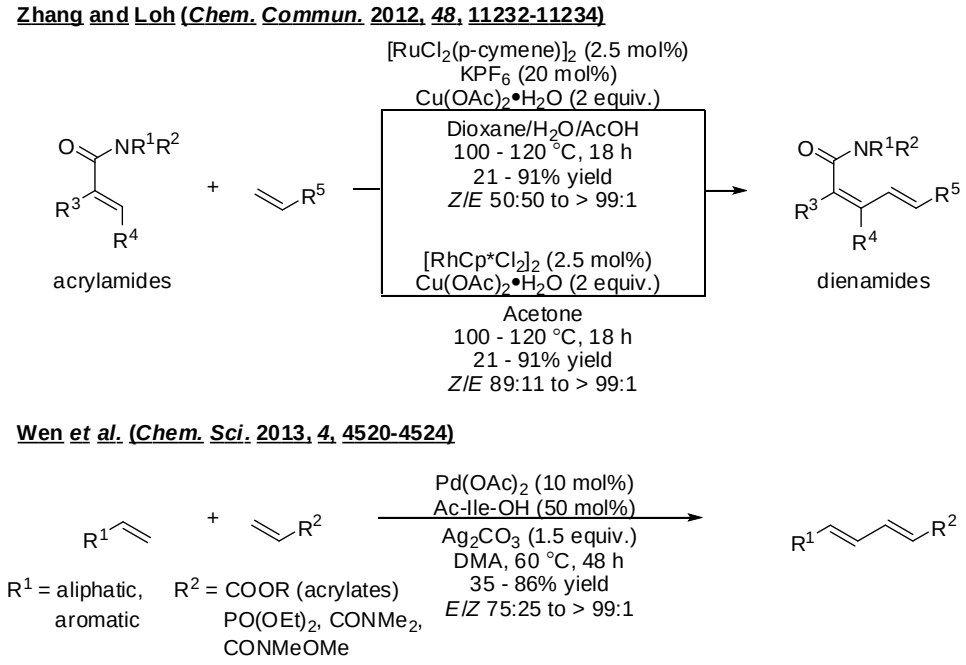

Scheme 1.3.30 Ru- and Rh-catalyzed direct cross coupling and Pd-catalyzed direct cross coupling which employed monoprotected amino acid as ligand developed in Loh's group.

Most of the examples of direct cross coupling reaction used acrylates as coupling partner. Vinyl ketones, on the other hand, seldom became an effective coupling partner until palladium-catalyzed direct cross coupling reaction between 1,1-disubstituted alkene and vinyl ketones was reported by Zhang et al. Among the examples shown, dienyl ketones could be obtained at moderate yield up to 60% with *E*/*Z* selectivity up to 84:16. Instead of employing $Cu(OAc)_2$ or oxygen as oxidant, AgOAc became the most effective oxidant in

[50] (a) Wang, D.-H.; Engle, K. M.; Shi, B.-F.; Yu, J.-Q. *Science* **2010**, *327*, 315; (b) Engle, K. M.; Wang, D.-H.; Yu, J.-Q. *J. Am. Chem. Soc.* **2010**, *132*, 14137; (c) Cheng, X. F.; Li, Y.; Su, Y. M.; Yin, F.; Wang, J. Y.; Sheng, J.; Vora, H. U.; Wang, X. S.; Yu, J. Q. *J. Am. Chem. Soc.* **2013**, *135*, 1236; (d) Leow, D.; Li, G.; Mei, T. S.; Yu, J. Q. *Nature* **2012**, *486*, 518; (e) Li, G.; Leow, D. S.; Wan, L.; Yu, J. Q. *Angew. Chem. Int. Ed.* **2013**, *52*, 1245.
[51] Wen, Z.-K.; Xu, Y.-H.; Loh, T.-P. *Chem. Sci.* **2013**, *4*, 4520-4524.

this synthesis. Besides, application of this synthetic methodology in synthesis of Vitamin A1 also proved that the methodology is useful and practical in value-added application.[52] (Scheme 1.3.31)

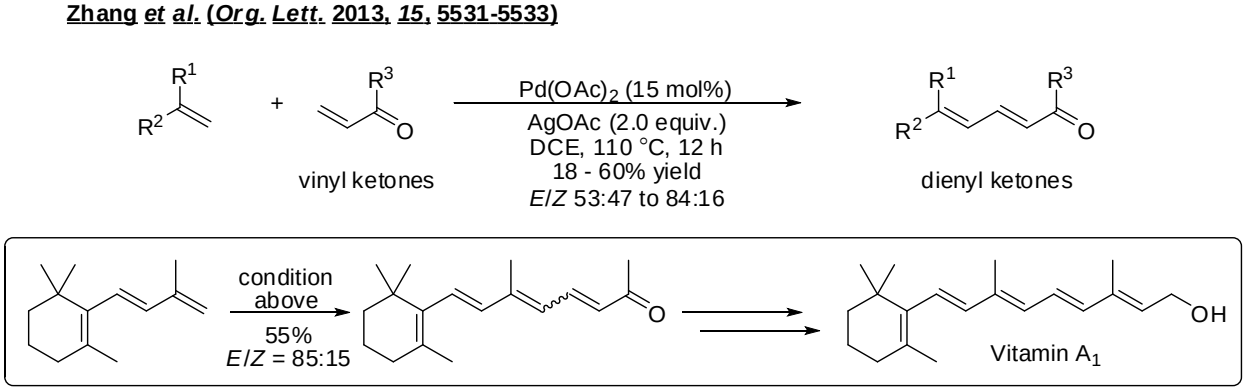

Scheme 1.3.31 Pd-catalyzed direct cross coupling between simple alkenes and vinyl ketones and its synthetic application in synthesis of Vitamin A1.

As introduced before, Ishii and co-workers demonstrated synthesis of muconates *via* direct cross coupling reaction under $Pd(OAc)_2$/HPMoV/O_2 system. (Scheme 1.3.26) However, one of the major drawbacks of this strategy is the *E*/*Z* selectivity of the muconate products, which only range from 56:44 to 66:34. Therefore, a highly *E*/*Z* stereoselective cross coupling becomes essential in order to be applied in practical application. This challenging work was resolved by Hu *et al.* after their report on the synthesis of (*Z*,*E*)-muconates from two electron-deficient acrylates. This ruthenium-catalyzed direct cross coupling reaction provided muconates with (*Z*,*E*)/(*E*,*E*) selectivity up to 98:2.[53] Another (*Z*,*E*)-diene-preferred cross coupling reaction was also reported by Hu *et al.*, which features the synthesis of enol phosphates. This cross coupling reaction was catalyzed by ruthenium catalyst and provided (*Z*,*E*)/(*Z*,*Z*) selectivity up to 92:8.[54] (Scheme 1.3.32)

[52] Zhang, X.; Wang, M.; Zhang, M.-X.; Xu, Y.-H.; Loh, T.-P. *Org. Lett.* **2013**, *15*, 5531-5533.
[53] Hu, X.-H.; Zhang, J.; Yang, X.-F.; Xu, Y.-H.; Loh, T.-P. *J. Am. Chem. Soc.* **2015**, *137*, 3169-3172.
[54] Hu, X.-H.; Yang, X.-F.; Loh, T.-P. *Angew. Chem. Int. Ed.* **2015**, *54*, 15535-15539.

Hu *et al.* (*J. Am. Chem. Soc.* 2015, *137*, 3169-3172)

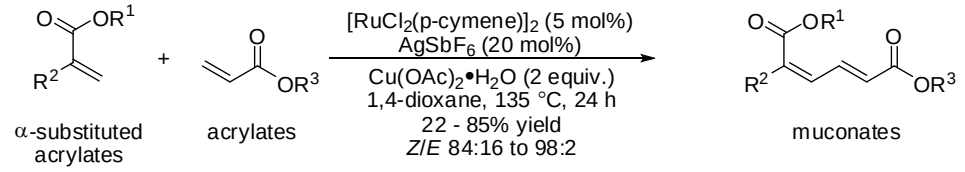

Hu *et al.* (*Angew. Chem. Int. Ed.* 2015, *54*, 15535-15539)

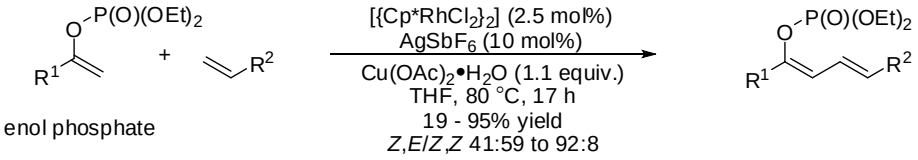

Scheme 1.3.32 Ru- and Rh-catalyzed direct cross coupling in synthesis of muconates and enol phosphates.

The proposed mechanism of typical direct cross coupling reaction is shown in Scheme 1.3.33.[49] In the synthesis of dienoates from simple alkene and acrylate, which catalyzed by palladium catalyst and participation of monoprotected amino acid as ligand, the catalytic cycle started from the formation of Pd(II)-ligand complex **A**. The complex **A** then activates alkenyl C-H bond of simple alkenes, leads to the formation of favourable vinyl-Pd intermediate **B** (intermediate **B'** is less favourable due to steric effect). Carbopalladation of intermediate **B** with acrylate results in intermediate **C**, which subsequently undergoes *β*-H elimination to release final product, dienoates, preferable in (*E*,*E*)-configuration. The Pd(II)-ligand complex **D** is deprotonated by base, followed by disassociation of the complex. The Pd(0) species is then oxidized into Pd(II) by Ag_2CO_3.

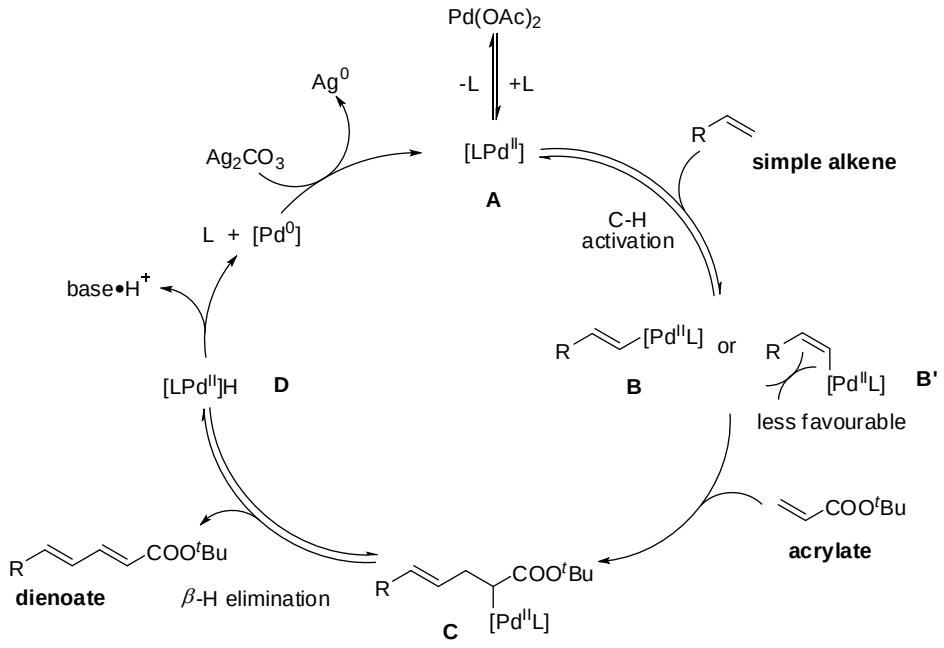

Scheme 1.3.33 Proposed mechanism of the dehydrogenative cross-coupling reaction.

As introduced above, our methodologies to construct conjugated diene structures are mostly catalyzed by palladium, except in the case of dienamide, muconate and enol phosphate. Besides, the methodologies developed above exhibit high stereoselectivity, mostly provide (*E*,*E*)-diene, in large scope of substrate. Directing groups, such as amide, ester and enol phosphate, are required in obtaining (*Z*)-selectivity diene product. Since direct cross coupling is high atom-economy and catalytically driven, it will be employed and further studied in the synthetic application in synthesis of dactylolide.

CHAPTER TWO

ZAMPANOLIDE

AND

DACTYLOLIDE

In line with our special interest to the application of environmental-friendly reactions in total synthesis, dactylolide, a marine natural product which consists of conjugated diene and tetrahydropyran motifs, was chosen as the target molecule to demonstrate the feasibility of $In(OTf)_3$-catalyzed intramolecular (2,5)-oxonium-ene reaction and direct cross coupling reaction.

This chapter will provide an overview of dactylolide and its analogue, zampanolide, from their discovery and biological activity, to reported total synthesis and formal synthesis of these two compounds.[55]

2.1 Discovery and structural elucidation of (–)-zampanolide (1) and (+)-dactylolide (2)

(−)-Zampanolide (**1**; Figure 2.1), an unsaturated 20-membered macrolide with an *N*-acyl hemiaminal side-chain, was first isolated by Tanaka and Higa in 1996, from the marine sponge *Fasciospongia rimosa* at Okinawa, Japan.[56] They obtained (−)-zampanolide at a mass of 3.9 mg (or 8.1 ppm) from repeated chromatography on extracts of 480 g sponge sample. Later in 2009, Northcote and Miller and co-workers isolated (−)-zampanolide from Tongan marine sponge *Cacospongia mycofijiensis*.[57] The latter isolation was obtained in a lower concentration of 5.0 ppm.

In 2001, another macrolide, (+)-dactylolide (**2**; Figure 2.1), was discovered in the Vanuatu sponge *Dactylospongia sp.* by Riccio and co-workers.[58] It was isolated at a concentration of 15.6 ppm from 353 g of sponge sample. This marine natural product has strikingly similar unsaturated 20-membered macrolide core but with opposite configurations and lack of the *N*-acyl hemiaminal side-chain compared with (−)-zampanolide (**1**).

[55] During the course of this research, a comprehensive review on zampanolide and dactylolide was published by Chen and Kingston in 2014. Ref: Chen, Q.-H.; Kingston, D. G. I. *Nat. Prod. Rep.* **2014**, *31*, 1202-1226.
[56] Tanaka, J.; Higa, T., *Tetrahedron Lett.* **1996,** *37*, 5535-5538.
[57] Field, J. J.; Singh, A. J.; Kanakkanthara, A.; Halafihi, T. I.; Northcote, P. T.; Miller, J. H., *J. Med. Chem.* **2009,** *52*, 7328-7332.
[58] Cutigano, A.; Bruno, I.; Bifulco, G.; Casapullo, A.; Debitus, C. C.; Gomez-Paloma, L.; Riccio, R., *Eur. J. Org. Chem.* **2001**, 775-778.

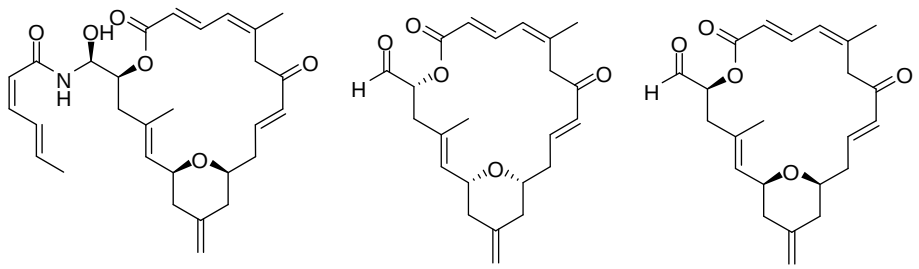

(−)-zampanolide (**1**) (+)-dactylolide (**2**) (−)-dactylolide (*ent*-**2**)

***Figure 2.1*:** (−)-zampanolide (**1**), (+)-dactylolide (**2**) and (−)-dactylolide (*ent*-**2**).

Initially, only the structure and relative stereochemistry of chiral centers of (−)-zampanolide were deduced by Tanaka and Higa alongside with their discovery. Based on 2D NMR observation, zampanolide consists of a 20-membered macrolactone core and an *N*-acyl hemiaminal side chain. The macrolactone core features interesting structures, including northern C1 – C5 (*E*,*Z*)-dienoate and southern 2,6-*syn*-4-exomethylene tetrahydropyran. Besides that, the core structure also consists of 3 chiral centers (C11, C15, C19) and a total of 5 olefins. On the other hand, the *N*-acyl hemiaminal side chain also has one chiral center (C20) and (*Z*,*E*)-dienamide. Stereochemistry of C11, C15 and C19 were deduced as 11*R*, 15*R*, 19*R*, while stereochemistry of C20 could not be confirmed in Tanaka and Higa's isolation. Later in 2001, the absolute stereochemistry of these chiral centers in (−)-zampanolide were corrected to 11*S*, 15*S*, 19*S*, 20*S*, after total synthesis of (+)-zampanolide (*ent*-**1**), the unnatural enantiomer of **1**, was completed by Smith and co-workers.[59]

In the isolation work done by Riccio and co-workers, relative stereochemistry of C11 and C14 of (+)-Dactylolide (**2**) was deduced as *syn*, while chirality of C19 was not determined. This uncertainty was then also resolved after Smith and co-workers' total synthesis of (+)-Dactylolide (**2**).

The striking similarities of zampanolide and dactylolide imply that (i) dactylolide might be the potential biogenic precursor of zampanolide or (ii) dactylolide might be an artefact produced from the decomposition of zampanolide during extraction of sponge sample. The second hypothesis was further questioned after Smith and co-workers' synthesis of

[59] (a) Smith, A. B., III; Safonov, I. G.; Corbett, R. M., *J. Am. Chem. Soc.* **2001,** *123*, 12426-12427; (b) Smith, A. B., III; Safonov, I. G., *Org. Lett.* **2002,** *4*, 635-637; (c) Smith, A. B., III; Safonov, I. G.; Corbett, R. M., *J. Am. Chem. Soc.* **2002,** *124*, 11102-11113.

(+)-dactylolide (**2**) from (+)-zampanolide (*ent*-**1**) *via* thermolysis. In order to verify the hypothesis, Uenishi and co-workers exposed (–)-zampanolide (**1**), the natural macrolide and the sponge to the extraction conditions reported by Riccio *et al.*, but no trace of (–)-dactylolide (*ent*-**2**) was detected.[60] As such, it is concluded that dactylolide is a natural product instead of artifact from decomposition of zampanolide. However, the first hypothesis remained unproven up to date.

[60] Uenishi, J.; Iwamoto, T.; Tanaka, J., *Org. Lett.* **2009,** *11*, 3262-3265.

2.2 Biological activity of (–)-zampanolide (1) and (+)-dactylolide (2)

The marine sponges that (−)-zampanolide (**1**) and (+)-dactylolide (**2**) are originated from, do not only provide these two macrolides, but also consists of different types of bioactive natural products, such as latrunculin A and laulimalide.[56-58] Therefore, as an effort to explore potential bioactive cytotoxic natural products, (−)-zampanolide (**1**) and (+)-dactylolide (**2**) were also subjected into various cancer cell lines since its discovery. (Table 2.1)

Tanaka and Higa revealed that (−)-zampanolide (**1**) exhibits potent cytotoxicity against P388 (leukaemia), A549 (lung cancer), HT29 (colon cancer) and SK-Mel-28 (melanoma cancer) cell lines, ranged from 2 nM to 10 nM, upon the discovery of **1**.[56] Northcote and Miller,[57] Uenishi,[60] Ghosh,[61] Altmann[62] later reported that (−)-zampanolide also exhibits cytotoxicity against various cell lines, from ovarian and prostate cancer to different type of leukaemia. The cytotoxicities obtained are mostly in low nanomolar range (< 10 nM). Among these biological activities, the most attractive result is (−)-zampanolide's bioactivity against A2780D[57] and NCI/ADR-RES[61] cell lines, which are multi-drug resistant cancer cells. These cancer cells express resistance towards paclitaxel (or Taxol) by overexpressing P-glycoprotein, an important cellular drug efflux pump, which ultimately lead to clinical loss of sensitivity.[63] Therefore, (−)-zampanolide becomes a potential lead in drug discovery. There is no biological test on artificial, unnatural (+)-zampanolide (*ent*-**1**) up to date.

(+)-Dactylolide (**2**), the natural occurring macrolide, exhibits cytotoxicity at micromolar range in L1210 (lymphatic leukaemia) and SK-OV-3 (ovarian cancer) cell lines.[58] Due to the synthetic efforts made on (–)-dactylolide (*ent*-**2**) by Altmann[62] and Jennings,[64] there is more bioactivity data obtained from the unnatural (–)-dactylolide. As shown in Table 2.1, (–)-dactylolide exhibits cytotoxicity in various cancer cell lines, including A549 (lung cancer),[62,64] HT29 (colon cancer),[64] SK-Mel-28 (melanoma cancer),[64] HL-60 (leukemia),[64] MCF-7 (breast cancer),[62,64] HCT116 (colon cancer)[62,64] and PC3 (prostate cancer)[62b] that have also been tested for (−)-zampanolide. However, the cytotoxicity

[61] Ghosh, A. K.; Cheng, X.; Bai, R.; Hamel, E., *Eur. J. Org. Chem.* **2012**, 4130-4139.
[62] (a) Zurwerra, D.; Gertsch, J.; Altmann, K.-H., *Org. Lett.* **2010,** *12*, 2302-2305; (b) Zurwerra, D.; Glaus, F.; Betschart, L.; Schuster, J.; Gertsch, J.; Ganci, W.; Altmann, K.-H., *Chem. Eur. J.* **2012,** *18*, 16868-16883.
[63] Rohena, C. C.; Mooberry, S. L. *Nat. Prod. Rep.* **2014**, *31*, 335-355.
[64] Ding, F.; Jennings, M. P., *J. Org. Chem.* **2008,** *73*, 5965-5976.

exhibited by (–)-dactylolide is about 30-fold to 1000-fold less potent than (**–**)-zampanolide. This suggests that the *N*-acyl hemiaminal side chain of (**–**)-zampanolide contributes to the cytotoxicity difference.

The structure-activity relationship of dactylolide and zampanolide was further studied by Altmann group.[62b] Analogues of the macrolides, which are shown in Table 2.2, were synthesized and subjected into four different cancer cell lines to understand the importance of sub-structure of macrolide in the antiproliferative activity. Epimer of **1** was found to be about one order of magnitude less potent than natural macrolide **1**. Altering the substituents at C20 of (–)-dactylolide (*ent*-**2**) resulted in highly less potent macrolide (ranged from 3 to 30-fold) as compared with *ent*-**2**, except **3** (hydroxyl group on C20) showed about one-fold more potent than *ent*-**2**. However, macrolide **3** is still less effective than (–)-zampanolide (**1**).

Macrolide **7** and **8**, which were synthesized by omitting the exomethylene group, showed similar cytotoxicity as macrolide **3**. This suggests that exomethylene group and aldehyde group of (–)-dactylolide (*ent*-**2**) are not role-playing groups in the relatively low potency of (–)-dactylolide. Besides, Altmann's group also synthesized analogue **9**, **10** and *epi*-**11**, which correspond to de-tetrahydropyran version of **3**, *ent*-**2**, *epi*-**1**, to investigate the effect of tetrahydropyran motif in biological activity. The de-tetrahydrofuran analogues **9** and **10** show one order of magnitude less potent when compared with tetrahydropyran-containing macrolides **3** and *ent*-**2**. In the case of *epi*-**11**, due to the isomeric mixture used in the biological test, the actual IC_{50} value might be closer to that of *epi*-**1**. These data implies that the chiral tetrahydropyran ring might play certain role in the structure-activity relationship.

Cell lines	Cancer type	(–)-Zampanolide (1)	(+)-Dactylolide (2)	(–)-Dactylolide (*ent*-2)
P388	Leukaemia (mice)	2-10 nM[56]		
A549	Lung	2-10 nM[56] 3.2 ± 0.4 nM[62b]		1.72 μg/mL[64] 301.5 nM[62a] 301 ± 4.3 nM[62b]
HT29	Colon	2-10 nM[56]		0.101 μg/mL[64]
SK-Mel-28	Melanoma	2-10 nM[56]		2.0 μg/mL[64]
SKM-1	Leukaemia	1.1 nM[60]		
U937	Leukaemia	2.9 nM[60]		
L1210	Lymphatic leukaemia (mice)		63% at 8.3μM[58]	
SK-OV-3	Ovarian		40% at 8.3μM[58]	1.8 μg/mL[64]
HL-60	Leukemia	4.3 ± 1.1 nM[57]		243 nM[64[a]]
K-562	Leukemia			63.8 nM[64[a]]
HCC- 2998	Colon			200 nM[64[a]]
SF-539	Central Nervous System			258 nM[64[a]]
MCF-7	Breast	4.0 nM[61] 6.5 ± 0.7 nM[62b]		198 nM[64[a]] 247.6 nM[62a] 247 ± 2.6 nM[62b]
HCT116	Colon	7.2 ± 0.8 nM[62b]		346 nM[64] 210.4 nM[62a] 210 ± 4.7 nM[62b]
OVCAR 8	Ovarian	20 nM[61]		
NCI/ADR-RES	Ovarian	25 nM[61]		
1A9	Ovarian	14.3 ± 2.4 nM[57]		
A2780D	Ovarian	7.5 ± 0.6 nM[57]		
CA46 Burkitt	Lymphoma	100 nM[61]		
PC3	Prostate	2.9 ± 0.4 nM[62b]		751 ± 69 nM[62b]

Table 2.1 IC_{50} (or GI_{50} for superscript [a]) of **1**, **2** and *ent*-**2** on various cancer cell lines.

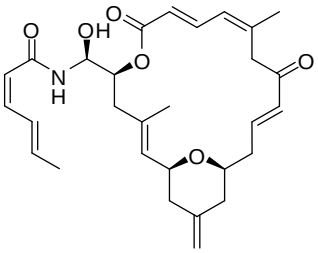

(–)-zampanolide (**1**)

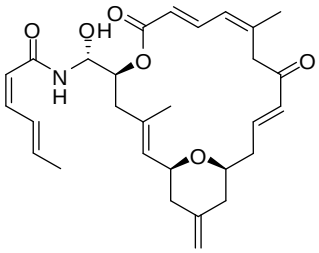

epi-zampanolide (*epi*-**1**)

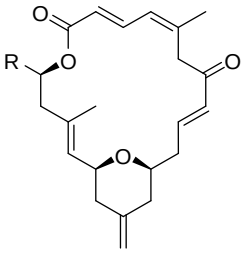

ent-**2**: R = CHO ((–)-dactylolide)
3: R = CH_2OH
4: R = CH_2OMe
5: R = COOH
6: R = $CONH(CH_2)_5CH_3$

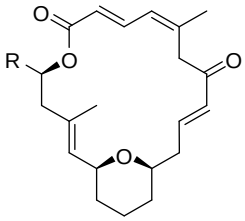

7: R = CH_2OH
8: R = CHO

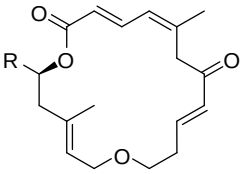

9: R = CH_2OH
10: R = CHO

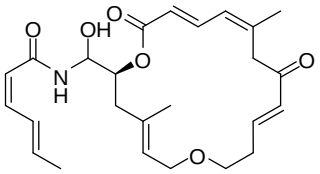

epi-**11** (ca. 1.6:1)

Compound	A549 (lung)	MCF-7 (breast)	HCT116 (colon)	PC-3 (prostate)
1	3.2 ± 0.4	6.5 ± 0.7	7.2 ± 0.8	2.9 ± 0.4
epi-**1**	53 ± 5.9	42 ± 9.3	88 ± 5.1	50 ± 11.7
ent-**2**	301 ± 4.3	247 ± 2.6	210 ± 4.7	751 ± 69
3	127 ± 2.9	106 ± 3.6	155 ± 2.1	320 ± 26
4	1072 ± 103	1489 ± 83	1603 ± 122	1274 ± 117
5	9732 ± 260	7624 ± 303	12733 ± 379	9338 ± 242
6	973 ± 90	1138 ± 72	1204 ± 63	829 ± 27
7	189 ± 19.3	114 ± 10.2	74 ± 1.5	104 ± 4.1
8	149 ± 12.8	68 ± 5.6	249 ± 28	n.d
9	2378 ± 70	3891 ± 102	1846 ± 92	3051 ± 178
10	3921 ± 216	2894 ± 144	2653 ± 68	4021 ± 102
epi-**11**	n.d	165 ± 13	309 ± 47	218 ± 7

Table 2.2 IC_{50} (in nM) of zampanolide, dactylolide and their analogues on various cancer cell lines, conducted by Altmann's group.[62b] n.d. = not determined.

The main reason of the universal antiproliferative activity observed from various cancer cell lines relies on zampanolide and dactylolide's microtubulin stabilizing activity. This biological mechanism of action blocks cell division in the G2/M phase of the cell cycle by enhancing the microtubule assembly into polymerized tubulin.[57,65] Although taxane-based anticancer drugs taxol, docetaxel and cabazitaxel or the epothilone derivative ixabepilone also inhibit cancer cell growth by polymerizing tubulin,[66] the mechanism of action induced by zampanolide and dactylolide is different from taxane-based anticancer drugs. Instead of non-covalent binding of taxol to β-tubulin, zampanolide binds covalently at His^{229} and Asn^{228} (to a lesser extent) residues on tubulin.[67] This binding action, first conducted by Diaz and co-workers, was further solidified by Steinmetz and co-workers after tubulin-zampanolide crystal complex was reported.[68] The complex revealed that (a) C9 at the eastern enone system of zampanolide covalently binds to the NE2 atoms of His^{229} of *β*-tubulin; (b) hydroxyl group at C20 and carbonyl group at C1' of zampanolide are hydrogen bonded to Thr^{276}; (c) helical conformation of the M-loop of tubulin, which favour in further polymerization, is induced by the *N*-acyl hemiaminal side chain.[68] The above observation is consistent with the bioactivity shown in Table 2.1 and 2.2 and confirms that *N*-acyl hemiaminal side chain plays critical role in bioactivity and altering chirality of C20 results in lesser binding affinity.[55] However, the effect of tetrahydropyran ring still remains questionable. It shows minimal effect in the tubulin-zampanolide complex, which is roughly consistent with the bioactivity observed for *epi*-**1** and *epi*-**11**, but the complex does not prove the huge difference of bioactivity observed for macrolide **9** and **10** with respect to **3** and *ent*-**2**.

[65] Qi, Y.; Ma, S., *ChemMedChem* **2011,** *6*, 399-409.
[66] Altmann, K.-H.; Gertsch, J., *Nat. Prod. Rep.* **2007,** *24*, 327-357.
[67] Field, J. J.; Pera, B.; Calvo, E.; Canales, A.; Zurwerra, D.; Trigili, C.; Rodriguez-Salarichs, J.; Matesanz, R.; Kanakkanthara, A.; Wakefield, S. J.; Singh, A. J.; Jimenez-Barbero, J.; Northcote, P.; Miller, J. H.; Lopez, J. A.; Hamel, E.; Barasoain, I.; Altmann, K.-H.; Díaz, J. F., *Chem. Biol.* **2012,** *19*, 686-698.
[68] Prota, A. E.; Bargsten, K.; Zurwerra, D.; Field, J. J.; Díaz, J. F.; Altmann, K.-H.; Steinmetz, M. O. *Science* **2013**, *339*, 587-590.

2.3 Previous reported synthesis

Up to date, there are 13 enantioselective syntheses of **1**,[60,61,64,69,70] *ent*-**1**,[59a,59c] **2**[59b,71,72] and *ent*-**2**[62a,64,73,74,75,76] have been reported by 11 research groups, together with a total of 5 formal syntheses[23,77] towards **1** and **2** and their enantiomers. This section will provide an overview of these syntheses, including the key reactions, number of steps required, overall yield and its impact from the viewpoint of green chemistry at the final summary.

2.3.1 Smith's synthesis of (+)-zampanolide (*ent*-1) and (+)-dactylolide (2)[59]

The first total synthesis of zampanolide and dactylolide was achieved by Smith's group in 2002. The absolute configuration of two natural products was also confirmed right after the synthetic work above. Retrosynthesis of Smith's synthesis of (+)-zampanolide (*ent*-**1**), which is outlined in Scheme 2.3.1, shows that the macrolide was dissected into 4 major fragments, namely Fragment **A** to **D**. Fragment **D**, the component to form *N*-acyl hemiaminal side chain, was planned to be installed to the macrolide core *via* Curtius rearrangement. The macrolide core was closed by Horner-Emmons macrolactonization after Fragment **ABC** was synthesized. The featured tetrahydropyran ring in Fragment **B** was synthesized *via* the Petasis-Ferrier rearrangement, which was developed by Smith and also employed in their synthesis of enigmazole A (Section 1.3.2.1.2). Kociensky-Julia olefination was employed in joining Fragment **A** and **B** and furnished the olefin C8 – C9. Nucleophilic ring-opening of epoxide **C** formed carbon-carbon bond between C17 and C18.

---

[69] Hoye, T. R.; Hu, M., *J. Am. Chem. Soc.* **2003,** *125*, 9576-9577.
[70] Ghosh, A. K.; Cheng, X., *Org. Lett.* **2011,** *13*, 4108-4111.
[71] (a) Aubele, D. L.; Wan, S.; Floreancig, P. E., *Angew. Chem. Int. Ed.* **2005,** *44*, 3485-3488; (b) Aubele, D. L.; Wan, S.; Floreancig, P. E., *Angew. Chem.* **2005,** *117*, 3551-3554.
[72] Sanchez, C. C.; Keck, G. E., *Org. Lett.* **2005,** *7*, 3053-3056.
[73] Ding, F.; Jennings, M. P., *Org. Lett.* **2005,** *7*, 2321-2324.
[74] Louis, I.; Hungerford, N. L.; Humphries, E. J.; McLeod, M. D., *Org. Lett.* **2006,** *8*, 1117-1120.
[75] (a) Yun, S. Y.; Hansen, E. C.; Volchkov, I.; Cho, E. J.; Lo, W. Y.; Lee, D., *Angew. Chem. Int. Ed.* **2010,** *49*, 4261-4263; (b) Lee, D.; Volchkov, I. *Strategies Tactics Org. Synth.* **2012**, *8*, 171-197.
[76] Lee, K.; Kim, H.; Hong, J., *Angew. Chem. Int. Ed.* **2012,** *51*, 5735-5738.
[77] (a) Troast, D. M.; Yuan, J.; J. A. Porco, J., *Adv. Synth. Catal.* **2008,** *350*, 1701-1711; (b) Troast, D. M.; J. A. Porco, J., *Org. Lett.* **2002,** *4*, 991-994; (c) Reddy, C. R.; Srikanth, B., *Synlett* **2010,** *10*, 1536-1538; (d) Wilson, M. R.; Taylor, R. E., *Org. Lett.* **2012,** *14*, 3408-3411; (e) Wang, J.; Ting, S. Z. Y.; Harvey, J. E. Beilstein *J. Org. Chem.* **2015**, *11*, 1815-1822.

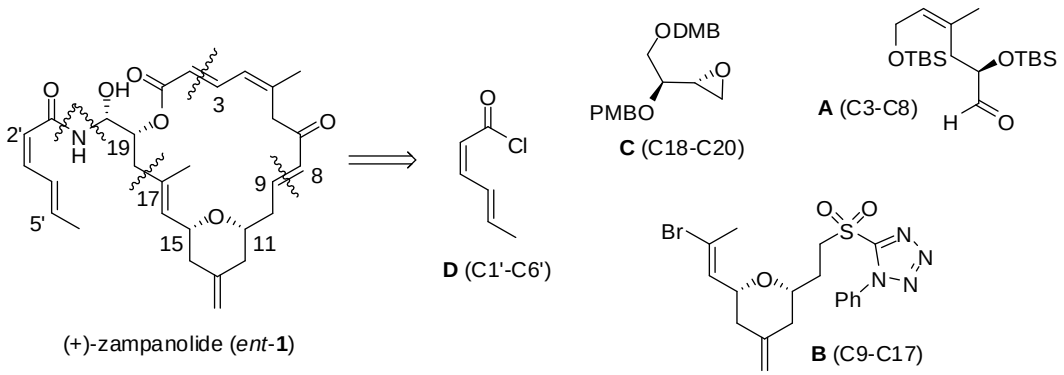

Scheme 2.3.1 Retrosynthesis of Smith's synthesis of (+)-zampanolide (*ent*-**1**).

The detailed synthetic flow is shown in Scheme 2.3.2. Synthesis of Fragment **A** was started from (–)-epichlorohydrin. Smith and co-workers first employed Ogasawara's procedure[78] to synthesize alkynoate, followed by Michael addition to yield alkenoate, then furnished Fragment **A** after a sequential of 4 steps transformation, i.e. reduction, protection, deprotection and oxidation. The highlight of Smith's synthesis is their Petasis-Ferrier rearrangement in constructing tetrahydropyran of Fragment **B**. Started from modified 1,3-propanediol, a sequence of Brown asymmetric allylation, silylation and ozonolysis, yielded pentanal, which was then converted to *β*–hydroxy ester in another 3-step reaction. The *β*–hydroxy ester was condensed with bromobutenal and cyclized into dioxanone, then Petasis olefination yielded enol acetal and followed by rearrangement under Me_2AlCl and methylene ylide to obtain 2,6-*syn*-4-exomethylene tetrahydropyran. Deprotection, incorporation of thiotetrazole and oxidation furnished the target sulfone **B**. (Scheme 2.3.2a)

On the other hand, epoxide **C** was synthesized from (–)-dimethyl tartrate. The first four steps were established protocol reported by Somfai and Yonemitsu,[79] while the subsequent steps converted diethyl ketal towards target epoxide **C**. With the availability of designated Fragment **A**, **B** and **C**, the convergent synthesis started from union of aldehyde **A** and sulfone **B** *via* Kociensky-Julia olefination, followed by nucleophilic ring opening of epoxide **C** *via* mixed cyano-Gilman cuprate formed from Fragment **AB**, then Mitsunobu reaction to yield phosphonate. The macrolide core was finally closed *via* Horner-Emmons macrocyclization at C2 – C3. The last part of the synthesis was the

[78] Oizumi, M.; Takahashi, M.; Ogasawara, K. *Synlett* **1997**, 1111-1113.
[79] (a) Somfai, P.; Olsson, R. *Tetrahedron* **1993**, *49*, 6645-6650; (b) Horita, K.; Sakurai, Y.; Hachiya, S.; Nagasawa, M.; Yonemitsu, O. *Chem. Pharm. Bull.* **1994**, 683-685.

installation of *N*-acyl hemiaminal side chain *via* Curtius rearrangement and acylation with Fragment **D**. (Scheme 2.3.2b)

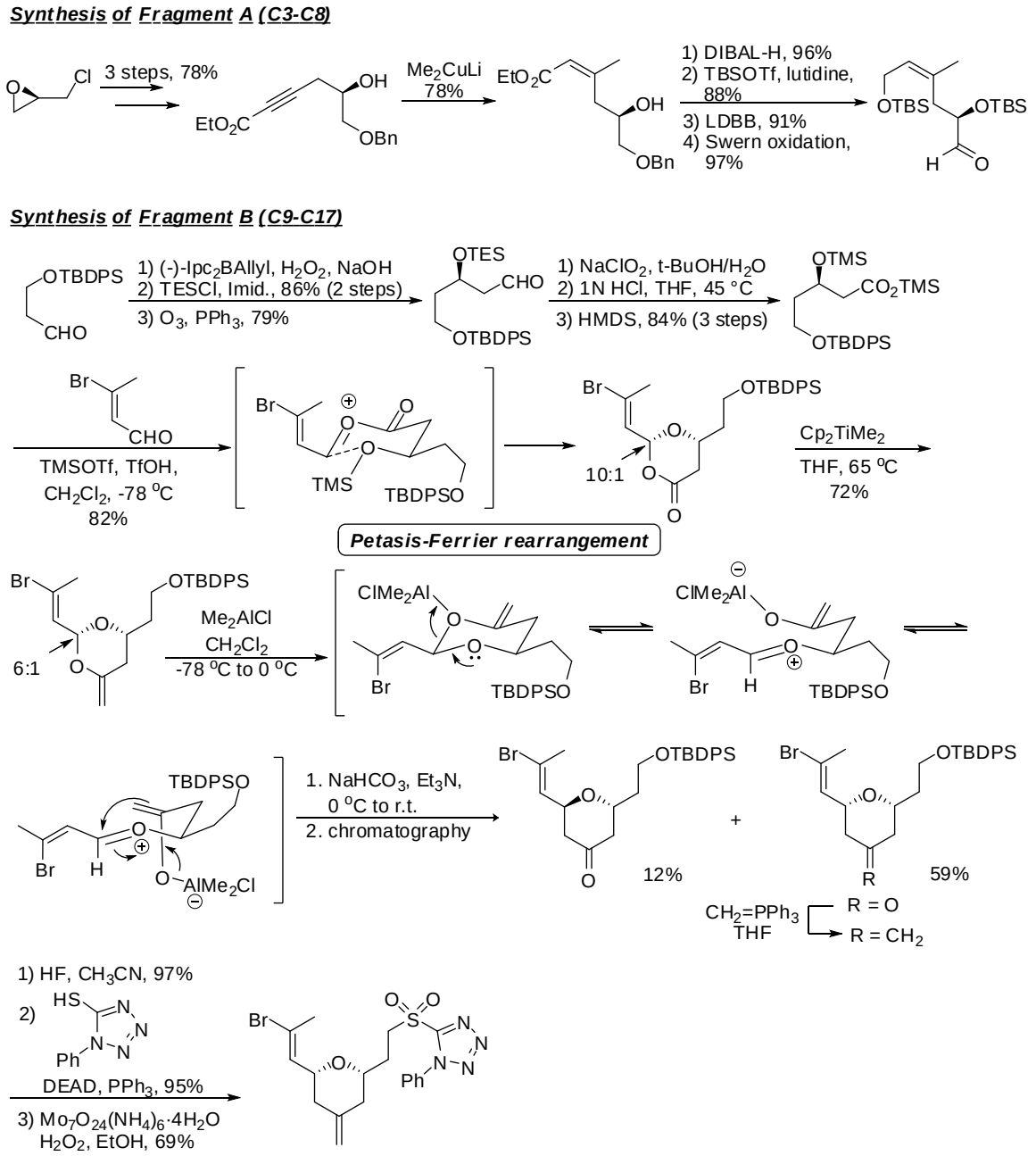

Scheme 2.3.2a Smith's synthesis of (+)-zampanolide (*ent*-**1**).

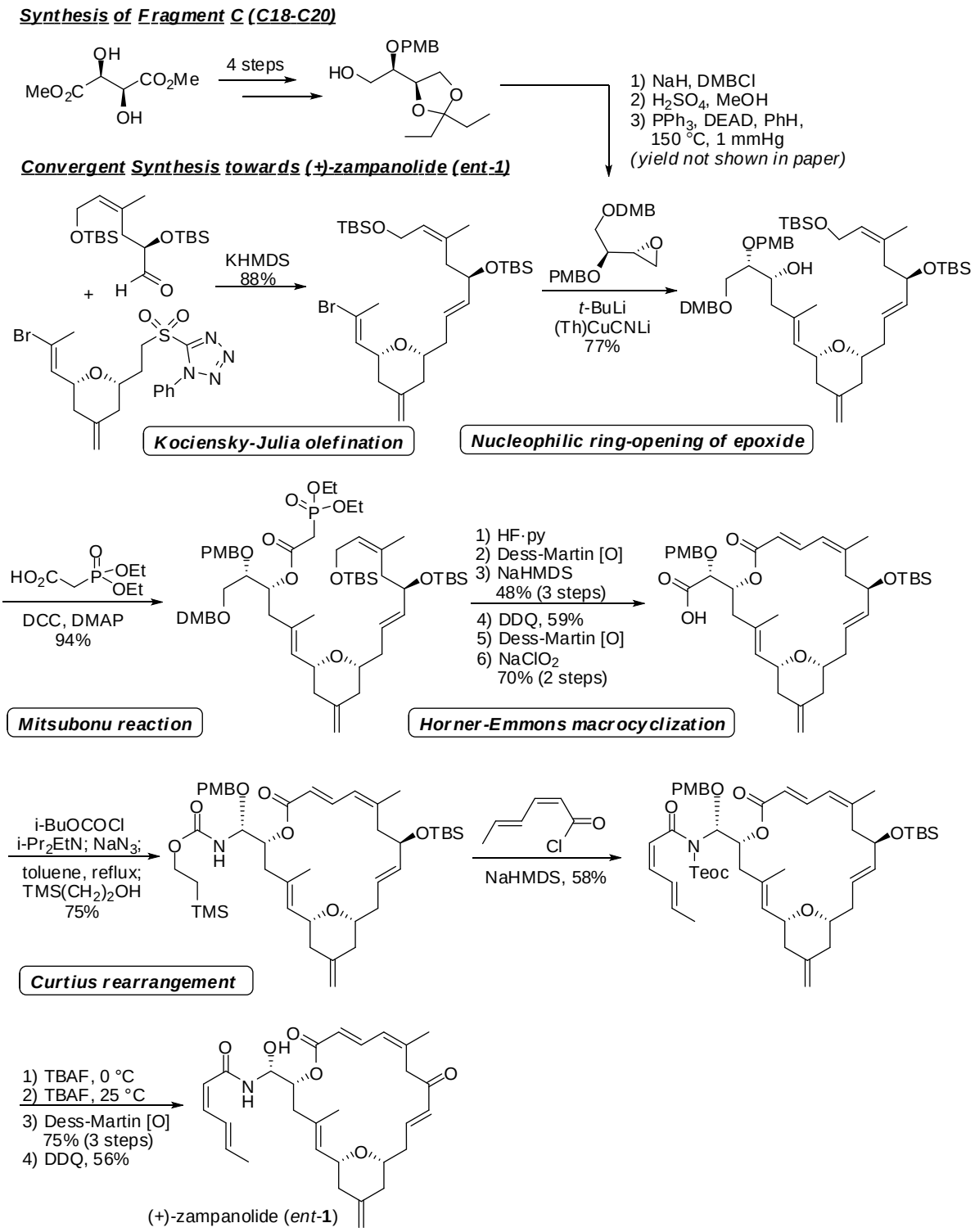

Scheme 2.3.2b Smith's synthesis of (+)-zampanolide (*ent*-**1**). (continued)

Since (+)-zampanolide (*ent*-**1**) shares same macrolide core as (+)-dactylolide (**2**), Smith and co-workers also synthesized the latter from the union of Fragment **AB** in the synthesis of (+)-zampanolide. As outlined in Scheme 2.3.3, instead of reacting with epoxide **C**, a new epoxide, derived from (*S*)-(–)-glycidol in single protection step, was employed in the synthesis of Fragment C3 – C20. Next, followed the same strategy employed in the synthesis of (+)-zampanolide, phosphonate was formed *via* Mitsunobu reaction and the macrocycle was closed *via* Horner-Wadsworth macrocyclization. Without extra installation of *N*-acyl hemiaminal side chain, the silyl (TBS) and benzyl (DMB) protecting group were removed and further oxidized into carbonyl to furnish (+)-dactylolide (**2**).

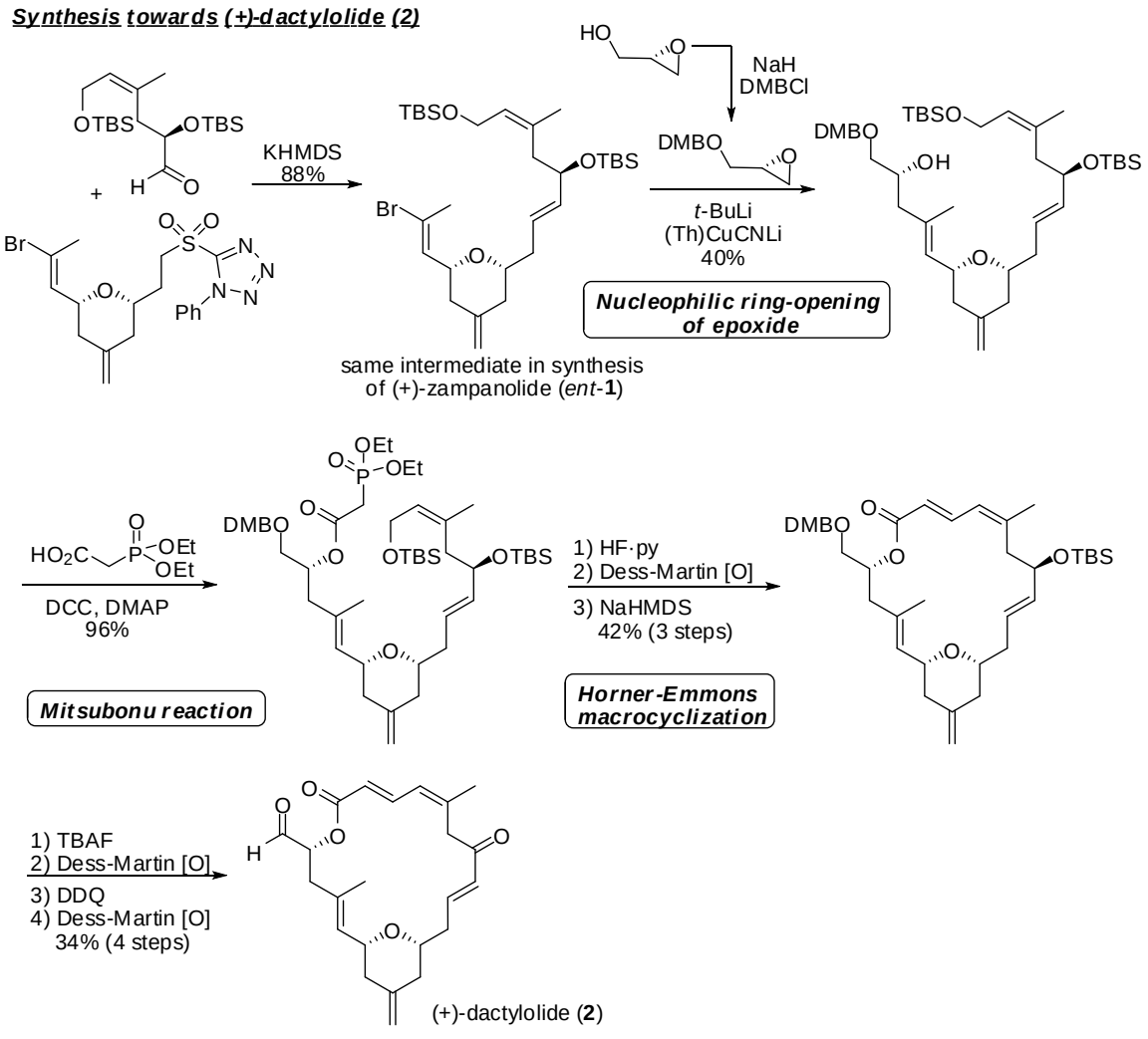

Scheme 2.3.3 Smith's synthesis of (+)-dactylolide (**2**).

2.3.2 Hoye's synthesis of (–)-zampanolide (1) and (–)-dactylolide (*ent*-2)[69]

Hoye and co-workers reported two different pathways to synthesize (–)-dactylolide (*ent*-**2**), and a single step installation of *N*-acyl hemiaminal side chain on *ent*-**2** to furnish (–)-zampanolide (**1**). The strategies applied by the authors are (a) macrolactonization via Ti(IV)-mediated epoxy-acid coupling (path a) and (b) ring-closing metathesis (RCM) macrocyclization (path b). Retrosyntheses of these two strategies are shown in Scheme 2.3.4. Disconnection at C1 – O20 and C7 – C8 of macrolide core resulted in aldehyde **A** and vinyl iodide **BC** (path a); while disconnection at C1 – O20 and C8 – C9 of macrolide core resulted alkene **A'** and alkene **BC'** (path b). The tetrahydropyran ring of vinyl iodide **BC** and alkene **BC'** was planned to be synthesized from conjugated aldehyde **B** and allyl silane **C** *via* intramolecular Sakurai cyclization.

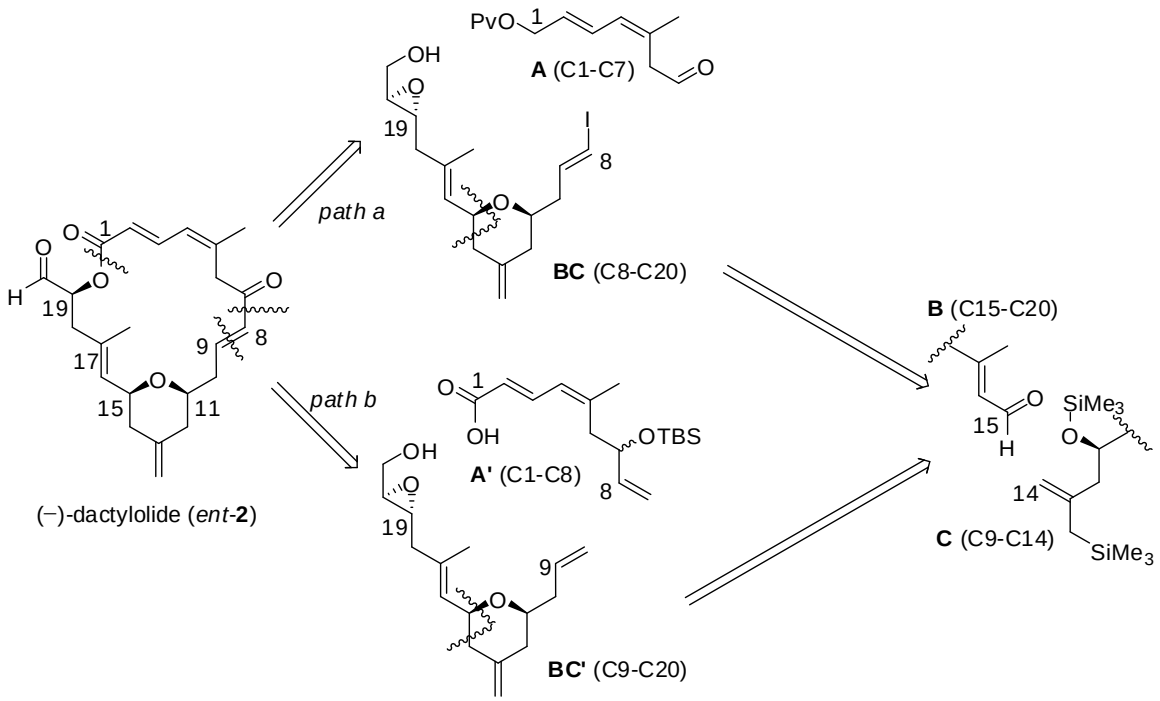

Scheme 2.3.4 Retrosynthesis of Hoye's synthesis of (–)-dactylolide (*ent*-**2**).

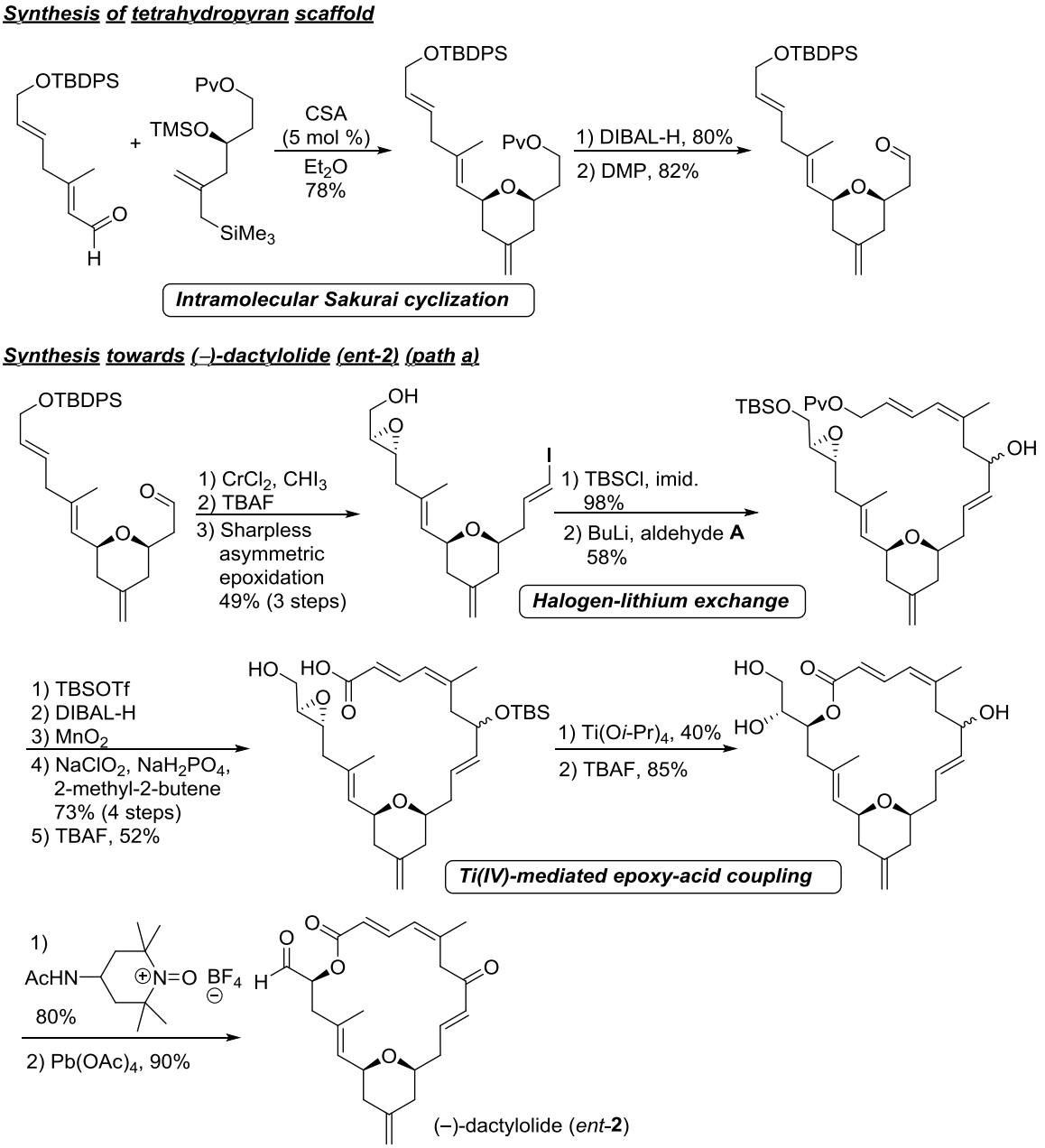

Scheme 2.3.5 Syntheses of common tetrahydropyran scaffold and (–)-dactylolide (*ent*-**2**) *via* Ti(IV)-mediated epoxy-acid coupling macrolactonization strategy (path a).

Without demonstrating the syntheses of conjugated aldehyde **B** and allyl silane **C**, the author reported that 2,6-*syn*-4-exomethylene tetrahydropyran scaffold was synthesized from **B** and **C** under catalytic amount of camphorsulfonic acid (CSA). The pivaloxyl group at C9 was further reduced and oxidized into aldehyde, which was later transformed into vinyl iodide **BC** and alkene **BC'** respectively. (Scheme 2.3.5)

Vinyl iodide **BC** in path a was obtained in a sequence of 3-step transformation, namely Takai olefination, deprotection and Sharpless asymmetric epoxidation, from the precursor aldehyde. Reprotection with *tert*-butyldimethylsilyl (TBS) group and halogen-lithium exchange reaction with aldehyde **A** formed carbon-carbon bond between C7 and C8. The enol was then further protected and underwent another 4 steps of transformation to yield epoxy-carboxylic acid, which was macrocyclized *via* Ti(IV)-mediated epoxy-acid coupling. The macrocycle was subjected into deprotection conditions and oxidation to furnish eastern enone motif, while cleavage of diol side chain by lead(IV) acetate yielded (–)-dactylolide (*ent*-**2**). (Scheme 2.3.5)

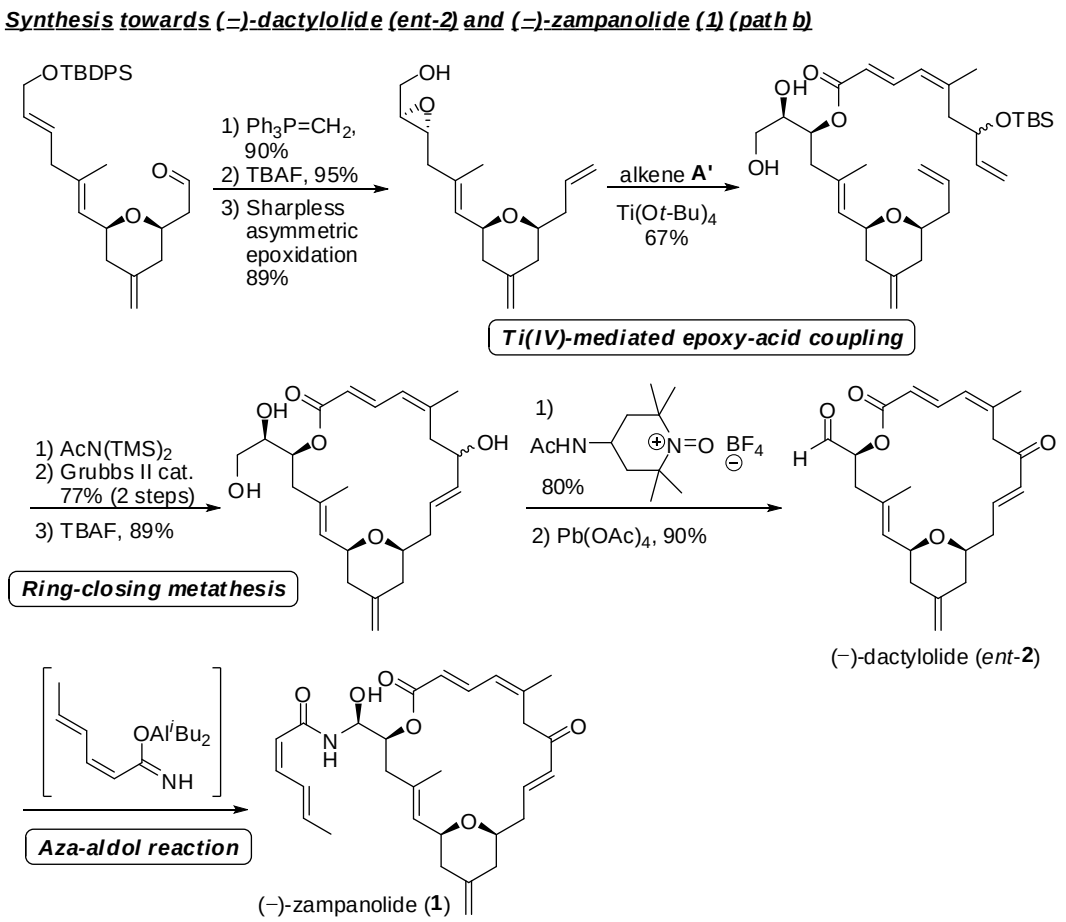

Scheme 2.3.6 Synthesis of (–)-dactylolide (*ent*-**2**) and (–)-zampanolide (**1**) *via* ring-closing metathesis (RCM) macrolactonization strategy (path b).

On the other hand, alkene **BC** in path b was synthesized in a similar sequence of 3-step transformation, namely Wittig olefination, deprotection and Sharpless asymmetric epoxidation, from the precursor aldehyde. Ti(IV)-mediated epoxy-acid coupling with alkene **A'** resulted in diene precursor, which was first protected at its C20 – C21 diol and further macrocyclized *via* ring-closing metathesis (RCM). The triol macrolide was revealed by deprotection, and further transformed into (–)-dactylolide (*ent*-**2**) under same conditions in path a. Installation of *N*-acyl hemiaminal side chain *via* aza-aldol reaction furnished the natural occurring (–)-zampanolide (**1**). (Scheme 2.3.6)

2.3.3 Floreancig's synthesis of (+)-dactylolide (2)[71]

Floreancig and co-workers aimed to synthesize dactylolide with maximum convergency and minimal carbon-carbon bond forming reactions. In their retrosynthesis of (+)-dactylolide (**2**), shown in Scheme 2.3.7, the maximum convergency was planned to be achieved by union of conjugated aldehyde **A** and diol **B** through an acetal linkage, while the latter objectives was postulated to be achieved by applying asymmetric vinylogous Mukaiyama aldol reactions,[80] which will be shown in the detailed synthetic route hereafter. The macrolide was planned to be closed *via* Horner-Wadsworth macrolactonization, which is similar strategy that employed by Smith and co-workers.[59]

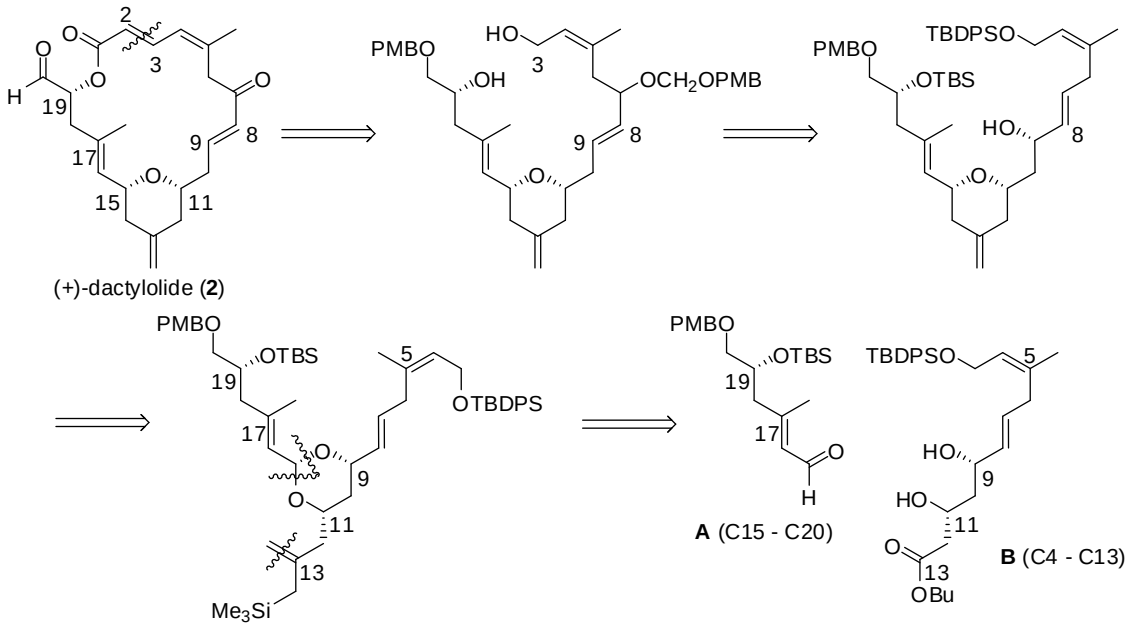

Scheme 2.3.7 Retrosynthesis of Floreancig's synthesis of (+)-dactylolide (**2**).

Conjugated aldehyde **A** was synthesized from *p*-methoxybenzyloxyacetaldehyde and silyl ketene acetal. The synthetic sequence was referred to Evans's synthesis of callipeltoside.[81] The conjugated ester was obtained *via* asymmetric vinylogous Mukaiyama aldol reaction, which employed catalytic amount of Cu pybox. Subsequent protection, reduction and oxidation furnished the target Fragment **A**. (Scheme 2.3.8a)

Synthesis of Fragment **B** was started from 2-butynol. Treatment with Red-Al, tributyltin chloride and *tert*-butyldiphenylsilyl chloride resulted in (*Z*)-vinyl stannane. Palladium-

[80] For a review, see: Casiraghi, G.; Zanardi, F.; Appendino, G.; Rassu, G. *Chem. Rev.* **2000**, *100*, 1929-1972.
[81] Evans, D. A.; Hu, E.; Burch, J. D.; Jaeschke, G. *J. Am. Chem. Soc.* **2002**, *124*, 5654-5655.

mediated coupling with allyl bromide and acetal hydrolysis yielded enal, which underwent another asymmetric Mukaiyama aldol reaction, catalyzed by Denmark's catalyst[82] and $SiCl_4$, to afford dioxinane. Thermolysis of dioxinane in butanol and subsequent *syn*-reduction of keto ester yielded diol **B**. (Scheme 2.3.8a)

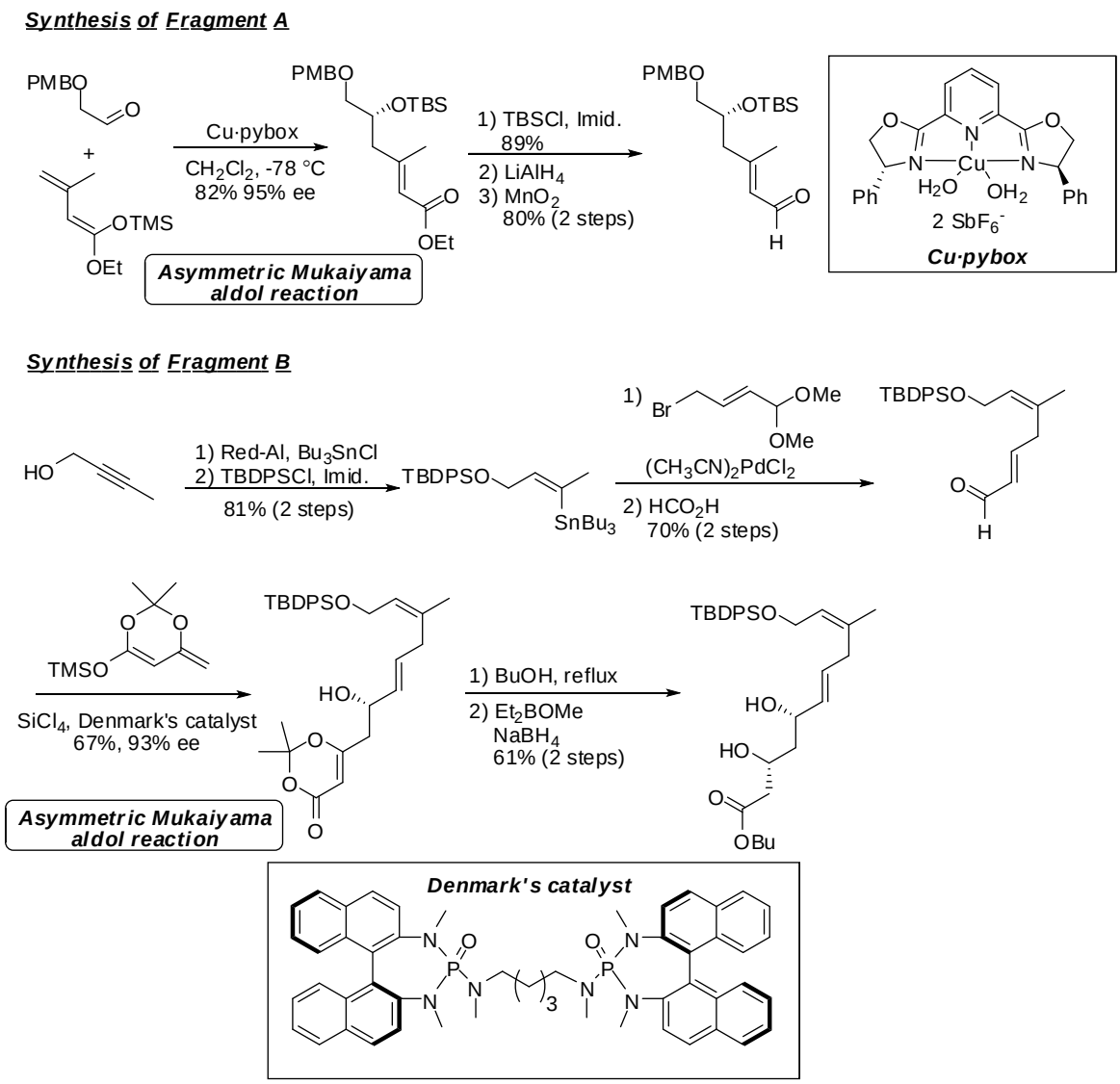

Scheme 2.3.8a Floreancig's synthesis of (+)-dactylolide (**2**).

With the availability of Fragment **A** and **B**, Fluoreancig and co-workers continued their convergent synthesis towards (+)-dactylolide (**2**). Noyori's TMSOTf-mediated protocol[83] was employed by the authors to couple aldehyde **A** with bis-TMS ether of diol **B**. The resulted key acetal was then exposed to excess $TMSCH_2MgCl$ and $CeCl_3$ to perform

[82] Denmark, S. E.; Jones, T. K. *J. Org. Chem.* **1982**, *47*, 4595-4597.
[83] Noyori, R.; Murata, S.; Suzuki, M. *Tetrahedron* **1981**, *37*, 3899-3910.

Peterson olefination at the butyl ester group. Under conditions of pyridinium triflate (act as Lewis acid) and $MgSO_4$, the allyl silane intermediate was converted into oxonium intermediate and underwent intramolecular Prins reaction to afford 2,6-*syn*-4-exomethylene tetrahydropyran unit.

Next, transposition of the C9 allylic alcohol *via* selenium variant of Mislow-Evans rearrangement[84] corrected the conformation of allylic alcohol. Further protection of allylic alcohol and desilylation yielded diol precursor, which was oxidized under $PhI(OAc)_2$ and TEMPO conditions to yield enal at C3 – C5. The secondary alcohol at C19 was then acylated with diethylphosphonoacetic acid and underwent Horner-Emmons macrolactonization, similar strategy employed in Smith's synthesis. The protection group on resulted macrolide was removed and oxidation at C20 alcohol furnished the target (+)-dactylolide (**2**). (Scheme 2.3.8b)

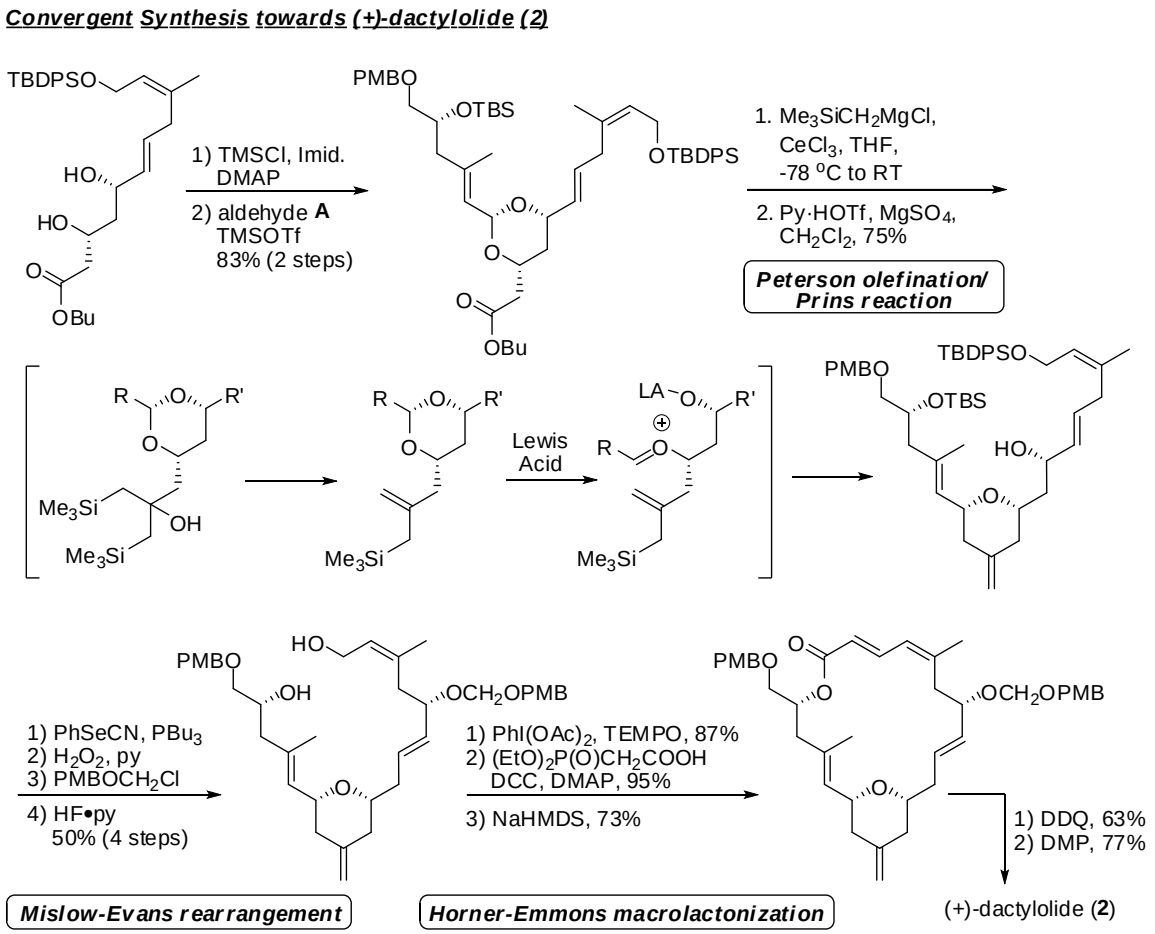

Scheme 2.3.8b Floreancig's synthesis of (+)-dactylolide (**2**). (continued)

[84] Evans, D. A.; Andrews, G. C. *Acc. Chem. Res.* **1974**, *7*, 147-155.

2.3.4 Jennings's synthesis of (–)-dactylolide (*ent*-2)[64,73]

Ding and Jennings reported a total synthesis of (–)-dactylolide (*ent*-**2**), which highlighted target oriented *β*-*C*-glycoside (tetrahydropyran motif) formation. As illustrated in Scheme 2.3.9, they postulated that the macrolide core could be synthesized from Fragment **A** (C9 – C20) and Fragment **B** (C1 – C8). The connection between O20 and C1 was achieved *via* Yamaguchi esterification,[85] while ring-closing metathesis (RCM) was applied in closing the macrolide core at C8 – C9 olefinic bond.

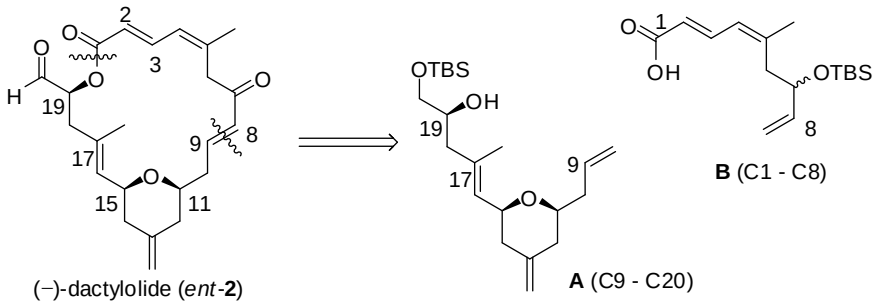

Scheme 2.3.9 Retrosynthesis of Jennings's synthesis of (–)-dactylolide (*ent*-**2**).

Synthesis of Fragment **A** was started from (*R*)-(+)-glycidol. A sequence of three-step transformation, which previously reported by Nicolaou and co-workers in their synthesis of CP-molecules,[86] yielded protected propargylic alcohol, which was further deprotonated and nucleophilic substitution with ethyl chloroformate. The *α*,*β*-acetylenic ester was then subjected into four-step sequence, included Michael addition of thiolate, copper-mediated 1,4-addition-elimination, DIBAL-H reduction and oxidation by PCC, to yield conjugated aldehyde. Brown's asymmetric allylation and esterification with acryloyl chloride furnished acrylate ester, which contained two terminal olefins. These terminal olefins were then joined into a single olefin *via* ring-closing metathesis. Epoxidation and regioselective reduction of the resulting oxirane yielded 4-hydroxytetrahydropyranone. Next, a tandem nucleophilic addition-oxocarbenium cation generation-diasteroselective reduction sequence converted the tetrahydropyranone into 2,6-*syn*-tetrahydropyran. The silyl groups of resulting tetrahydropyran were totally removed, followed by reprotection of the 1,2-diol in order to perform oxidation on hydroxyl group at 4-position of

[85] Inanaga, J.; Hirata, K.; Saeki, H.; Katsuki, T.; Yamaguchi, M. *Bull. Chem. Soc. Jpn.* **1979**, *52*, 1989-1993.
[86] Nicolaou, K. C.; Jung, J.; Yoon, W. H.; Fong, K. C.; Choi, H.-S.; He, Y.; Zhong, Y.-L.; Baran, P. S. *J. Am. Chem. Soc.* **2002**, *124*, 2183-2189.

tetrahydropyran. The resulted carbonyl group was converted to alkene *via* Wittig reaction, then removal of diol protecting group and reprotection of primary alcohol furnished Fragment **A**. (Scheme 2.3.10a)

Synthesis of Fragment A

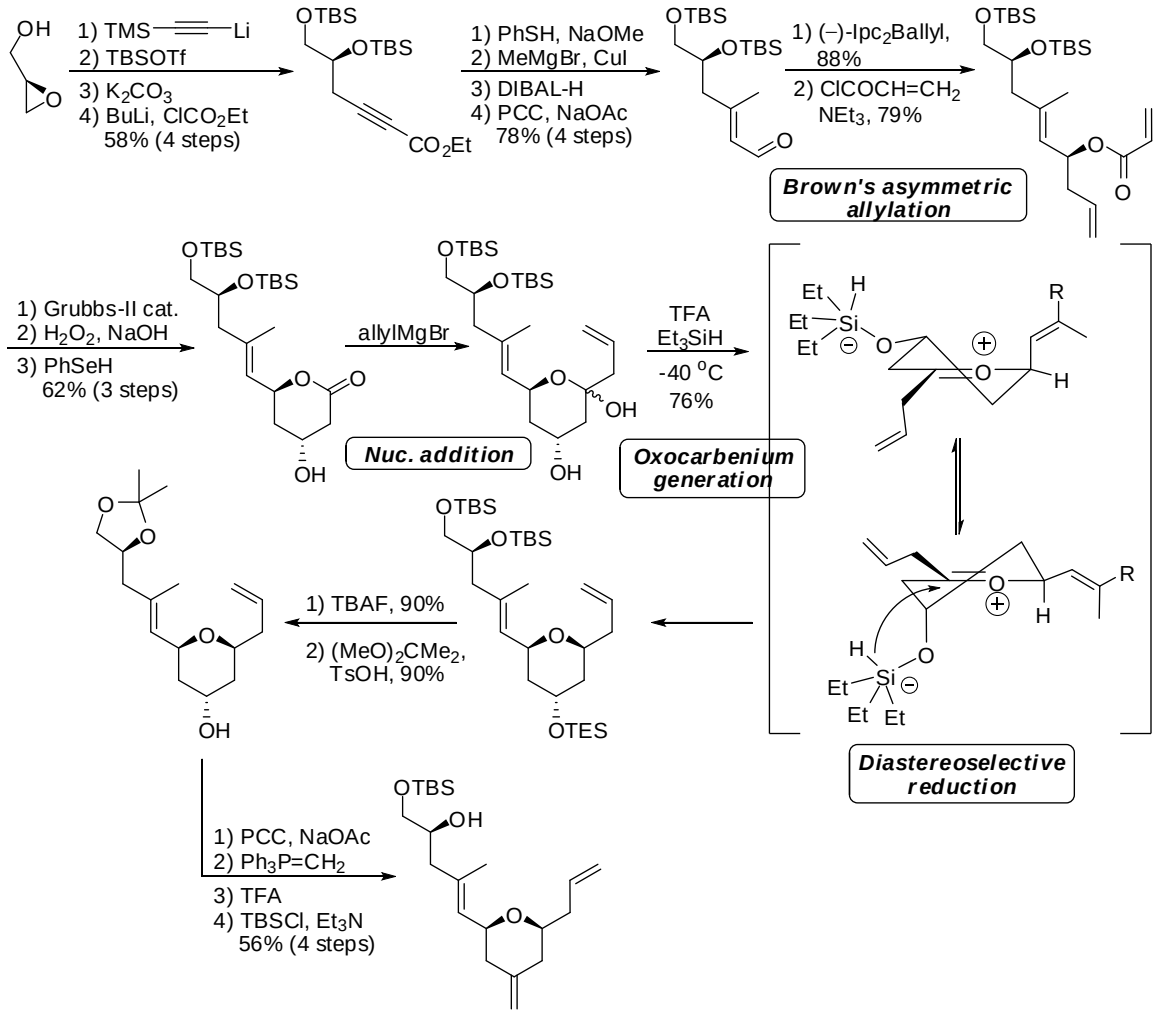

Scheme 2.3.10a Jennings's synthesis of (–)-dactylolide (*ent*-**2**).

On the other hand, synthesis of Fragment **B** was initiated from an established protocol by McLaughlin and Hsung in the synthesis of (*Z*)-enal from dihydropyranone.[87] Horner-Wadsworth-Emmons reaction, deprotection and oxidation yielded C1 – C7 fragment, which was then elongated to designated Fragment **B** *via* a three-step sequence, including Grignard reaction, protection and hydrolysis. (Scheme 2.3.10b)

The following convergent synthesis was achieved *via* Yamaguchi esterificaton and ring-closing metathesis to yield macrolide core. The protected hydroxyl group at C20 was deprotected and oxidized into aldehyde as an effort to complete the total synthesis of (–)-dactylolide (*ent*-**2**). (Scheme 2.3.10b)

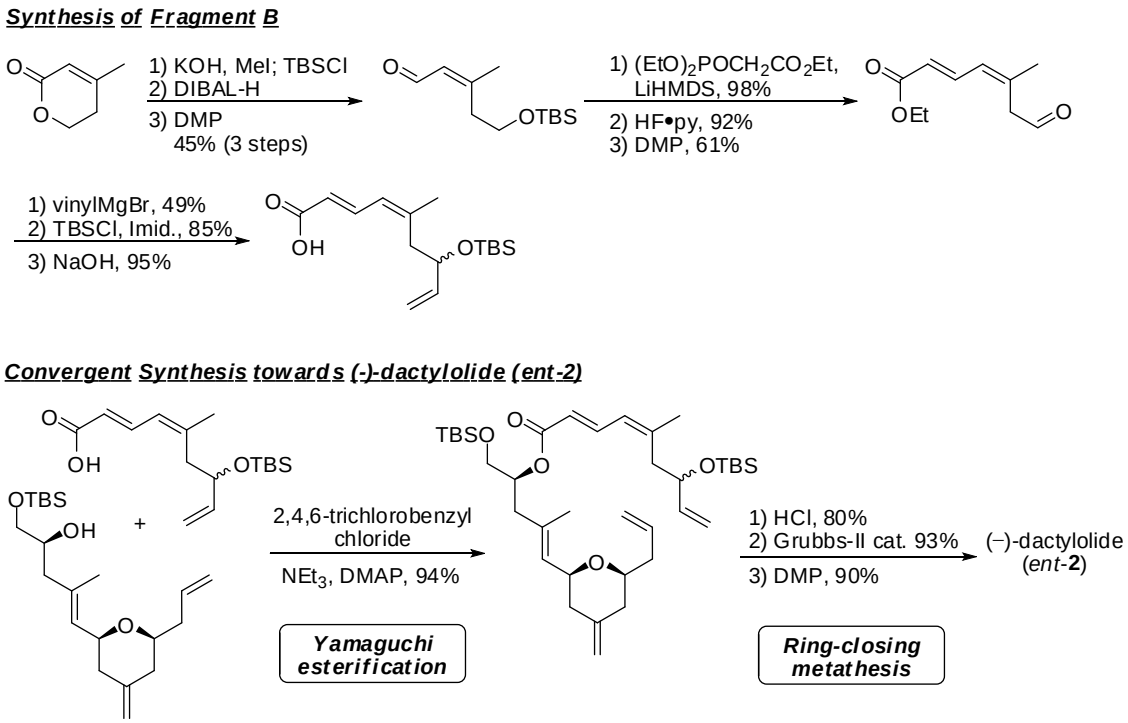

Scheme 2.3.10b Jennings's synthesis of (–)-dactylolide (*ent*-**2**).

[87] McLaughlin, M. J.; Hsung, R. P. *J. Org. Chem.* **2001**, *66*, 1049-1053.

2.3.5 Keck's synthesis of (+)-dactylolide (2)[72]

Sanchez and Keck reported a total synthesis of (+)-dactylolide (**2**), featuring a Horner-Wadsworth-Emmons (HWE) macrocyclization, diastereoselective pyran annulations and catalytic asymmetric allylation. As shown in Scheme 2.3.11, the macrolide core was expected to be formed from tetrahydropyran **A** and phosphonate **B**.

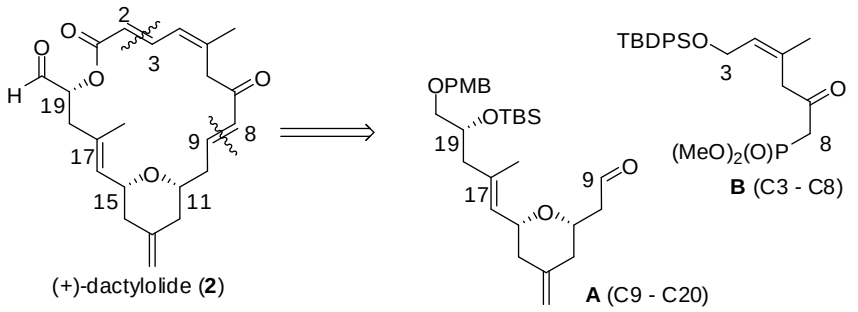

Scheme 2.3.11 Retrosynthesis of Keck's synthesis of (+)-dactylolide (**2**).

The synthesis of tetrahydropyran **A** was synthesized from two chiral alcohols *via* diastereoselective pyran annulations. Chiral alcohol **A1** (Fragment C15 – C20) could be afforded in five steps, as shown in Scheme 2.3.12. The first step was asymmetric allylation of aldehyde with allylstannane catalyzed by BINOL titanium tetraisopropoxide (BITIP), which provided allylic alcohol at 93% *ee*. After protected the hydroxyl group, isomerization of terminal alkene into α,β-unsaturated ester (E/Z = 32:1) was achieved by NaH. Reduction of ester group to alcohol and subsequent oxidiation with TPAP/NMO afforded enal **A1**. On the other hand, preparation of allylic alcohol **A2** was straightforward, which also featured an asymmetric allylation strategy as employed in enantioselective synthesis of chiral C19. Instead of (*R*)-BITIP, its enantiomer, (*S*)-BITIP, was used as catalyst in this case. Aldehyde **A1** and homoallylic alcohol **A2** were then condensed into tetrahydropyran *via* pyran annulations under stoichiometric amount of TMSOTf. Single diasteroisomer of tetrahydropyran was obtained. Deprotection and oxidation with TPAP/NMO furnished designated aldehyde **A**.

Synthesis of phosphonate **B** was started a sequence of transformation: reduction, protection and selective deprotection, of pre-formed (*Z*)-α,β-unsaturated ester[88] into trisubstituted alkene. Oxidation, addition of phosphonate and oxidation of C7 hydroxyl group into ketone yielded target phosphonate **B**. The union between phosphonate **B** and aldehyde **A** under $Ba(OH)_2$[89] achieved Horner-Wadsworth-Emmons olefination product. In order to prevent possible enolization at eastern enone system in further synthesis, the ketone was reduced and protected with *p*-methoxybenzyl (PMB) group. Then, desilylation and installation of phosphonate at C19 hydroxyl group, followed by another desilylation and oxidation at C3 hydroxyl group were conducted in order to perform Horner-Wadsworth-Emmons macrolactonization in subsequent step. Removal of PMB protecting groups at C20 and C7 hydroxyl groups was done under DDQ conditions in a single reaction, and final DMP oxidation converted both free hydroxyl groups into carbonyl groups to furnish (+)-dactylolide (**2**).

[88] Still, W. C.; Gennari, C.; Nogues, J. A.; Pearson, D. A. *J. Am. Chem. Soc.* **1984**, *106*, 260-262.
[89] (a) Paterson, I.; Yeung, K.-S. *Tetrahedron Lett.* **1993**, *34*, 5347-5350; (b) Paterson, I.; Yeung, K.-S.; Smaill, J. B. *Synlett* **1993**, 774-776.

Synthesis of Fragment A

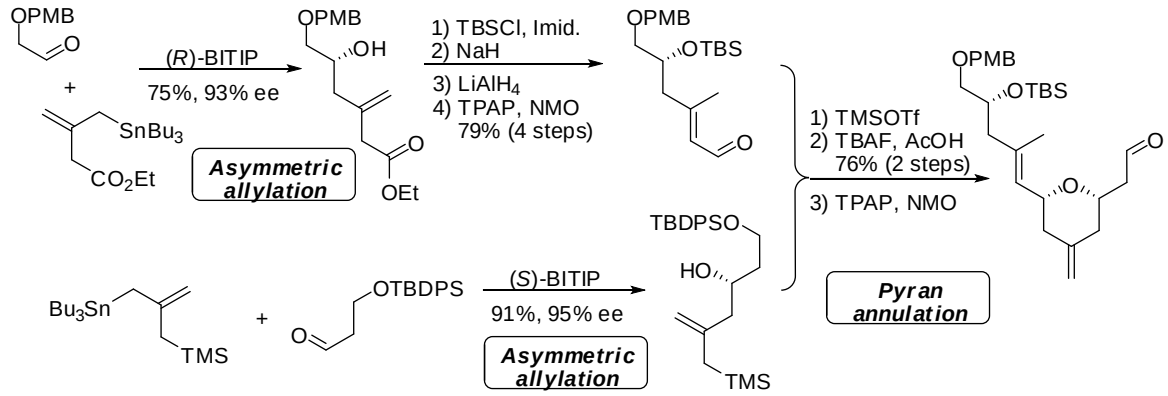

Synthesis of Fragment B

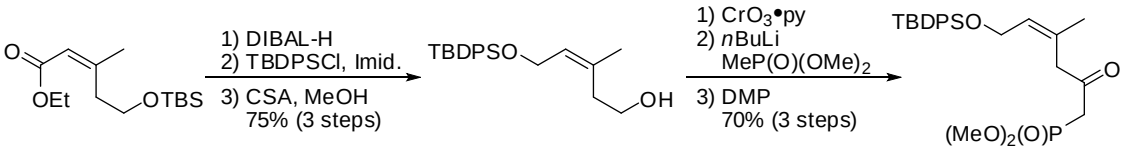

Convergent Synthesis towards (+)-dactylolide (2)

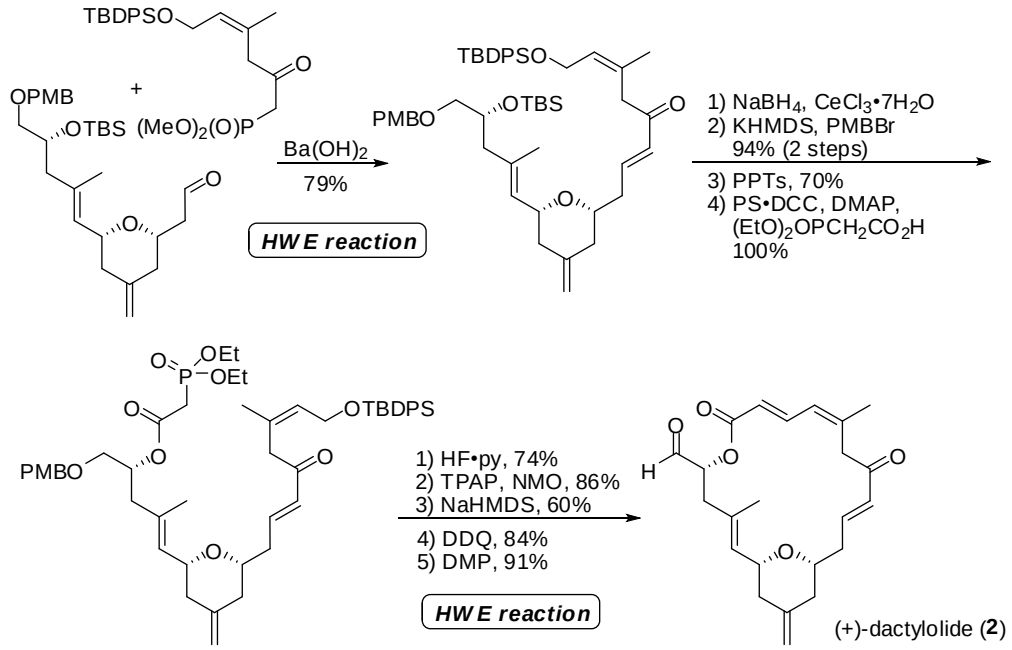

Scheme 2.3.12 Keck's synthesis of (+)-dactylolide (**2**).

2.3.6 McLeod's synthesis of (–)-dactylolide (*ent*-2)[74]

In McLeod's synthesis of (–)-dactylolide (*ent*-**2**), the key reactions that applied in the final convergent synthesis included Mitsunobu esterification and ring-closing metathesis, which led to Fragment **A** (tetrahydropyran unit) and **B** (triene unit) shown in Scheme 2.3.13. The construction of tetrahydropyran was achieved by catalytic asymmetric Jacobsen hetero-Diels-Alder reaction,[90] while the stereocontrolled synthesis of chiral C19 was achieved *via* chelation-controlled Grignard addition and Ireland-Claisen rearrangement.[91]

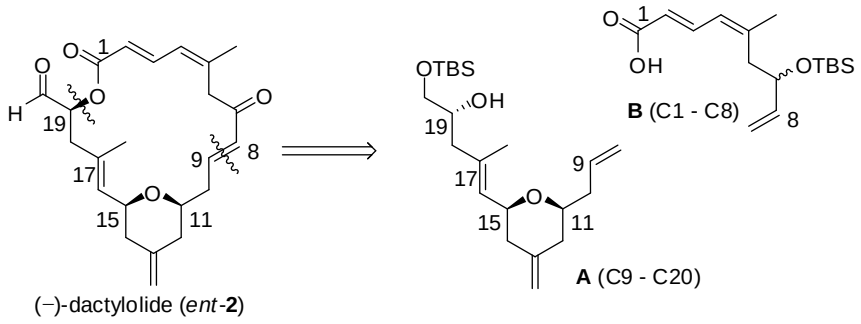

Scheme 2.3.13 Retrosynthesis of McLeod's synthesis of (–)-dactylolide (*ent*-**2**).

As illustrated in Scheme 2.3.14, synthesis of Fragment **A** commenced with the Jacobsen hetero-Diels-Alder reaction catalyzed by a sophisticated chromium reagent (catalyst A). The reaction joined aldehyde and diene into tetrahydropyranone, which was converted to tetrahydropyran *via* Wittig reaction, that transformed two carbonyl groups (one at tetrahydropyran unit, another one at C9) into olefin. The resulted tetrahydropyran underwent oxidation and allylation at C16 position, which formed chiral allylic alcohol. The hydroxyl group was then esterified and underwent Ireland-Claisen [3,3] sigmatropic rearrangement-reduction to yield fragment C9 – C20. Protection and deprotection steps prepared Fragment **A** for the convergent synthesis.

The conjugated dienoate was synthesized from a diene, which was cyclized into dihydropyranone *via* ring-closing metathesis. The resulted dihydropyranone was then reduced and reacted under Horner-Wadsworth-Emmons conditions. A sequence of four-

[90] Dossetter, A. G.; Jamison, T. F.; Jacobsen, E. N. *Angew. Chem. Int. Ed.* **1999**, *38*, 2398-2400.
[91] (a) Ireland, R. E.; Mueller, R. H.; Willard, A. K. *J. Am. Chem. Soc.* **1976**, *98*, 2868-2877; (b) Martin-Castro, A. M. *Chem. Rev.* **2004**, *104*, 2939-3002.

step transformation converted the dienoate into designated Fragment **B**, which was then joined with Fragment **A** *via* Mitsunobu esterification. The macrolide core was later closed by ring-closing metathesis to furnish the target molecule, (–)-dactylolide (*ent*-**2**).

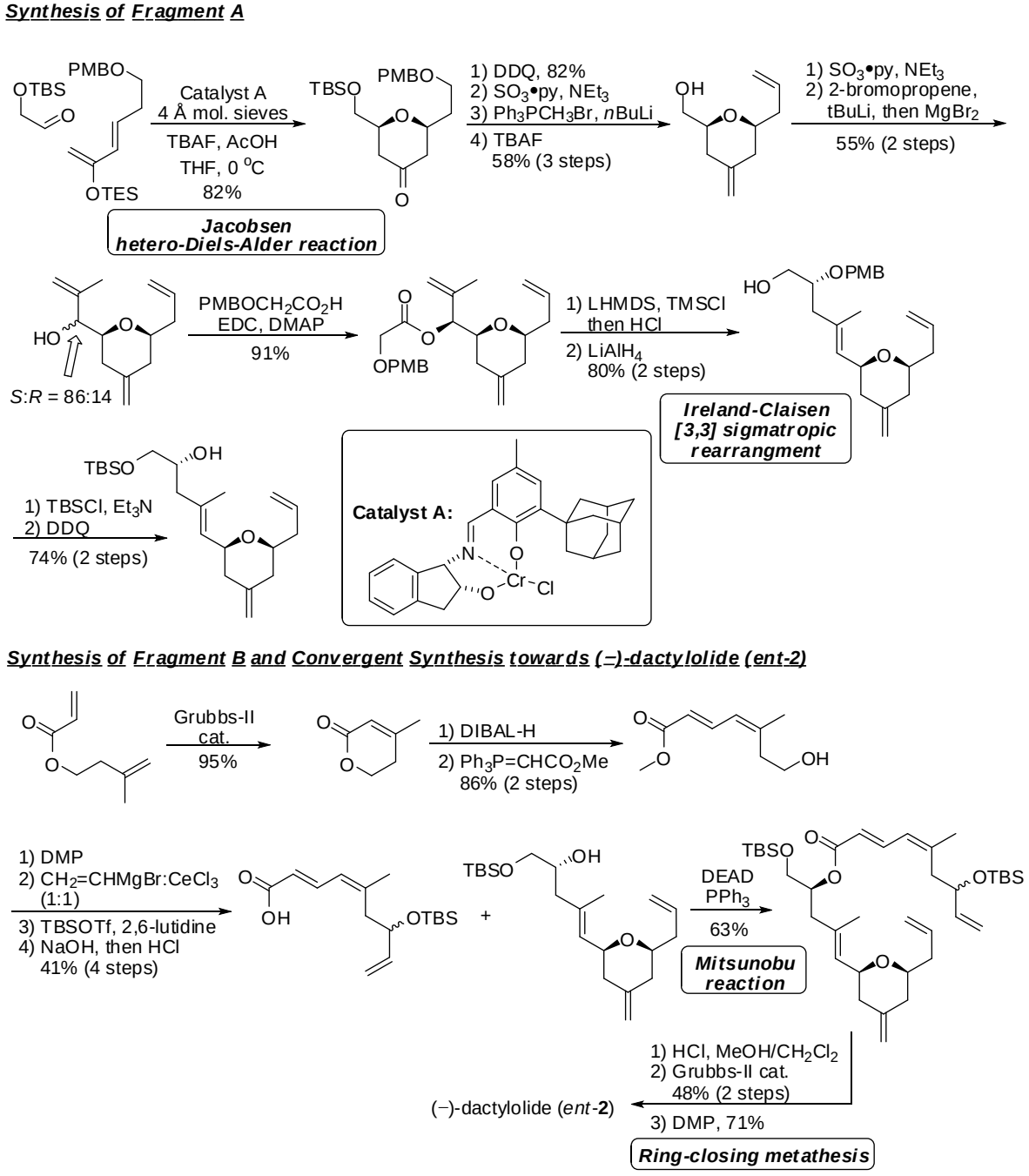

Scheme 2.3.14 McLeod's synthesis of (–)-dactylolide (*ent*-**2**).

2.3.7 Porco's synthesis of macrolide core of (–)-zampanolide (1)[75a,75b]

Porco and co-workers' work on synthesis of macrolide core of (–)-zampanolide (**1**) was initiated by their earlier synthesis of *N*-acyl hemiaminal side chain and its apparent stabilization through intramolecular hydrogen bond network.[75b] As illustrated in Scheme 2.3.15, *N*-acyl hemiaminal side chain was planned to be installed on protected amino alcohol-bearing macrolide in a later stage. Disconnections at the northern dienoate revealed that the macrolide could be formed from fragment C7 – C20 with two smaller fragments, which are vinyl stannane (C1 – C3) and allylic silane (C4 – C6). Disconnection at the tetrahydropyran unit of fragment C7 – C20 showed that conjugated aldehyde **A** and homoallylic alcohol **B** were essential in the construction of tetrehydropyran ring. Conjugated aldehyde **A** was synthesized from protected serine derivative and dienol ether.

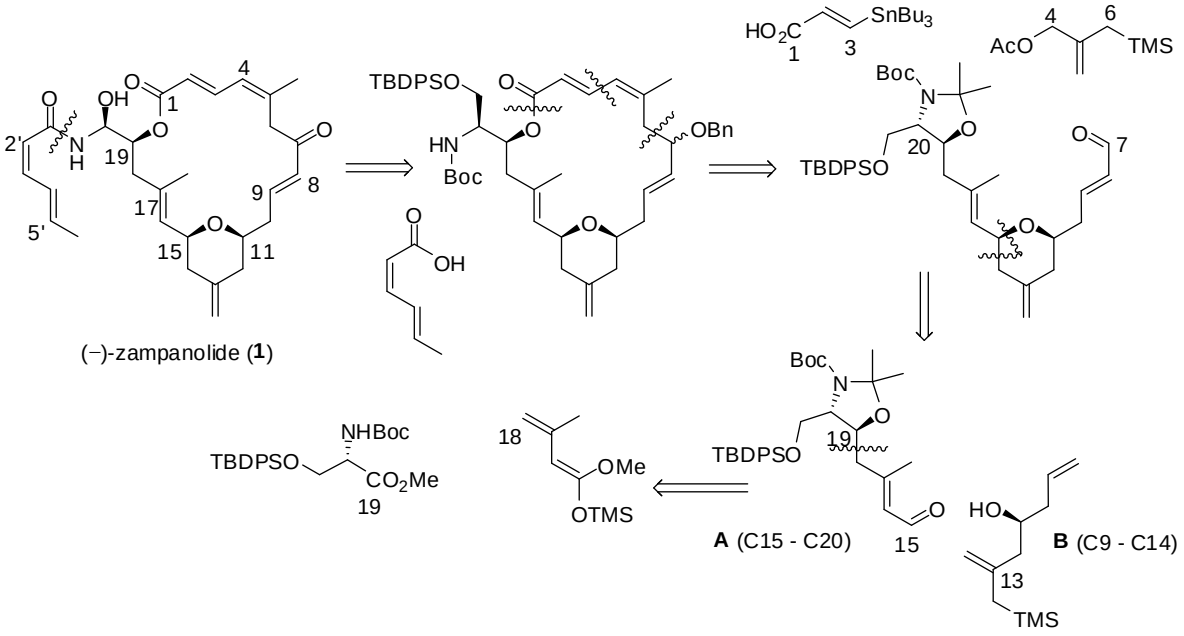

Scheme 2.3.15 Retrosynthesis of Porco's synthesis of macrolide core of (–)-zampanolide (**1**).

The detailed synthesis is shown in Scheme 2.3.16. As planned before, Porco and co-workers synthesized Fragment **A** from protected serine derivative. One-pot reduction/vinylogous aldol reaction yielded conjugated ester, which was further protected at its amino alcohol motif before subsequent reduction/oxidation at conjugated ester group. On the other hand, the homoallylic alcohol **B** was synthesized from chiral epoxide, which was exposed to a sequence of Grignard reaction, desilylation and alkyne reduction. Conjugated aldehyde **A** and homoallylic alcohol **B** were then merged into tetrahydropyran ring under stoichiometric amount of $Bi(OTf)_3$ *via* intramolecular silyl-modified Sakurai (ISMS) reaction.[92] Subsequent olefin metathesis with acrolein was employed to lengthen the fragment to C7 and allylation with allylsilane further extended the fragment to C4. Removal of acetonide and esterification with vinyl stannane provided macrocyclization precursor, which was cyclized under a $Pd(PPh_3)_4$/DIEA/Bu_4NI system *via* sp^2-sp^3 Stille coupling. However, the resulted macrolide consisted of 1,4-diene instead of 1,3-diene. The abnormal diene structure was then corrected by DBU, but a 1:1 mixture of (*E*,*E*) and (*E*,*Z*)-1,3-diene was afforded.

The authors envisioned that the resulted macrolide could be further transformed into macrolide core of (–)-zampanolide with subsequent removal of benzyl group at eastern enone system and ready for installation of N-*acyl* hemiaminal side chain in final stage.

[92] Leroy, B.; Marko, I. E. *Tetrahedron Lett.* **2001**, *42*, 8685-8688.

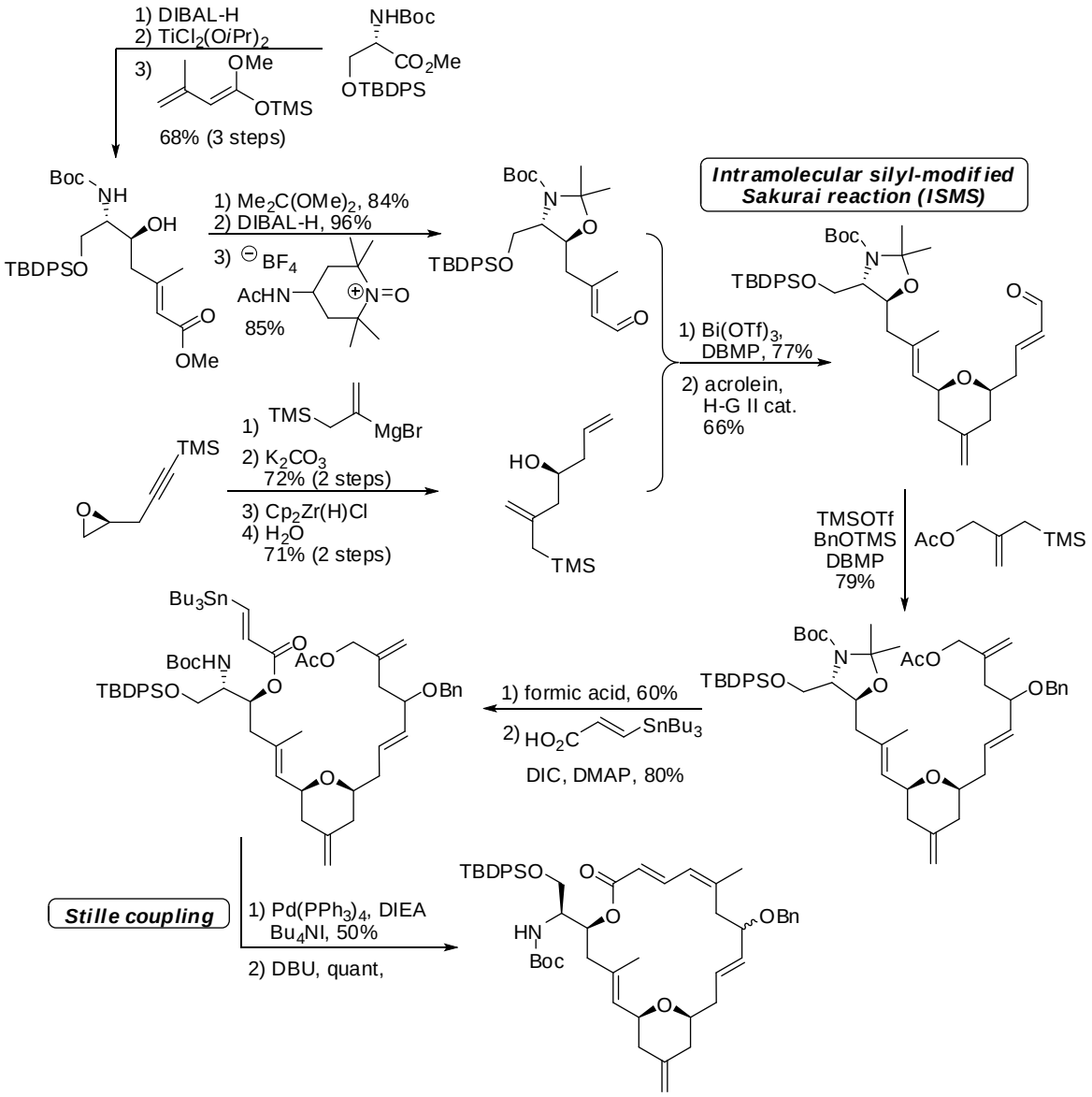

Scheme 2.3.16 Porco's synthesis of macrolide core of (–)-zampanolide (**1**).

2.3.8 Uenishi's synthesis of (–)-zampanolide (1) and (–)-dactylolide (*ent*-2)[60]

Uenishi and co-workers demonstrated another strategy in their synthesis of (–)-zampanolide (**1**) and (–)-dactylolide (*ent*-**2**). (–)-dactylolide (*ent*-**2**) was envisioned to be synthesized from Fragment **A** (C9 – C20) and phosphonate **B** (C1 – C8) *via* macrolactonization and Horner-Wadsworth-Emmons reaction. The tetrahydropyran unit was synthesized *via* Hosomi-Sakurai reaction and *O*-Michael reaction, which will be discussed (vide infra). Installation of *N*-acyl hemiaminal side chain was performed after completion of (–)-dactylolide (*ent*-**2**) *via* CSA-promoted reaction. (Scheme 2.3.17)

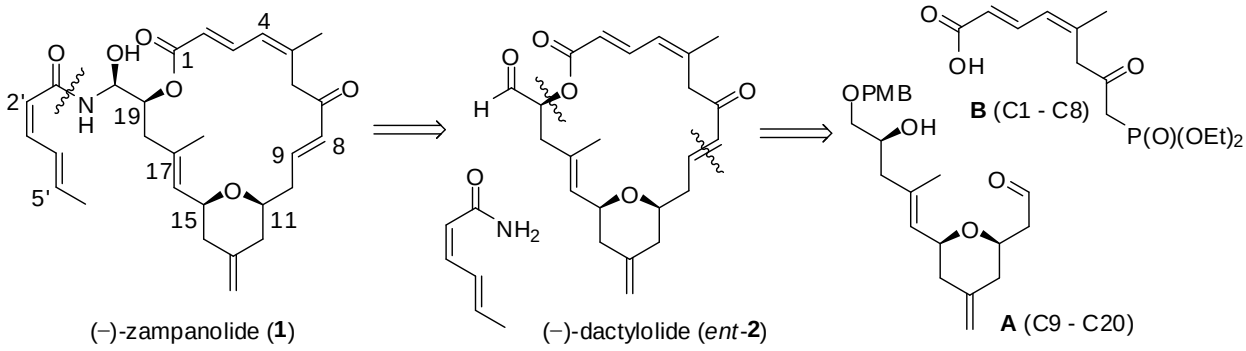

Scheme 2.3.17 Retrosynthesis of Uenishi's synthesis of (–)-zampanolide (**1**) and (–)-dactylolide (*ent*-**2**).

Fragment **A** was synthesized from (*R*)-(+)-glycidol, which was protected with PMB and ring opening by a vinyl lithium derivative. The resulted chiral alcohol was protected with pivalic group, and underwent desilylation/oxidation to yield conjugated aldehyde. On the other hand, allylsilane was synthesized from TBDPS-acetaldehyde with a three-step transformation, namely dibromomethylenation,[93] Kumado-Tamao-Corriu coupling and protodesilylation.[94] Union of conjugated aldehyde and allylsilane into homoallylic alcohol was achieved with $SnCl_4$ *via* Hosomi-Sakurai reaction, but a mixture of diasteromers was obtained. However, the author was able to convert (15*R*)-homoallylic alcohol into (15*S*)-analogue with Mitsunobu reaction and methanolysis. A subsequent five-step transformation, included protection of secondary alcohol, desilylation, oxidation, Wittig reaction and deprotection on secondary alcohol, was applied to produce cyclization precursor, which underwent *O*-Michael reaction and yielded tetrahydropyran ring

[93] Corey, E. J.; Fuchs, P. L. *Tetrahedron Lett.* **1972**, *13*, 3769-3772.
[94] Uenishi, J.; Iwamoto, T.; Ohmi, M. *Tetrahedron Lett.* **2007**, *48*, 1237-1240.

(mixture of *cis*- and *trans*-isomers). Final reduction step furnish the designated Fragment **A**.

Diene fragment **B** was synthesized from *α*,*β*-unsaturated aldehyde. Dibromomethylenation and stereoselective Sonagashira coupling yielded dienyne, which was introduced with a methyl group by replacing the bromine *via* Kumada-Tamao-Corriu coupling.[95] The terminal TMS-acetylene unit was converted to ester *via* a sequence of hydroboration, oxidation and esterification. Deprotection, installation of phosphonate and two oxidations furnished the target diene fragment **B**.

Fragment **A** and **B** were then bonded at C8 – C9 position with Cs_2CO_3, followed by macrolactonization using ruthenium-based catalyst to complete the macrolide core. Final deprotection and oxidation yielded (–)-dactylolide (*ent*-**2**). Installation of *N*-acyl hemiaminal side chain was achieved with camphor sulfonic acid (CSA), albeit in lower yield (11%) with the presence of C20 epimer and bis(*N*-acyl)product.

[95] Uenishi, J.; Matsui, K.; Ohmi, M. *Tetrahedron Lett.* **2005**, *46*, 225-228.

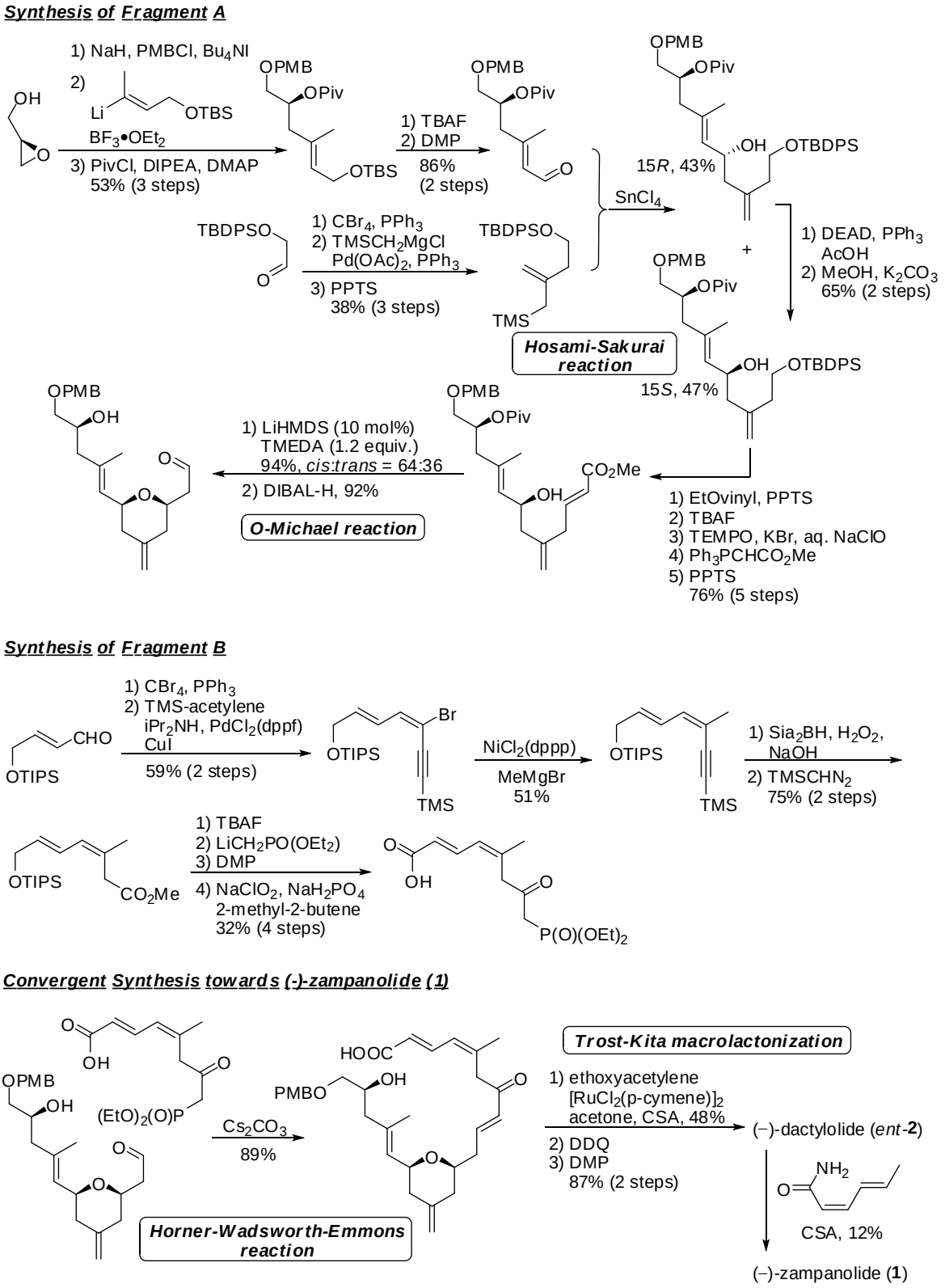

Scheme 2.3.18 Uenishi's synthesis of (–)-zampanolide (**1**) and (–)-dactylolide (*ent*-**2**).

2.3.9 Lee's synthesis of (–)-dactylolide (*ent*-2)[75]

As an application to show the practicability of their own synthetic methods for construction of *Z*-vinyl boronates and 2,6-*syn*-4-exomethylene tetrahydropyrans, Lee and co-workers viewed that (–)-dactylolide (*ent*-**2**) could be synthesized from *Z*-vinyl boronate **A** and vinyl iodide **B** *via* ring-closing metathesis and Suzuki coupling.[96] (Scheme 2.3.19) The tetrahydropyran unit was envisioned to be constructed with a tandem ruthenium-catalyzed Alder-ene reaction (RCAER)[97] and palladium-catalyzed ring closure.[98] These transition metal based strategies were considered as an effort to minimize functional group transformation and protection/deprotection steps in their total synthetic work.[99]

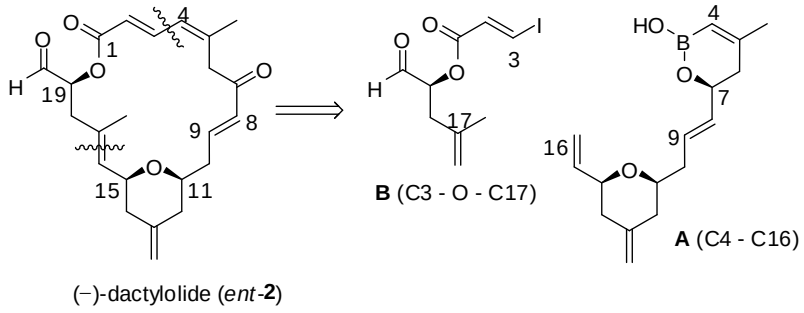

Scheme 2.3.19 Retrosynthesis of Lee's synthesis of (–)-dactylolide (*ent*-**2**).

The synthesis of tetrahydropyran motif was begun with an one-pot reaction, firstly RCAER by joining ethyl carbonate and homopropargylic alcohol[100] into 1,4-diene, followed by palladium-catalyzed cyclization into tetrahydropyran. Reduction and oxidation at C9 allowed Leighton allylation[101] and protection to proceed and yield homoallylic alcohol, which was transformed into vinyl boronate *via* RCAER. Subsequent

[96] For a review, see: Miyaura, N.; Suzuki, A. *Chem. Rev.* **1995**, *95*, 2457-2483.
[97] For a review, see: Trost, B. M.; Frederiksen, M. U.; Rudd, M. T. *Angew Chem.* **2005**, *117*, 6788-6825; *Angew. Chem. Int. Ed.* **2005**, *44*, 6630-6666.
[98] Hansen, E. C.; Lee, D. *Tetrahedron Lett.* **2004**, *45*, 7151-7155.
[99] (a) Ho, T.-L. *Tandem Organic Reactions*, Wiley: New York, **1992**; (b) Tietze, L. F. *Chem. Rev.* **1996**, *96*, 115-136; (c) Wasilke, J.-C.; Obrey, S. J.; Baker, R. T.; Bazan, G. C. *Chem. Rev.* **2005**, *105*, 1001-1020.
[100] Synthesis of homopropargylic alcohol, see: Pattenden, G.; Gonzalez, M. A.; Little, P. B.; Millan, D. S.; Plowright, A. T.; Tornos, J. A.; Ye, T. *Org. Biomol. Chem.* **2003**, *1*, 4173-4208.
[101] Kinnaird, J. W. A.; Ng, P. Y.; Kubota, K.; Wang, X.; Leighton, J. L. *J. Am. Chem. Soc.* **2002**, *124*, 7920-7921.

treatment with rhenium oxide transposited allylic alcohol and yielded a relatively unstable cyclic boronic acid half ester **A**.[102]

On the other hand, the coupling partner of cyclic boronic acid **A**, vinyl iodide **B**, was synthesized from TBS-protected (*S*)-(–)-glycidol. Two-step transformation, including epoxide ring opening by 2-propenylmagnesium chloride and Mitsunobu reaction, prepared the target vinyl iodide **B**. Suzuki coupling between **A** and **B** under $Pd(PPh_3)_4$/TlOEt completed the northern dienoate scaffold. Oxidation of C7 hydroxyl group, ring-closing metathesis, desilylation and oxidation furnished (–)-dactylolide (*ent*-**2**), which shown in Scheme 2.3.20.

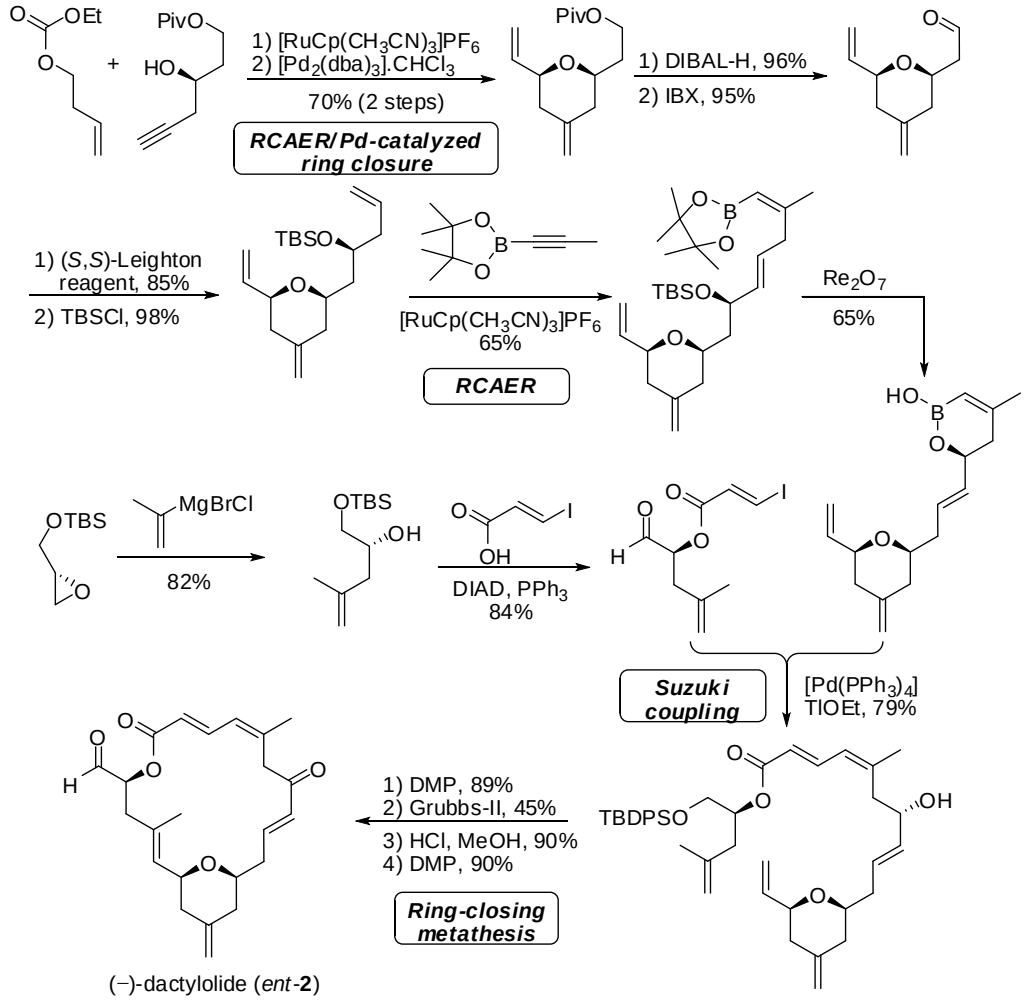

Scheme 2.3.20 Lee's synthesis of (–)-dactylolide (*ent*-**2**).

[102] (a) Bellemin-Laponnaz, S.; Gisie, H.; Le Ny, J. P.; Osborn, J. A. *Angew. Chem.* **1997**, *109*, 1011-1013; *Angew. Chem. Int. Ed. Engl.* **1997**, *36*, 976-978; (b) Bellemin-Laponnaz, S.; Gisie, H.; Le Ny, J. P.; Osborn, J. A. *Tetrahedron Lett.* **2000**, *41*, 1549-1552.

2.3.10 Kim and Hong's synthesis of (+)-dactylolide (2)[76]

Kim and Hong and co-workers featured *N*-heterocyclic carbene catalyzed oxidative macrolactonization in their synthesis of (–)-dactylolide (*ent*-**2**). As shown in Scheme 2.3.21, such strategy was applied in connecting C1 to O20 atom of macrolide. Further disconnection at C6 and C7 showed that the macrolide could be constructed from aldehyde **A** and chloride **B** *via* cyanohydrins umpolung alkylation. Disconnection at tetrahydropyran motif envisioned that Fragment **A** could be synthesized from vinyl iodide **A1**, dithiane **A2** and dienyl chloride **A3**.

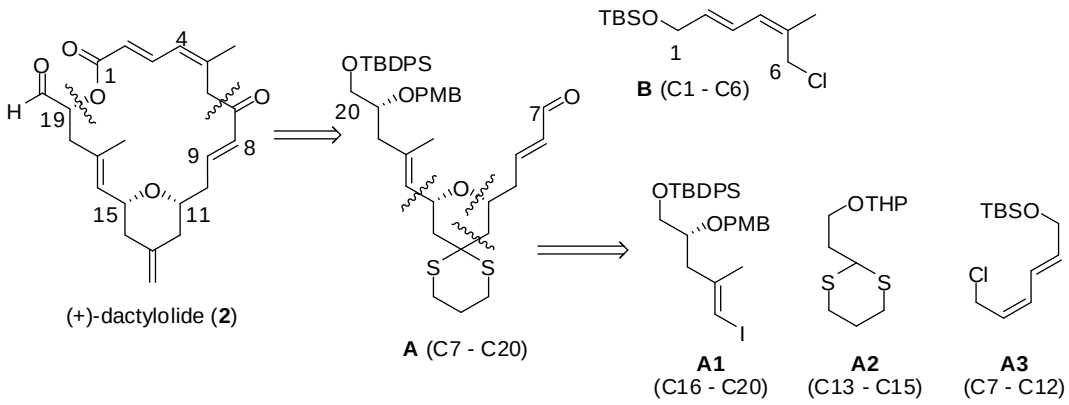

Scheme 2.3.21 Retrosynthesis of Hong's synthesis of (+)-dactylolide (**2**).

Detailed Hong's synthesis of (+)-dactylolide (**2**) is illustrated in Scheme 2.3.22. Dithiane derivative **A2** was prepared from 1,3-dithiane with a four-step transformation,[103] while dienyl chloride **A3** was obtained *via* a five-step sequence from (*Z*)-butenediol.[104] Coupling of these two fragments was then achieved under *n*BuLi/*n*Bu_2Mg conditions.[105] Removal of THP group by $ZnCl_2$ and oxidation prepared aldehyde precursor for next coupling with vinyl iodide **A1**, which was synthesized from (*S*)-(–)-glycidol in 4 steps. Asymmetric organozinc addition was employed as the coupling strategy and yielded chiral allylic alcohol. Deprotection and oxidation into aldehyde was conducted at C7 before key intramolecular 1,6-oxa conjugate addition with the presence of chiral pyrollidine was performed to afford tetrahydropyran. The resulted intermediate was then converted into TBS-protected cyanohydrins, which underwent cyanohydrins umpolung

[103] Gaunt, M. J.; Jessiman, A. S.; Orsini, P.; Tanner, H. R.; Hook, D. F. Ley, S. V. *Org. Lett.* **2003**, *5*, 4819-4822.
[104] Caussanel, F.; Deslongchamps, P.; Dory, Y. L. *Org. Lett.* **2003**, *5*, 4799-4802.
[105] (a) Ide, M.; Yasuda, M.; Nakata, M. *Synlett* **1998**, 936-938; (b) Ide, M.; Nakata, M. *Bull. Chem. Soc. Jpn.* **1999**, *72*, 2491-2499; (c) Ichige, T.; Okano, Y.; Kanoh, N.; Nakata, M. *J. Org. Chem.* **2009**, *74*, 230-243.

alkylation with dienyl chloride **B**, which prepared from (*E*)-butenediol. Further treatment with DDQ resulted in dienal precursor, which was macrocyclized *via* NHC-catalyzed oxidative macrolactonization. It was achieved when DBU, DMAP, 3,3',5,5'-tetra-*tert*-butyldiphenoquinone (as oxidant) and catalytic amount of 1,4-dimethyl-4*H*-1,2,4-triazolium iodide (NHC compound) was added into the reaction. Removal of dithiane of resulted macrolide, installation of exomethylene group *via* Wittig reaction, removal of TBS and TBDPS group and subsequent oxidation marked the completion of (+)-dactylolide (**2**).

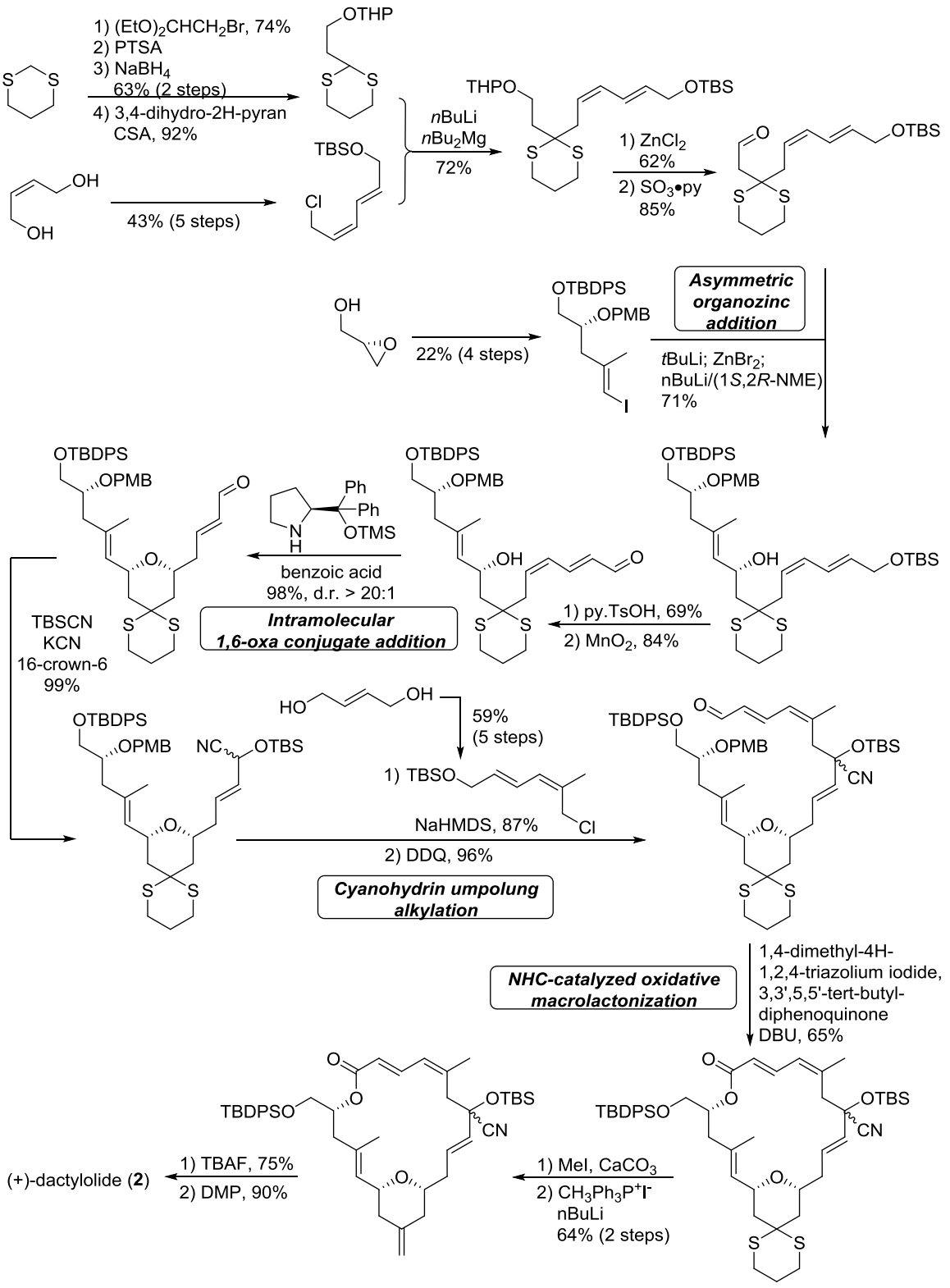

Scheme 2.3.22 Hong's synthesis of (+)-dactylolide (**2**).

2.3.11 Ghosh's synthesis of (–)-zampanolide (1)[61,70]

Ghosh and co-workers featured oxidative intramolecular cyclization-based strategy in their enantioselective synthesis of (–)-zampanolide (**1**). Similar as Uenishi's work, Ghosh disconnected (–)-zampanolide (**1**) into (–)-dactylolide (*ent*-**2**) and hexadienamide, while (–)-dactylolide (*ent*-**2**) was further disconnected at C1 – O bond and C8 – C9 olefin bond, revealed that the macrolide could be synthesized from Fragment **A** and **B** *via* Yamaguchi esterification and ring-closing metathesis respectively. (Scheme 2.3.23) Olefin metathesis and oxidative intramolecular cyclization were employed as key strategies in the synthesis of Fragment **A**, which will be discussed below.

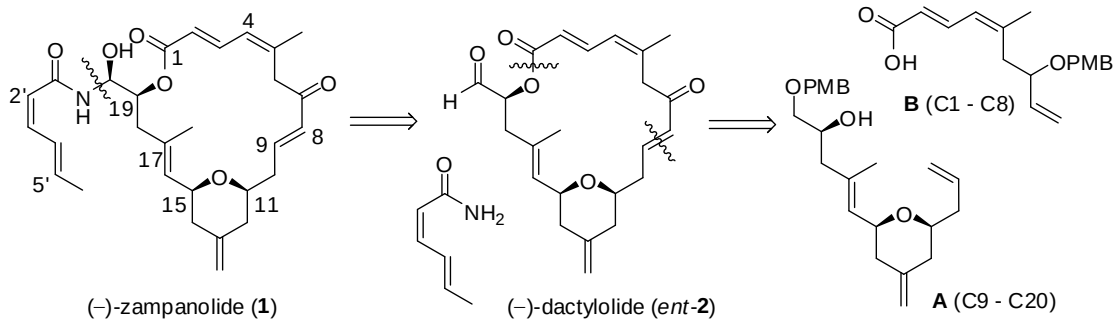

Scheme 2.3.23 Retrosynthesis of Ghosh's synthesis of (–)-zampanolide (**1**).

Synthesis of Fragment **A** started from benzyl-monoprotected 1,3-propanediol. Swern oxidation, treatment with N_2CHCO_2Et and asymmetric Noyori hydrogenation yielded chiral alcohol,[106] which further underwent deprotection/protection at primary alcohol. The resulted chiral alcohol was esterified with *tert*-butyl cinnamyl carbonate at the presence of catalytic amount of $Pd(PPh_3)_4$.[107] The cinnamyl ether was then converted to allylsilane,[108] which underwent oxidative intramolecular cyclization with DDQ catalyzed by PPTS to furnish 2,6-*syn*-4-exomethylene tetrahydropyran unit. After a three-step sequence,[109] the phenyl group was replaced with H atom, and became a terminal olefin, which was coupled with another terminal olefin, represented fragment C17 – C20, *via* olefin cross metathesis. The coupling partner was constructed from (*R*)-(+)-glycidol in 3 steps. After olefin cross metathesis, the resulted fragment was underwent a series of transformation,

[106] Claffey, M. M.; Hayes, C. J.; Heathcock, C. H. *J. Org. Chem.* **1999**, *64*, 8267-8274.
[107] Chrobok, A.; Gossinger, E.; Grunberger, K.; Kahlig, H.; White, M. J.; Wuggenig, F. *Tetrahedron* **2007**, *63*, 8336-8350.
[108] Narayanan, B. A.; Bunnelle, W. H. *Tetrahedron Lett.* **1987**, *28*, 6261-6264.
[109] Zhang, W.; Carter, R. G. *Org. Lett.* **2005**, *7*, 4209-4212.

included desilylation, selective oxidation of primary alcohol and Wittig reaction, to furnish the target Fragment **A**. (Scheme 2.3.24a)

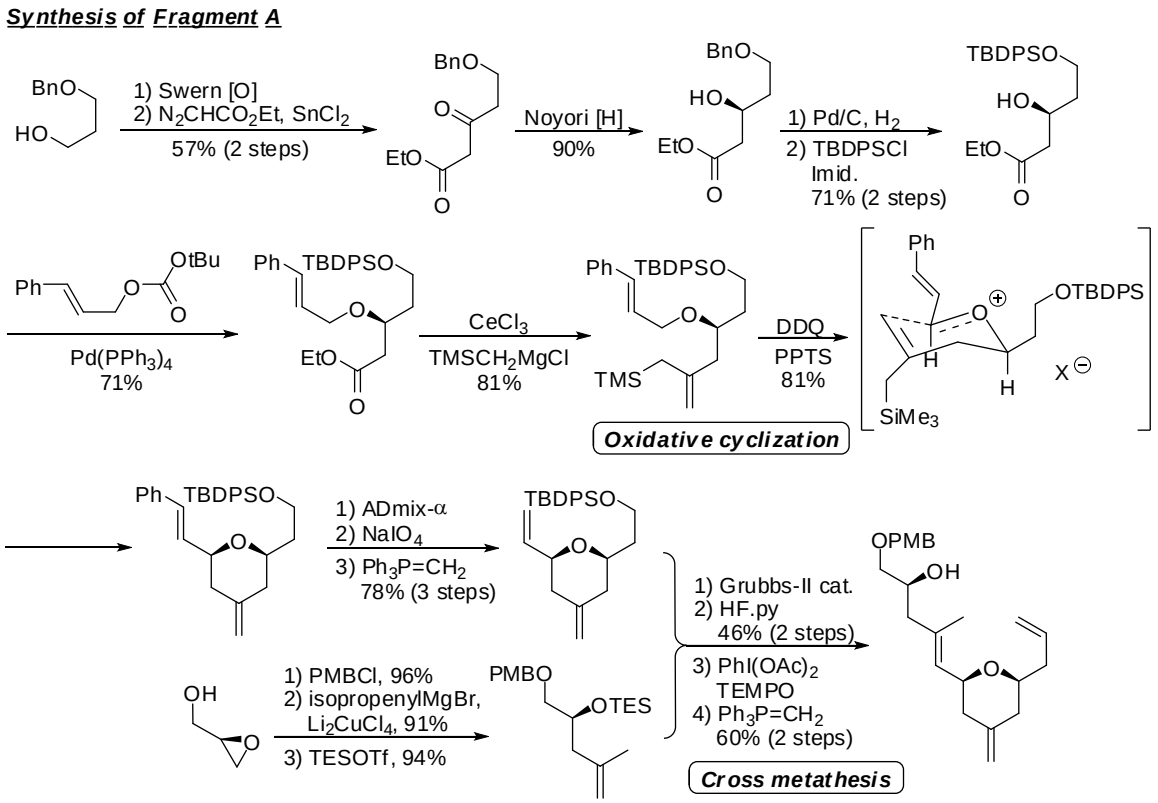

Scheme 2.3.24a Ghosh's synthesis of (–)-zampanolide (**1**).

On the other hand, Fragment **B** was synthesized from methyl 3-methylbut-2-enoate. Bromination resulted in a mixture of *E*- and *Z*-isomers,[110] which was cyclized into dihydropyranone with acrolein and zinc dust. Similar as McLeod's work in preparation of northern dienoate motif,[74] the dihyropyranone was opened by reduction and extended *via* Horner-Wadsworth-Emmons reaction. Protection of secondary alcohol with PMB and reduction of ethyl ester provided the target Fragment **B**. Convergent synthesis of Fragment **A** and **B** was achieved *via* Yamaguchi esterification,[85] while ring-closing metathesis was employed in final closing of macrolide core. Removal of PMB group and oxidation yielded (–)-dactylolide (*ent*-**2**). With various failed attempts, Ghosh and co-workers decided to optimize Uenishi's amidation strategy[60] in the installation of *N*-acyl hemiaminal side chain on (–)-dactylolide (*ent*-**2**). They discovered that with the presence of catalytic amount of (*S*)-TRIP,[111] (–)-zampanolide (**1**) was obtained in a yield of 51%

[110] Lei, B.; Fallis, A. G. *Can. J. Chem.* **1991**, *69*, 1450-1456.
[111] For a review of TRIP in organocatalysis, see: Akiyama, T. *Chem. Rev.* **2007**, *107*, 5744-5758.

(11% obtained by Uenishi) with 18% of C20 epimer. There was no bis(*N*-acyl)product observed in Ghosh's conditions. (Scheme 2.3.24b)

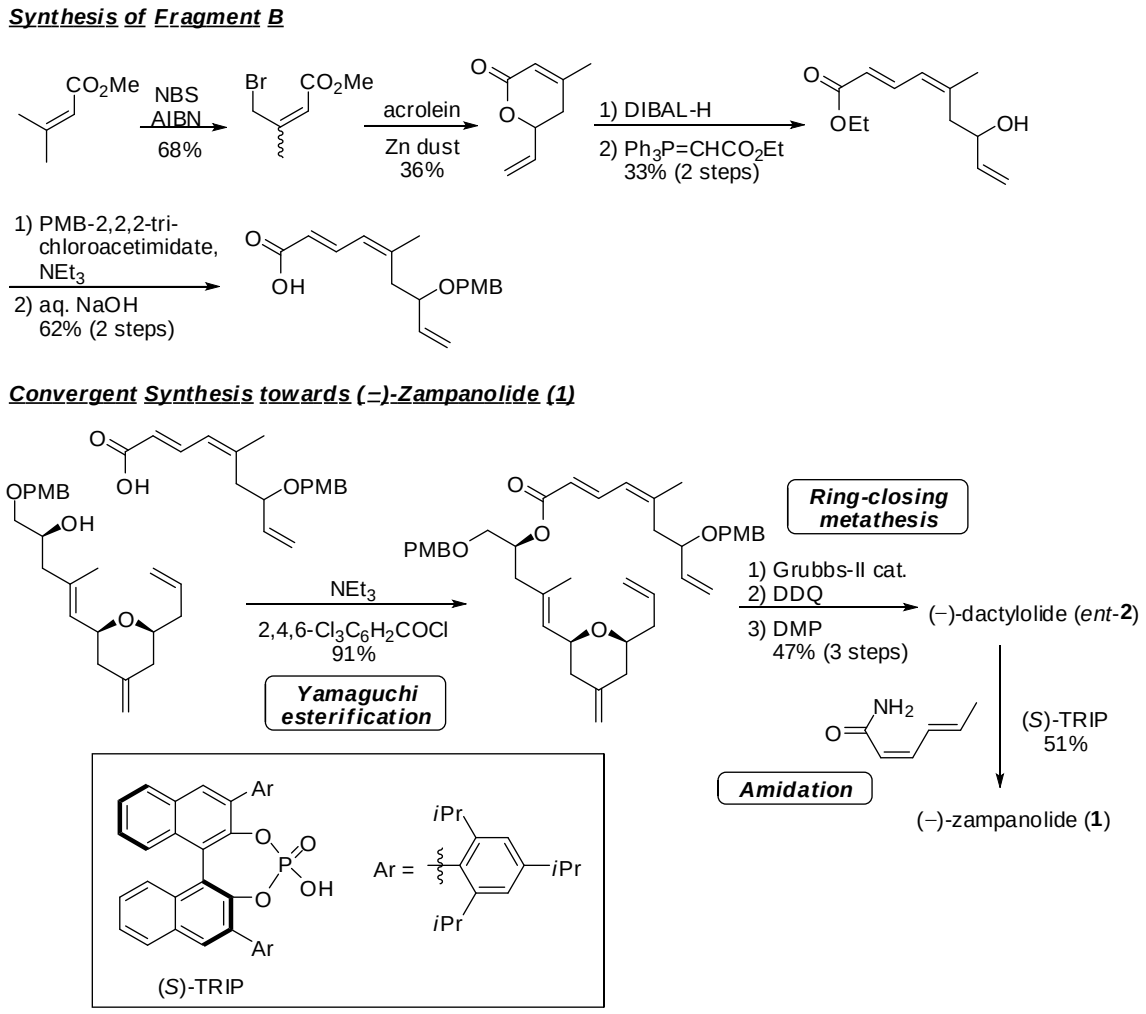

Scheme 2.3.24b Ghosh's synthesis of (–)-zampanolide (**1**). (continued)

2.3.12 Altmann's synthesis of (–)-zampanolide (1)[62]

Retrosynthesis of Altmann's synthesis of (–)-zampanolide (**1**), as outlined in Scheme 2.3.25, showed that Hoye's aza-aldol strategy[69] was used by authors in the installation of *N*-acyl hemiaminal side chain on (–)-dactylolide (*ent*-**2**). Subsequent disconnections on macrolide core envisioned that Yamaguchi esterification[85] and Horner-Wadsworth-Emmons macrocyclization were strategies to construct macrolide from Fragment **A** (C9 – C20) and Fragment **B** (C1 – C8). Fragment **A** was synthesized *via* epoxide opening (C18 – C19), carbostannylation iodination (C16 – C17) and Prins reaction (tetrahydropyran), while Fragment **B** was synthesized *via* Horner-Wadsworth-Emmons reaction (C2 – C3) and epoxide opening (C5 – C6).

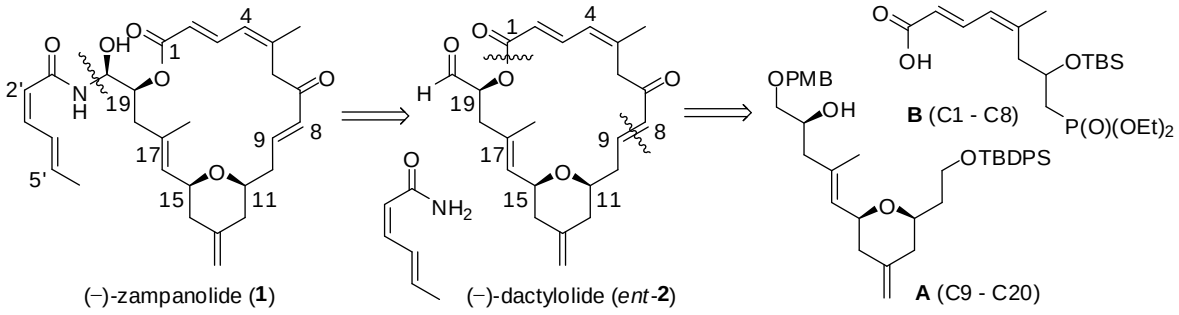

Scheme 2.3.25 Retrosynthesis of Altmann's synthesis of (–)-zampanolide (**1**).

Fragment **A** was synthesized from (*R*)-aspartic acid. A sequence of bromination, epoxide formation and alcohol protection provided epoxide precursor, which was opened by regioselective nucleophilic attack with vinylmagnesium bromide. The resulted chiral secondary alcohol was esterified, reduction and acetylation to yield terminal olefin, which underwent Prins reaction with the presence of trimethylsilyl iodide and 2,6-lutidine to yield 4-iodotetrahydropyran.[112] A sequence of iodine displacement, hydrolysis, Swern oxidation and Wittig reaction converted 4-iodotetrahydropyran to 4-exomethylene tetrahydropyran. Carbostannylation iodination transformed alkyne into alkenyl iodide, which underwent epoxide opening with PMB-protected (*R*)-(+)-glycidol at the presence of *t*-butyl lithium, furnish the target Fragment **A**.

[112] Jasti, R.; Vitale, J.; Rychnovsky, S. D. *J. Am. Chem. Soc.* **2004**, *126*, 9904-9905.

Fragment **B** was constructed from butynol. With a two step transformation, alkenyl iodide was obtained and performed epoxide opening with epichlorohydrin to yield chlorohydrin, which was deprotonated by KOH to yield epoxide, while latter was opened again to yield phosphonate. A sequence of silylation, removal of PMB group and Swern oxidation yielded conjugated aldehyde, which was extended *via* Horner-Wadsworth-Emmons (HWE) reaction and further hydrolysis to furnish Fragment **B**.

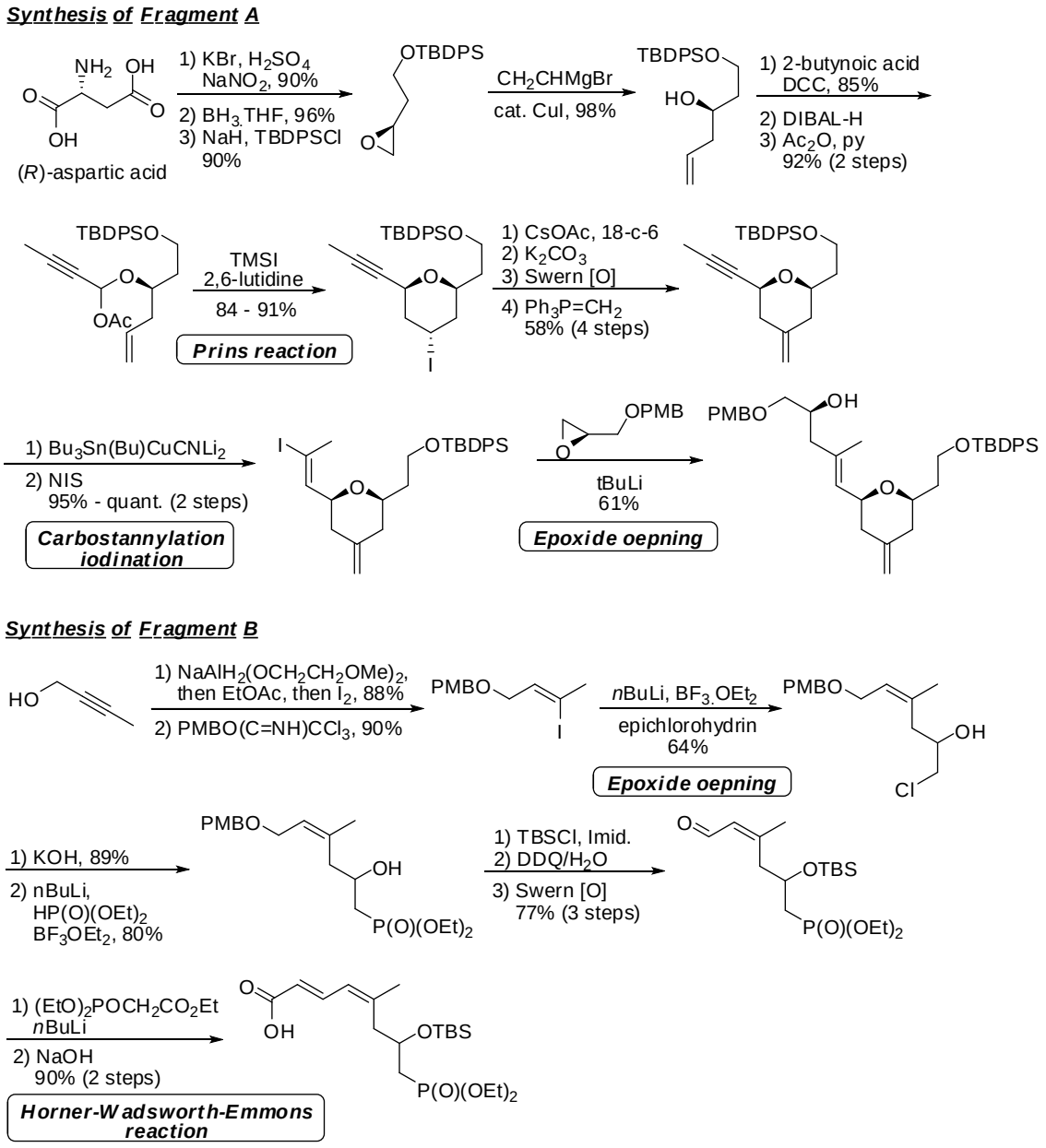

Scheme 2.3.26 Altmann's synthesis of (–)-zampanolide (**1**).

With the availability of Fragment **A** and **B**, Altmann and co-workers esterified both fragments into macrolide precursor. Subsequent desilylation and oxidation into ketone, HWE macrocyclization which furnish the macrolide core, and final removal of PMB group and oxidation yielded (–)-dactylolide (*ent*-**2**). Hoye's aza-aldol reaction allowed the installation of *N*-acyl hemiaminal side chain at C20 aldehyde and furnish (–)-zampanolide (1).

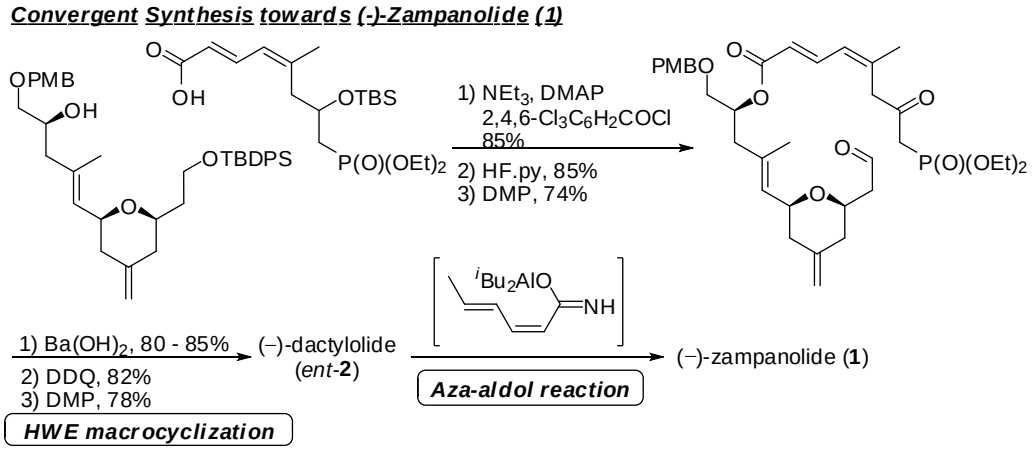

Scheme 2.3.26 Altmann's synthesis of (–)-zampanolide (**1**). (continued)

2.3.13 Other formal synthesis

Besides the aforementioned syntheses, our group (which has been discussed in Section 1.3.2.2.4),[23] Reddy,[77c] Taylor[77d] and Harvey[77e] also reported formal syntheses of zampanolide and dactylolide. Our group, Reddy and Taylor focused the synthesis of southern tetrahydropyran unit, while Harvey demonstrated a three-component synthesis of northern conjugated diene unit.

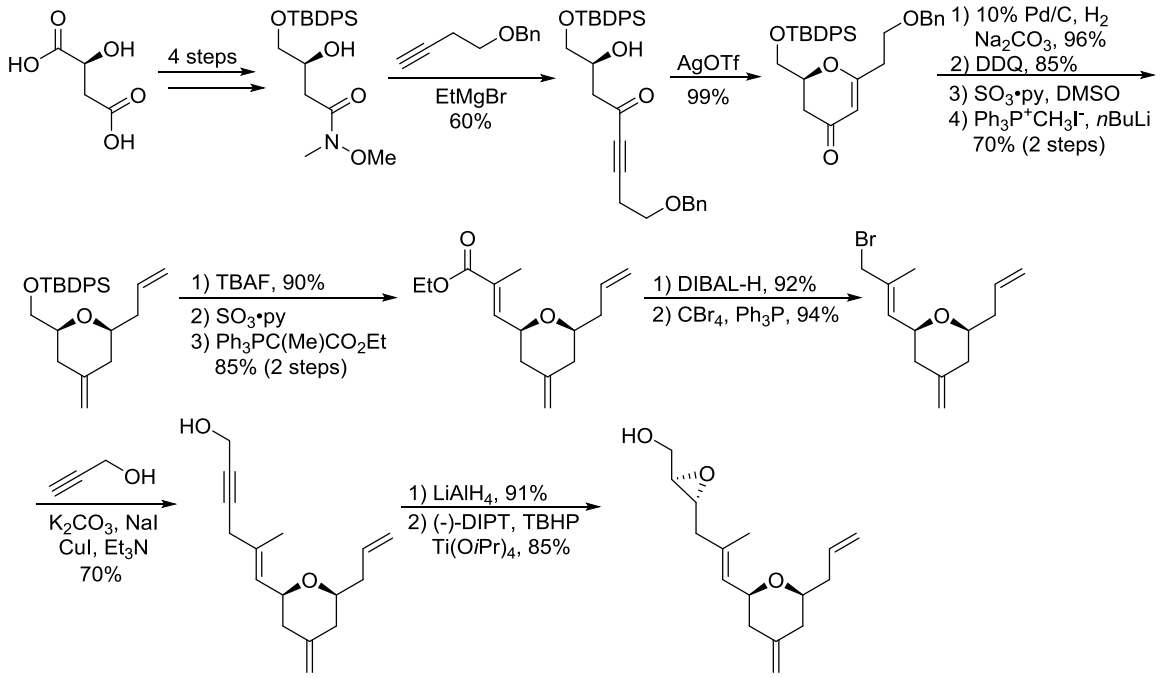

Scheme 2.3.27 Reddy's synthesis of C8 – C20 fragment of (–)-zampanolide (**1**).

Reddy and Srikanth demonstrated an alternative synthetic strategy towards tetrahydropyran fragment that synthesized by Hoye and co-workers[69] before. (Scheme 2.3.27) The synthesis was commenced from L-malic acid, which was transformed to a Weinreb amide with a reported 4-step protocol.[113] The extension of four-carbon fragment on Weinreb amide was performed at the presense of ethyl magnesium bromide. Key cyclization of alkynone into dihydropyranone was achieved at 99% yield under the treatment of AgOTf. Subsequent four-step transformation, included hydrogenation of alkene, removal of benzyl group, oxidation and Wittig reaction furnished the 2,6-*syn*-4-exomethylene tetrahydropyran. Subsequent treatment with TBAF (remove TBDPS), SO_3 py (oxidation) and Wittig reagent provided ethyl ester product, which was reduced

[113] Shioiri, T.; McFarlane, N.; Hamada, Y. *Heterocycles* **1998**, *47*, 73-76.

and brominated. The resulted bromide compound was introduced with another three carbon unit under a CuI/K_2CO_3/NaI-mediated coupling reaction.[114] The alkyne was then reduced to alkene and subsequent Sharpless asymmetric epoxidation provided the target tetrahydropyran fragment.

Taylor and co-workers demonstrated synthesis of C9 – C20 fragment of (–)-zampanolide (**1**) by applying their ether *transfer* methodology under treatment of iodine monochloride (ICl).[115] As shown in Scheme 2.3.28, they started the synthesis from an epoxide, which prepared from (*R*)-aspartic acid *via* a modified procedure.[116] The epoxide was opened *via* nucleophilic attack by vinyl magnesium bromide and the resulted chiral alcohol was further protected with benzyloxy methyl (BOM) group. Electrophilic activation by ICl resulted in 1,3-*syn*-diol monoether, which was transformed into *β*-alkoxyacrylate *via* tributylphosphine-catalyzed conjugate addition [117] with methyl propiolate. [118] Intramolecular radical cyclization converted the *β*-alkoxyacrylate into 2,6-*syn*-tetrahydropyran with high diasteroselectivity (d.r. > 20:1). Subsequent reduction and Grieco-Sharpless olefination[119] furnished the terminal olefin, which was subjected into olefin cross metathesis and Horner-Wadsworth-Emmons reaction to extend the fragment. Resulted dienoate was then reduced, transformed to epoxide *via* Sharpless asymmetric epoxidation, and its primary alcohol was protected with TBS group. Regioselctive epoxide opening was achieved by DIBAL-H subsequently, followed by desilylation and protection of 1,2-diol, to furnish the target C9 – C20 fragment of (–)-zampanolide (**1**).

[114] Yoshinari, T.; Ohmori, K.; Schrems, M. G.; Pfaltz, A.; Suzuki, K. *Angew. Chem. Int. Ed.* **2010**, *49*, 881-885.
[115] Liu, K.; Taylor, R. E.; Kartika, R. *Org. Lett.* **2006**, *8*, 5393-5395.
[116] Frick, J. A.; Klassen, J. B.; Bathe, A.; Abramson, J. M.; Rapoport, H. *Synthesis* **1992**, 621-623.
[117] Inanaga, J.; Baba, Y.; Hanamoto, T. *Chem. Lett.* **1993**, 241-244.
[118] Kartika, R.; Gruffi, T. R.; Taylor, R. E. *Org. Lett.* **2008**, *10*, 5047-5050.
[119] Grieco, P. A.; Gilman, S.; Nishizawa, M. *J. Org. Chem.* **1976**, *41*, 1485-1486.

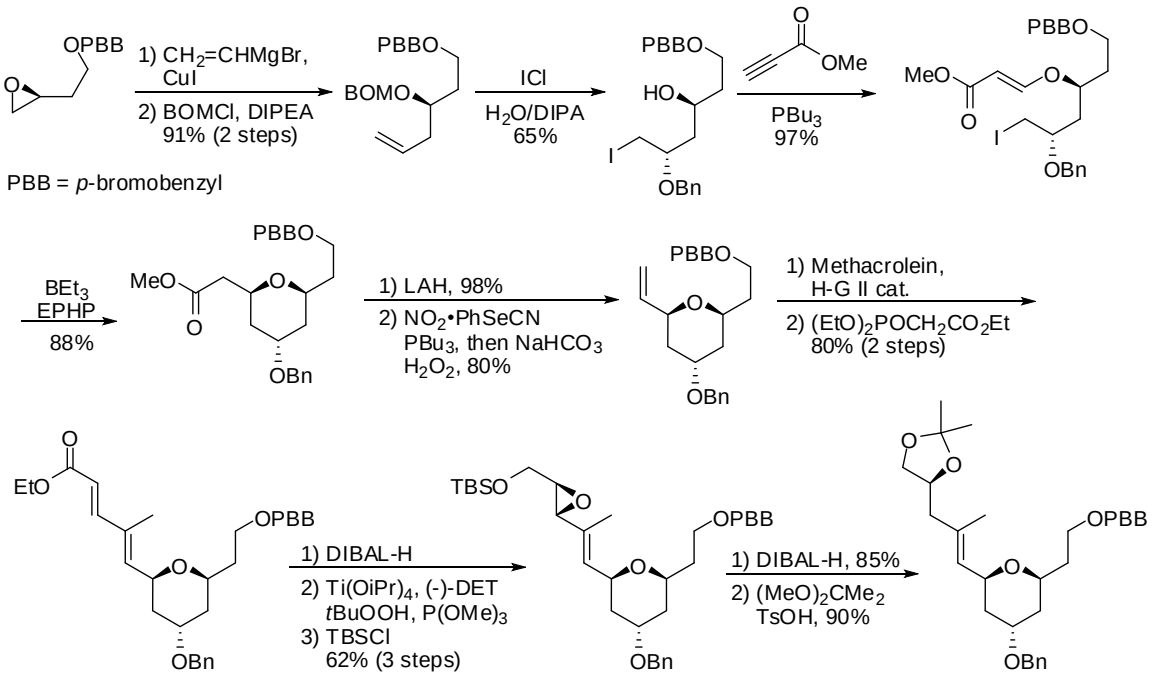

Scheme 2.3.28 Taylor's synthesis of C9 – C20 fragment of (–)-zampanolide (**1**).

On the other hand, Harvey and co-workers reported a three-component synthesis of conjugated dienoate, which involved an alcohol, enal and (triphenylphosphoranylidene)ketene (Ph3P=C=C=O, also known as Bestmann ylide[120]). They applied this methodology in synthesis of northern fragment (C9 – O – C16) of zampanolide. (Scheme 2.3.29) Preparation of enal component was started from acrolein, which was transformed into enyne *via* Barbier reaction and further protected with TBS group. Nucleophilic addition of alkyne onto methyl chloroformate yielded internal alkene, which was reduced into conjugated enoate. Reduction and oxidation of methyl ester group provided the enal for the three-component synthesis. A secondary alcohol, represented C16 – C20 fragment, and Bestmann ylide were introduced together with enal in toluene and finally furnished the target northern fragment of zampanolide.

[120] (a) Bestmann, H. J.; Sandmeir, D. *Chem. Ber.* **1980**, *113*, 274-277; (b) Bestmann, H. J.;Schobert, R. *Synthesis* **1989**, 419-423; (c) Bestmann, H. J.; Kellermann, W. *Synthesis* **1994**, 1257-1261.

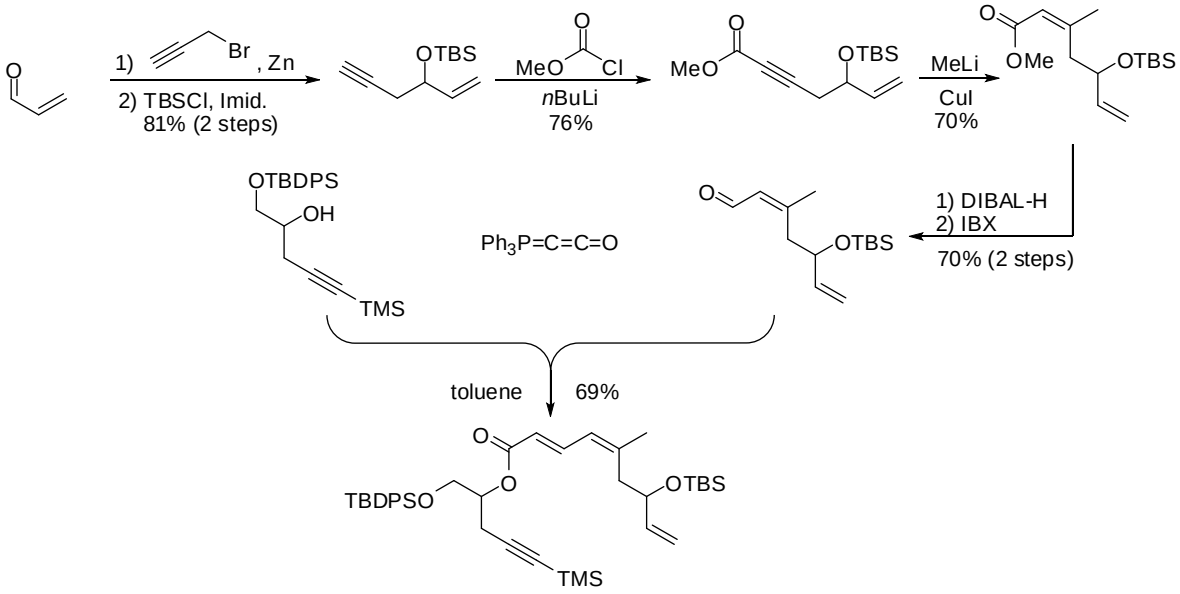

Scheme 2.3.29 Harvey's synthesis of C9 – O – C16 fragment of zampanolide.

2.3.14 Summary on reported total syntheses of zampanolide and dactylolide

This summary will provide an overview and comparison among reported total syntheses of zampanolide and dactylolide that introduced in previous section. The first syntheses of zampanolide and dactylolide were completed by Smith and co-workers in 2002.[59] Subsequently, another 11 research groups[60-62,64,69-76] completed these two compounds or their enantiomers in following decade. (Table 2.3.1, except Porco's group, who only achieved a formal synthesis towards macrolide core[77a,77b]) The highest overall yield towards macrolide core was 7.1%, which achieved by Keck's group on their synthesis of (+)-dactylolide (**2**),[72] while the shortest linear sequence was achieved by Uenishi's group.[60] They completed the synthesis of (–)-dactylolide (**2**) within 17 steps as of their longest sequence.

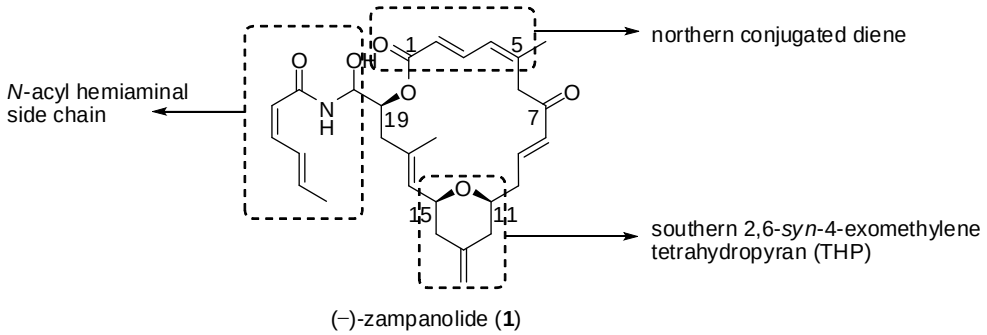

Scheme 2.3.30 Featured structures of (–)-zampanolide (**1**).

As shown in Scheme 2.3.30, there are three featured structures, namely *N*-acyl hemiaminal side chain, northern conjugated diene and southern 2,6-*syn*-4-exomethylene tetrahydropyran, identified in zampanolide. The latter diene and tetrahydropyran are common structures presented in dactylolide. Among the reported syntheses of zampanolide, *N*-acyl hemiaminal side chain was normally installed onto dactylolide,[60,61,62b,69,70] except Smith's Curtius rearrangement/acylation strategy.[59a,59c] (Scheme 2.3.31) Northern conjugated diene was mainly constructed *via* Horner-Wadsworth-Emmons reaction and its analogue, Wittig reaction. Metal-catalyzed cross coupling was also employed as synthetic strategy in the construction of northern conjugated diene. From the viewpoint of green chemistry, these synthetic strategies have their limitations, such as low atom economy (HWE and Wittig reaction), pre-installed activation group required and usage of toxic metal (metal-catalyzed coupling). (Scheme 2.3.32)

Year	Group	Cpd	Synthesis towards macrolide core			Highlights/Remarks
			Overall Yield	Total No. of Steps	Longest Sequence Steps	
2002	Smith[59a, 59c]	*ent*-**1**	5.0%[a]	36	14	1st reported synthesis Petasis-Ferrier Rearrangement (THP)
2002	Smith[59b]	**2**	0.6%	42	27	
2003	Hoye[69]	**1**	1.2%[b]	17	17	1st synthesis which install *N*-acyl hemiaminal side chain in one step Macrolactonization *via* Tin(IV)-mediated epoxy-acid coupling
2005	Floreancig[71]	**2**	3.0%[b]	23	19	
2005	Keck[72]	**2**	7.1%	25	20	One of the highest overall yield reported
2006	McLeod[74]	*ent*-**2**	2.5%[b]	23	16	
2008	Porco[75a,75b]	-	4.5%[a]	> 18	14	Synthesis was ended at macrolide core without converting to **1** or **2** or their enantiomer
2008	Jennings[64,73]	*ent*-**2**	6.2%[b]	32	24	
2009	Uenishi[60]	**1**	6.5%	37	17	Ru-catalyzed Kita-Trost macrolactonization at C1/O20
2010	Lee[75]	*ent*-**2**	8.2%[b]	21	17	
2010	Altmann[62a]	*ent*-**2**	4.8%	26	18	HWE-based macrocyclization at C8/C9
2012	Kim and Hong[76]	**2**	1.4%	33	19	NHC-catalyzed oxidative macrolactonization at C1/O20
2012	Ghosh[61,70]	**1**	1.4%	29	20	Chiral phosphoric acid promoted *N*-acyl hemiaminal side chain formation
2012	Altmann[62b]	**1**	See *ent*-**2** by Altmann in 2010			

***Table 2.3.1*:** Reported total syntheses from 2002 to 2012. [a] Calculated until ring closing. [b] Synthetic steps not fully reported, so actual overall yield should be lower than the value shown above.

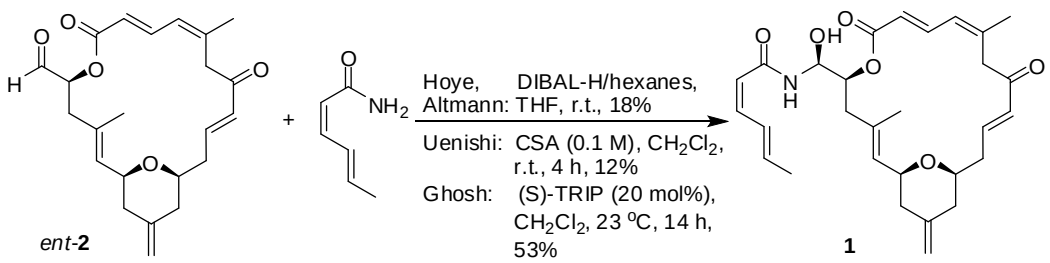

Scheme 2.3.31 Direct installation of *N*-acyl hemiaminal side chain onto (–)-dactylolide (*ent*-**2**).[60,61,62b,69,70]

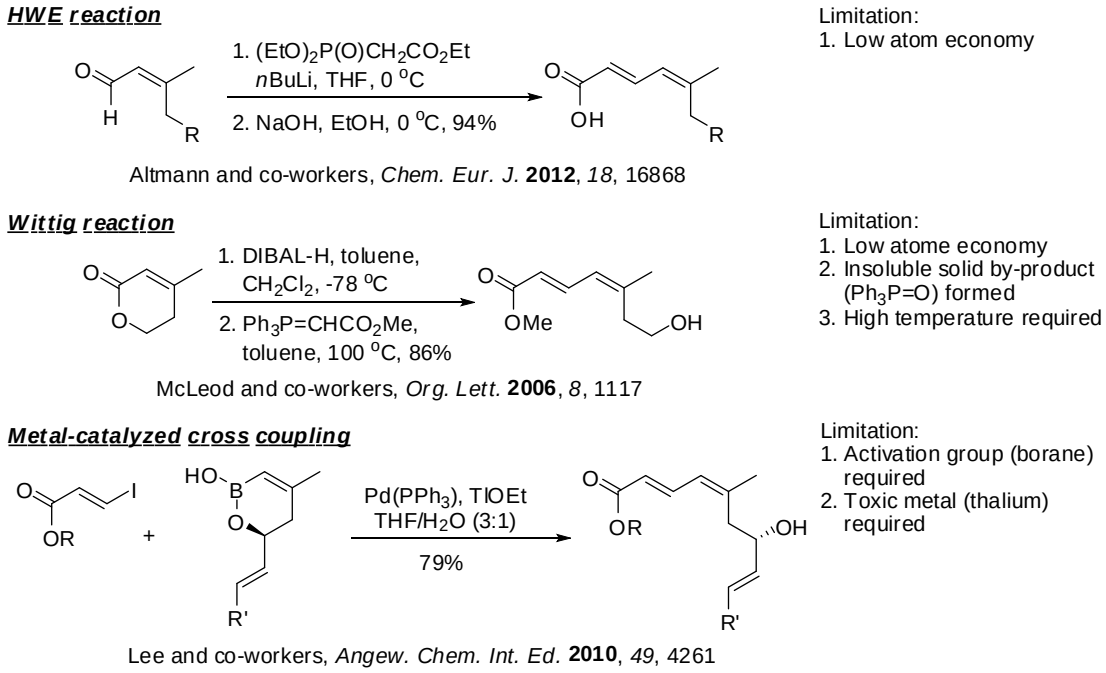

Scheme 2.3.32 Common strategies in the construction of northern conjugated diene.

Reported syntheses of southern tetrahydropyran ring are various from each other but could be categorized into two major groups of strategies, namely (a) involvement of trialkylsilyl-related reagent and (b) participation of sophisticated designed catalyst. Trialkylsilyl-related reagents, especially allylsilane, are proved to be efficient in the synthesis of tetrahydropyran ring. Such examples include Petasis-Ferrier union/rearrangement (Smith's synthesis),[59] intramolecular Sakurai cyclization (Hoye's[69] and Porco's[75a,75b] synthesis), Prins cyclization (Fluoreancig's[71] and Altmann's[62] synthesis), pyran annulations (Keck's synthesis),[72] oxocarbenium reduction (Jenning's synthesis)[64,73] and oxidative C-H activation (Ghosh's synthesis).[61,70] Although different

names were introduced in these syntheses, the formation of oxonium ion under Lewis acid conditions is involved in these strategies. These strategies are excellent in convergent synthesis of tetrahydropyran, however, in the expense of atom economy due to the removal of trialkylsilyl group at the end of the reaction.

On the other hand, Jacobsen hetero-Diels-Alder reaction (McLeod's strategy),[74] *O*-Michael reaction (Uenishi's strategy),[60] ruthenium-catalyzed Alder-ene reaction/palladium-catalyzed ring closure (Lee's strategy)[75] and organocatalytic 1,6-oxa conjugate addition (Kim and Hong's strategy)[76] required sophisticated catalyst, sometimes are expensive in cost economy perspective. However, these strategies are effective in the perspective of green chemistry.

In previous chapter, new methodologies in the construction of tetrahydropyran and conjugated diene that developed in our group were introduced. We envisioned that these strategies could provide a *greener* access to the synthesis of dactylolide. $In(OTf)_3$-catalyzed intramolecular 2,5-oxonium-ene cyclization[23] shows several advantages from the perspective of green chemistry and cost-effectiveness, include (a) increasing atom economy (no pre-installation of trialkylsilyl group and losing of 1 oxygen atom and 2 hydrogen atoms only), (b) using common, relatively safe and cheaper indium salt and (c) ambient reaction temperature. Metal-catalyzed direct cross coupling reaction also shows high atom economy because no pre-installation of activating group on participating alkenes is required and only 2 hydrogen atoms are removed during the reaction. In next chapter, we will demonstrate the application of these *green* strategies in the synthesis of dactylolide.

CHAPTER THREE

SYNTHETIC EFFORT TOWARDS TOTAL SYNTHESIS OF DACTYLOLIDE

As a continuous effort in demonstrating the practicability of our research group's methodologies, which provided *greener* access to 2,6-*syn*-4-exomethylene tetrahydropyrans and conjugated dienoates, dactylolide was chosen as our target natural product for demonstration. This chapter will introduce detailed synthetic efforts during these four-years of studies.

3.1 Retrosynthetic analysis

In this section, an overview of retrosynthetic analysis of target molecule, dactylolide, is provided as outlined in Scheme 3.1.1. During the course of our synthetic study towards the macrolide, we derived two synthetic routes, namely 1st Generation and 2nd Generation, which the latter replaced the unsuccessful former route.

We envisioned that the macrolide core of dactylolide could be constructed *via* esterification between C1 and O20. In 1st Generation Synthetic Route, the requisite conjugated diene ester/alcohol **ABC** precursor would be obtained by the formation of tetrahydropyran (THP) ring *via* Prins cyclization. The disconnection was planned at C11 – C12 and C15 – O bonds. This would result in homoallylic alcohol **A1** and aldehyde **BC**. We then anticipated that Fragment **BC** could be prepared from the union of vinyl iodide **B1** and aldehyde **C1** *via* Nozaki-Hiyama-Kishi (NHK) coupling.[121] Fragment **B1** could be accessed from 1,3-propanediol (**B3-1**), a main by-product in bio-fuel synthesis of fermentation,[122] while the featured diene structure within Fragment **C1** revealed that it could be arisen from two terminal alkenes, which were acrylate (**E1**) and protected isoprenol (**D1**), *via* our strategic dissection, namely metal-catalyzed direct cross coupling reaction.

On the other hand, the initial disconnection in 2nd Genration Synthetic Route, which enlightened by Altmann's work,[62] was planned at olefin C8 – C9 of precursor **ABC**. We anticipated that precursor **ABC** could be synthesized from aldehyde **AB** and phosphonate **C2** *via* Horner-Wadsworth-Emmons (HWE) reaction. The conjugated diene structure of

[121] (a) Takai, K.; Kimura, K.; Kuroda, T.; Hiyama, T.; Nozaki, H., *Tetrahedron Lett.* **1983,** *24*, 5281-5284; (b) Jin, H.; Uenishi, J.; Christ, W. J.; Kishi, Y., *J. Am. Chem. Soc.* **1986,** *108*, 5644-5646; (c) Takai, K.; Tagashira, M.; Kuroda, T.; Oshima, K.; Utimoto, K.; Nozaki, H., *J. Am. Chem. Soc.* **1986,** *108*, 6048-6050; (d) Stamos, D. P.; Sheng, X. C.; Chen, S. S.; Kishi, Y., *Tetrahedron Lett.* **1997,** *38*, 6355-6358.

[122] (a) Mendes, F. S.; González-Pajuelo, M.; Cordier, H.; François, J.M.; Vasconcelos, I. *Appl. Microbiol. Biotechnol.* **2011**, *92*, 519-527; (b) Barbirato, F.; Himmi, E. H.; Conte, T.; Bories, A. *Industrial Crops and Products* **1998**, *7*, 281-289.

phosphonate **C2** could be constructed from acrylate (**E1**) and phosphonate (**P1**) by employing metal-catalyzed direct cross coupling reaction. Disconnection at C14 – C15 and C11 – O bonds of THP unit of aldehyde **AB** resulted in aldehyde **A2** and homoallylic alcohol **B2**. Similar as 1st Generation Synthetic Route, homoallylic alcohol **B2** could be derived from 1,3-propanediol (**B3-1**).

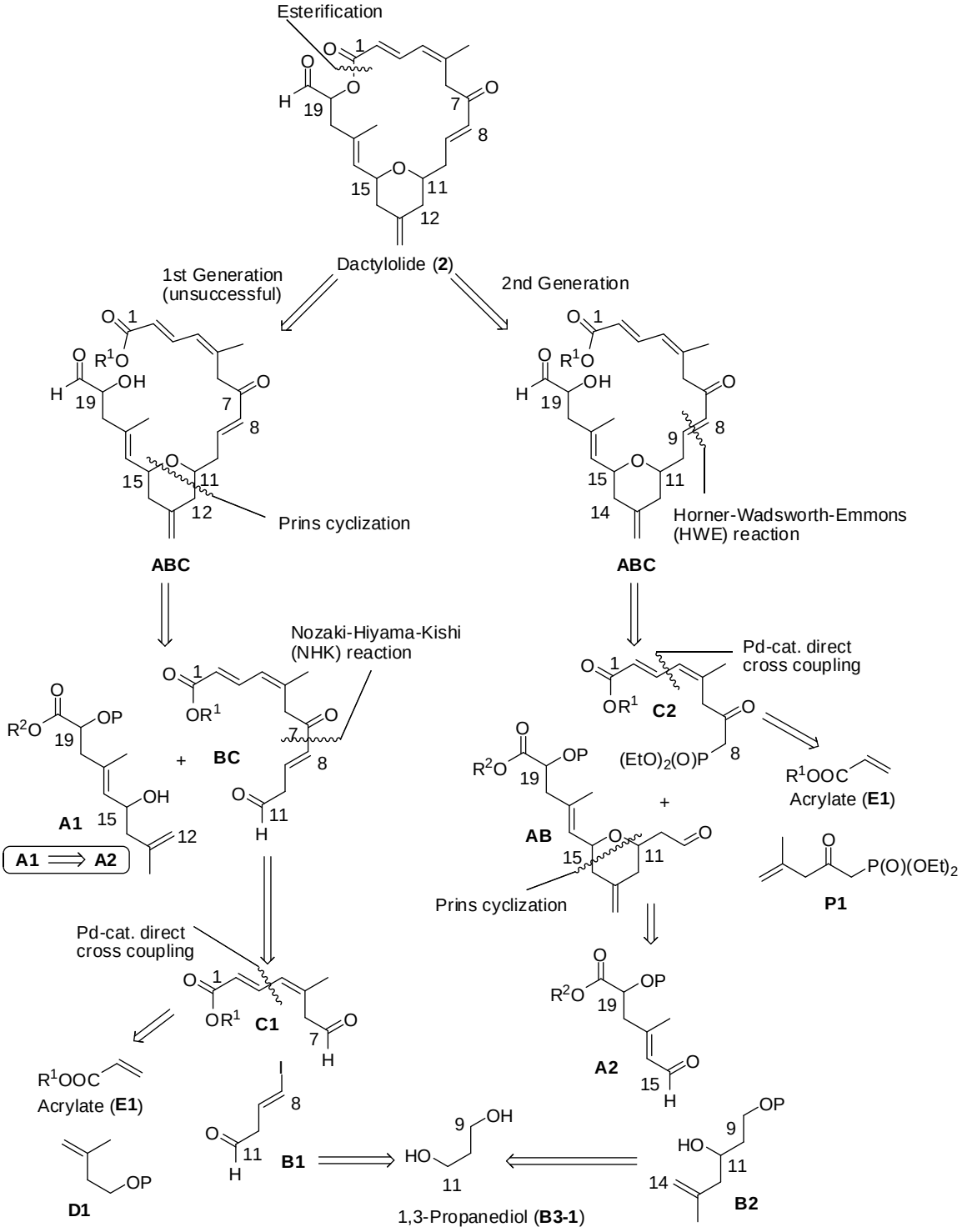

Scheme 3.1.1 An overview of retrosynthetic analysis of dactylolide.

3.2 Synthesis towards Fragment A and attempts to shorten the synthesis

3.2.1 Retrosynthetic analysis

As shown in the retrosynthetic analysis (Section 3.1.1), Fragment **A** could be designed as homoallylic alcohol **A1** or conjugated aldehyde **A2**. We envisioned that both molecules could be synthesized *via* a single synthetic route as shown in Scheme 3.2.1. Homoallylic alcohol **A1** could be transformed from aldehyde **A2** by employing indium-mediated allylation,[23,123] while conjugated aldehyde **A2** could be obtained *via* Horner-Wadsworth-Emmons (HWE) Reaction and selective functional group interconversion (FGI) from ketone **A3**. In order to achieve selective reduction in latter step, syntheses of ketone **A3** with different alkyl groups (R^2 = Et or *t*-Bu) were planned in this retrosynthetic analysis. The ketone **A3** could be derived from commercially available diethyl L-tartrate (**A4-1**) or ethyl glyoxalate[124] (**A5-1**) for R^2 = Et, and naturally occurring L-tartaric acid (**A4-2**) and *tert*-butanol (**12**) for R^2 = *t*-Bu.

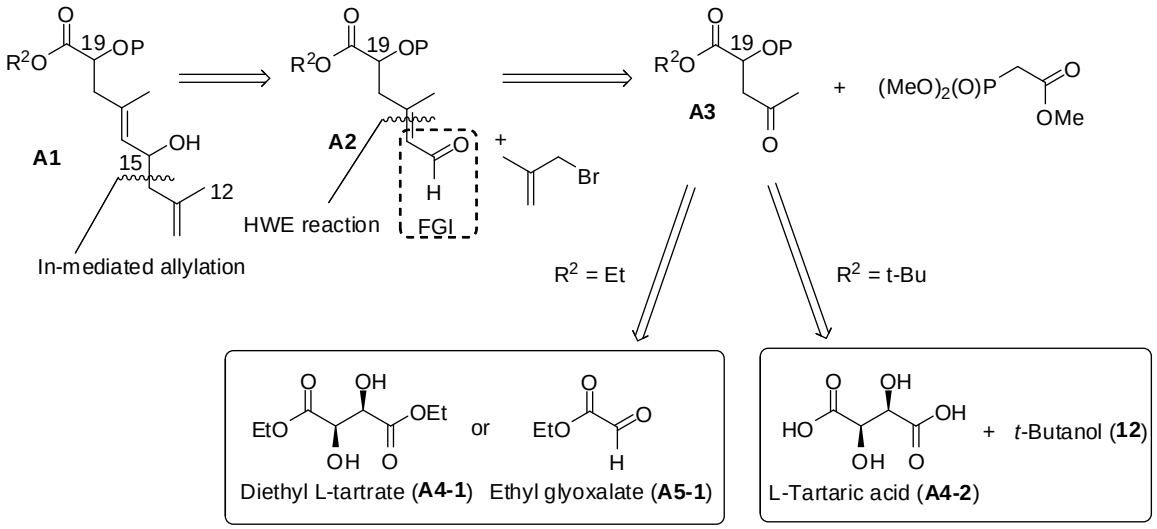

Scheme 3.2.1 Retrosynthetic analysis of Fragment **A1** and **A2**.

[123] Other examples of indium-mediated allylation: (a) Araki, S.; Ito, H.; Katsumura, N.; Butsugan, Y. *J. Org. Chem.* **1988**, 53, 1831-1833; (b) Li, C.-J.; *Chem. Rev.* **1993**, 93, 2023-2035; (c) Chan, T. H.; Li, C.-J.; Lee, M.-C.; Wei, Z. Y. *Can. J. Chem.* **1994**, 72, 1181-1192; (d) Cintas, P. *Synlett* **1995**, 1087-1096; (e) Chan, T. H.; Yang, Y. *J. Am. Chem. Soc.* **1999**, 121, 3228-3229.

[124] Also known as ethyl glyoxylate.

3.2.2 Synthetic efforts towards ketone A3

As illustrated in Scheme 3.2.1, ketone **A3** with two different alkyl groups, namely ethyl and *t*-butyl, were synthesized. Four different routes were employed and tested in the synthetic study towards ketone **A3**. Chronologically, route A and B were conducted in parallel to obtain ketone **A3-1** to **A3-4**. Route C and D were developed later in order to obtain ketone **A3-1** and **A3-4** in higher yield.

3.2.2.1 Route A

Synthesis of ketone **A3-1** (R^2 = Et, PG = TIPS), **A3-2** (R^2 = Et, PG = PMB), **A3-3** (R^2 = Et, PG = TBDPS) could be achieved in 3 steps. The synthetic route was started with conversion of diethyl L-tartrate (**A4-1**) into ethyl glyoxalate hydrate (**A6-1**),[125] followed by aldol reaction in aqueous solution. (Scheme 3.2.2) The common conditions of aldol condensation, which employed lithium diisopropylamide (LDA) as base and THF as solvent, was tested initially, but only provided trace amount of desired ketone **A7-1**. Alternatively, a catalytic aldol reaction in aqueous solution,[126] which utilized 20 mol% diethylenetriamine as base and 40 mol% D-(–)-tartaric acid as additive, was employed and successfully provided ketone **A7-1** with a yield of 38% over two steps albeit progressing slowly (4 days).

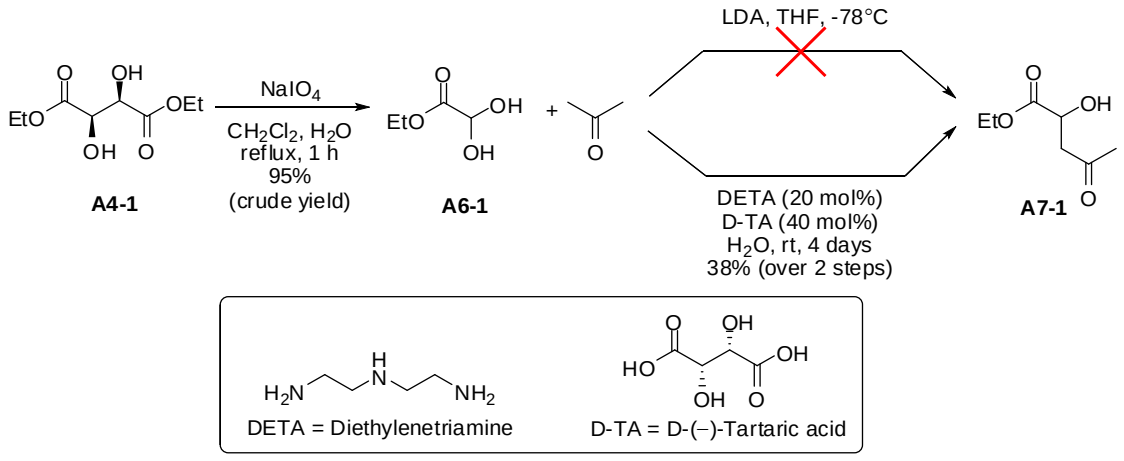

Scheme 3.2.2 Synthetic Route A towards ketone **A7-1**.

[125] (a) Hursthouse, M. B.; Malik, K. M. A.; Hibbs, D. E.; Roberts, S. M.; Seago, A. J. H.; Sik, V.; Storer, R. *J. Chem. Soc., Perkin Trans. 1* **1995**, 2419-2425; (b) Bailey, P. D.; Smith, P. D.; Pederson, F.; Clegg, W.; Rosaira, G. M.; Teatb, S. J. *Tetrahedron Lett.* **2002**, *43*, 1067-1070.

[126] The condition employed in the aldol reaction is adapted from a preliminary study in our research group.

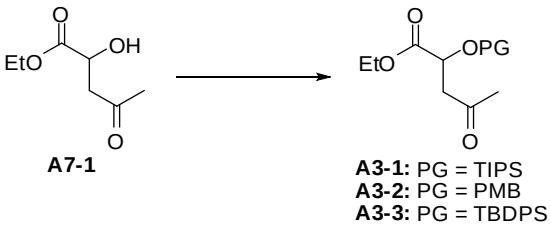

Entry	Reagent	Base	Catalyst	Solvent	Temp.	t	Product	Yield
1	TIPSOTf	2,6-lutidine	-	CH_2Cl_2,	0 ℃ – rt	16 h	A3-1	0%
2	TIPSCl	pyridine	-	DMF	rt	16 h	A3-1	0%
3	TIPSCl	TEA	-	DMF	rt	16 h	A3-1	0%
4	TIPSCl	2,6-lutidine	-	DMF	rt	16 h	A3-1	0%
5	**TIPSCl**	**imidazole**	**-**	**DMF**	**rt**	**16 h**	**A3-1**	**76%[a]**
6	TIPSCl	imidazole	-	DMF	100 ℃	16 h	A3-1	56%
7	TIPSCl	imidazole	-	DMF	reflux	16 h	A3-1	0%
8	TIPSCl	imidazole	DMAP	DMF	rt	2 days	A3-1	70%
9	TIPSCl	imidazole	DMAP	CH_2Cl_2	reflux	16 h	A3-1	57%
10	TIPSCl	imidazole	DMAP	THF	reflux	1 day	A3-1	NC[b]
11	PMBCl	NaH	-	THF	0 ℃		A3-2	0%
12	TBDPSCl	imidazole	-	CH_2Cl_2	0 ℃ – rt	2 h	A3-3	70%

Table 3.2.1 Screening of reaction conditions for alcohol protection of ketone **A7-1**. [a] Yield based on recovered starting materials (brsm); [b] NC: Not completed.

With ketone **A7-1** in hand, the synthesis was continued with alcohol protection to obtain ketone **A3**. A series of conditions screening was conducted and listed in Table 3.2.1. Initially, a relatively reactive silylating reagent, TIPSOTf, was attempted and resulted in complex compound without yielding any desired product **A3-1**. (Entry 1) Next, TIPSCl, a milder silylating reagent, was tested with various types of bases. Among bases attempted in Entry 2 to 5, only imidazole provided ketone **A3-1** with a yield of 76% (brsm) under rt. (Entry 5) Increasing temperature (Entry 6 and 7) did not enhance the reaction. Addition of DMAP as catalyst in different solvents (Entry 8 to 10) also failed to accelerate the reaction. In addition, alcohol protection with PMB group to obtain ketone **A3-2** was failed. (Entry 11) It was noticed that vigorous reaction happened once alcohol **A7-1** was added into solution of sodium hydride (NaH). Alcohol protection with TBDPS group was smoothly completed with a yield of 70%. (Entry 12)

The overall yield of Route A towards ketone **A3-1** was 29% (3 steps). Major drawbacks of this route included low overall yield, long reaction time and inconsistent yield in alcohol protection.

3.2.2.2 Route B

Synthesis of ketone **A3-4** (R^2 = *t*-Bu, PG = TIPS) was also conducted in this synthetic study. (Scheme 3.2.3) Since there was no commercially available di-*t*-butyl-L-tartrate (**A4-3**), Luthman's method was adapted to synthesize **A4-3** and subsequent *t*-butyl glyoxalate hydrate (**A6-2**).[127] During the synthesis of **A6-2**, we noticed that extra peaks were showed in ^{1}H NMR spectrum of **A6-2**. This situation was also reported in other's work.[128] It is strongly believed that a mixture of *t*-butyl glyoxalate and *t*-butyl glyoxalate hydrate **A6-2** was obtained eventually.

Ketone **A7-2** was then obtained *via* catalytic aldol reaction described in Route A. With ketone **A7-2** in hand, the hydroxyl group was subsequently protected with TIPS group by employing the optimal conditions in Route A. The desired ketone **A3-4** was finally obtained in high yield of 99%. Meanwhile, attempt to protect the hydroxyl group of **A7-2** with acetyl group (Ac) only provided 20% of desired ketone **A3-5**. The major product obtained in this protection was highly conjugated bicarbonyl compound **A3-5b**, which implies that the α-proton next to carbonyl group in ketone **A7-2** was highly susceptible to base. This also explained why reaction became vigorous when ketone **A7-1** was added in NaH solution. (Table 3.2.1, Entry 11)

The overall yield of Route B towards ketone **A3-4** was 14% (4 steps).

[127] Våbenø, J.; Brisander, M.; Lejon, T.; Luthman, K. *J. Org. Chem.* **2002**, *67*, 9186-9191.
[128] Anderson, I. Synthesis of Amide Bond Isosteres Incorporated in the Minimal Glycopeptide Recognized by T Cells in a Mouse Model for Rheumatoid Arthritis. Master Thesis in Organic Chemistry, Umeå University, Sweden, **2005**.

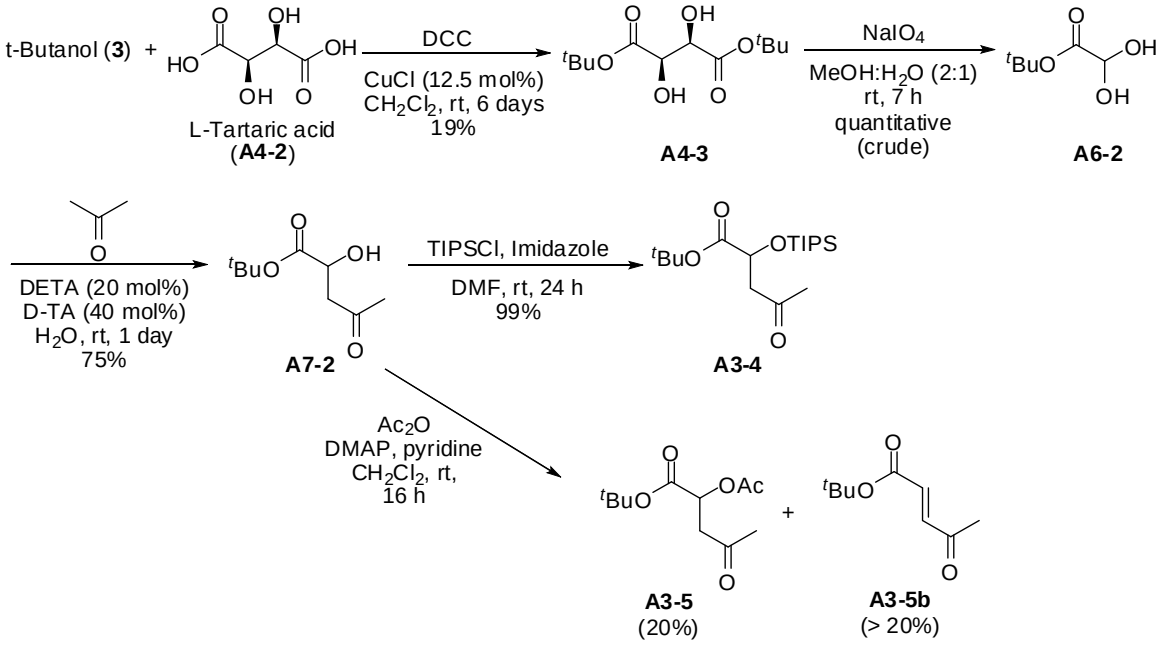

Scheme 3.2.3 Synthetic Route B towards ketone **A3-4**.

3.2.2.3 Route C

Due to the low efficiency in Route A and B, we then redesigned our synthetic route (Scheme 3.2.4) by first synthesizing homoallylic alcohol **A8-1** from commercially available ethyl glyoxalate (**A5-1**) *via* indium-mediated allylation, which was reported by our group in 2002.[23] Although insufficient stirring happened during gram-scale synthesis due to clumping of indium metal, the homoallylic alcohol **A8-1** was obtained successfully in an average yield of 72%. (Highest yield of a single reaction could reach 99%)

The synthesis was then continued by alcohol protection with TIPS group. Compared with alcohol protection of **A7-1** in Route A, the lack of reactive α-proton in **A8-1** allowed the alcohol reacting with more reactive silylating reagent, TIPSOTf, without causing any side reactions, and yielded the desired alkene **A9-1** at an excellent yield of 94%. The alkene **A9-1** was oxidized by ozonolysis to yield target ketone **A3-1** with a moderate yield of 74%.

This new route provided higher overall yield of 50% (3 steps).

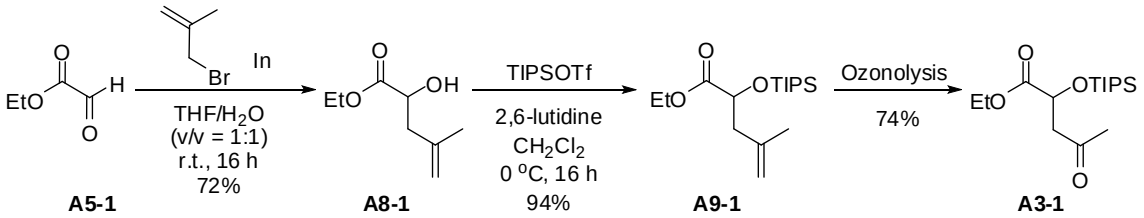

Scheme 3.2.4 Synthetic Route C towards ketone **A3-1**.

3.2.2.4 Route D

With well established synthetic route towards ethyl ester **A3-1**, *t*-butyl ester analogue **A3-4** was planned to be synthesized with similar methods applied in Route C. The synthesis was started with esterification of L-tartaric acid (**A4-2**), followed by cleavage of diol **A4-3** into *t*-butyl glyoxalate **A5-2** as introduced in Route B. Initially, crude mixture of *t*-butyl glyoxalate hydrate **A6-2** was subjected into subsequent indium-mediated allylation[23] but to no avail. Therefore, distillation was performed on the crude mixture in order to acquire pure *t*-butyl glyoxalate **A5-2**.[129] With the pure **A5-2** in hand, the allylation processed albeit only a yield of 29% was achieved. The resulted homoallylic alcohol **A8-2** was then protected with TIPS group by employing conditions applied in Route B. However, due to the failure in subsequent Horner-Wadsworth-Emmons reaction (Entry 3, Table 3.2.3), this route was abandoned without further attempt on ozonolysis.

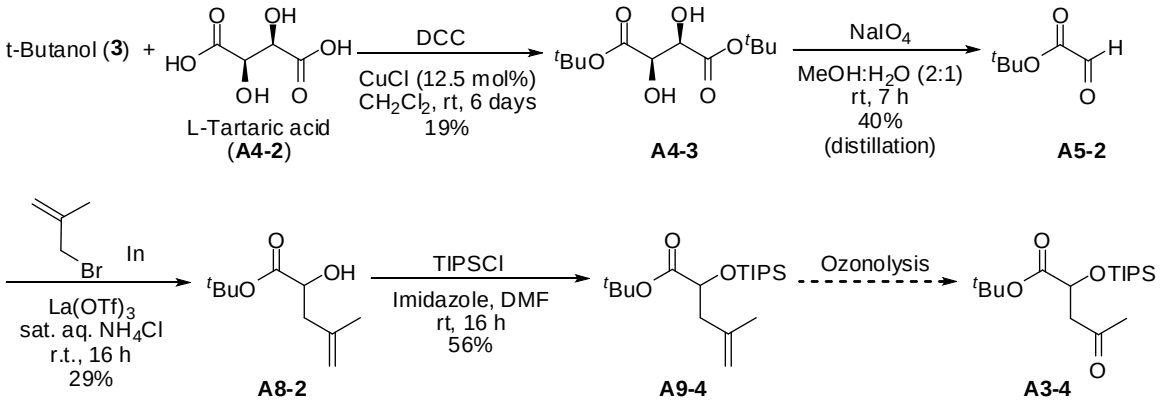

Scheme 3.2.5 Synthetic Route D towards ketone **A3-4**.

[129] Distillation of *t*-butyl glyoxalate **A5-2** was performed at 2.4 kPa, 40 – 41°C. Ref: Yamamoto, Y.; Shirai, T.; Miyaura, N. *Chem. Commun.* **2012**, *48*, 2803-2805.

3.2.2.5 Summary of synthetic efforts towards ketone A3

A summary of synthetic efforts towards ketone **A3** is listed in Table 3.2.2. Route C was the most optimum route for further synthesis of Fragment **A** due to its relatively high yield and shorter reaction time compared with another three routes. An overview of these four synthetic routes is summarized in Scheme 3.2.6.

Synthetic Route	Final Product	Overall Yield	No. of Steps	Reaction Time[a]	Major Drawbacks
Route A	A3-1	29%	3	5 days	Low overall yield, inconsistent yield due to reactive α-proton
Route B	A3-4	14%	4	9 days	Long reaction time
Route C	**A3-1**	**50%**	**3**	**< 2 days**	
Route D	A9-4	1.2%	4	9 days	Extremely low overall yield, long reaction time

Table 3.2.2 Summary of synthetic efforts towards ketone **A3**. [a] Approximate period, not included work-up and purification steps.

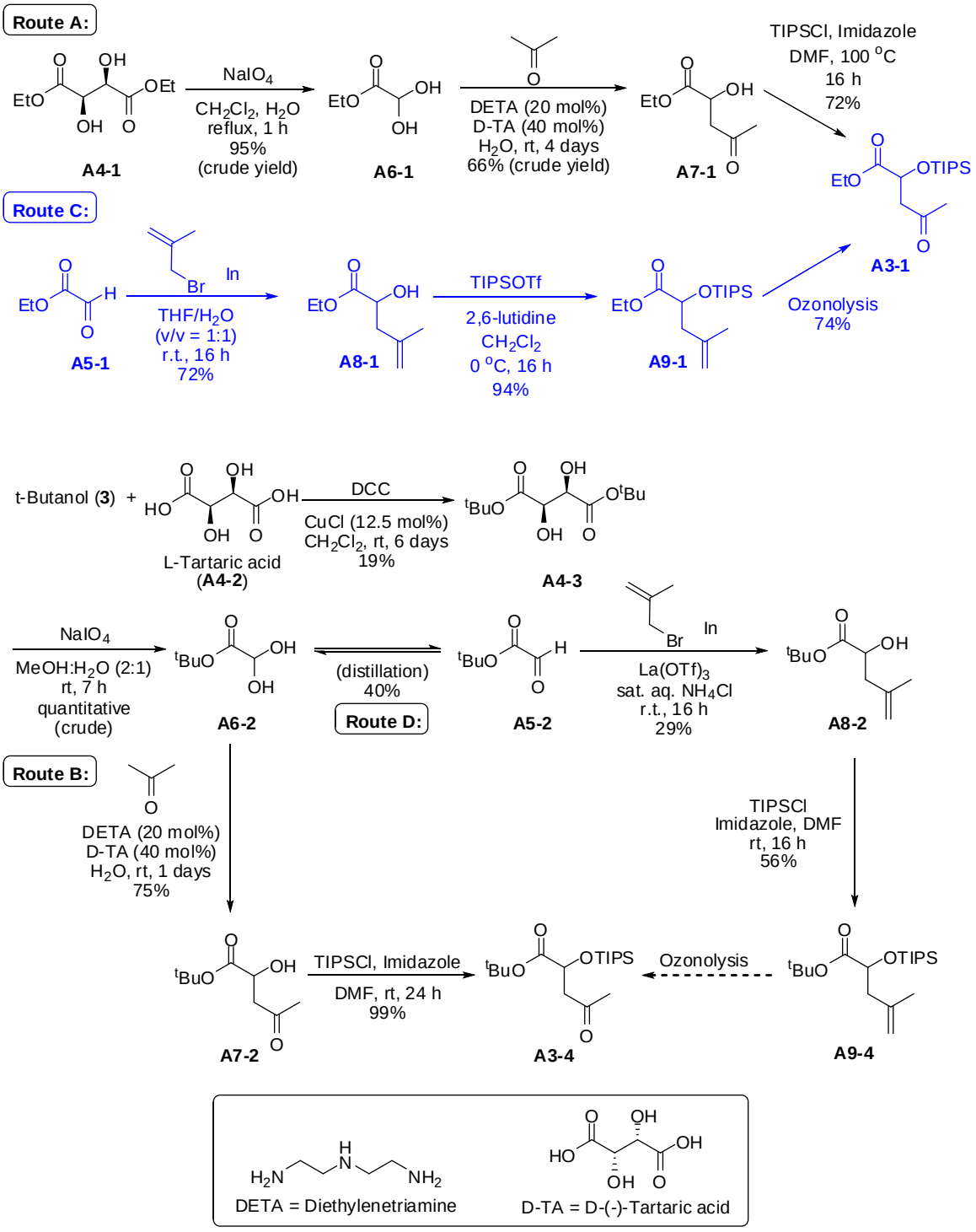

Scheme 3.2.6 An overview of synthetic efforts towards ketone **A3**.

3.2.3 Synthetic efforts towards aldehyde A2 and homoallylic alcohol A1

3.2.3.1 Olefin C16 – C17 construction

The olefin C16 – C17 of the macrolide core of dactylolide was planned to be synthesized *via* Wittig reaction or its analogue Horner-Wadsworth-Emmons (HWE) reaction, common strategies that chemistry communities utilize in olefin construction. (Section 1.3.3.1)

Initially, non-protected alcohol **A7-1** was coupled with phosphonate-stabilized carbanion, generated from trimethyl phosphonoacetate by NaH in toluene. As part of the effort to synthesize the target molecule through Green Chemistry, this reaction would allow us to skip protection step. However, instead of desired product, a highly conjugated diester **A13** was obtained. (Scheme 3.2.7)

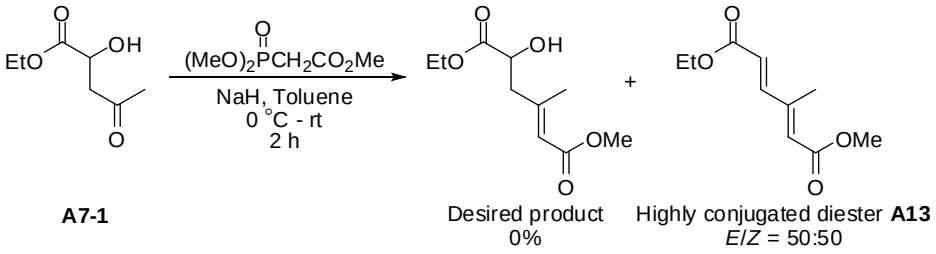

Scheme 3.2.7 Attempt to construct olefin C16-C17 from non-protected alcohol **A7-1**.

Due to inaccessibility from **A7-1**, synthesis was continued with coupling reaction between ketone **A3**, which alcohol had been protected in advance, and phosphonium ylide (Wittig reagent) or phosphonate-stabilized carbanion to construct target olefin C16 – C17. The coupling reaction was tested with three different ketone **A3**s that were synthesized before. (Table 3.2.3) But unfortunately, coupling reaction between ketone **A3-3** (R^2 = Et, PG = TBDPS) and phosphonium ylide (Entry 1) or triethyl phosphonoacetate (Entry 2) did not provide any product. Discouraging result was also obtained when ketone **A3-4** (R^2 = *t*-Bu, PG = TIPS) reacted with trimethyl phosphonoacetate (Entry 3), even though temperature was increased to 100 ℃. The unsuccessful attempt to synthesize **A10-4** from **A3-4** ultimately led to cessation of Route D, which was initially developed to synthesize ketone **A3-4** in higher yield. (Section 3.2.2.4)

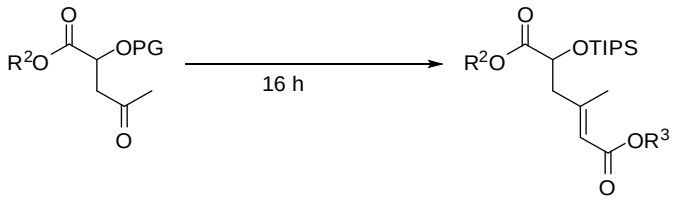

A3-1: R^2 = Et, PG = TIPS
A3-3: R^2 = Et, PG = TBDPS
A3-4: R^2 = t-Bu, PG = TIPS

A10-1: R^2 = Et, PG = TIPS, R^3 = Me
A10-2: R^2 = Et, PG = TBDPS, R^3 = Me
A10-3: R^2 = Et, PG = TBDPS, R^3 = Et
A10-4: R^2 = t-Bu, PG = TIPS, R^3 = Me

Entry	Ketone	Reagent[a]	Base	Solvent	Temp.	Product	Yield (*E*/*Z*)
1	A3-3	I	-	THF	reflux	A10-2	0%
2	A3-3	II	NaH	toluene	0 ℃ - rt	A10-3	0%
3	A3-4	III	NaH	toluene	rt – 100 ℃	A10-4	0%
4	A3-1	I	-	THF	reflux	A10-1	0%
5	A3-1	III	NaH	toluene	0 ℃ - rt	A10-1	NC
6	A3-1	III	NaH	toluene	70 ℃	A10-1	39% (67:33)
7	A3-1	III	NaH	toluene	100 ℃	A10-1	28%
8	A3-1	III	NaH	THF	60 ℃	A10-1	7%
9	A3-1	III	PhLi	THF	rt	A10-1	28% (63:37)
10	**A3-1**	**III**	**BuLi**	**THF**	**rt**	**A10-1**	**42% (67:33)**
11	A3-1	III	MeMgBr	THF	reflux	A10-1	0%
12	A3-1	III	DBU, LiCl	CH_3CN	rt	A10-1	0%

Table 3.2.3 Screening of reaction conditions for olefin synthesis from ketone **A3**. [a] Reagent I: $Ph_3P{=}CHCO_2Me$; II: $(EtO)_2POCH_2CO_2Et$, III: $(MeO)_2POCH_2CO_2Me$

Effort to construct olefin C16 – C17 from ketone **A3-1** (R^2 = Et, PG = TIPS) with the presence of phosphonium ylide did not yield any desired product **A10-1**. (Entry 4) However, by changing the coupling reagent to trimethyl phosphonoacetate, the conjugated ester **A10-1** was finally obtained at a yield of 39% with *E*/*Z* selectivity of 67:33 under the most optimal temperature of 70 ℃. (Entry 6)

During the screening of reaction conditions, we observed that the viscous suspension of NaH in toluene led to inefficient stirring. Changing the solvent from toluene to THF resulted in less viscous suspension but the yield was lowered. (Entry 8) Stronger base, including PhLi (Entry 9) and BuLi (Entry 10), were investigated next. To our delight, a better average yield of 42% was obtained when BuLi was used in THF as solvent. The *E*/*Z* selectivity remained as 67:33.

Apart from conventional HWE reaction, MeMgBr-promoted highly (*E*)-selective Wadsworth-Emmons Reaction,[130] which claimed by Davies's group that it supersedes Masumune-Roush conditions (DBU/LiCl)[131] in terms of (*E*)-selectivity, was also applied in our synthesis of **A10-1**. However, Davies's strategy, as well as Masumune-Roush strategy, failed to provide any product. (Entry 11 and 12)

3.2.3.2 Selective ester reduction

With the mixture of *E*- and *Z*-conjugated ester **A10-1** in hand, we next intended to reduce the conjugated methyl ester of **A10-1** to alcohol **A11**. However, this reduction needed to be conducted selectively because **A10-1** has an ethyl ester, which is easier to be reduced compared with conjugated methyl ester.

A series of conditions were screened to find the most optimum conditions for the selective reduction. (Table 3.2.4) $NaBH_4$, a common reduction agent, failed to provide any reaction. (Entry 1) Then, different types of diisobutylaluminum hydride (DIBAL-H) solutions were tested along with various reaction solvents at -78 ℃ for 24 h. The search of most optimum conditions for obtaining alcohol **A11** was challenging at the beginning. No reaction was observed when DIBAL-H solution in cyclohexane was tested in two different reaction solvents, which were THF and CH_2Cl_2. (Entry 2 - 3) Same discouraging results were obtained when DIBAL-H solution in THF was tested in heptane and CH_2Cl_2. (Entry 4 - 5) Performing the reaction in toluene, however, over-reduced the diester **A10-1** and yielded undesired diol product. (Entry 6)

Changing DIBAL-H to its toluene solution, surprisingly, provided solvent-dependent results. Performing the reaction in diethyl ether and heptane did not yield any products but recovered starting materials. (Entry 7 - 8) Changing solvent to THF provided the desired allylic alcohol **A11** in a yield of 23% together with undesired side product aldehyde **A14** (10%). (Entry 9) Conducting the reaction in CH_2Cl_2 yielded single product **A11** in a yield of 44%, but the *E*/*Z* selectivity was slightly deteriorated. (Entry 10)

[130] Claridge, T. D. W.; Davies, S. G.; Lee, J. A.; Nicholson, R. L.; Roberts, P. M.; Russell, A. J.; Smith, A. D.; Toms, S. M. *Org. Lett.* **2008**, *10*, 5437.
[131] Blanchette, M. A.; Choy, W.; Davis, J. T.; Essenfield, A. P.; Masamune, S.; Roush, W. R.; Sakai, T. *Tetrahedron Lett.* **1984**, *25*, 2183.

DIBAL-H solution in heptanes was also tested in the screening. As shown in Table 3.2.4, only undesired aldehyde **A14** was obtained when hexane, CH_2Cl_2 and toluene were employed as solvent. (Entry 11 to 13) In contrast to the results above, changing solvent to ether solvents, such as diethyl ether and THF, provided our desired allylic alcohol **A11** as sole product. Alcohol **A11** was obtained at a yield of 22% when the reaction was conducted in diethyl ether (Entry 14), while higher yield of 45% was achieved when THF was chosen as reaction solvent. (Entry 15)

Next, we investigated the effect of reaction temperature in this selective reduction. Increasing the temperature from -78 ℃ to -40 ℃ had a positive effect on reaction yield. The yield was raised from 45% to 58%. (Entry 16) However, further increasing the temperature to 0 ℃ deteriorated the reaction yield to 32%. (Entry 17)

As a result, the best conditions to perform selective reduction of **A10-1** were employing DIBAL-H solution in heptanes as base and THF as reaction solvent at -40 ℃ for 24 h.

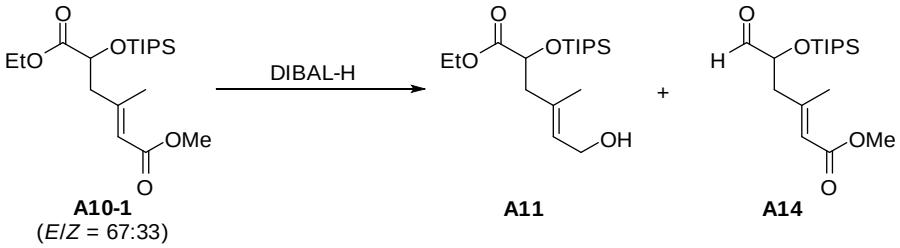

A10-1 (*E*/*Z* = 67:33) **A11** **A14**

Entry	Solvent of DIBAL-H solution	Solvent	temp.	t	A11 (*E*/*Z*)	A14[a]
1	$NaBH_4$	MeOH	Reflux	> 24 h	No reaction	
2	Cyclohexane	THF	-78 ℃	24 h	No reaction	
3	Cyclohexane	CH_2Cl_2	-78 ℃	24 h	No reaction	
4	THF	Heptane	-78 ℃	24 h	No reaction	
5	THF	CH_2Cl_2	-78 ℃	24 h	No reaction	
6	THF	Toluene	-78 ℃	24 h	diol found	
7	Toluene	Et_2O	-78 ℃	24 h	No reaction	
8	Toluene	Heptane	-78 ℃	24 h	No reaction	
9	Toluene	THF	-78 ℃	24 h	23% (65:35)	10%
10	Toluene	CH_2Cl_2	-78 ℃	24 h	44% (62:38)	-
11	Heptane	Hexane	-78 ℃	1 h	-	found
12	Heptane	CH_2Cl_2	-78 ℃	3 h	-	17%
13	Heptane	Toluene	-78 ℃	24 h	-	20%
14	Heptane	Et_2O	-78 ℃	24 h	22% (66:34)	-
15	Heptane	THF	-78 ℃	24 h	45% (70:30)	-
16	**Heptane**	**THF**	**-40 ℃**	**24 h**	**58% (67:33)**	-
17	Heptane	THF	0 ℃	24 h	32% (63:37)	-

Table 3.2.4 Screening of selective reduction of **A10-1**. [a] Only yield of **A14**, if shown, was determined, *E*/*Z* ratio was not determined.

3.2.3.3 Synthesis of conjugated aldehyde A2 and homoallylic alcohol A1

The targeted homoallylic alcohol **A1** in 1st Generation Synthetic Route and conjugated aldehyde **A2** in 2nd Generation Synthetic Route could be synthesized once (*E*)-allylic alcohol **A11** was ready. Upon stirring with Dess-Martin periodinane (DMP), a common oxidizing reagent for the synthesis of aldehyde, conjugated aldehyde (*E*)-**A2** was obtained in a yield of 75%. During the preparation of **A2**, we noticed that the conjugated aldehyde (*E*)-**A2** was highly unstable and gradually interconvert to a mixture of (*E*)- and (*Z*)-isomers even under -20 ℃.

Due to its instability, the crude product of (*E*)-**A2** was subjected into the subsequent synthesis of homoallylic alcohol **A1**. Without concerning of enantioselectivity of the final product, indium-mediated allylation in aqueous media that adapted in the early synthesis of Fragment **A**, was utilized. However, higher temperature (40 ℃) and longer reaction time (48 h) were required to drive the reaction to completion.

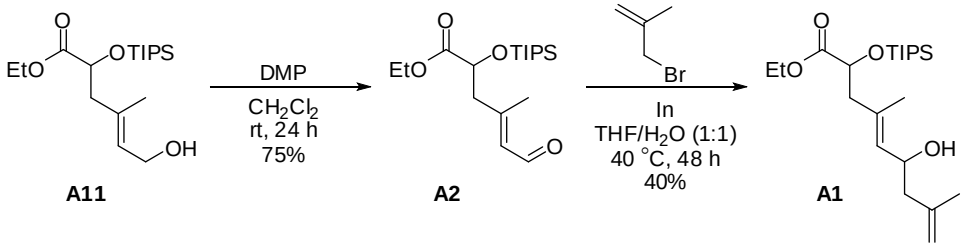

A11 **A2** **A1**

Scheme 3.2.8 Synthesis of conjugated aldehyde **A2** and homoallylic alcohol **A1**.

3.2.3.4 Summary of synthesis of Fragment A and attempt to shorten the synthetic route

As illustrated previously, synthesis of homoallylic alcohol **A1** required in 1st Generation Synthetic Route was achieved in 7 steps with an overall yield of 4.5% (*E*/*Z* = 67:33), while conjugated aldehyde **A2**, which was the essential fragment in 2nd Generation Synthetic Route, was achieved in 6 steps with an overall yield of 11.3% (*E*/*Z* = 67:33).

In spite of successful synthesis of Fragment **A**, several improvements could be made in order to fulfill Green Chemistry. One of them was reducing derivatives during synthesis. We noticed that other than Horner-Wadsworth-Emmons reaction, the Nobel prize-awarded olefin metathesis could be a *greener* strategy to construct alkene C16 – C17.[132] By bypassing the ozonolysis, conjugated ester **A10-1** could be synthesized from alkene **A9-1** directly if olefin metathesis worked in our case. However, this intention was disrupted since there was no reaction observed when the coupling was attempted between alkene **A9-1** and methyl acrylate **E1-3** with 5 mol% Hoveyda-Grubbs II catalyst in either dichloroethane or toluene under reflux.[133]

With the failure in olefin metathesis, we also intended to shorten the synthesis by omitting reduction-oxidation from conjugated ester **A10-1** to aldehyde **A2**. This attempt was made by constructing olefin C16 – C17 of aldehyde **A2** *via* Horner-Wadsworth-Emmons reaction directly from ketone **A3-1** with a prepared phophonate.[134] However, no reaction was observed either BuLi or LiCl/DIPEA[131] was employed.

As a result, the synthesis of Fragment **A** remained as what we had achieved early.

[132] Similar strategy was employed by Ghosh's group in their synthesis of (–) -zampanolide (see Section 2.3.11).
[133] Chatterjee, A. K.; Choi, T.-L.; Sanders, D. P.; Grubbs, R. H. *J. Am. Chem. Soc.* **2003**, *125*, 11360-11370.
[134] Nagata, W.; Wakabayashi, T.; Hayase, Y. *Organic Syntheses* **1973**, *53*, 44-48.

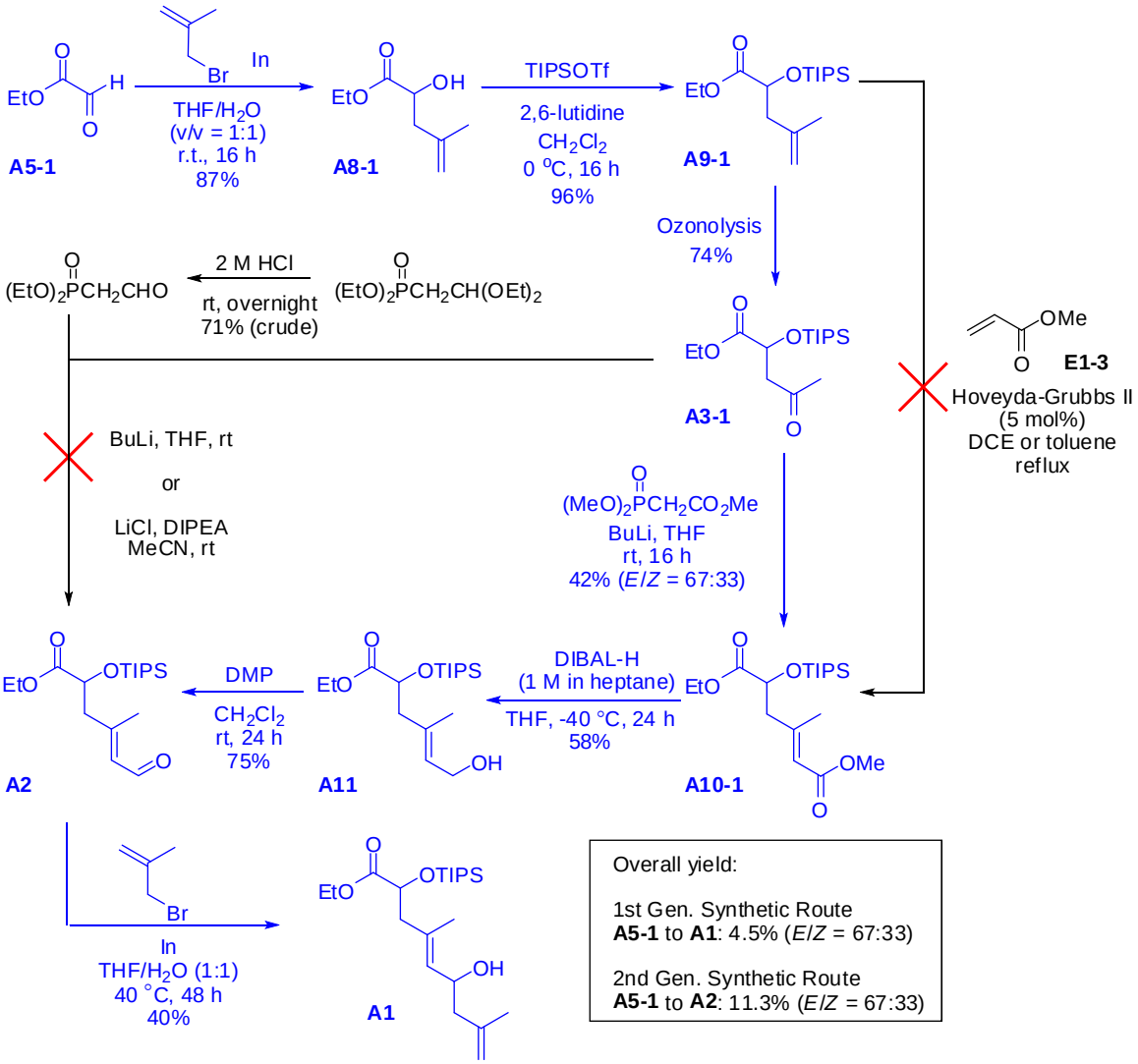

Scheme 3.2.9 Summary of synthesis of Fragment **A** and attempt to shorten the synthetic route.

3.3 Synthesis from 1,3-propanediol towards homoallylic alcohol B2

3.3.1 Retrosynthetic analysis

Fragment **B** in our synthetic plan of dactylolide, as illustrated in retrosynthetic analysis (Section 3.1), was to construct the hydrocarbon chain C9 – C11 and its extension in macrolide core. It was an important bridge to link the western part of macrolide core (Fragment **A**) and northern diene Fragment **C**. On top of that, it was also an indispensable fragment in construction of tetrahydropyran ring (Section 3.4).

Fragment **B** could be designed as vinyl iodide **B1** and homoallylic alcohol **B2**, respective to 1st Generation and 2nd Generation Synthetic Route. The synthesis could be derived from a simple diol, 1,3-propanediol (**B3-1**), followed by monoprotection of hydroxyl group and oxidation of another. The resulted aldehyde could be turned into vinyl iodide **B1** *via* Takai olefination[135] or homoallylic alcohol **B2** *via* indium-mediated allylation. (Scheme 3.3.1)

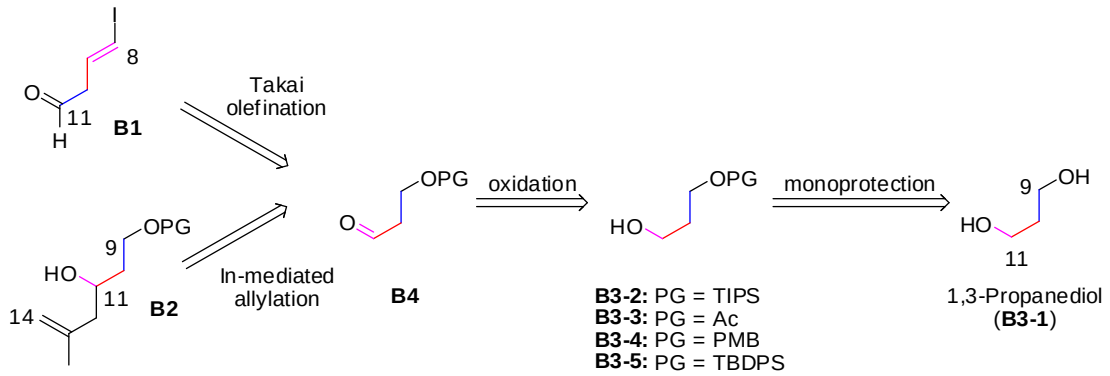

Scheme 3.3.1 Retrosynthetic analysis of Fragment **B1** and **B2**.

Three different types of protecting groups, which were silyl ethers (including triisopropylsilyl or TIPS, *t*-butyldiphenylsilyl or TBDPS), ester (acetate or Ac) and benzyl ether (*p*-methoxybenzyl or PMB), were employed in the investigation of the synthesis of Fragment **B**. Chronologically, monoprotected alcohol **B3-2** (PG = TIPS), **B3-3** (PG = Ac) and **B3-4** (PG = PMB) were synthesized in parallel to obtain vinyl iodide **B1** or its

[135] Takai, K.; Nitta, K.; Utimoto, K., *J. Am. Chem. Soc.* **1986,** *108*, 7408-7410.

derivatives under 1st Generation Synthetic Plan, while the synthesis of **B3-5** (PG = TBDPS) was started in a later time under 2nd Generation Synthetic Plan.

3.3.2 Attempt to synthesize vinyl iodide B1

One of the protecting groups that used in monoprotection of 1,3-propanediol (**B3-1**) was triisopropylsilyl (TIPS) group. The monoprotected alcohol **B3-2** was obtained in a high yield of 85%. The synthesis was continued with oxidation by Dess-Martin Periodinane (DMP) and a moderate yield of 70% was achieved for the desired aldehyde **B4-1**. (Scheme 3.3.2)

As illustrated in Scheme 3.3.1, the target vinyl iodide **B1** was planned to be synthesized *via* Takai olefination. Takai olefination is a name reaction, which employs iodoform and chromium(II) chloride to synthesize high (*E*)-selectivity vinyl iodide from aldehyde. This strategy, if successful, not only could establish the geometry of olefin C8 – C9 of the macrolide core, but also provides opportunity to access the eastern hemisphere of macrolide core by connecting vinyl iodide **B1** and Fragment **C1**.

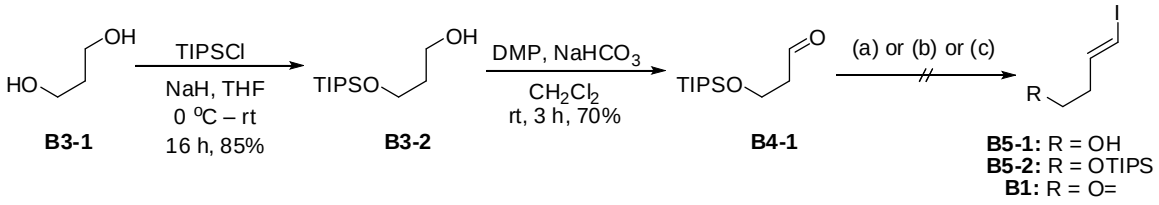

	Conditions	Result
(a)	CHI_3, $CrCl_2$, THF, 0 ℃, 2.5 h	mixture of **B5-1** and **B5-2**
(b)	1. CHI_3, $CrCl_2$, THF, 0 ℃, 2.5 h 2. 5% HCl/ 95% EtOH, 0 ℃, 2 h	**B5-1** 10%, E/Z = 6:1
(c)	1. CHI_3, $CrCl_2$, THF, 0 ℃, 2.5 h 2. TBAF, THF, rt, 5h 3. DMP, THF, rt, 16 h *or* PCC, CH_2Cl_2, rt, 16 h *or* Swern oxidation	**B1** No desired product

Scheme 3.3.2 Attempt to synthesize vinyl iodide **B1** from TIPS-monoprotected alcohol **B3-2**

However, the plan did not proceed as what we had planned. Crude mixture of deprotected vinyl iodide **B5-1** and TIPS-protected vinyl iodide **B5-2** was observed from ^{1}H NMR

spectrum when Takai olefination was employed. (Conditions a, Scheme 3.3.2) Due to unexpected deprotection, the crude product of Takai olefination, without any prior purification, was subjected into deprotection conditions of 5% HCl in ethanol solution.[136] As a result, only vinyl iodide **B5-1** was obtained albeit a yield of 10% and *E*/*Z* selectivity of 6:1 were achieved. (Conditions b, Scheme 3.3.2) Other than low yield, the technical difficulty to purify **B5-1** from crude which contained iodine also prompt us to oxidize the crude vinyl iodide **B5-1** into target Fragment **B1** directly. Unfortunately, no desired product was obtained under common oxidation methods, such as Dess-Martin Periodinane (DMP), pyridinium chlorochromate (PCC) or Swern oxidation. (Conditions c, Scheme 3.3.2)

3.3.3 Attempt to improve efficiency in the synthesis of vinyl iodide B5 and the failure of convergent synthesis of Fragment BC

Due to the failed attempts to oxidize (*E*)-4-iodobut-3-en-1-ol (**B5-1**) to target vinyl iodide **B1** (Conditions c, Scheme 3.3.2), the plan to synthesize Fragment **BC** was slightly revised as illustrated in Scheme 3.3.3. Instead of oxidize **B5-1** before the Nozaki-Hiyama-Kishi (NHK) coupling, the NHK coupling was planned to be conducted first from vinyl iodide **B5-1** and aldehyde **C1-4**, followed by an oxidation of C7 and C11 hydroxyl groups into carbonyl groups to afford target Fragment **BC**. As a continuous effort to obtain vinyl iodide **B5-1** in higher yield, acetate (Ac) and *p*-methoxybenzyl (PMB) group were chosen as protecting group due to its stability in Takai olefination conditions.[137]

As shown in Scheme 3.3.3, the acetate-monoprotected alcohol **B3-3** was successfully obtained from 1,3-propanediol (**B3-1**) with a high yield of 80%. However, an unexpected major obstacle happened in the subsequent oxidation step. Common oxidation strategies, such as Dess-Martin Periodinane (DMP) and pyridinium chlorochromate (PCC), did not yield any desire aldehyde **B4-2**. Different type of PCC[138] and changes in solvent did not provide any product too. As a result, synthetic route to synthesize vinyl iodide **B5-1** from acetate-monoprotected alcohol **B3-3** was abandoned.

---

[136] Cunico, R.F.; Bedell, L. *J. Org. Chem.* **1980**, *45*, 4797-4798.
[137] T. W. Green, P. G. M. Wuts, *Protective Groups in Organic Synthesis*, Wiley-Interscience, New York, **1999**, 76-86, 708-711.
[138] Oxidation by PCC on alumina, ref: Vinczer, P., Baán, G., Novák, L., Szántay, C. *Tetrahedron Lett.* **1984**, *25*, 2701-2704.

Meanwhile, the synthesis of vinyl iodide **B5-1** was initiated with monoprotection of 1,3-propanediol (**B3-1**) with *p*-methoxybenzyl (PMB) group. The resulted alcohol **B3-4** was further oxidized *via* Swern oxidation to produce aldehyde **B4-3**. The aldehyde **B4-3** was then subjected into Takai olefination conditions to yield desired vinyl iodide **B5-4** at a yield of 34% with *E*/*Z* selectivity of 80:20 under 0 ℃. The *E*/*Z* selectivity could be improved by decreasing the reaction temperature to -20 ℃ albeit in lower yield of 15%. Despite the successful synthesis, vinyl iodide **B5-4** was unstable even at -20 ℃.

At the same time as we synthesized vinyl iodide **B5-4**, synthesis of northern conjugated dienoate Fragment **C** was also conducted.[139] With modification of the Pd-catalyzed direct cross coupling strategy developed by our group,[48] the conjugated dienoate **C1-3** was formed from *n*-butyl acrylate **E1-1** and acetate-protected isoprenol **D1-3** at a yield of 65% and *E*/*Z* selectivity of 54:46. Subsequent reduction with sodium borohydride yielded alcohol **C1-1** at a yield of 61%. However, attempt to oxidize alcohol **C1-1** to aldehyde **C1-4** was failed under common oxidation strategies, such as DMP and Swern oxidation. This unexpected failure in obtaining aldehyde **C1-4** discontinued the subsequent deprotection of vinyl iodide **B5-3**, which also marked the end of synthetic effort to construct Fragment **BC** *via* NHK coupling as key strategy.

[139] Condition screening of the synthesis of Fragment **C** in 1st Generation Synthetic Plan is shown in Section 4.2.

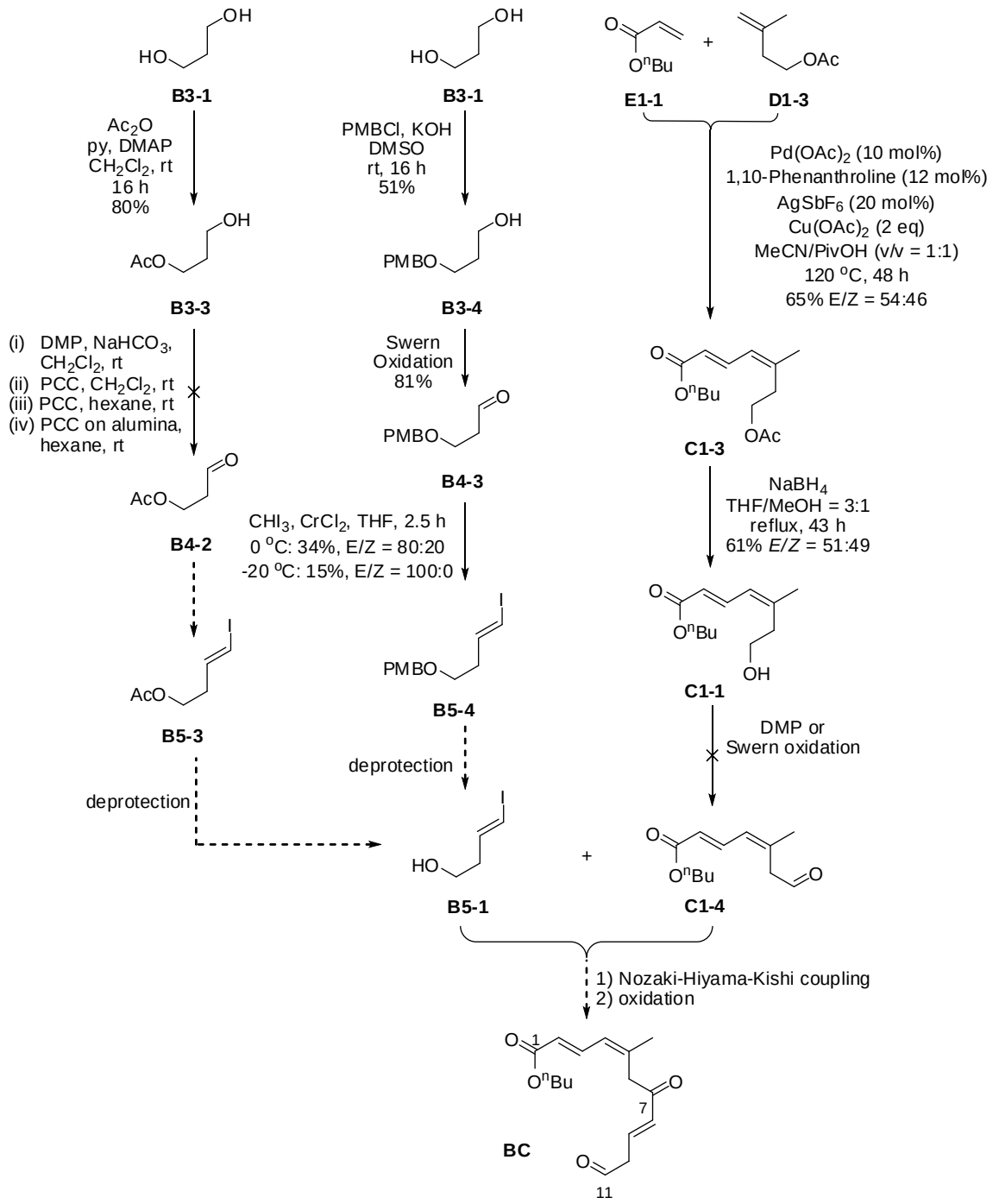

Scheme 3.3.3 Convergent synthetic plan for Fragment **BC1**, derived from vinyl iodide **B5-1** and aldehyde **C1-4**. Failure to obtain aldehyde **C1-4** marked the end of this synthetic strategy.

3.3.4 Synthesis of homoallylic alcohol B2

Due to inaccessibility to synthesize Fragment **BC**, we initially revised our synthetic strategy as shown in Scheme 3.3.4. Instead of synthesizing tetrahydropyran motif in later stage, we planned to construct this southern featured unit first with the available homoallylic alcohol **A1** and aldehyde **B4-3** *via* $In(OTf)_3$-catalyzed intramolecular 2,5-oxonium-ene cyclization. The resulted tetrahydropyran **AB-1** was then planned to be subjected for removal of *p*-methoxybenzyl (PMB) group and oxidation to yield aldehyde **AB-2**. Horner-Wadsworth-Emmons reaction between **AB-2** and phosphonate **C2** would result in macrolide precursor **ABC**. Subsequent desilylation, esterification and reduction of ethyl ester would provide target dactylolide.

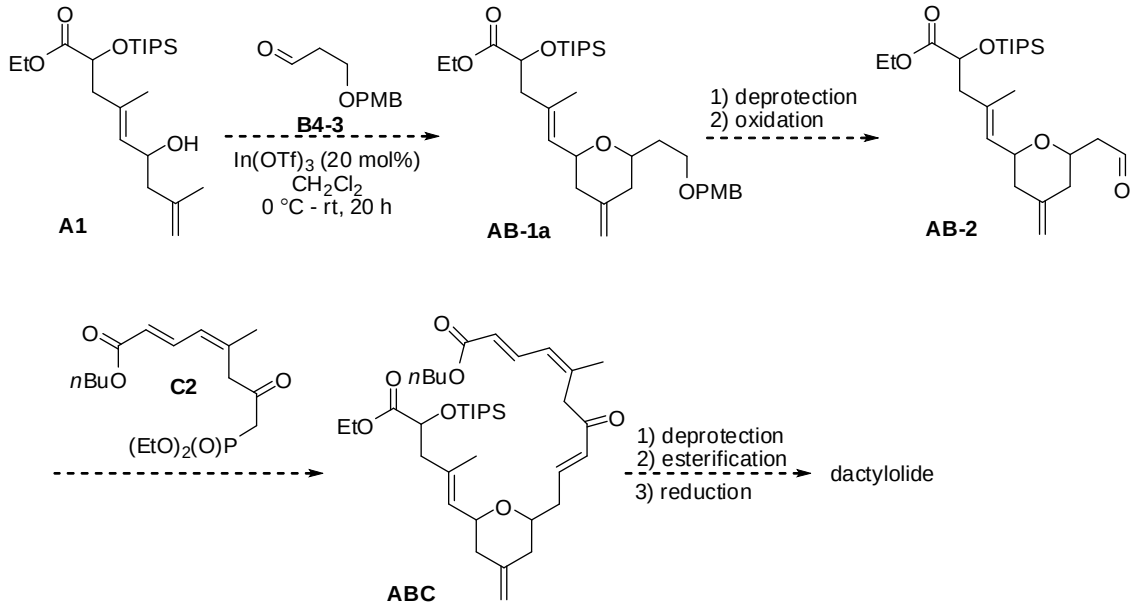

Scheme 3.3.4 Revised strategy for the synthesis of dactylolide.

However, the tetrahydropyran ring synthesis from homoallylic alcohol **A1** and aldehyde **B4-3** did not provide the target compound **AB-1**. An unexpected dihydrofuranone **A15** was formed. (Section 3.3.5) Due to this surprising result, we revised the synthetic strategy by disconnecting C14 – C15 and C11 – O bonds of tetrahydropyran unit, and envisioned that the tetrahydropyran ring could be synthesized from aldehyde **A2** and homoallylic alcohol **B2**. In order to ensure selective deprotection was feasible after tetrahydropyran ring synthesis, the protecting group of **B2** could not be triisopropylsilyl (TIPS) group. Hereafter, the synthetic effort towards dactylolide was shifted to 2nd Generation Synthetic

Route, which featured the new way of tetrahydropyran synthesis and Horner-Wadsworth-Emmons reaction in the construction of olefin C8-C9.

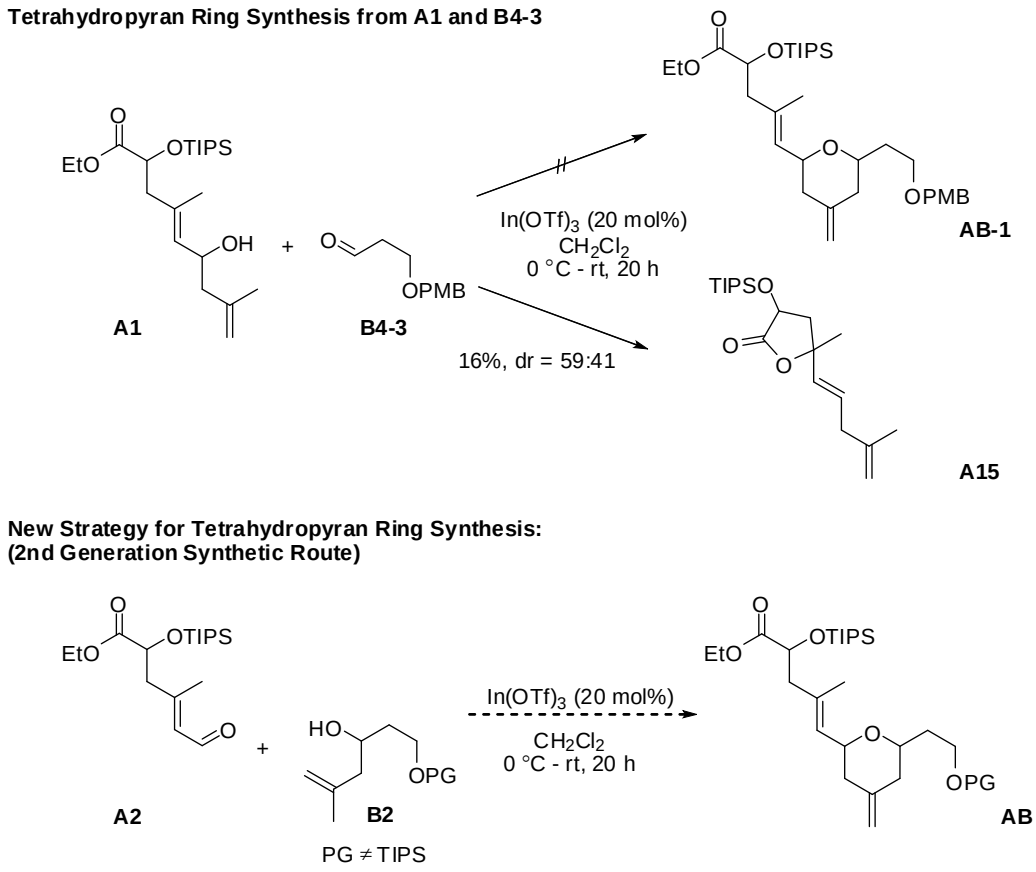

Scheme 3.3.5 Failure synthesis of tetrahydropyran ring from homoallylic alcohol **A1** and aldehyde **B4-3**, and new strategy on tetrahydropyran ring synthesis.

In order to continue our synthesis, two different homoallylic alcohol **B2**s were prepared from its respective aldehyde precursor **B4** in parallel. As shown in Scheme 3.3.6, aldehyde **B4-3**, whose hydroxyl group had been protected with *p*-methoxybenzyl (PMB) group, was transformed into homoallylic alcohol **B2-1** by employing indium-mediated allylation with a high yield of 89%. On the other hand, *t*-butyldiphenylsilyl or TBDPS-analogue **B2-2** was synthesized by employing similar synthetic route for **B2-1**. The synthesis was started from monoprotection of 1,3-propanediol (**B3-1**), which produced monoprotected alcohol **B3-5** at a higher yield of 73% when *n*BuLi acted as base compared with imidazole (43%). Subsequent Swern oxidation and indium-mediated allylation yielded the final homoallylic alcohol product **B2-2** at an overall yield of 48% in 3 steps.

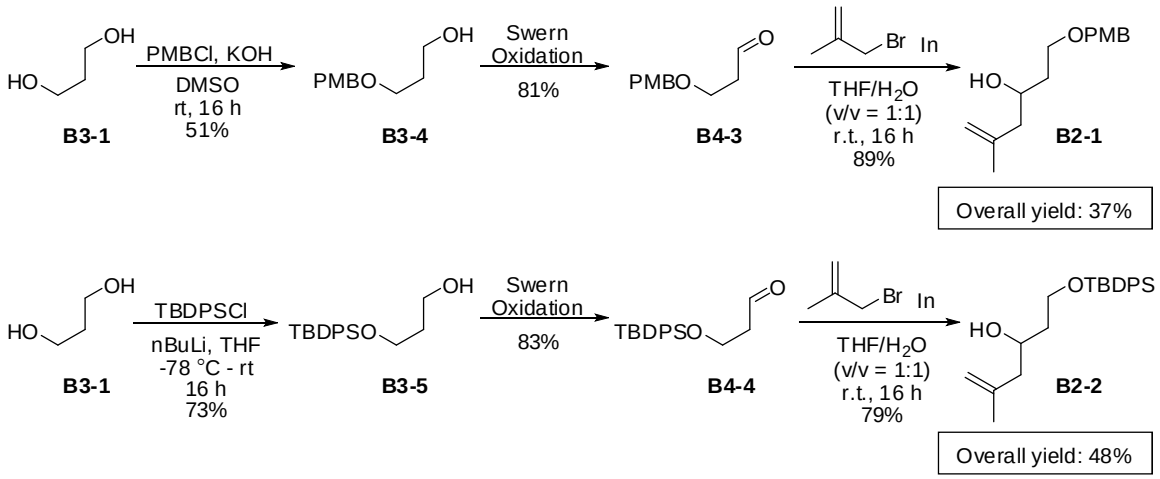

Scheme 3.3.6 Synthesis towards homoallylic alcohol **B2** in 2nd Generation Synthetic Plan.

3.4 Convergent synthesis towards tetrahydropyran

With aldehyde **A2** and homoallylic alcohol **B2** in hand, we continued our synthesis of dactylolide by combining these two fragments to construct tetrahydropyran ring. As introduced in Section 1.3, the $In(OTf)_3$-catalyzed intramolecular 2,5-oxonium-ene cyclization, which was developed by our group in 2002, would be our main strategy in the study.[23] Compared with others' strategies, this Prins-type reaction provided more advantages in terms of green chemistry, such as higher atom efficiency and catalytic reaction.

3.4.1 Initial attempts on tetrahydropyran synthesis in 2nd Generation Synthetic Route

As planned in 2nd Generation Synthetic Route, initial attempt to synthesize tetrahydropyran **AB-1a** was conducted under standard conditions, i.e. 20 mol% $In(OTf)_3$ subjected into CH_2Cl_2 solution of aldehyde and homoallylic alcohol,[140] reported by our group in 2002. Surprisingly, no desired tetrahydropyran product was observed when aldehyde **A2** and homoallylic alcohol **B2-1** were used. On top of that, the recovered aldehyde **A2** was transformed into a mixture of (*E*) and (*Z*)-isomers. Replacing the catalyst with $InCl_3$ showed same result as $In(OTf)_3$, while $InBr_3$ provided a mixture of unidentified products. $BF_3 \cdot OEt_2$, a Lewis acid which reported to be effective in tetrahydropyran ring synthesis,[24] did not provide desired results too. (Table 3.4.1)

[140] This addition sequence was reported as superior than the sequence of adding aldehyde and homoallylic alcohol into CH_2Cl_2 solution of 20 mol% $In(OTf)_3$.

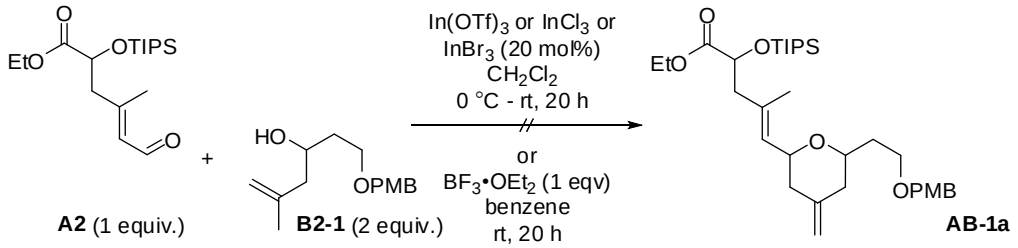

Entry	Lewis acid	Solvent	temp.	AB-1a	Recovered A2
1	$In(OTf)_3$ (20 mol%)	CH_2Cl_2	0 ℃ - rt	-	Mixture of (*E*) and (*Z*)-isomers
2	$InCl_3$ (20 mol%)	CH_2Cl_2	0 ℃ - rt	-	Mixture of (*E*) and (*Z*)-isomers
3	$InBr_3$ (20 mol%)	CH_2Cl_2	0 ℃ - rt	Mixture of unidentified compounds	
4	$BF_3 \cdot OEt_2$ (1 equiv.)	benzene	rt	Mixture of unidentified compounds	

Table 3.4.1 Initial attempts on tetrahydropyran ring synthesis in 2nd Generation Synthetic Route.

3.4.2 Reexamination on tetrahydropyran synthesis *via* intramolecular 2,5-oxonium-ene cyclization

The unexpected setbacks occurred in the initial attempts prompted us to reexamine the effectiveness of tetrahydropyran synthesis *via* intramolecular 2,5-oxonium-ene cyclization. As shown in Table 3.4.2, selected conjugated enals were coupled with homoallylic alcohol **B2** under standard conditions. (Entry 1 to 4) It was surprising to find that a mixture of tetrahydropyran ring (THP) **I** and dihydropyran ring (DHP) **II** was formed under the conditions reported. The ratio of **I** to **II** ranged from 50:50 to 64:36, showed that the formation of tetrahydropyran was slightly favaourable compared with dihydropyran. Both pyrans had same polarity, which caused the separation *via* column chromatography became impossible. Besides, NOESY experiment revealed that both pyrans were in *syn* configuration only. This finding contradicted with the reported result, which claimed that a mixture of *syn*- and *anti*-tetrahydropyrans was obtained.[141] (Entry 2 and 3)

We also investigated the effect of ratio between two coupling partners. Acrolein (**E2-3**) and homoallylic alcohol **B2-2** were employed in the investigation. Decreasing the ratio of **E2-3** to **B2-2** to 1:1 deteriorated the overall yield but THP formation was more favourable than DHP formation. (Entry 5) Increasing the equivalent of **B2-2** to 3 equivalents increased the yield, but did not show any improvement on the ratio of THP/DHP product.

[141] This contradictory result was also observed in experiments involved coupling between benzaldehyde or aliphatic aldehyde and other homoallylic alcohol. Detailed experiment data is shown in Section 4.2.3.

(Entry 6) As acrolein (**E2-3**) is volatile and easily polymerized, therefore we expected that increasing the amount of acrolein might improve the yield. However, neither desired THP nor DHP was obtained. (Entry 7) Addition of tributylamine (Entry 8), which acted as acid scavenger, to the reaction showed no difference if compared to Entry 4.

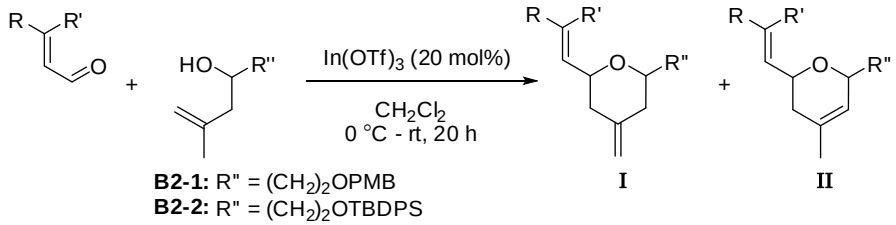

B2-1: R" = $(CH_2)_2$OPMB
B2-2: R" = $(CH_2)_2$OTBDPS

Entry	Aldehyde	Alcohol	Desired Product	Yield of I	Total Yield (I+II)	Ratio of I:II[a]
1	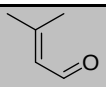 **E2-1** (1 equiv.)	**B2-1** (2 equiv.)	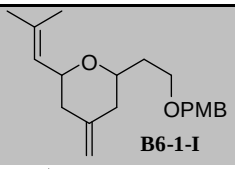 **B6-1-I**	2%	4%	50:50
2	**E2-1** (1 equiv.)	**B2-2** (2 equiv.)	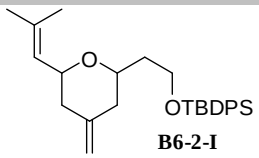 **B6-2-I**	7%	11%	64:36
Ref	(Table 1, Entry 12 reported in *TL*, **2002**, *43*, 7193)			55%, *syn*:*anti* = 75:25		
3	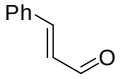 **E2-2** (1 equiv.)	**B2-2** (2 equiv.)	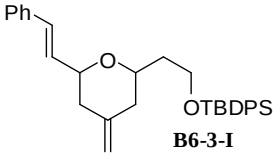 **B6-3-I**	47%	74%[b]	63:37
Ref	(Table 1, Entry 10 reported in *TL*, **2002**, *43*, 7193)			90%, *syn*:*anti* = 75:25		
4	 **E2-3** (1 equiv.)	**B2-2** (2 equiv.)	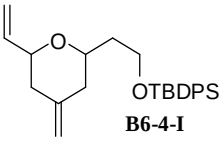 **B6-4-I**	28%	53%	53:47
5	**E2-3** (1 equiv.)	**B2-2** (1 equiv.)	**B6-4-I**	17%	26%	65:35
6	**E2-3** (1 equiv.)	**B2-2** (3 equiv.)	**B6-4-I**	30%	64%	47:53
7	**E2-3** (2 equiv.)	**B2-2** (1 equiv.)	**B6-4-I**	0%	0%	-
8[c]	**E2-3** (1 equiv.)	**B2-2** (2 equiv.)	**B6-4-I**	26%	50%	52:48

Table 3.4.2 Reexamination of tetrahydropyran ring synthesis catalyzed by $In(OTf)_3$. [a] determined from ^1H NMR; [b] calculated from ^1H NMR with $PhNO_2$ as internal standard; [c] NBu_3 (1 equiv.) was added.

A plausible mechanism[21,24] is shown in Scheme 3.4.1 to explain the formation of tetrahydropyran **I** and dihydropyran **II**. Two types of oxonium were expected to form under this mechanism, where oxonium A was more favourable compared with oxonium B. This was because steric hindrance resulted from the alkyl groups (R or R') and hydrogen in oxonium B is larger than steric hindrance in oxonium A. This could explain why only *syn* product was formed in oxonium-ene reaction.

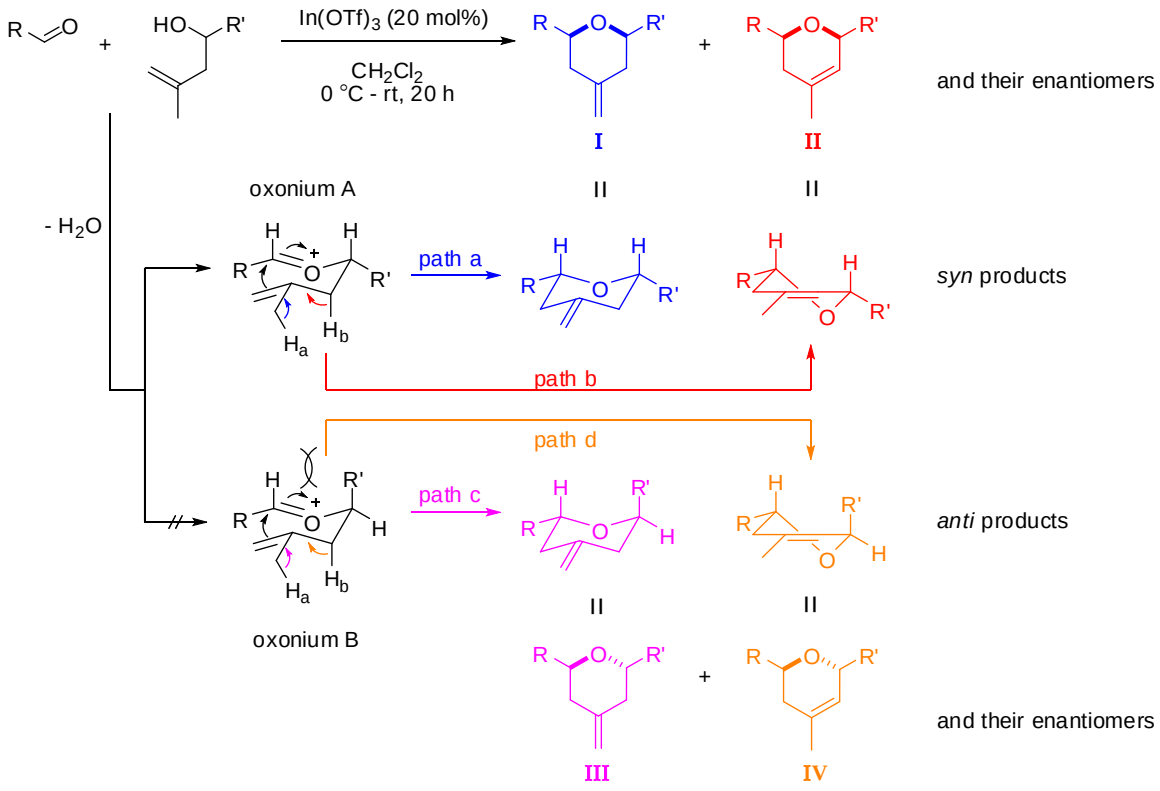

Scheme 3.4.1 Plausible mechanism of $In(OTf)_3$-catalyzed intramolecular 2,5-oxonium-ene cyclization.

Oxonium ion subsequently underwent deprotonation, followed by ring closure to form pyran ring. Two pathways were suggested for each oxonium ion. For favourable oxonium A, removal of H_a on methyl group leads to the formation of exomethylene group on tetrahydropyran **I** (path a), while removal of H_b leads to dihydropyran **II**, which consists of a thermodynamically-stable trisubstituted alkene (path b).

3.4.3 Conditions screening on synthesis of tetrahydropyran ring in 2nd Generation Synthetic Route

With the findings above, we continued the synthesis of dactylolide with conjugated aldehyde **A2** and homoallylic alcohol **B2-2** under the standard conditions despite that a mixture of tetrahydropyran and dihydropyran would be obtained. Meanwhile, screening of catalysts and hindered base was also conducted to search the most optimum conditions, which shown in Table 3.4.3.

As expected, the desired tetrahydropyran **AB-1b-I** was obtained in a yield of 15% alongside with undesired dihydropyran **AB-1b-II** (15%) when 20 mol% of $In(OTf)_3$ was used as catalyst. (Entry 1) Changing catalyst to $Zn(OTf)_2$ and $Cu(OTf)_2$ (Entry 2, 3, 5) did not drive the reaction to the end and only provided lower yield after prolonged reactions and high catalyst loading. TMSOTf, a relatively strong Lewis acid, not only failed to provide desired tetrahydropyran ring but also destroyed both starting materials. (Entry 4)

Catalytic amount of methyl aluminum dichloride ($MeAlCl_2$), a strong Lewis acid as well as proton scavenger, was added along with $In(OTf)_3$ in Entry 6. This conditions deteriorated the yield and also induced the formation of dihydropyran **AB-1b-II**. Addition of hindered bases,[75a,75b, 142] such as 2,6-di-tert-butylpyridine (DTBP), lithium bis(trimethylsilyl)amide (LiHMDS), diisopropylethylamine (DIPEA) and tributylamine (NBu_3), did not show higher conversion and selectivity. (Entry 7 - 10)

On top of these discouraging results, the recovered aldehyde in Entry 2, 3, 5, 7 and 9 was found to be isomerized into a mixture of (*E*) and (*Z*)-isomers. However, this isomerization did not affect the alkene geometry of desired tetrahydropyran product **AB-1b-I**.

As a result, the most optimum way to synthesize tetrahydropyran of dactylolide in 2nd Generation Synthetic Route was using $In(OTf)_3$ as catalyst, which was the original conditions. This reaction provided target tetrahydropyran **AB-1b-I** at a yield of 15% together with 15% of dihydropyran **AB-1b-II**.

[142] Hindered bases are reported as efficient triflic acid scavenger, see (a) Brown, H. C.; Kanner, B. *J. Am. Chem. Soc.* **1966**, *88*, 986–992; (b) Dumeunier, R.; Markó, I. E. *Tetrahedron Lett.* **2004**, *45*, 825-829.

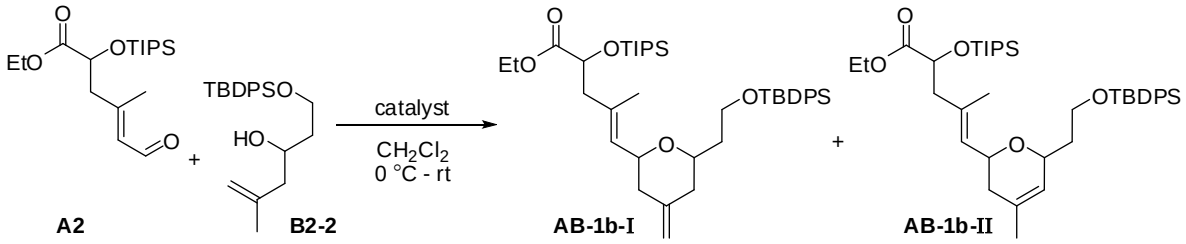

Entry	Catalyst	Additive	t	Yield of AB-1b-I	Total Yield (AB-1b-I+ AB-1b-II)	Ratio (AB-1b-I:AB-1b-II)[a]
1	$In(OTf)_3$ (20 mol%)	-	20 h	15%	30%	50:50
2[b]	$Zn(OTf)_2$ (60 mol%)	-	72 h	15%	26%	59:41
3[b]	$Cu(OTf)_2$ (60 mol%)	-	84 h	5%	9%	55:45
4	TMSOTf (20 mol%)	-	4 h	0%	0%	-
5[b]	$Zn(OTf)_2$ (100 mol%)	-	72 h	6%	11%	58:42
6	$In(OTf)_3$ (20 mol%)	$MeAlCl_2$ (20 mol%)	1 h	2%	8%	23:77
7[b]	$In(OTf)_3$ (100 mol%)	DTBP (100 mol%)	46 h	9%	20%	44:56
8	$In(OTf)_3$ (60 mol%)	LiHMDS (100 mol%)	40 h	6%	12%	54:46
9[b]	$In(OTf)_3$ (100 mol%)	DIPEA (100 mol%)	72 h	6%	12%	50:50
10	$In(OTf)_3$ (120 mol%)	NBu_3 (100 mol%)	20 h	14%	28%	51:49

Table 3.4.3 Conditions screening on synthesis of tetrahydropyran ring in 2nd Generation Synthetic Route. [a] determined from ^{1}H NMR; [b] yield calculated based on recovered starting materials.

3.5 Attempt to synthesize Fragment AB *via* olefin metathesis

As illustrated in previous sections, the desired tetrahydropyran **AB-1b-I** could be obtained *via* convergent strategy, which combining aldehyde **A2** and homoallylic alcohol **B2-2** through $In(OTf)_3$-catalyzed intramolecular 2,5-oxonium-ene reaction. This strategy required 7 steps of its longest linear sequence and yielded the product at an overall yield of 1.7%. (Scheme 3.5.1)

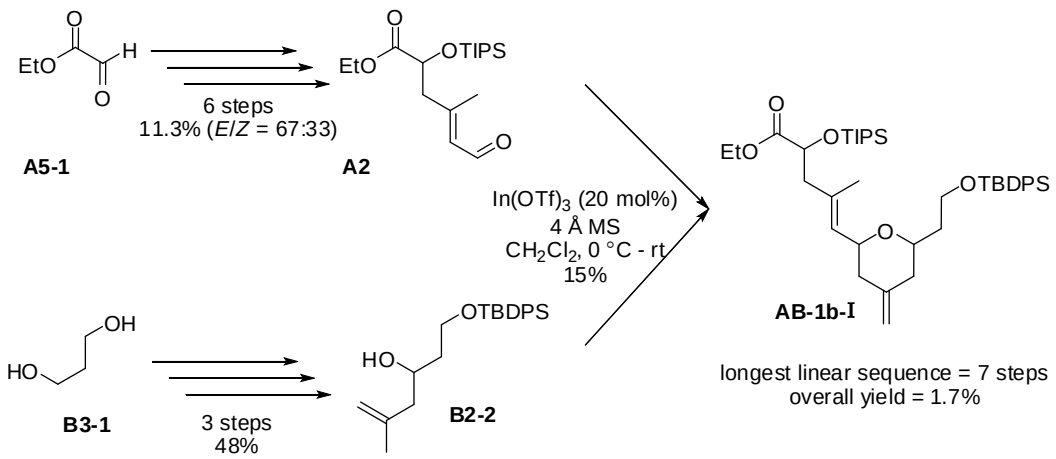

Scheme 3.5.1 Established convergent synthesis of Fragment **AB**.

Low overall yield implied that the effort to continue the synthesis would be even harder. Therefore, we attempted to modify the synthetic route by employing olefin metathesis, a common green synthetic strategy in constructing carbon-carbon double bond. A successful example of such strategy in total synthesis of dactylolide has been reported by Ghosh *et al.*[61,70] They synthesized the C16 – C17 olefin by combining a disubstituted terminal olefin and a monosubstituted olefin with Grubbs 2nd generation catalyst. The fragment C9 – C19 was obtained in a yield of 57% with moderate *E*/*Z* selectivity of 63:37. This example inspired us to synthesize our designated Fragment **AB** with similar strategy. As shown in Scheme 3.5.2, alkene **A9-1** and alkene **B6-4-I** were used to examine the accessibility of this olefin metathesis strategy. Alkene **A9-1**, which was one of the synthesized compounds in synthesis of Fragment **A**, could be obtained in 2 steps, with a high overall yield of 84% from ethyl glyoxalate, while alkene **B6-4-I** could be generated by various transformation made on 1,3-propanediol (**B3-1**) and subsequent 2,5-oxonium-ene reaction (Table 3.4.2, Entry 4) with an overall yield of 13% in 4 steps. This strategy

could reduce the longest linear sequence from 7 steps to 5 steps and might increase the overall yield of Fragment **AB**. (Scheme 3.5.2)

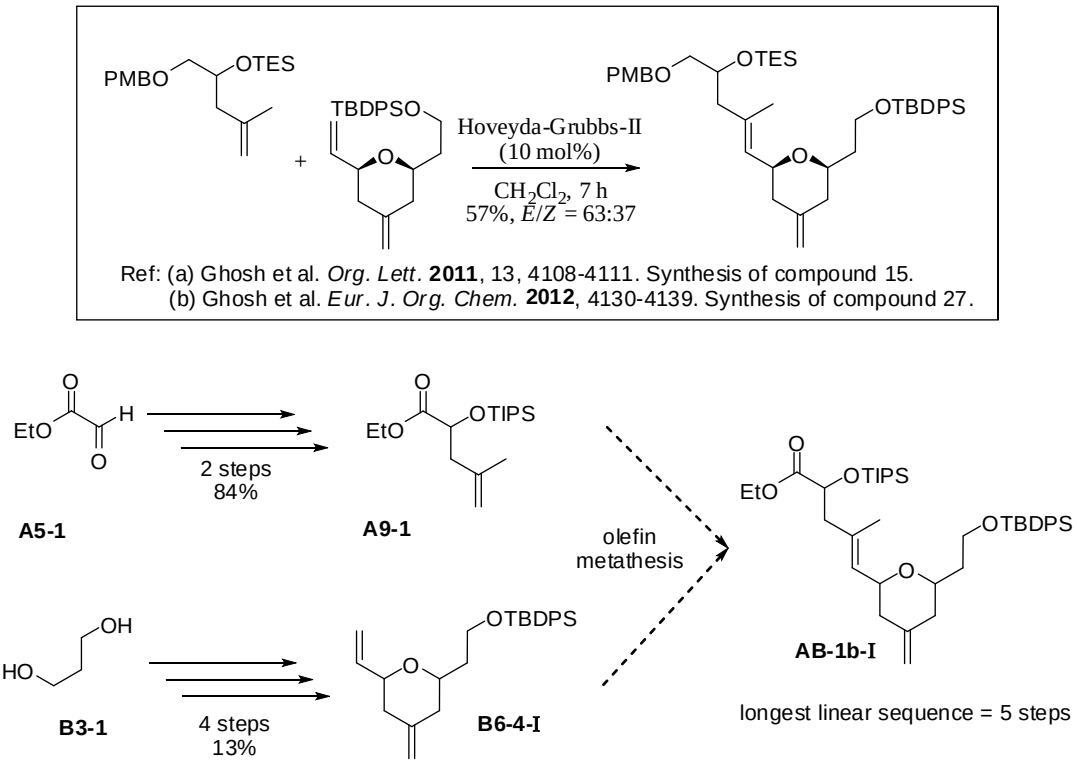

Scheme 3.5.2 Olefin metathesis strategy to access Fragment **AB**.

A complementary article, "*A General Model for Selectivity in Olefin Cross Metathesis*", reported by Grubbs and co-workers, showed that 1,1-disubstituted olefin is classified as Type III olefin, which homodimerization do not occur during cross metathesis, while terminal olefin is classified as Type I olefin, which homodimerization could be happened fast. 1,1-disubstituted olefin sometimes is classified as Type IV olefin, or spectators to cross metathesis, if less efficient Grubbs 1st Generation catalyst (Scheme 3.5.3, Cat. 1) is used.[39a] This implies that cross metathesis between less reactive 1,1-disubstituted olefin **A9-1** and reactive terminal olefin **B6-4-I** could be challenging. Competition between cross metathesis and homodimerization of **B6-4-I** could be expected. Although formation of trisubstituted olefins *via* cross metathesis was challenging, Grubbs and co-workers later demonstrated that bulkier NHC ligand ruthenium-based catalyst (Scheme 3.5.3, Cat. 4 and 5) was an efficient catalyst in formation of trisubstituted olefins.[143]

[143] Stewart, I. C.; Douglas, C. J.; Grubbs, R. H. *Org. Lett.* **2008**, *10*, 441-444.

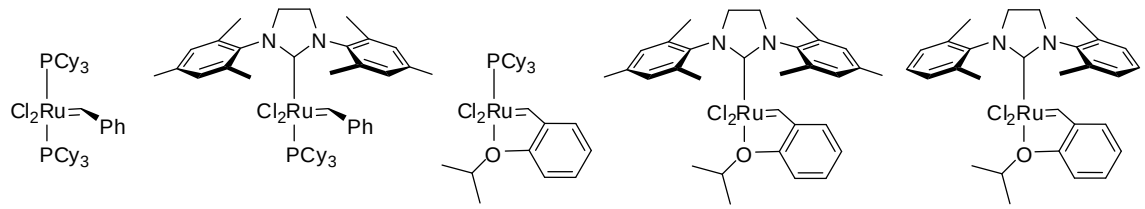

Cat. 1 (Grubbs 1st Gen.) **Cat. 2** (Grubbs 2nd Gen.) **Cat. 3** (Hoveyda-Grubbs 1st Gen.) **Cat. 4** (Hoveyda-Grubbs 2nd Gen.) **Cat. 5**

Scheme 3.5.3 Common ruthenium-based catalyst for cross metathesis.

With this in mind, different types of common olefin metathesis ruthenium-based catalysts (Scheme 3.5.3) were tested in our reaction. With the conditions reported by Ghosh *et al.*, [61,70] a series of screening was made and summarized in Table 3.5.1. As expected, only Grubbs 2nd Generation catalyst and Hoveyda-Grubbs 2nd Generation catalyst, which possess bulky NHC ligand, yielded desired product. However, the cross metathesis did not work as efficient as other reported, extremely low yield (3 – 4%) was obtained after prolonged reflux (3 – 5 days). (Entry 2 and 4) No desired product **AB-1b** but only dimer product from homodimerization of terminal olefin **B6-4-I** was observed if Grubbs 1st Generation or Hoveyda-Grubbs 1st Generation catalyst was used. (Entry 1 and 3)

We also investigated the solvent effect on cross metathesis. Toluene did not yield desired product (Entry 5), while chlorine-based solvents, such as dichloromethane (Entry 4) and dichloroethane (Entry 6), only yielded desired product in very poor yield after prolonged reflux.

We then tested conditions adopted from Grubbs's group.[143] (Entry 7) Although moderate yield (> 70%) was obtained in their model study, their conditions did not provide any desired product in our case. Changing TIPS protecting group on hydroxyl group of alkene **A9-1** to less bulky methoxymethyl (MOM) group also resulted in dissatisfactory result. (Entry 8)

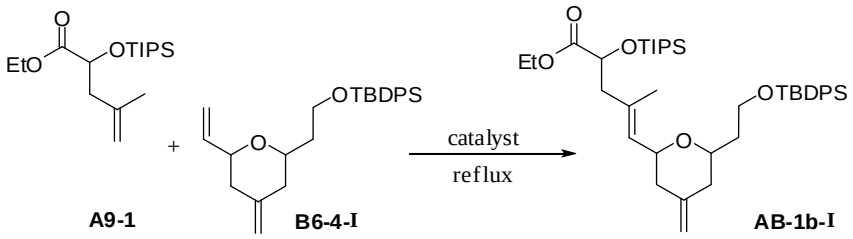

Entry	Catalyst	Solvent	t	Yield of AB-1b-I	E/Z
1	Cat. 1	CH_2Cl_2	24 h	0%	-
2	Cat. 2	CH_2Cl_2	3 d	4%	100:0
3	Cat. 3	CH_2Cl_2	5 d	0%	-
4	Cat. 4	CH_2Cl_2	5 d	3%	100:0
5	Cat. 4	toluene	4 d	NR	-
6	Cat. 4	DCE	7 d	3%	100:0
7	Cat. 4	CH_2Cl_2	7 d	NR	-
8[a]	Cat. 4	CH_2Cl_2	24 h	NR	

Table 3.5.1 Screening of cross metathesis between **A9-1** and **B6-4-I**. [a] Protecting group of **A9-1** was methoxymethyl (MOM) group.

*Ghosh's conditions (Entry 1 - 6): **A9-1** (10 equiv.) and mixture of **B6-4-I/B6-4-II** (1 equiv.) were dissolved in solvent (0.14 M wrt **B6-4**) and treated with 10 mol% catalyst for timing stated above.*

*Grubbs' conditions (Entry 7 - 8): **A9-1** (1 equiv.) and mixture of **B6-4-I/B6-4-II** (3 equiv.) were dissolved in solvent (0.25 M wrt **A9-1**) and treated with 5 mol% catalyst for timing stated above.*

The unexpected failure of cross metathesis could be rationalized by catalyst deactivation by chelation of carbonyl group to the metal center. (Scheme 3.5.4) This phenomenon was first observed by Cossy and BouzBouz.[144] They found that hydroxyolefin was functionalized twice while acetoxyolefin was only functionalized at its homoallylic unit when both olefins were treated with acrolein as coupling partner and Hoveyda-Grubbs 2nd Generation Catalyst as catalyst. They proposed that the chemoselectivity was arised from the chelation of acetoxy group to the ruthenium at allylic side, which resulted in a 6-membered ring intermediate **A** in the catalytic cycle. Therefore, the unreactive ring **A** caused acrolein selectively coupled with homoallylic unit. On the other hand, chelation of acetoxy group to ruthenium center at homoallylic side was unfavourable because of the formation of 7-membered ring **B**, which was less stable. As a result, chemoselective cross metathesis was achieved *via* deactivation of catalyst.

[144] BouzBouz, S.; Cossy, J. *Org. Lett.* **2001**, *3*, 1451-1454.

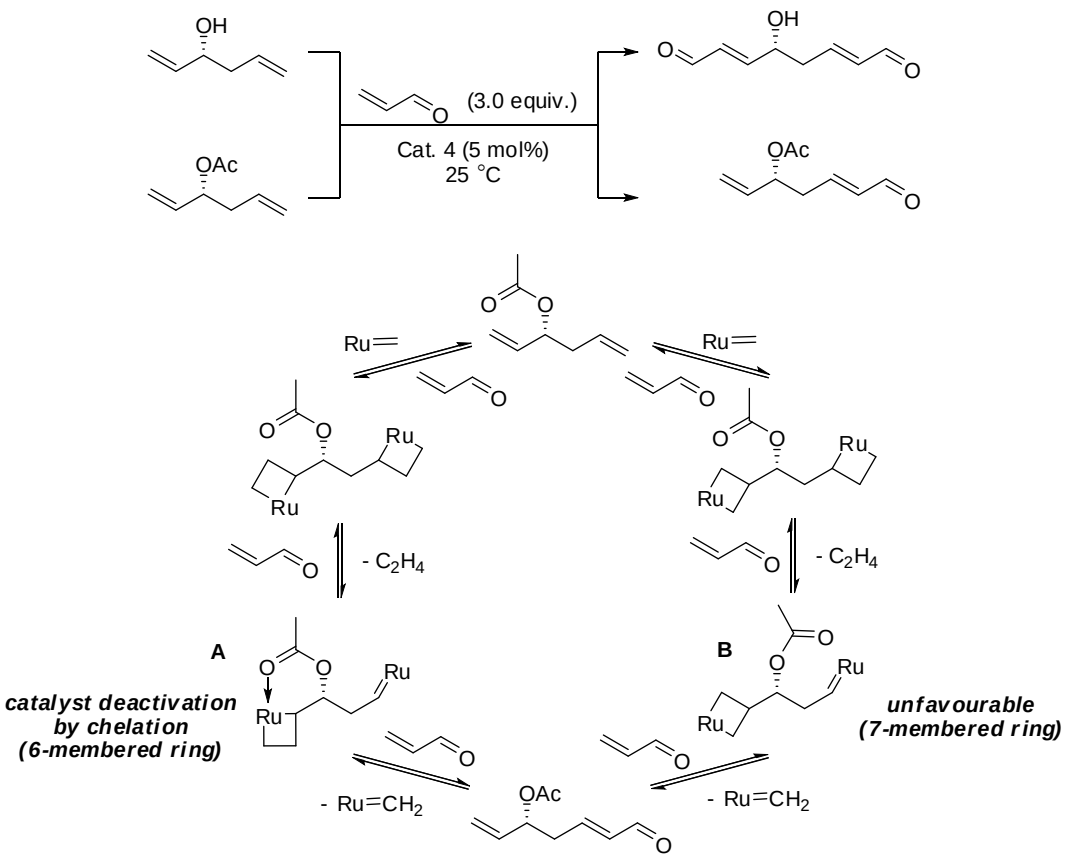

Scheme 3.5.4 Chelation effects in chemoselective cross metathesis and its proposed mechanism.

With this proposed mechanism, we speculated that the chelation effect might cause the cross metathesis of our case became unreactive than expected. (Scheme 3.5.5) As shown in the catalytic cycle, a 6-membered ring could also be formed if carbonyl group of alkene **A9-1** chelates with ruthenium metal. This leads to the deactivation of catalyst and halt the catalytic cycle to produce desired product **AB-1b-I**. Therefore, we reduced the ethyl ester group of alkene **A9-1** to alcohol and then further protected with methoxymethyl (MOM) protecting group. However, alkene **A12-9** was still unable to couple with alkene **B6-4-I** under Ghosh's conditions or Grubbs's conditions. Only homodimerization of alkene **B6-4-I** and unreacted alkenes were observed from crude NMR analysis. (Scheme 3.5.6)

As a result, the attempt to shorten the synthesis *via* olefin cross metathesis was failed and the synthesis of compound **AB-1b-I** remained as what we have described in previous section.

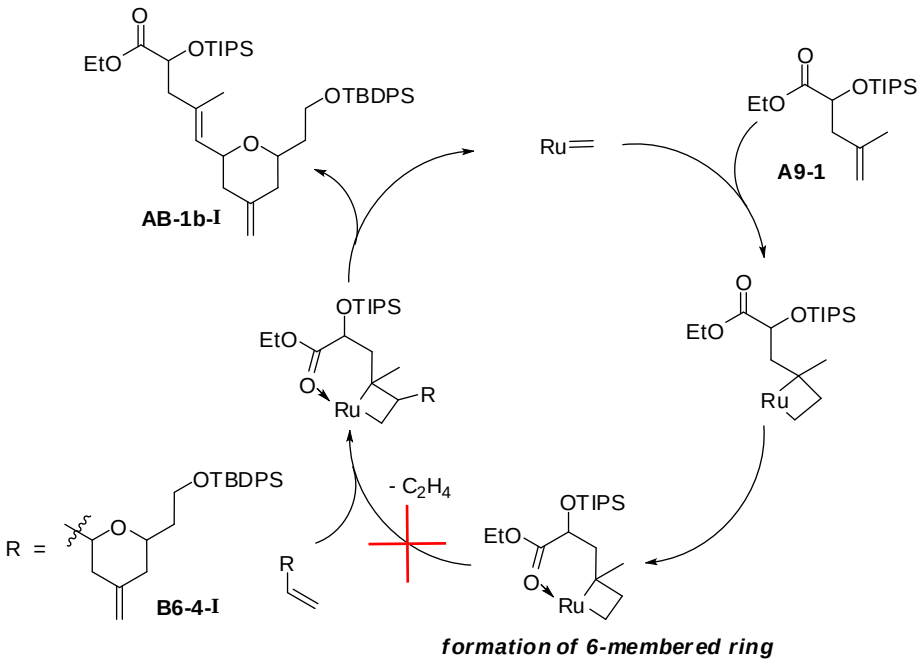

Scheme 3.5.5 Chelation effects in ineffective olefin cross metathesis between **A9-1** and **B6-4-I**.

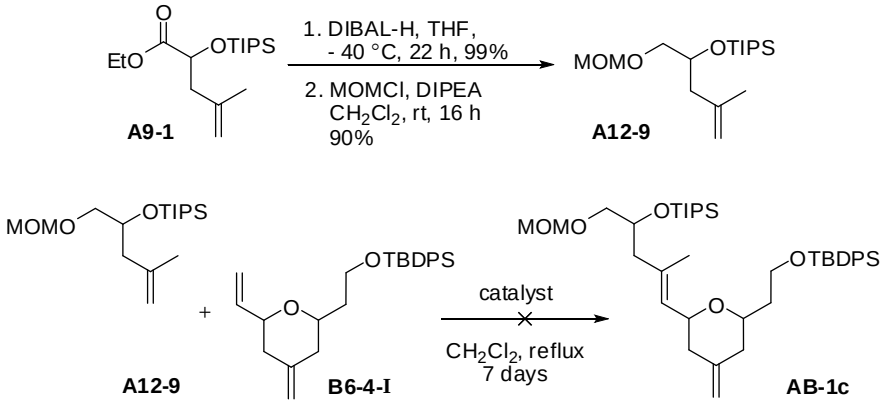

Scheme 3.5.6 Conversion of alkene **A9-1** to alkene **A12-9** and olefin cross metathesis between alkene **A12-9** and alkene **B6-4-I**. Conditions tested for cross metathesis includes: (a) Cat. 2, Ghosh's conditions; (b) Cat. 4 or cat. 5, Grubbs's conditions.

3.6 Synthesis towards conjugated diene (Fragment C)

3.6.1 Retrosynthetic analysis

As illustrated in Section 3.1, the northern diene of dactylolide was fragmented out from the macrolide core and be an important fragment in convergent synthesis. The configuration of diene was identified as (2*E*,4*Z*)-diene. As part of the effort to synthesize dactylolide in *greener* way, metal-catalyzed direct cross coupling, developed by our group, would be the key step of synthesis of conjugated diene. As 1st Generation Synthetic Route had been abandoned, this section will discuss the synthesis of conjugated diene under 2nd Generation Synthetic Route. As illustrated in Scheme 3.6.1, the conjugated diene **C2**, which featured a phosphonate group at **C8**, could be derived from acrylate and phosphonate **P1** with the key strategy, while phosphonate **P1** could be synthesized from (±)-epichlorohydrin (**4**).

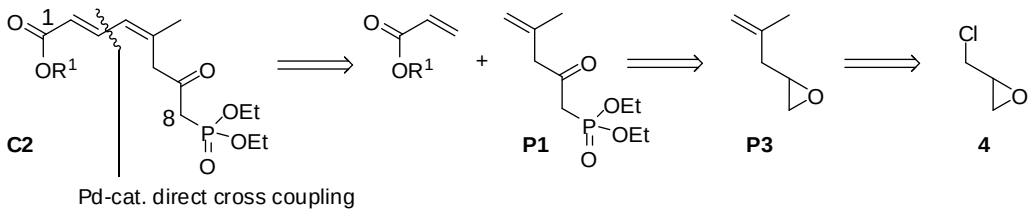

Scheme 3.6.1 Retrosynthetic analysis of Fragment **C2**.

3.6.2 Synthetic effort towards Fragment C2 and C3

Initial effort to synthesize phosphonate **P2-1** was started by transforming alkene **A9-1**, which was one of the compounds synthesized in synthetic route of Fragment **A**. (Scheme 3.6.5) This synthetic strategy required five steps of reactions, started from ester reduction to alcohol, alcohol protection with tosyl group, removal of triisopropylsilyl group to yield alcohol **A12-5**, followed by epoxidation and formation of phosphonate **P2-1** *via* epoxide ring opening. This synthetic route yielded phosphonate **P2-1** at an overall yield of 11%.

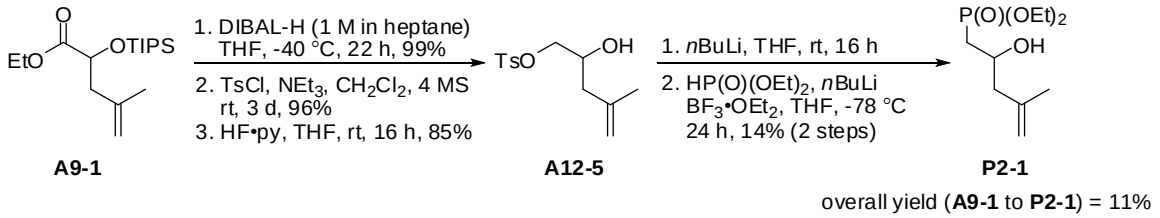

Scheme 3.6.5 Initial effort of synthesizing phosphonate **P2-1** from alkene **A9-1**.

Due to multiple protection and deprotection steps required, we decided to synthesize phosphonate **P2-1** from epichlorohydrin (**4**). (Scheme 3.6.6) Dai's method was employed in the preparation of epoxide **P3**.[145] The phosphonate **P2-1** could be obtained in 3 steps with an overall yield range of 5 – 10%.

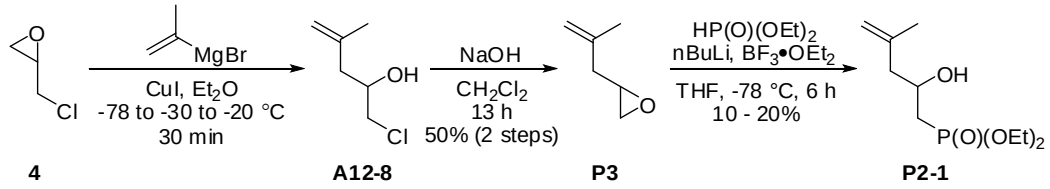

Scheme 3.6.6 Shortened synthetic route towards phosphonate **P2-1**.

With phosphonate **P2-1** in hand, we next oxidized the alcohol to ketone **P1** and subjected into direct cross coupling reaction. The methodologies reported by our group before, including Pd-catalyzed,[48] Ru-catalyzed[53] and Rh-catalyzed,[54] did not provide our intended diene **C2**. Instead, the ketone **P1** was isomerized into a conjugated ketone. (Scheme 3.6.7) Without further oxidized into ketone **P1**, alcohol **P2-1** was subjected into direct cross coupling reaction. Under the same conditions applied above, none of them provided

[145] Dai, M.; Krauss, I. J.; Danishefsky, S. J. *J. Org. Chem.* **2008**, *73*, 9576-9583.

desired diene **C3-1**. Instead, alcohol **P2-1** was dehydrated and became a dienylphosphonate.

From these reactions, we understood that the phosphonate **P2-1** and **P1** are susceptible to metal-catalyzed conditions. Therefore, alcohol protection made on phosphonate **P2-1** might able to allow us to access conjugated dienoate. At the beginning, alcohol protection with PMB and TIPS were failed. Fortunately, alcohol protection with TBDPS was successful. With the phosphonate **P2-4** in hand, we subjected it to Pd-catalyzed direct cross coupling reaction and obtained the desired dienoate **C3-2** at a yield of 36% albeit of *Z*/*E* selectivity of 35:65.

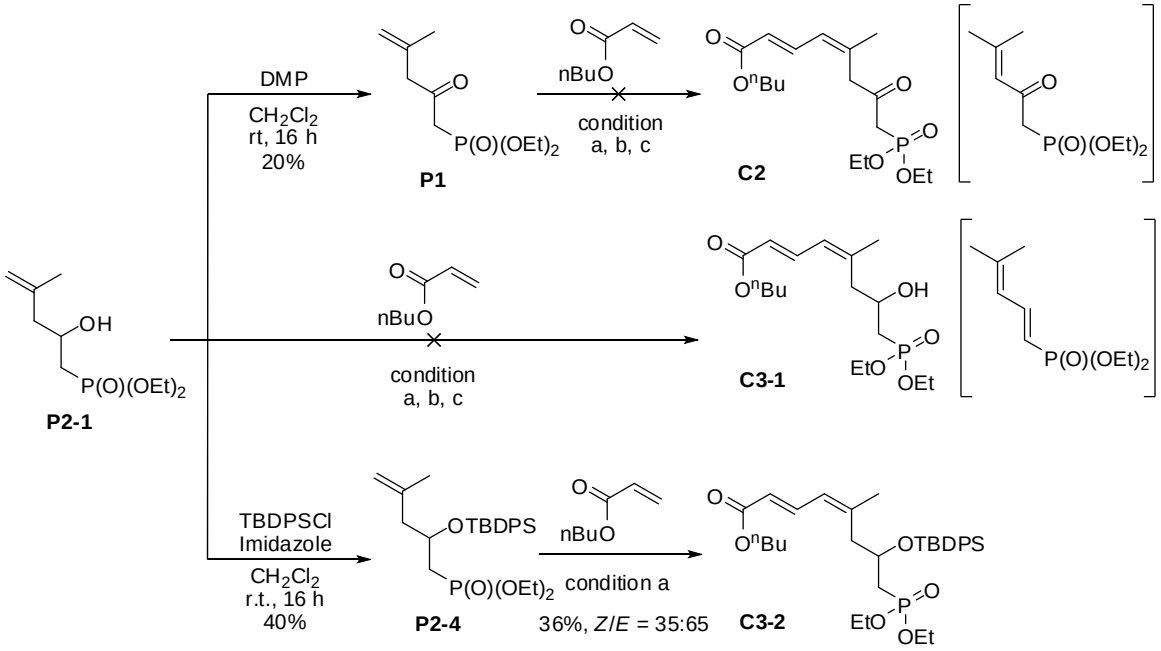

Scheme 3.6.7 Diene synthesis from phosphonate **P2-1**.

Conditions a: $Pd(OAc)_2$ (10 mol%), 1,10-phenanthroline (12 mol%), $AgSbF_6$ (20 mol%), $Cu(OAc)_2$ (2 equiv.), MeCN/PivOH (v/v = 1:1), 120 ℃, 48 h. [48]

Conditions b: $[RuCl_2(p\text{-cymene})]_2$ (5 mol%), $AgSbF_6$ (20 mol%), $Cu(OAc)_2 H_2O$ (2 equiv.), 1,4-dioxane, 135 ℃, 24 h. [53]

Conditions c: $[Cp^*RhCl_2]_2$ (2.5 mol%), $AgSbF_6$ (10 mol%), $Cu(OAc)_2 H_2O$ (1.1 equiv.), THF, 80 ℃, 17 h. [54]

3.7 Conclusion

In a nutshell, we were able to synthesize C1-C8 fragment (or Fragment **C**) and C9-C19 fragment (Fragment **AB**) of dactylolide *via* 2nd Generation Synthetic Route, which summarized in Scheme 3.7.1 and 3.7.2. The synthesis demonstrated that $In(OTf)_3$-catalyzed intramolecular 2,5-oxonium-ene cyclization was feasible in construction of 2,6-*syn*-4-exomethylene tetrahydropyran of dactylolide albeit in a relative low yield (15%). Besides, palladium-catalyzed direct cross coupling was also feasible in construction of dienoate that bearing with phosphonate group although low *Z*-selectivity was observed. The synthesis of Fragment **A** was completed in 6 steps, with an overall yield of 11.3%, while synthesis of Fragment **B** was achieved in 3 steps with an overall yield of 48%. The convergent synthesis between Fragment **A** and **B** showed that tetrahydropyran **AB-1b-I** was obtained by a longest linear sequence of 7 steps with an overall yield of 1.7%. (Scheme 3.7.1) The major factors contributed to the low overall yield include (a) moderate yield obtained in Horner-Wadsworth-Emmons reaction and DIBAL-H chemoselective reduction; (b) formation of equivalent amount of dihydropyran in 2,5-oxonium-ene cyclization. Attempts to solve these obstacles, such as shortening the synthetic route to avoid moderate efficient reactions and searching for improvement by testing different conditions, were conducted but to no avail as discussed in previous section.

It was also noteworthy to mention that the previous reported results in the work of $In(OTf)_3$-catalyzed intramolecular 2,5-oxonium-ene cyclization was rectified during our work on synthesis of dactylolide. Mixture of *syn* and *anti* tetrahydropyrans was reported as final products in previous work, but extensive examination on NMR spectrum revealed that only *syn* tetrahydropyrans were obtained, along with undesired dihyropyrans side products.

Although low to moderate yields in each step deteriorated the efficiency of the synthetic route, the target phosphonate **C** was synthesized in 5 steps with an overall yield of 1.4%. (Scheme 3.7.2) We have yet to establish the convergent synthesis between Fragment **AB** and **C**. However, with the availability of these two fragments, it was envisioned that subsequent Horner-Wadsworth-Emmons olefination at C8/C9 and macrolactonization at C1/O20 should provide the macrolide core of dactylolide. (Scheme 3.7.3)

Synthesis of Fragment A

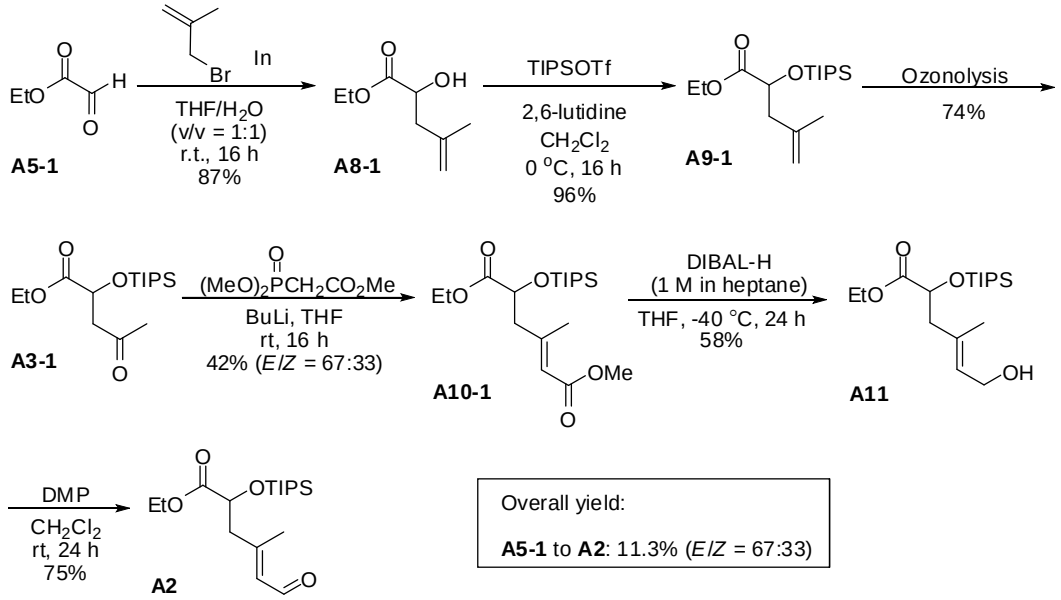

Synthesis of Fragment B

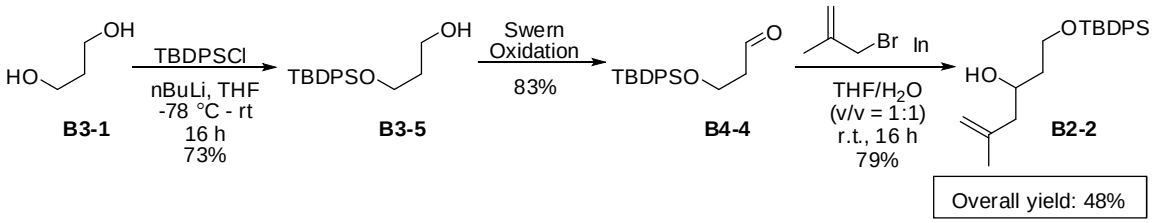

Convergent Synthesis towards Fragment AB

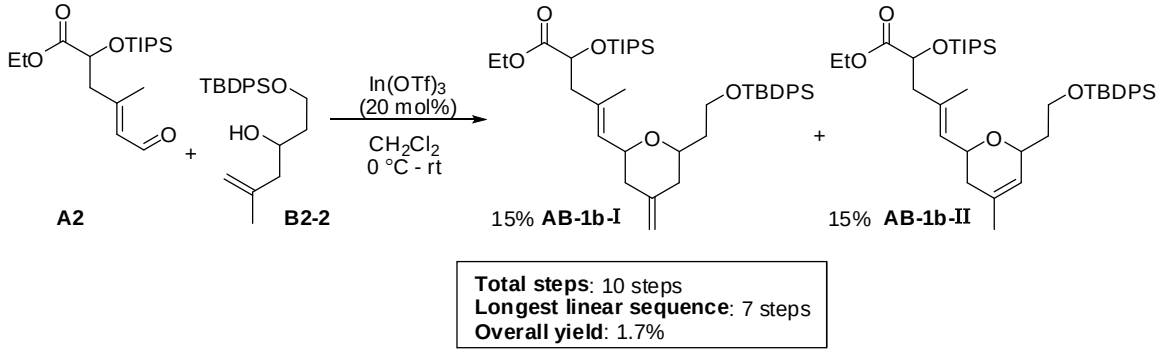

Scheme 3.7.1 Synthetic route towards Fragment **AB** *via* 2nd Generation Synthetic Plan.

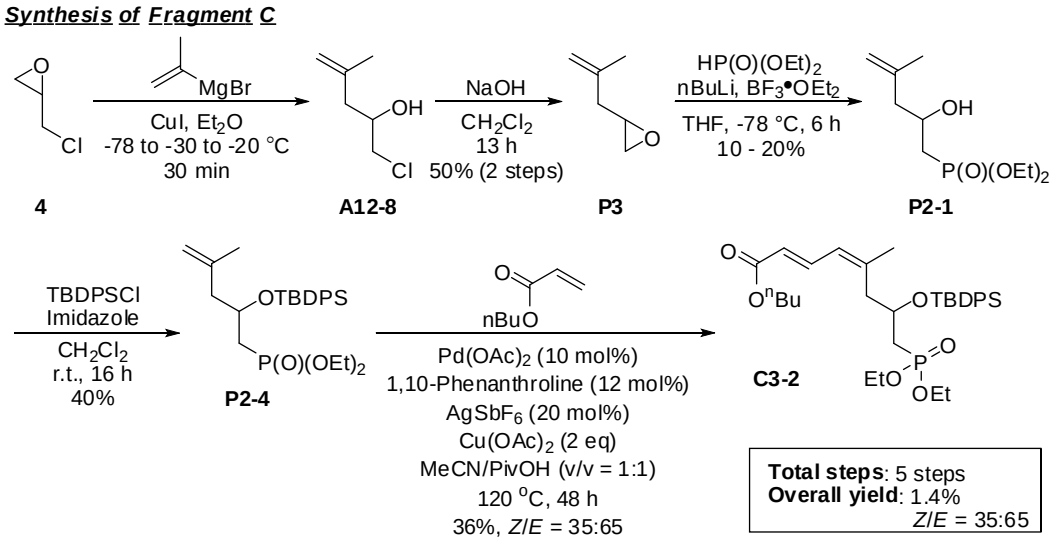

Scheme 3.7.2 Synthetic route towards Fragment **C** *via* 2nd Generation Synthetic Plan.

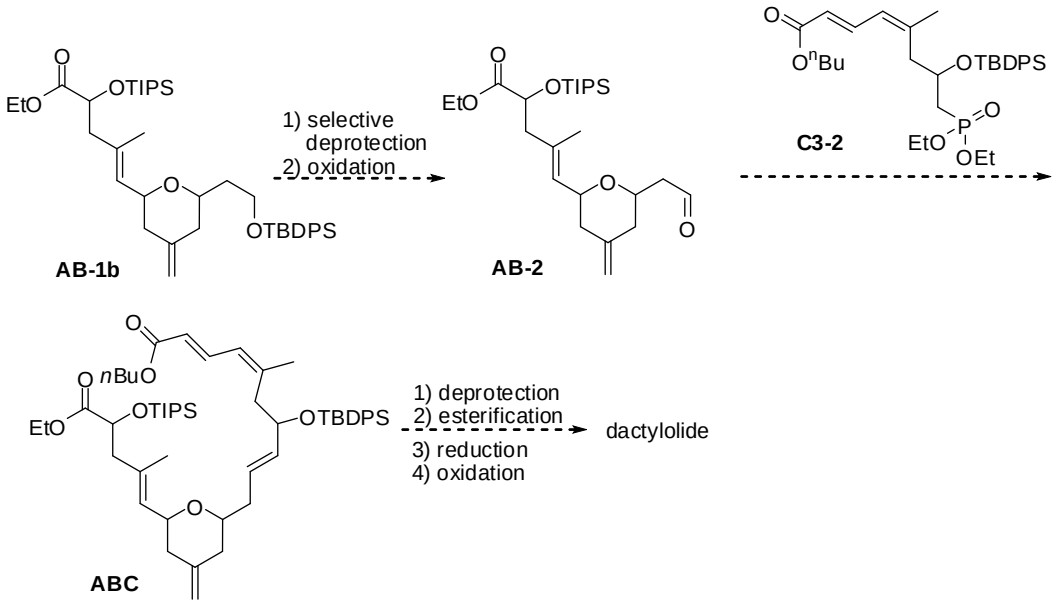

Scheme 3.7.3 Future work on synthesis of dactylolide.

CHAPTER FOUR

EXPERIMENTAL SECTION

4.1 General Method

All reactions requiring anhydrous conditions were conducted in oven-dried (124 ℃) glass apparatus under an atmosphere of N_2 using freshly distilled solvents. Commercial grade solvents and reagents were used without further purification unless otherwise indicated. Preparative chromatographic separations were performed on silica gel and reactions followed by TLC analysis using Merck 60 F254 precoated silica gel plate (0.2 mm thickness) and visualized with UV light or $KMnO_4$ or acidic solution of ceric molybdate. ^1H and ^{13}C NMR spectra were recorded in Fourier transform mode at the field strength specified and from the indicated deuterated solvents in standard 5 mm diameter tubes. Chemical shift in ppm is quoted relative to residual solvent signals calibrated as follows: $CDCl_3$ δH ($CHCl_3$) = 7.26 ppm, δC = 77.0 ppm. Multiplicities in the ^1H NMR spectra are described as: s = singlet, d = doublet, t = triplet, q = quartet, m = multiplet, br = broad. Elements in parentheses following carbon atom chemical shifts refer to the carbon atom and its attached hydrogen atoms as revealed by the DEPT spectral editing technique. The proportion of geometric isomers was determined from the integration of ^1H NMR and ^{13}C NMR spectra. The structure of *E/Z* regioisomers and *syn*/*anti* stereoisomers were identified from Nuclear Overhauser effect spectroscopy (NOESY). High resolution mass spectral analysis (HRMS) was performed on Water Q-TOF Premier mass spectrometer (Thermo Electron Corporation).

4.2 Experimental procedures and supporting information

4.2.1 Compounds synthesized in 2nd Generation Synthetic Route

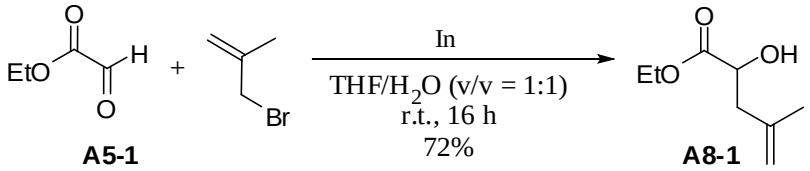

Ethyl 2-hydroxy-4-methylpent-4-enoate (A8-1):

Indium (6.89 g, 60.0 mmol) and 3-bromo-2-methylpropene (6.0 mL, 60.0 mmol) was added into a mixture of THF (75.0 mL) and H_2O (75.0 mL) at room temperature and allowed to stir for 30 mins. Ethyl glyoxalate (5.90 mL, ~50% in toluene solution, 30.0 mmol) was then added into the mixture and stirred for 16 h. After that, the reaction mixture was filtered through celite, extracted with Et_2O (3 x 50.0 mL) and washed with brine (50.0 mL). The combined organic extracts were dried over Na_2SO_4, filtered and concentrated in *vacuo*. The crude residue was purified by column chromatography (hexane/EtOAc = 5:1) to afford homoallylic alcohol **A8-1** (3.417 g, 21.6 mmol, 72% yield) as colorless liquid.

R_f value (hexane/EtOAc = 4:1): 0.30;

^{1}H NMR (400 MHz, $CDCl_3$): δ 4.88 (s, 1H), 4.82 (s, 1H), 4.34-4.29 (m, 1H), 4.25 (q, *J* = 7.2 Hz, 2H), 2.71 (d, *J* = 6.0 Hz, 1H), 2.53 (dd, *J* = 4.2, 14.2 Hz, 1H), 2.37 (dd, *J* = 8.2, 14.2 Hz, 1H), 1.79 (s, 3H), 1.30 (t, *J* = 7.2 Hz, 3H) ppm.

^{13}C NMR (100 MHz, $CDCl_3$): δ 174.7, 141.0, 114.0, 69.1, 61.7, 42.7, 22.5, 14.2 ppm.

HRMS (ESI): m/z calculated for $C_8H_{15}O_3$ $[M+H]^+$: 159.1021, found: 159.1024.

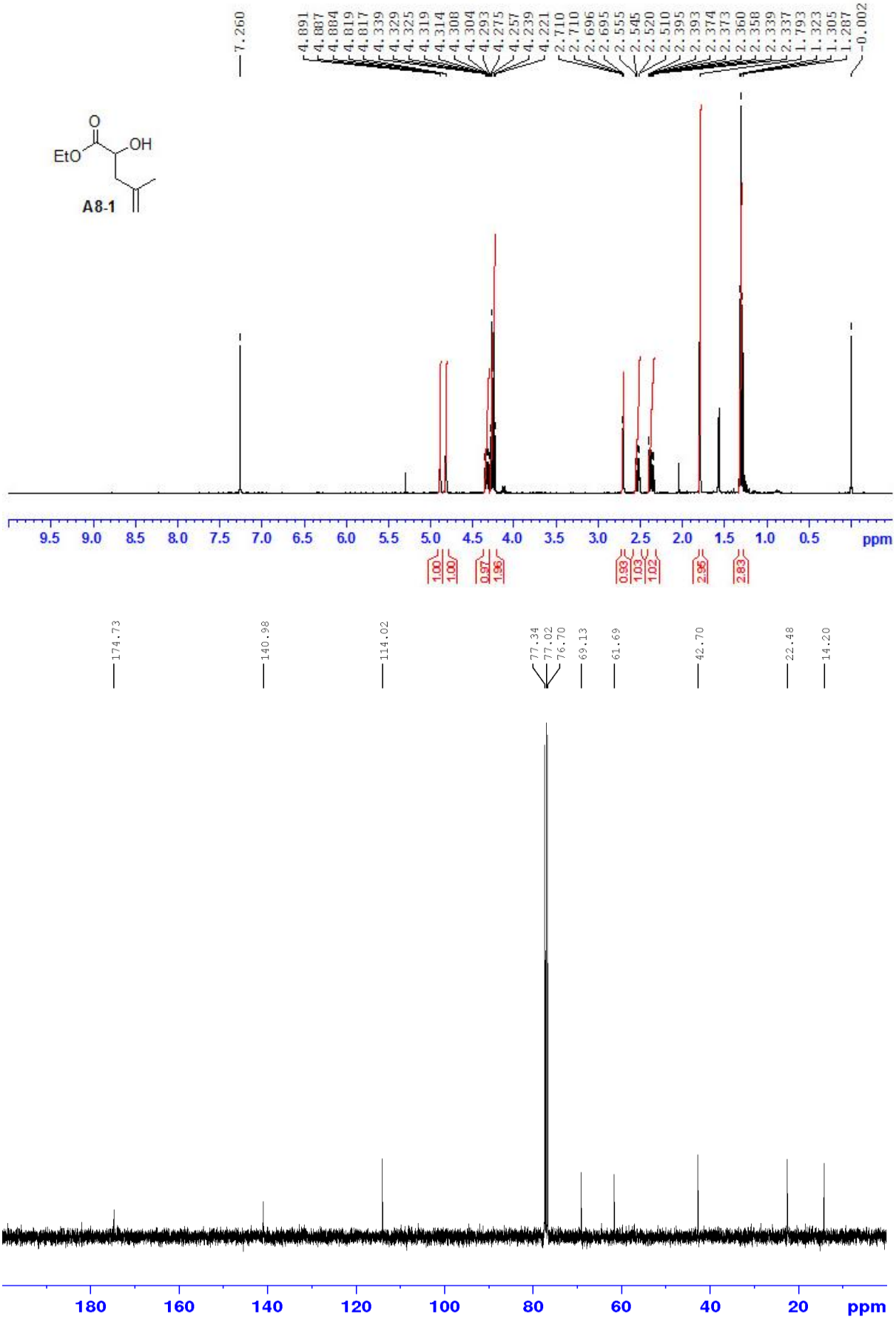
7.260
4.891
4.887
4.884
4.819
4.817
4.339
4.329
4.325
4.319
4.314
4.308
4.304
4.293
4.275
4.257
4.239
4.221
2.710
2.710
2.696
2.695
2.555
2.545
2.520
2.510
2.395
2.393
2.374
2.373
2.360
2.358
2.339
2.337
1.793
1.323
1.305
1.287
-0.002
O
EtO
OH
A8-1
9.5 9.0 8.5 8.0 7.5 7.0 6.5 6.0 5.5 5.0 4.5 4.0 3.5 3.0 2.5 2.0 1.5 1.0 0.5 ppm
1.00
1.00
0.97
1.96
0.93
1.03
1.02
2.95
2.83
174.73
140.98
114.02
77.34
77.02
76.70
69.13
61.69
42.70
22.48
14.20
180 160 140 120 100 80 60 40 20 ppm

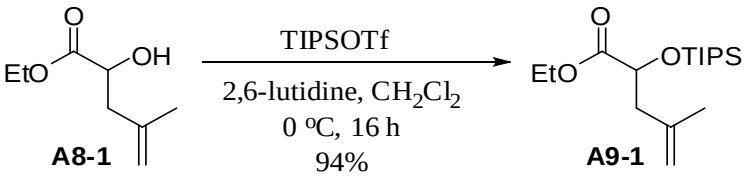

Ethyl 4-methyl-2-(triisopropylsilyloxy)pent-4-enoate (A9-1):

To a solution of alcohol **A8-1** (4.75 g, 30.0 mmol) in CH_2Cl_2 (60.0 mL) at 0 ^oC under N_2 atmosphere, 2,6-lutidine (4.86 mL, 42.0 mmol) and triisopropyl trifluoromethanesulfonate (9.68 mL, 36.0 mmol) was added dropwise. The reaction mixture was allowed to warm up to room temperature and stir 16 h. Then, the reaction was quenched by H_2O (30.0 mL), extracted with CH_2Cl_2 (3 x 30 mL) and washed with brine (30 mL). The combined organic extracts were dried over Na_2SO_4, filtered and concentrated in *vacuo*. The crude residue was purified by column chromatography (hexane/EtOAc = 50:1) to afford alkene **A9-1** (8.87 g, 28.2 mmol, 94% yield) as colorless liquid.

R_f value (hexane/EtOAc = 4:1): 0.67;

^{1}H NMR (400MHz, $CDCl_3$): δ 4.79 (s, 1H), 4.74 (s, 1H), 4.46 (t, *J* = 6.0 Hz, 1H), 4.16 (q, *J* = 7.2 Hz, 2H), 2.47 (d, *J* = 5.2 Hz, 2H), 1.78 (s, 3H), 1.26 (t, *J* = 7.2 Hz, 3H), 1.13-1.06 (m, 21H) ppm.

^{13}C NMR (100 MHz, $CDCl_3$): δ 173.2, 141.1, 113.9, 71.9, 60.5, 44.2, 22.9, 17.9, 14.2, 12.2 ppm.

HRMS (ESI): m/z calculated for $C_{17}H_{34}O_3SiNa$ $[M+Na]^+$: 337.2175, found: 337.2188.

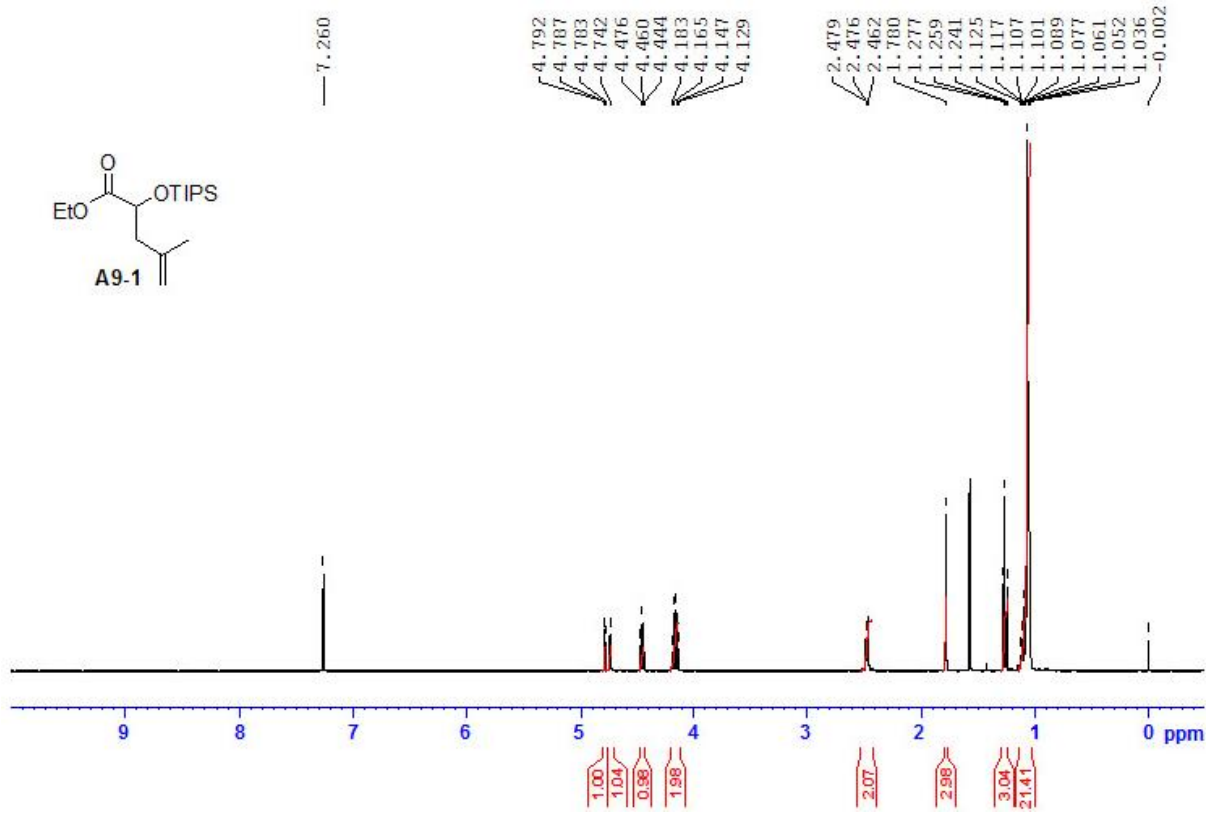
7.260
4.792
4.787
4.783
4.742
4.476
4.460
4.444
4.183
4.165
4.147
4.129
2.479
2.476
2.462
1.780
1.277
1.259
1.241
1.125
1.117
1.107
1.101
1.089
1.077
1.061
1.052
1.036
0.002
O
EtO
OTIPS
A9-1
9
8
7
6
5
4
3
2
1
0 ppm
1.00
1.04
0.98
1.98
2.07
2.98
3.04
21.41

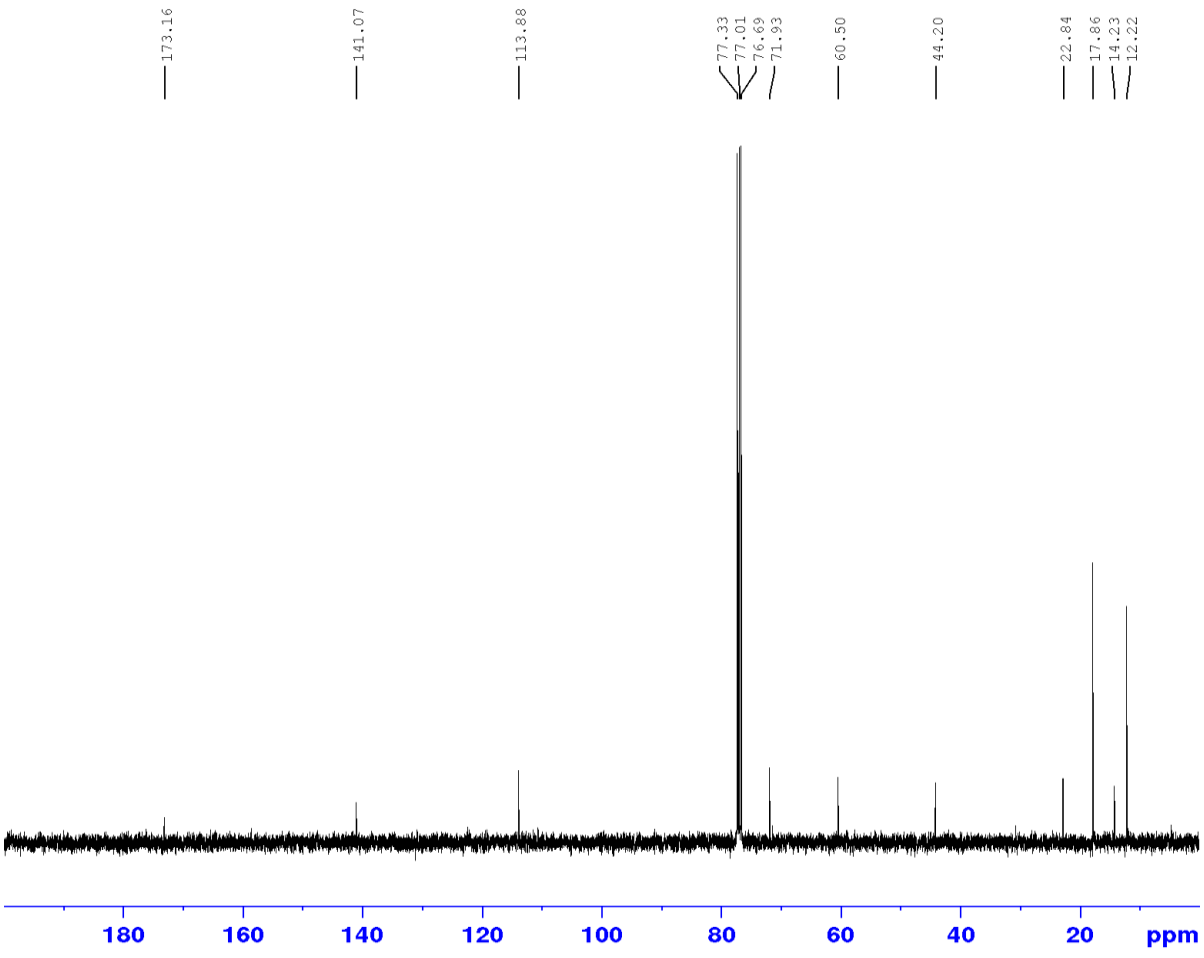
173.16
141.07
113.88
77.33
77.01
76.69
71.93
60.50
44.20
22.84
17.86
14.23
12.22
180
160
140
120
100
80
60
40
20
ppm

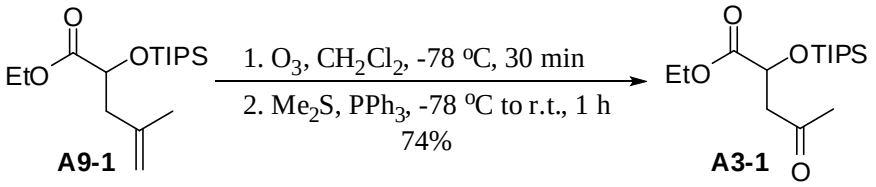

Ethyl 4-oxo-2-(triisopropylsilyloxy)pentanoate (A3-1):

Ozone was continuosly flushed into a solution of alkene **A9-1** (9.44 g, 30.0 mmol) in CH_2Cl_2 (300 mL) at -78 °C until the solution turned into blue in colour. Then, dimethyl sulfide (22.0 mL, 300 mmol) was added into the reaction mixture dropwise. The reaction mixture was allowed to warm to room temperature and stir for 1 h. After that, the reaction mixture was concentrated in *vacuo*. The crude residue was purified by column chromatography (hexane/EtOAc = 5:1) to afford ketone **A3-1** (7.03 g, 22.2 mmol, 74% yield) as colorless liquid.

R_f value (hexane/EtOAc = 4:1): 0.45;

^{1}H NMR (400MHz, $CDCl_3$): δ 4.75 (t, *J* = 6.4 Hz, 1H), 4.18 (q, *J* = 7.2 Hz, 2H), 2.87 (ddd, *J* = 5.8, 16.2, 41.4 Hz, 2H), 2.19 (s, 3H), 1.27 (t, *J* = 7.2 Hz, 3H), 1.14-1.04 (m, 21H) ppm.

^{13}C NMR (100 MHz, $CDCl_3$): δ 205.6, 172.7, 69.0, 61.1, 48.8, 31.0, 17.9, 14.1, 12.3 ppm.

HRMS (ESI): m/z calculated for $C_{16}H_{32}O_4SiNa$ $[M+Na]^+$: 339.1968, found: 339.1978.

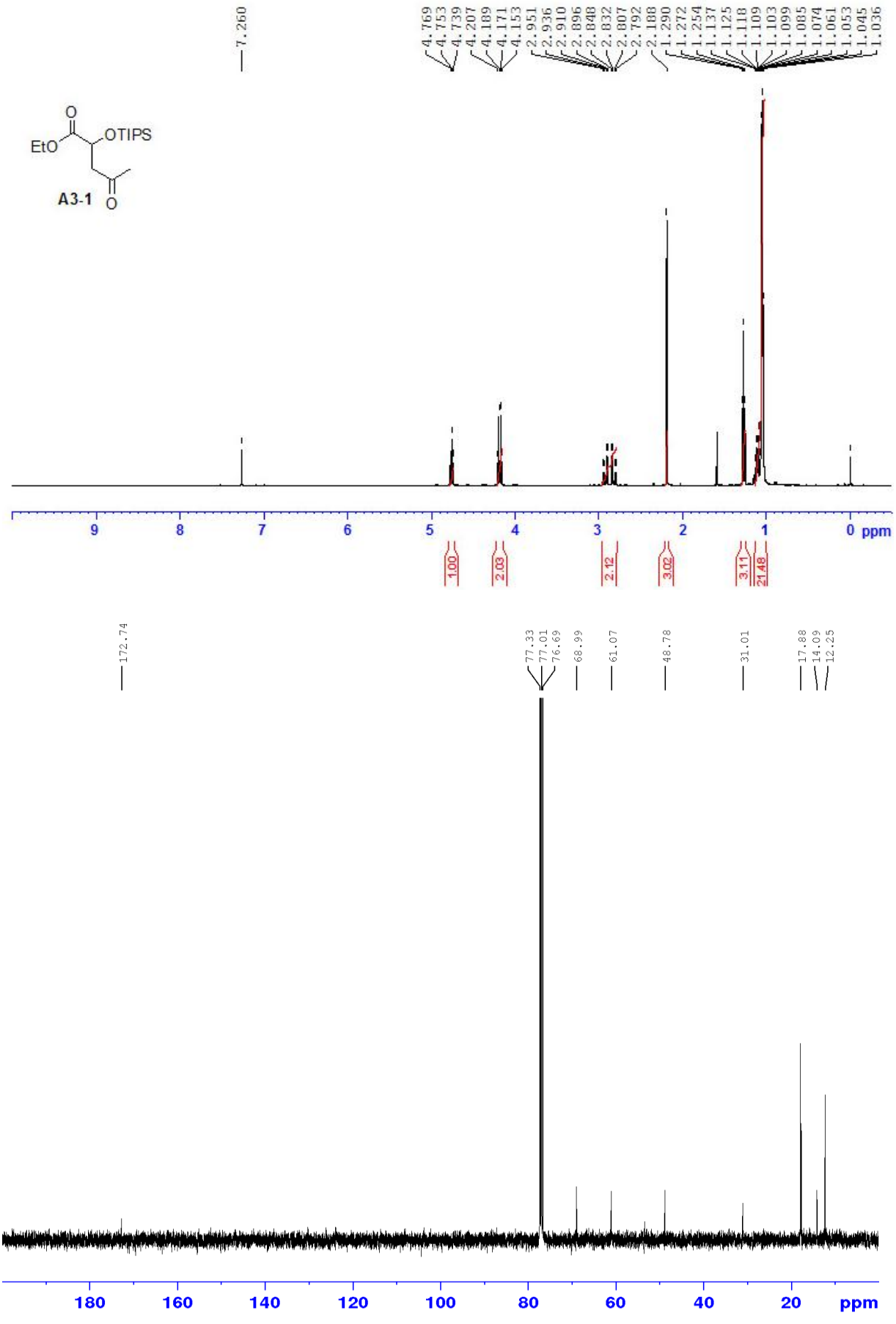
7.260
4.769
4.753
4.739
4.207
4.189
4.171
4.153
2.951
2.936
2.910
2.896
2.848
2.832
2.807
2.792
2.188
1.290
1.272
1.254
1.137
1.125
1.118
1.109
1.103
1.099
1.085
1.074
1.061
1.053
1.045
1.036
EtO
OTIPS
A3-1
9
8
7
6
5
4
3
2
1
0 ppm
1.00
2.03
2.12
3.02
3.11
21.48
172.74
77.33
77.01
76.69
68.99
61.07
48.78
31.01
17.88
14.09
12.25
180
160
140
120
100
80
60
40
20
ppm

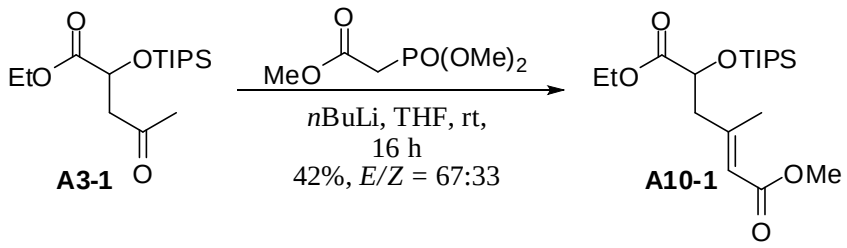

(*E*)-6-Ethyl 1-methyl 3-methyl-5-(triisopropylsilyloxy)hex-2-enedioate (A10-1):

n-BuLi (7.7 mL, Aldrich 2.0 M in cyclohexane, 15.3 mmol) was added dropwise into a solution of trimethylphosphonoacetate (3.2 mL, 19.5 mmol) in THF (15.0 mL) at room temperature under N_2 atmosphere. After stirring for 1 h, ketone **A3-1** (4.75 g, 15.0 mmol) was added into the mixture and allowed to stir for 16 h at room temperature. The reaction mixture was then quenched by saturated NH_4Cl aqueous solution (30.0 mL), extracted with Et_2O (3 x 30.0 mL), washed with brine (30.0 mL). The organic layer was dried over Na_2SO_4, filtered and concentrated in vacuo. The crude residue was further purified by column chromatography (eluting with hexane/EtOAc = 5:1) to yield conjugated ester **A10-1** (2.35 g, 6.3 mmol, 42% yield; *E*/*Z* = 67:33) as colorless liquid.

Note: *E* and *Z* isomers of **A10-1** could not be separated by column chromatography.

R_f value (hexane/EtOAc = 4:1): 0.55;

^{1}H NMR (400MHz, $CDCl_3$):

E-isomer: δ 5.72 (s, 1H), 4.51 (t, *J* = 6.2 Hz, 1H), 4.16 (q, *J* = 7.2 Hz, 2H), 3.67 (s, 3H), 2.56 (d, *J* = 6.4 Hz, 2H), 2.21 (s, 3H), 1.26 (t, *J* = 7.2 Hz, 3H), 1.14-1.04 (m, 21H) ppm.

Z-isomer: δ 5.76 (s, 1H), 4.63 (t, *J* = 6.4 Hz, 1H), 4.16 (q, *J* = 7.2 Hz, 2H), 3.67 (s, 3H), 3.12 (dd, *J* = 5.6, 12.8 Hz, 1H), 3.05 (dd, *J* = 7.2, 9.2 Hz, 1H), 1.98 (s, 3H), 1.26 (t, *J* = 7.2 Hz, 3H), 1.14-1.04 (m, 21H) ppm.

^{13}C NMR (100 MHz, $CDCl_3$):

E-isomer: δ 172.7, 166.8, 154.7, 118.6, 71.4, 60.9, 50.9, 46.9, 19.3, 17.7, 14.1, 12.3 ppm.

Z-isomer: δ 172.7, 166.8, 154.7, 118.3, 71.8, 60.7, 50.9, 39.0, 26.7, 17.7, 14.1, 12.3 ppm.

HRMS (ESI): m/z calculated for $C_{19}H_{37}O_5Si$ $[M+H]^+$: 373.2410, found: 373.2405.

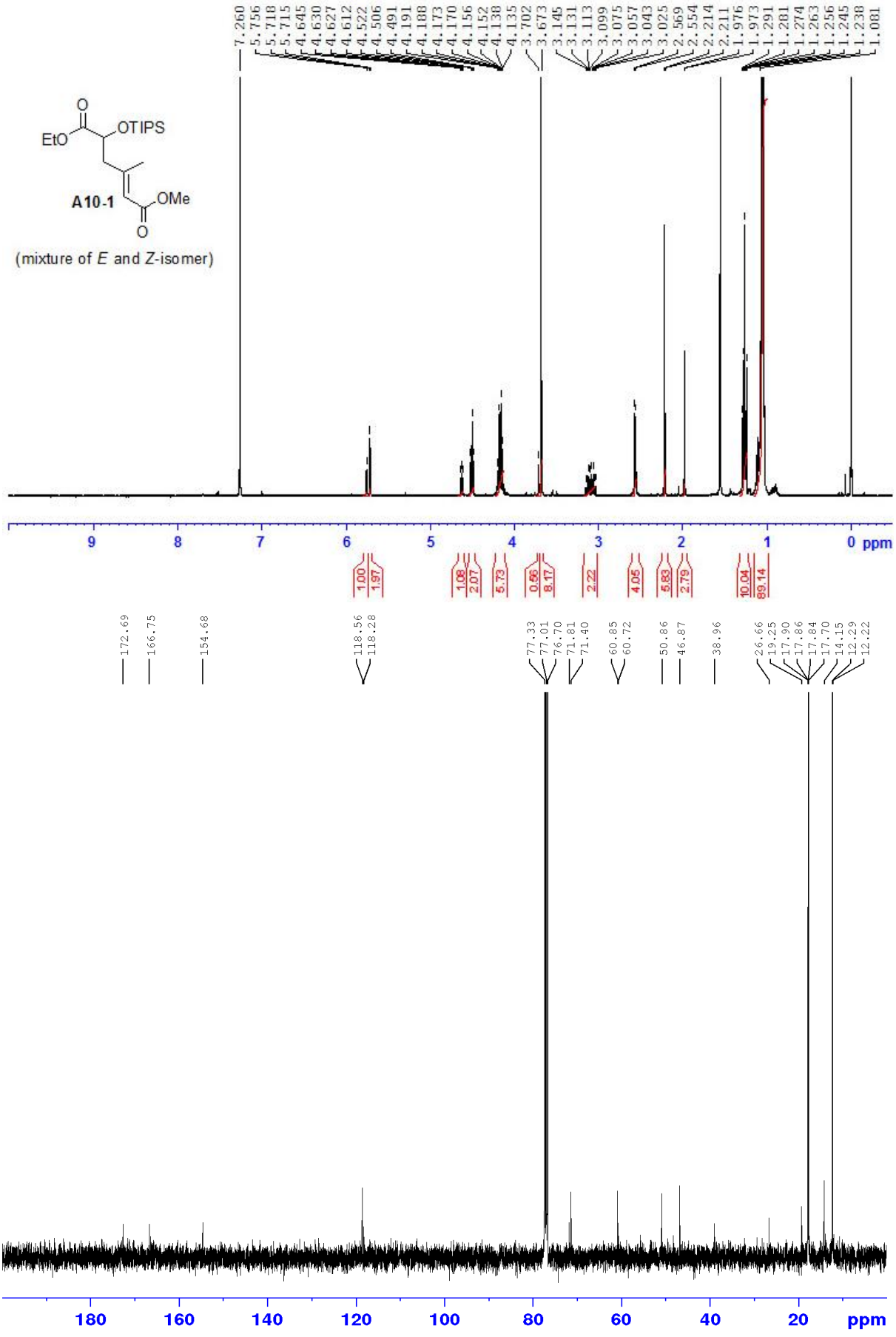
7.260
5.756
5.718
5.715
4.645
4.630
4.627
4.612
4.522
4.506
4.491
4.191
4.188
4.173
4.170
4.156
4.152
4.138
4.135
3.702
3.673
3.145
3.131
3.113
3.099
3.075
3.057
3.043
3.025
2.569
2.554
2.214
2.211
1.976
1.973
1.291
1.281
1.274
1.263
1.256
1.245
1.238
1.081
EtO
OTIPS
A10-1
OMe
O
O
(mixture of E and Z-isomer)
9
8
7
6
5
4
3
2
1
0 ppm
1.00
1.97
1.08
2.07
5.73
0.66
8.17
2.22
4.05
5.83
2.79
10.04
89.14
172.69
166.75
154.68
118.56
118.28
77.33
77.01
76.70
71.81
71.40
60.85
60.72
50.86
46.87
38.96
26.66
19.25
17.90
17.86
17.84
17.70
14.15
12.29
12.22
180
160
140
120
100
80
60
40
20
ppm

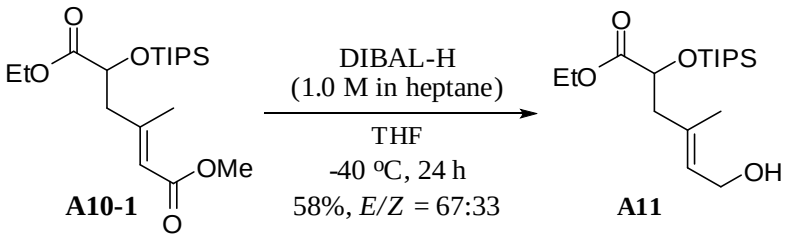

(*E*)-Ethyl 6-hydroxy-4-methyl-2-(triisopropylsilyloxy)hex-4-enoate (A11):

DIBAL-H (12.0 mL, Aldrich 1.0 M in heptane, 12.0 mmol) was added dropwise into a solution of conjugated ester **A10-1** (*E/Z* mixture; 2.24 g, 6.0 mmol) in THF (12.0 mL) at -40 ^{o}C under N_2 atmosphere. After stirring for 24 h, the reaction mixture was quenched by MeOH (0.54 mL, 13.2 mmol) and stirred for 15 mins. Saturated potassium sodium tartrate aqueous solution (12.0 mL) and THF (12.0 mL) was then added into the mixture and the mixture was allowed to warm to room temperature. The reaction mixture was extracted with Et_2O (3 x 20.0 mL) and washed with brine (20.0 mL). The organic layer was dried over Na_2SO_4, filtered and concentrated in vacuo. The crude residue was further purified by column chromatography (eluting with hexane/EtOAc = 2:1) to yield alcohol **A11** (1.20 g, 3.48 mmol, 58% yield; *E*/*Z* = 67:33) as colorless liquid.

Note: *E* and *Z* isomers of **A11** could be separated by column chromatography. Following data are that of (*E*)-**A11**.

R_f value (hexane/EtOAc = 4:1): 0.13;

^{1}H NMR (400MHz, $CDCl_3$): δ 5.46 (t, *J* = 6.4 Hz, 1H), 4.45 (t, *J* = 6.4 Hz, 1H), 4.19-4.11 (m, 4H), 2.46 (d, *J* = 6.4 Hz, 2H), 1.74 (s, 3H), 1.71 (s, 1H), 1.28 (t, *J* = 7.2 Hz, 3H), 1.13-1.03 (m, 21H) ppm;

^{13}C NMR (100MHz, $CDCl_3$): δ 173.1, 134.9, 127.4, 72.0, 60.6, 59.2, 45.8, 17.9, 16.8, 14.2, 12.2 ppm.

HRMS (ESI): m/z calculated for $C_{18}H_{36}O_4SiNa$ $[M+Na]^+$: 367.2281, found: 367.2281.

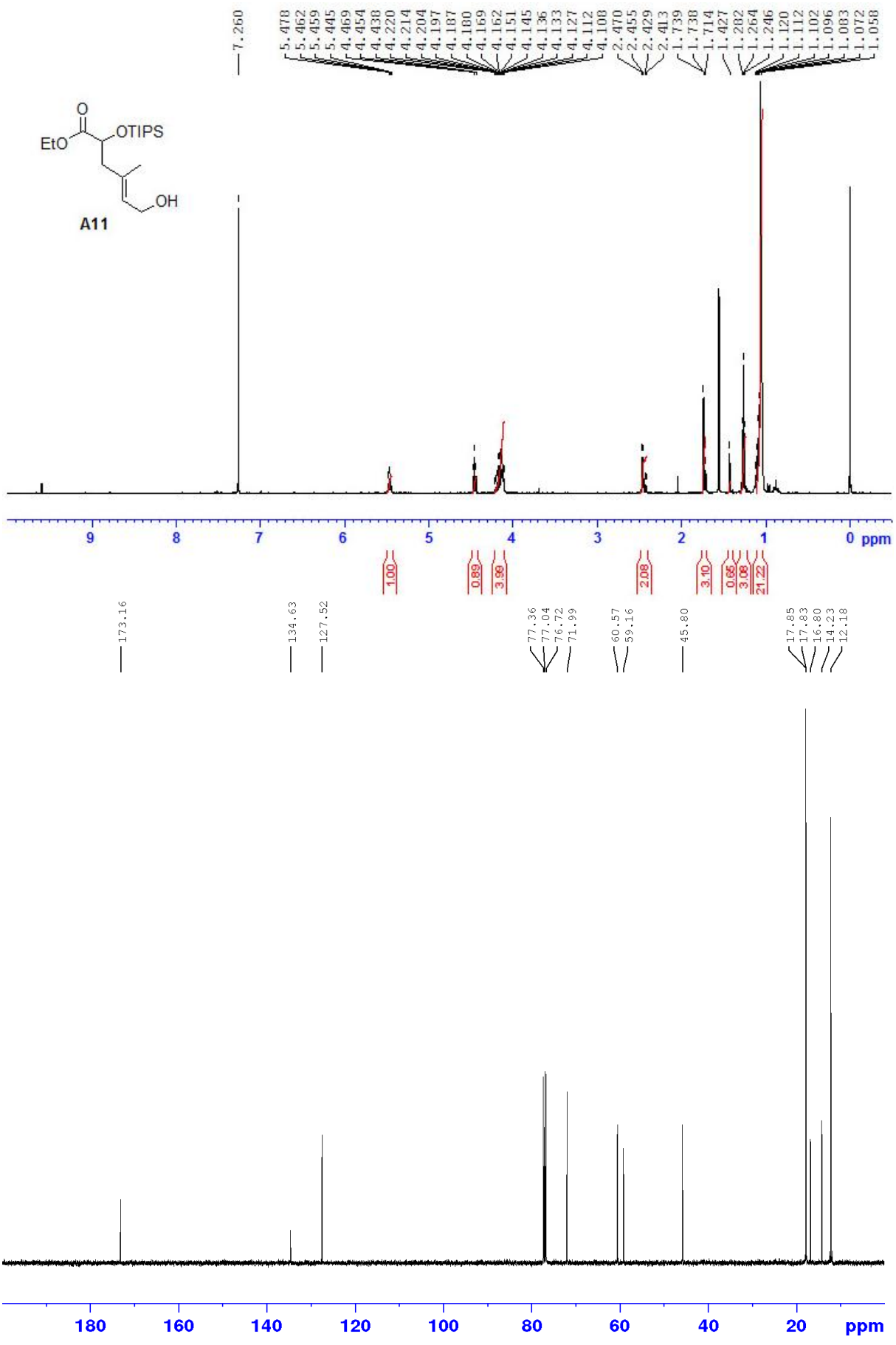
7.260
5.478
5.462
5.459
5.445
4.469
4.454
4.438
4.220
4.214
4.204
4.197
4.187
4.180
4.169
4.162
4.151
4.145
4.136
4.133
4.127
4.112
4.108
2.470
2.455
2.429
2.413
1.739
1.738
1.714
1.427
1.282
1.264
1.246
1.120
1.112
1.102
1.096
1.083
1.072
1.058
O
EtO
OTIPS
OH
A11
9
8
7
6
5
4
3
2
1
0 ppm
1.00
0.89
3.99
2.08
3.10
0.65
3.08
21.22
173.16
134.63
127.52
77.36
77.04
76.72
71.99
60.57
59.16
45.80
17.85
17.83
16.80
14.23
12.18
180
160
140
120
100
80
60
40
20
ppm

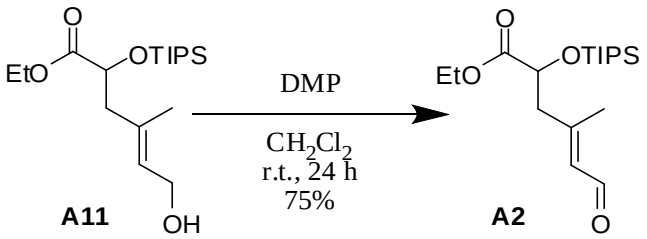

(*E*)-Ethyl 4-methyl-6-oxo-2-(triisopropylsilyloxy)hex-4-enoate (A2):

Dess-martin periodinane (1.70 g, 4.0 mmol) was added as a portion into a solution of alcohol **A11** (0.689 g, 2.0 mmol) in CH_2Cl_2 (20.0 mL) at room temperature. After stirring for 24 h, the reaction mixture was quenched by mixture of saturated sodium bicarbonate aqueous solution (20.0 mL) and saturated sodium thiosulfate aqueous solution (20.0 mL). The reaction mixture was then extracted with CH_2Cl_2 (3 x 20.0 mL) and washed with brine (20.0 mL). The organic layer was dried over Na_2SO_4, filtered and concentrated in vacuo. The crude residue was further purified by column chromatography (eluting with hexane/EtOAc = 5:1) to yield aldehyde **A2** (0.514 g, 1.50 mmol, 75% yield) as colorless liquid.

Note: (*E*)-**A2** is easily isomerized into a mixture of (*E*)-**A2** and (*Z*)-**A2**.

R_f value (hexane/EtOAc = 4:1): 0.39;

^{1}H NMR (400MHz, $CDCl_3$): δ 9.89 (d, *J* = 8.0 Hz, 1H), 5.81 (d, *J* = 7.6 Hz, 1H), 4.50 (t, *J* = 6.0 Hz, 1H), 4.12-4.06 (m, 2H), 2.58 (d, *J* = 6.0 Hz, 2H), 2.17 (s, 3H), 1.18 (t, *J* = 7.2 Hz, 3H), 1.04-0.98 (m, 21H) ppm.

^{13}C NMR (100MHz, $CDCl_3$): δ 190.6, 172.3, 158.5, 130.0, 71.4, 60.9, 46.3, 18.1, 17.8, 14.1, 12.1 ppm.

HRMS (ESI): m/z calculated for $C_{18}H_{34}O_4SiNa$ $[M+Na]^+$: 365.2124, found: 365.2119.

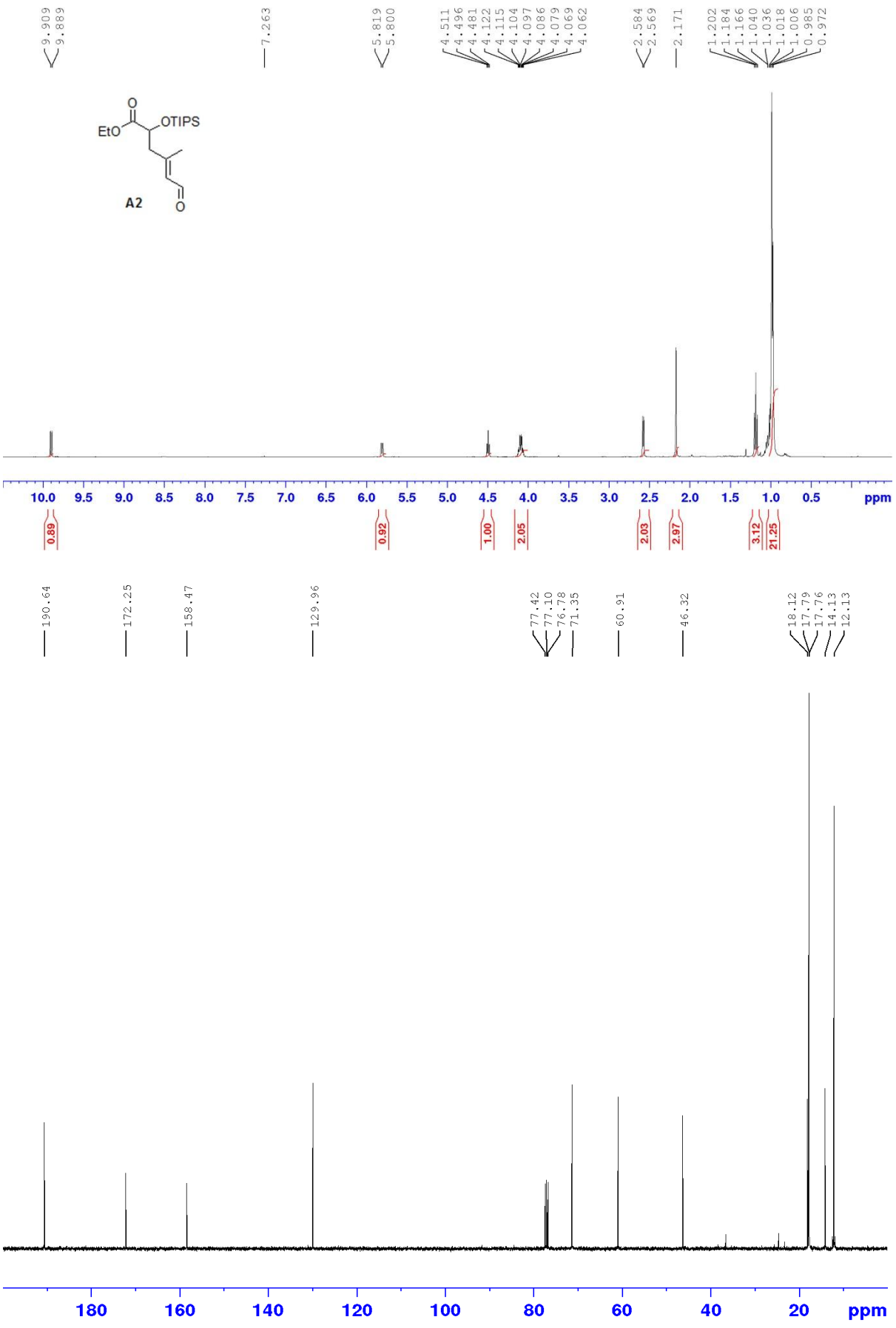
9.909
9.889
7.263
5.819
5.800
4.511
4.496
4.481
4.122
4.115
4.104
4.097
4.086
4.079
4.069
4.062
2.584
2.569
2.171
1.202
1.184
1.166
1.040
1.036
1.018
1.006
0.985
0.972
EtO
OTIPS
A2
O
O
10.0
9.5
9.0
8.5
8.0
7.5
7.0
6.5
6.0
5.5
5.0
4.5
4.0
3.5
3.0
2.5
2.0
1.5
1.0
0.5
ppm
0.89
0.92
1.00
2.05
2.03
2.97
3.12
21.25
190.64
172.25
158.47
129.96
77.42
77.10
76.78
71.35
60.91
46.32
18.12
17.79
17.76
14.13
12.13
180
160
140
120
100
80
60
40
20
ppm

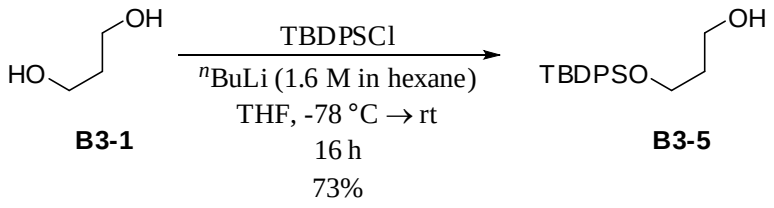

B3-1 **B3-5**

3-(*tert*-Butyldiphenylsilyloxy)propan-1-ol (B3-5):

n-Butyllithium (25.0 mL, Aldrich 1.6 M in hexane, 40.0 mmol) was added dropwise into a solution of 1,3-propanediol **B3-1** (2.90 ml, 40.0 mmol) in THF (80.0 mL) at -78 ^{o}C under N_2 atmosphere. *tert*-Butyldiphenylsilyl chloride (10.3 ml, 40.0 mmol) was then added and allowed the reaction warm to room temperature and stirred for 16 h. The reaction mixture was concentrated in *vacuo* and further purified by column chromatography (eluting with hexane/EtOAc = 3:1) to yield 3-(tert-butyldiphenylsilyloxy)propan-1-ol **B3-5** (9.18 g, 29.2 mmol, 73% yield) as colorless liquid.

R_f value (hexane/EtOAc = 4:1): 0.29;

^{1}H NMR (400MHz, $CDCl_3$): δ 7.69-7.67 (m, 4H), 7.44-7.40 (m, 6H), 3.87-3.84 (m, 4H), 2.33 (t, *J* = 5.4 Hz, 1H), 1.81 (tt, *J* = 5.2, 6.4 Hz, 2H), 1.06 (s, 9H) ppm.

^{13}C NMR (100MHz, $CDCl_3$): δ 135.6, 133.3, 129.8, 127.8, 63.3, 62.0, 34.3, 26.8, 19.1 ppm.

HRMS (ESI): m/z calculated for $C_{19}H_{26}O_2SiNa$ $[M+Na]^+$: 337.1600, found: 337.1603.

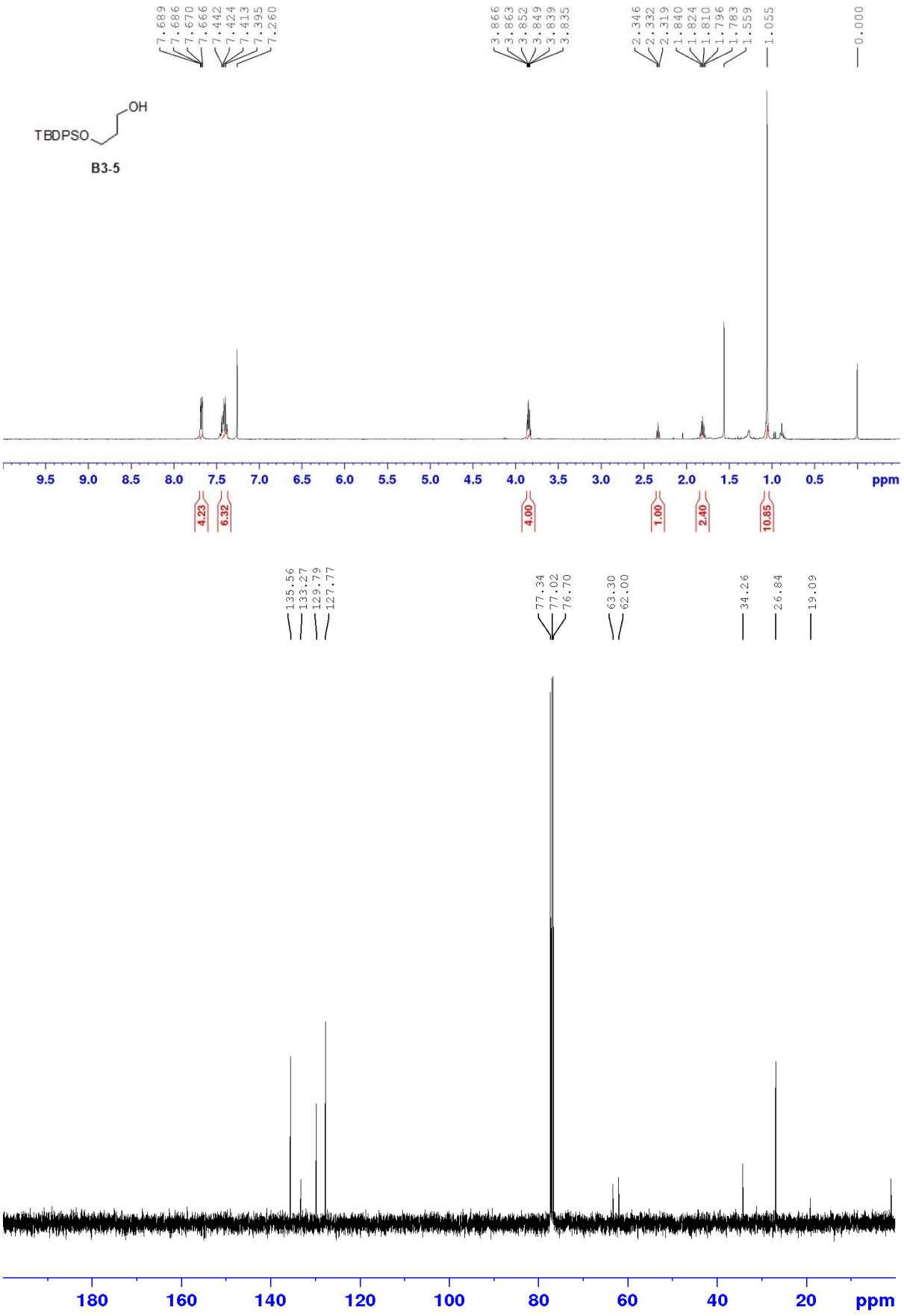
7.689
7.686
7.670
7.666
7.442
7.424
7.413
7.395
7.260
3.866
3.863
3.852
3.849
3.839
3.835
2.346
2.332
2.319
1.840
1.824
1.810
1.796
1.783
1.559
1.055
0.000
OH
TBDPSO
B3-5
9.5
9.0
8.5
8.0
7.5
7.0
6.5
6.0
5.5
5.0
4.5
4.0
3.5
3.0
2.5
2.0
1.5
1.0
0.5
ppm
4.23
6.32
4.00
1.00
2.40
10.85

135.56
133.27
129.79
127.77
77.34
77.02
76.70
63.30
62.00
34.26
26.84
19.09
180
160
140
120
100
80
60
40
20
ppm

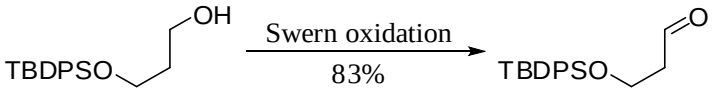

B3-5 **B4-4**

3-(*tert*-Butyldiphenylsilyloxy)propanal (B4-4):

Oxalyl chloride (1.89 mL, 22.0 mmol) was added into a solution of DMSO (3.41 mL, 48.0 mmol) in CH_2Cl_2 (20.0 mL) at -60 ^oC under N_2 atmosphere and allowed to stir for 10 mins. Then, 3-(tert-butyldiphenylsilyloxy)propan-1-ol **B3-5** (6.39 g, 20.0 mmol) was dissolved in CH_2Cl_2 (20.0 mL) and added into the reaction mixture. After stirred for 15 mins, triethylamine (13.9 mL, 100.0 mmol) was added dropwise and the reaction mixture was allowed to stir for 5 mins. Then, the mixture was warmed to room temperature, followed by addition of H_2O (40.0 mL) and stirred for 10 mins. The mixture was extracted with CH_2Cl_2 (3 x 40.0 mL), washed with dilute HCl (40.0 mL), H_2O (40.0 mL), dilute Na_2CO_3 (40.0 mL), H_2O (40.0 mL). The combined organic layer was dried over Na_2SO_4, filtered and concentrated in *vacuo*. The crude residue was further purified by column chromatography (eluting with hexane/EtOAc = 5:1) to yield aldehyde **B4-4** (5.19 g, 16.6 mmol, 83% yield) as colorless liquid.

R_f value (hexane/EtOAc = 4:1): 0.50;

^{1}H NMR (400MHz, $CDCl_3$): δ 9.82 (t, *J* = 2.2 Hz, 1H), 7.68-7.64 (m, 4H), 7.46-7.37 (m, 6H), 4.02 (t, *J* = 6.0 Hz, 2H), 2.61 (dt, *J* = 2.4, 6.0 Hz, 2H), 1.04 (s, 9H) ppm.

^{13}C NMR (100MHz, $CDCl_3$): δ 201.9, 135.6, 133.3, 129.8, 127.8, 58.3, 46.4, 26.8, 19.1 ppm.

HRMS (ESI): m/z calculated for $C_{19}H_{25}O_2Si$ $[M+H]^+$: 313.1624, found: 313.1633.

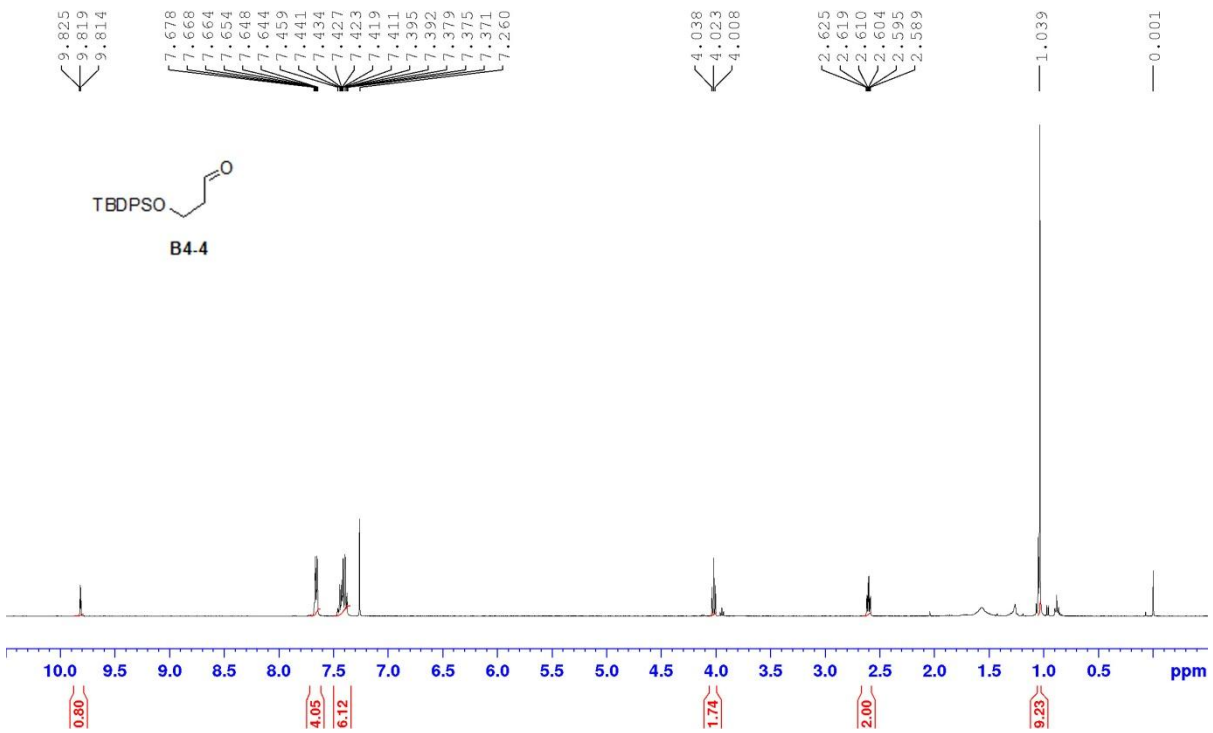
9.825
9.819
9.814
7.678
7.668
7.664
7.654
7.648
7.644
7.459
7.441
7.434
7.427
7.423
7.419
7.411
7.395
7.392
7.379
7.375
7.371
7.260
4.038
4.023
4.008
2.625
2.619
2.610
2.604
2.595
2.589
1.039
0.001
TBDPSO
O
B4-4
10.0 9.5 9.0 8.5 8.0 7.5 7.0 6.5 6.0 5.5 5.0 4.5 4.0 3.5 3.0 2.5 2.0 1.5 1.0 0.5 ppm
0.80
4.05
6.12
1.74
2.00
9.23

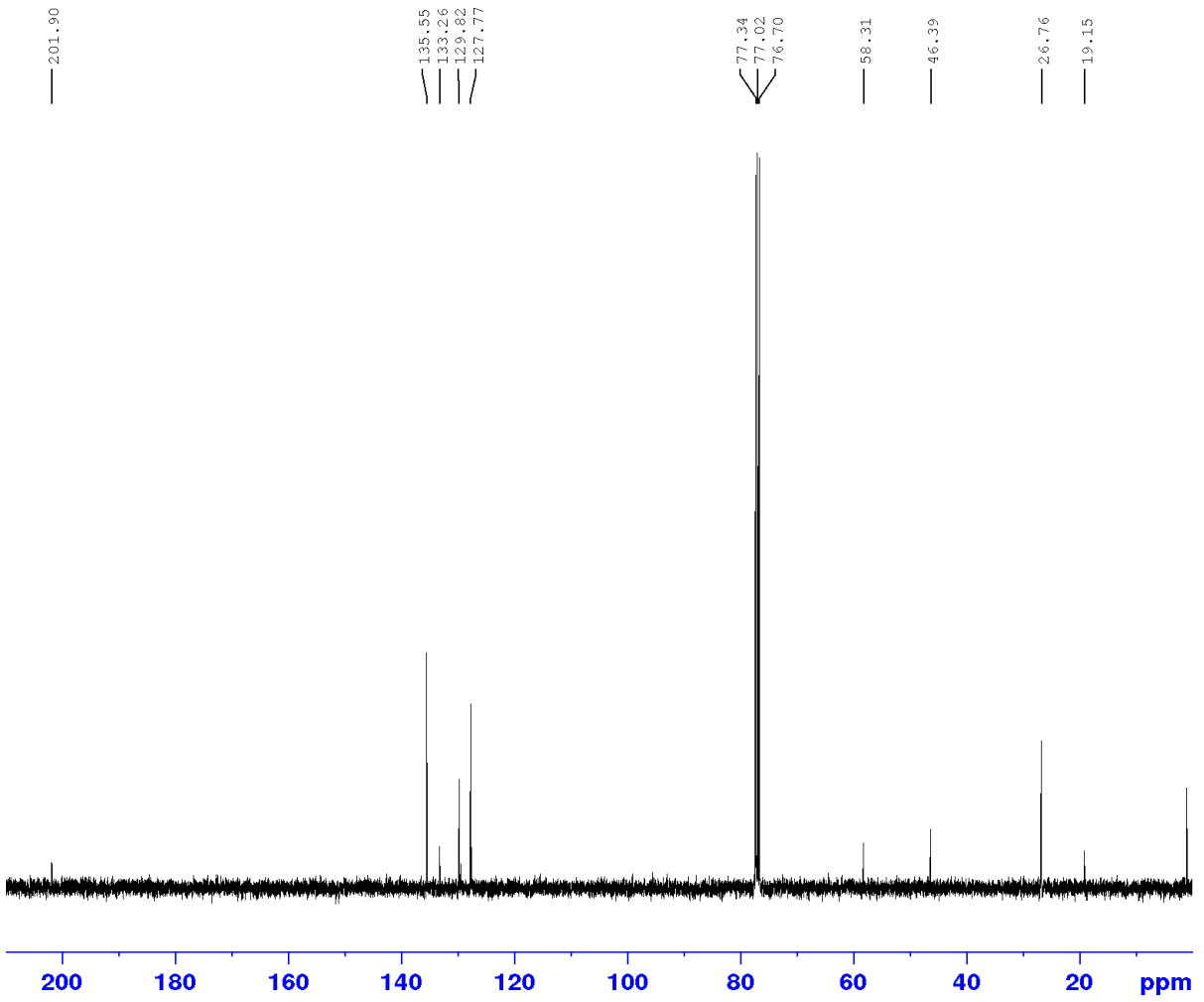
201.90
135.55
133.26
129.82
127.77
77.34
77.02
76.70
58.31
46.39
26.76
19.15
200 180 160 140 120 100 80 60 40 20 ppm

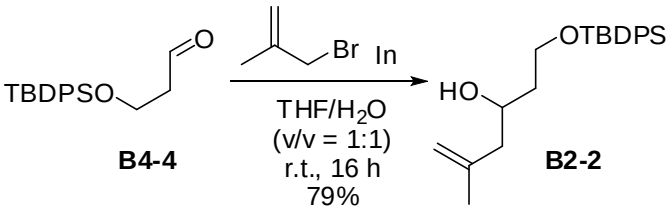

1-(*tert*-Butyldiphenylsilyloxy)-5-methylhex-5-en-3-ol (B2-2):

Indium (4.59 g, 40.0 mmol) and 3-bromo-2-methylpropene (4.0 mL, 40.0 mmol) was added into a mixture of THF (50.0 mL) and H_2O (50.0 mL) at room temperature and allowed to stir for 30 mins. 3-(tert-butyldiphenylsilyloxy)propanal **B4-4** (6.25 g, 20.0 mmol) was then added into the mixture and stirred for 16 h. After that, the reaction mixture was filtered through celite, extracted with Et_2O (3 x 50.0 mL) and washed with brine (50.0 mL). The combined organic extracts were dried over Na_2SO_4, filtered and concentrated in *vacuo*. The crude residue was purified by column chromatography (hexane/EtOAc = 5:1) to afford homoallylic alcohol **B2-2** (5.82 g, 15.8 mmol, 79% yield) as colorless liquid.

R_f value (hexane/EtOAc = 4:1): 0.40;

^{1}H NMR (400MHz, $CDCl_3$): δ 7.69-7.67 (m, 4H), 7.46-7.37 (m, 6H), 4.84 (s, 1H), 4.77 (s, 1H), 4.08-4.04 (m, 1H), 3.91-3.83 (m, 2H), 2.97 (d, *J* = 2.4 Hz, 1H), 2.25 (dd, *J* = 7.8, 13.8 Hz, 1H), 2.17 (dd, *J* = 5.0, 13.8 Hz, 1H), 1.77 (s, 3H), 1.73-1.69 (m, 2H), 1.05 (s, 9H) ppm.

^{13}C NMR (100MHz, $CDCl_3$): δ 142.8, 135.6, 135.2, 134.8, 133.3, 129.7, 127.8, 113.0, 68.7, 63.0, 46.1, 38.3, 26.8, 22.5, 19.2 ppm.

HRMS (ESI): m/z calculated for $C_{23}H_{32}O_2SiNa$ $[M+Na]^+$: 391.2069, found: 391.2067.

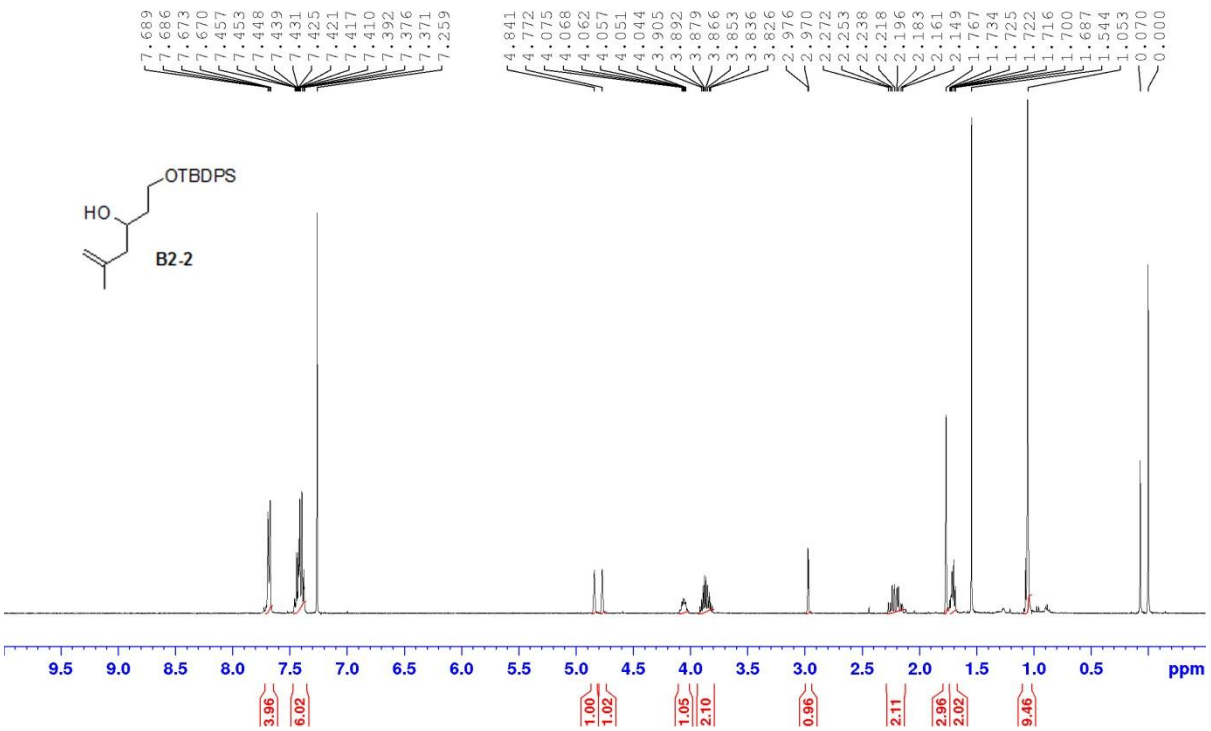
7.689
7.686
7.673
7.670
7.457
7.453
7.448
7.439
7.431
7.425
7.421
7.417
7.410
7.392
7.376
7.371
7.259
4.841
4.772
4.075
4.068
4.062
4.057
4.051
4.044
3.905
3.892
3.879
3.866
3.853
3.836
3.826
2.976
2.970
2.272
2.253
2.238
2.218
2.196
2.183
2.161
2.149
1.767
1.734
1.725
1.722
1.716
1.700
1.687
1.544
1.053
0.070
0.000
OTBDPS
HO
B2-2
9.5
9.0
8.5
8.0
7.5
7.0
6.5
6.0
5.5
5.0
4.5
4.0
3.5
3.0
2.5
2.0
1.5
1.0
0.5
ppm
3.96
6.02
1.00
1.02
1.05
2.10
0.96
2.11
2.96
2.02
9.46

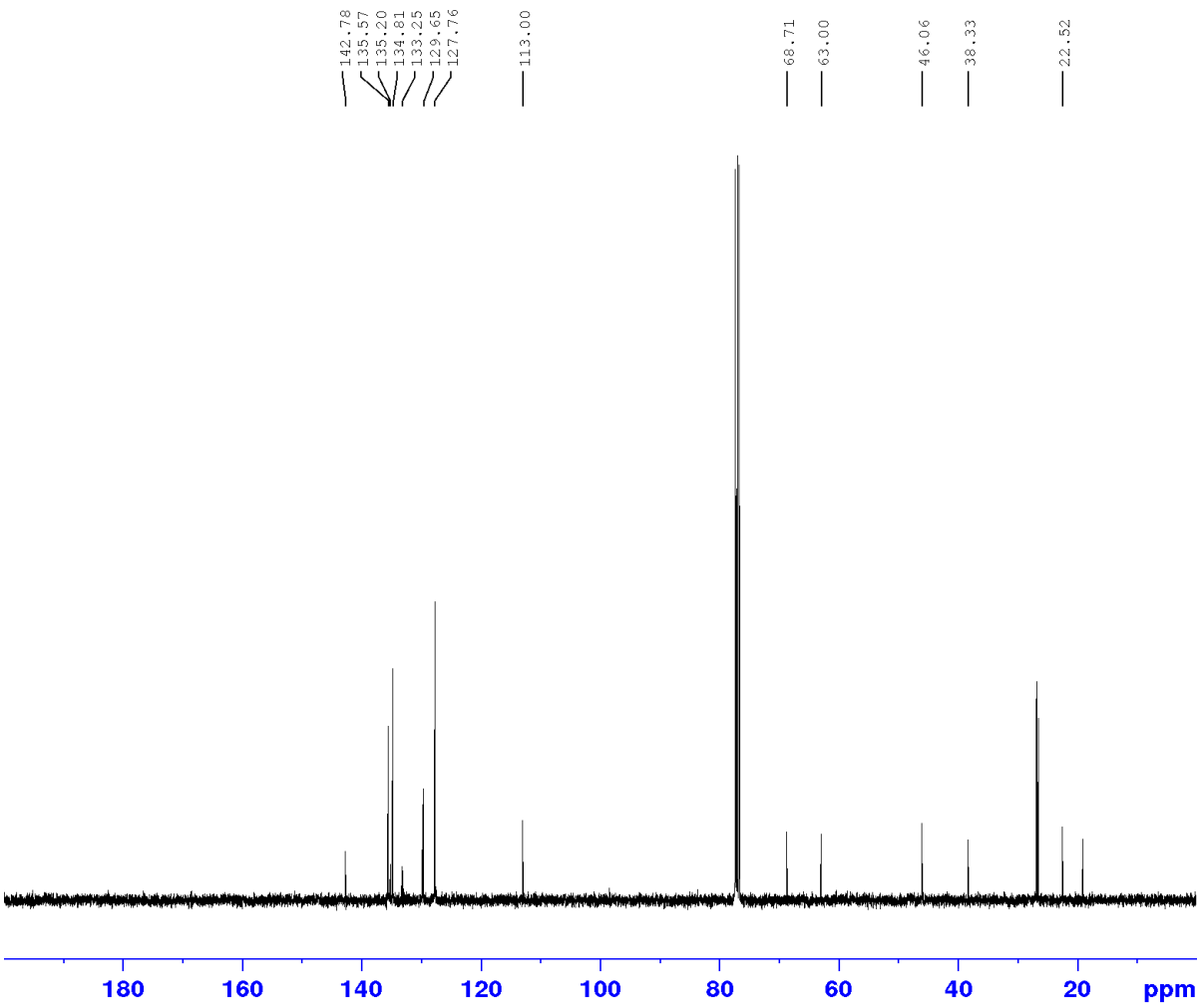
142.78
135.57
135.20
134.81
133.25
129.65
127.76
113.00
68.71
63.00
46.06
38.33
22.52
180
160
140
120
100
80
60
40
20
ppm

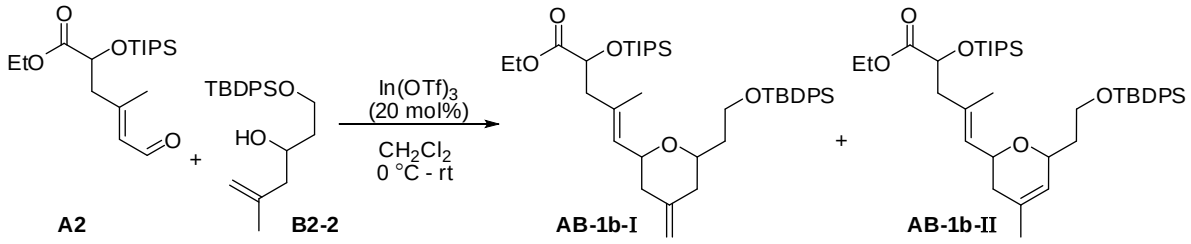

(*E*)-Ethyl 5-(6-(2-(*tert*-butyldiphenylsilyloxy)ethyl)-4-methylenetetrahydro-2*H*-pyran-2-yl)-4-methyl-2-(triisopropylsilyloxy)pent-4-enoate (AB-1b-I)

(*E*)-Ethyl 5-(6-(2-(*tert*-butyldiphenylsilyloxy)ethyl)-4-methyl-3,6-dihydro-2*H*-pyran-2-yl)-4-methyl-2-(triisopropylsilyloxy)pent-4-enoate (AB-1b-II)

A solution of aldehyde **A2** (0.171 g, 0.50 mmol) and homoallylic alcohol **B2-2** (0.369 g, 1.00 mmol) in anhydrous CH_2Cl_2 (2.0 mL) was treated with indium trifluormethanesulfonate (0.0562 g, 0.10 mmol) at 0 ^oC. The reaction was allowed to warm to room temperature and stir for 20 h. Then, the reaction mixture was diluted with CH_2Cl_2 (10.0 mL), extracted with saturated $NaHCO_3$ aqueous solution (10.0 mL), followed by CH_2Cl_2 (2 x 10.0 mL), and washed with brine (10.0 mL). The combined organic extracts were dried over Na_2SO_4, filtered and concentrated in *vacuo*. The crude residue was purified by column chromatography (hexane/EtOAc = 10:1) to afford mixture of tetrahydropyran **AB-1b-I** and dihydropyran **AB-1b-II** (0.104 g, 0.15 mmol, 30% yield; ratio of **AB-1b-I**:**AB-1b-II** = 50:50) as colorless liquid.

Note: Tetrahydropyran **AB-1b-I** and dihydropyran **AB-1b-II** could not be separated by column chromatography.

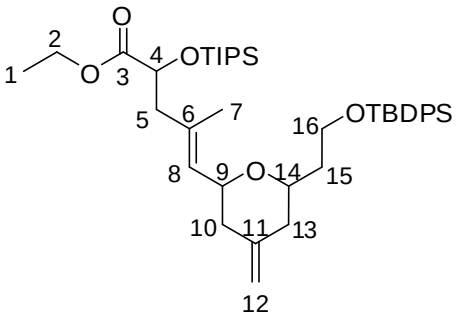

AB-1b-I

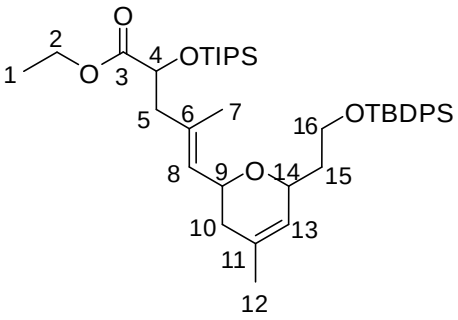

AB-1b-II

R_f value (hexane/EtOAc = 4:1): 0.67;

^{1}H NMR (400MHz, $CDCl_3$):

AB-1b-I: δ 7.70 – 7.66 (m, 4H, Ph of TBDPS), 7.44 – 7.37 (m, 6H, Ph of TBDPS), 5.32 – 5.26 (app q, 1H, H8), 4.74 (s, 2H, H12), 4.50 – 4.43 (app dt, 1H, H4), 4.19 – 4.10 (m, 2H, H2), 4.01 – 3.96 (m, 1H, H9), 3.89 – 3.72 (m, 2H, H16), 3.55 (br s, 1H, H14), 2.53 – 2.42 (m, 2H, H5), 2.24 – 1.91 (m, 4H, H10 & H13), 1.81 – 1.71 (m, 5H, H7 & H15), 1.28 – 1.23 (app t, 3H, H1), 1.08 – 1.02 (m, 30H, *i*Pr of TIPS & *t*Bu of TBDPS) ppm.

AB-1b-II: δ 7.70 – 7.66 (m, 4H, Ph of TBDPS), 7.44 – 7.37 (m, 6H, Ph of TBDPS), 5.35 (s, 1H, H13), 5.32 – 5.26 (app q, 1H, H8), 4.50 – 4.43 (app dt, 1H, H4), 4.32 (br s, 1H, H14), 4.26 – 4.20 (m, 1H, H9), 4.19 – 4.10 (m, 2H, H2), 3.89 – 3.72 (m, 2H, H16), 2.53 – 2.42 (m, 2H, H5), 1.81 – 1.71 (m, 7H, H7, H10 & H15), 1.67 (s, 3H, H12), 1.28 – 1.23 (app t, 3H, H1), 1.08 – 1.02 (m, 30H, *i*Pr of TIPS & *t*Bu of TBDPS) ppm.

^{13}C NMR (100MHz, $CDCl_3$):

AB-1b-I: δ 173.1 (C3), 144.7 (C11), 135.6 (Ph), 134.2 (C6), 134.0 (Ph), 129.9 (C8), 129.5 (Ph), 127.6 (Ph), 108.5 (C12), 75.5 (C9), 75.2 (C14), 72.1 (C4), 60.5 x 2 (C2 & C16), 46.1 (C5), 40.8 & 40.7 (C10 & C13), 38.8 (C15), 26.9 (**C**H_3 of TBDPS), 19.2 (C of TBDPS), 17.9 (**C**H_3 of TIPS), 17.5 (C7), 14.3 (C1), 12.2 (**C**H of TIPS) ppm.

AB-1b-II: δ 173.1 (C3), 135.6 (Ph), 134.2 (C6), 134.0 (Ph), 132.1 (C11), 129.9 (C8), 129.5 (Ph), 127.6 (Ph), 124.1(C13), 72.1 (C4), 71.8 (C14), 71.1 (C9), 60.5 x 2 (C2 & C16), 45.8 (C5), 39.2 (C10), 38.8 (C15), 26.9 (**C**H_3 of TBDPS), 22.9 (C12), 19.2 (C of TBDPS), 17.9 (**C**H_3 of TIPS), 17.5 (C7), 14.3 (C1), 12.2 (**C**H of TIPS) ppm.

HRMS (ESI): m/z calculated for $C_{41}H_{65}O_5Si_2$ $[M+H]^+$: 693.4371, found: 693.4371.

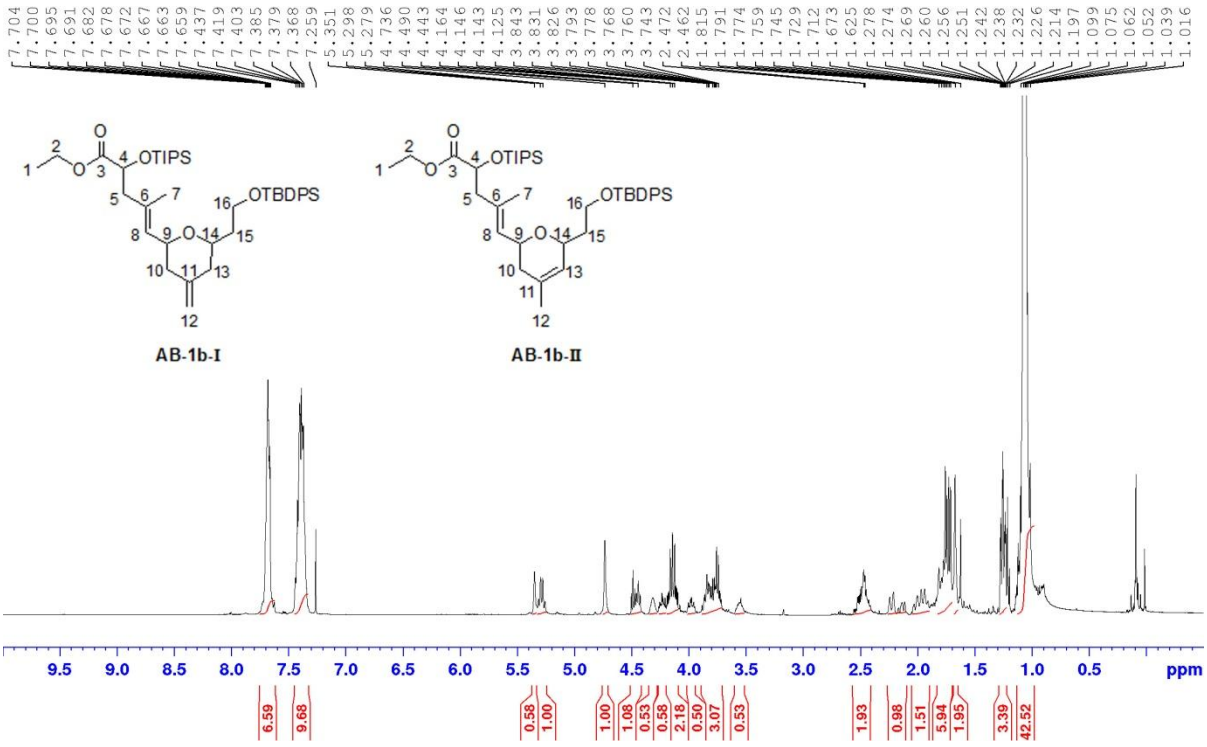
OTIPS
OTBDPS
AB-1b-I
AB-1b-II
ppm

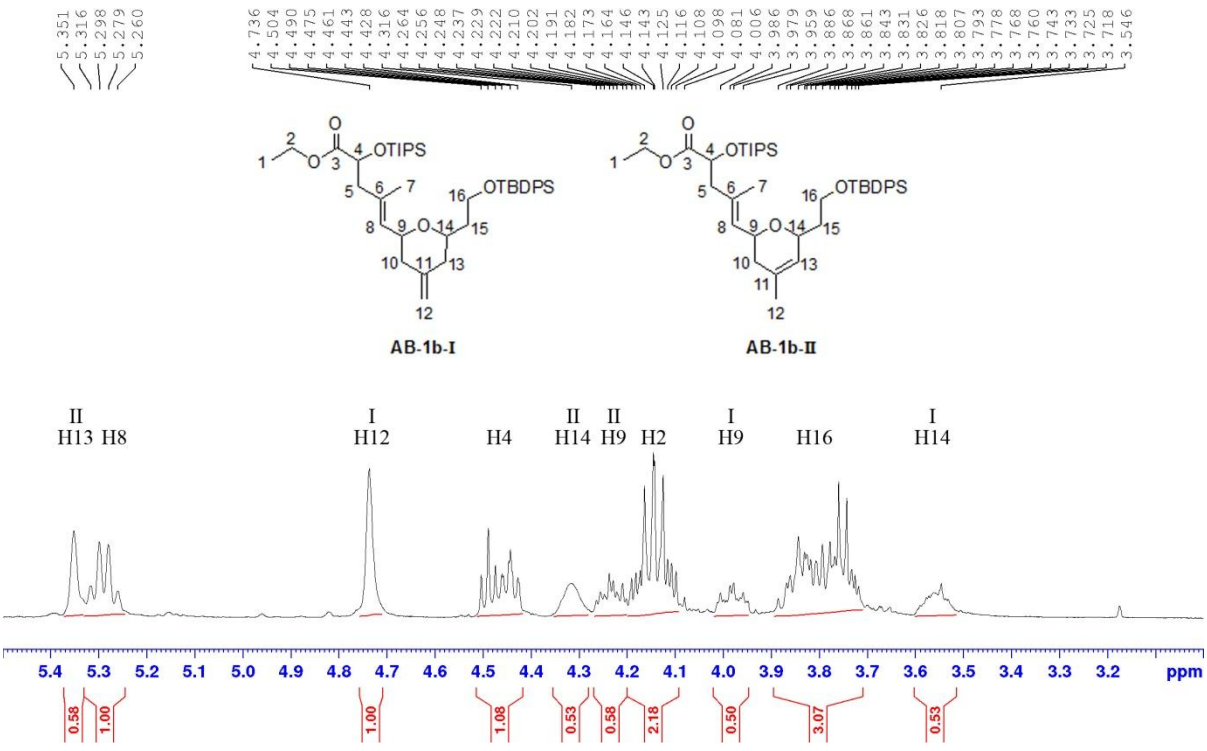
OTIPS
OTBDPS
AB-1b-I
AB-1b-II
II H13 H8
I H12
H4
II H14
II H9
H2
I H9
H16
I H14
ppm

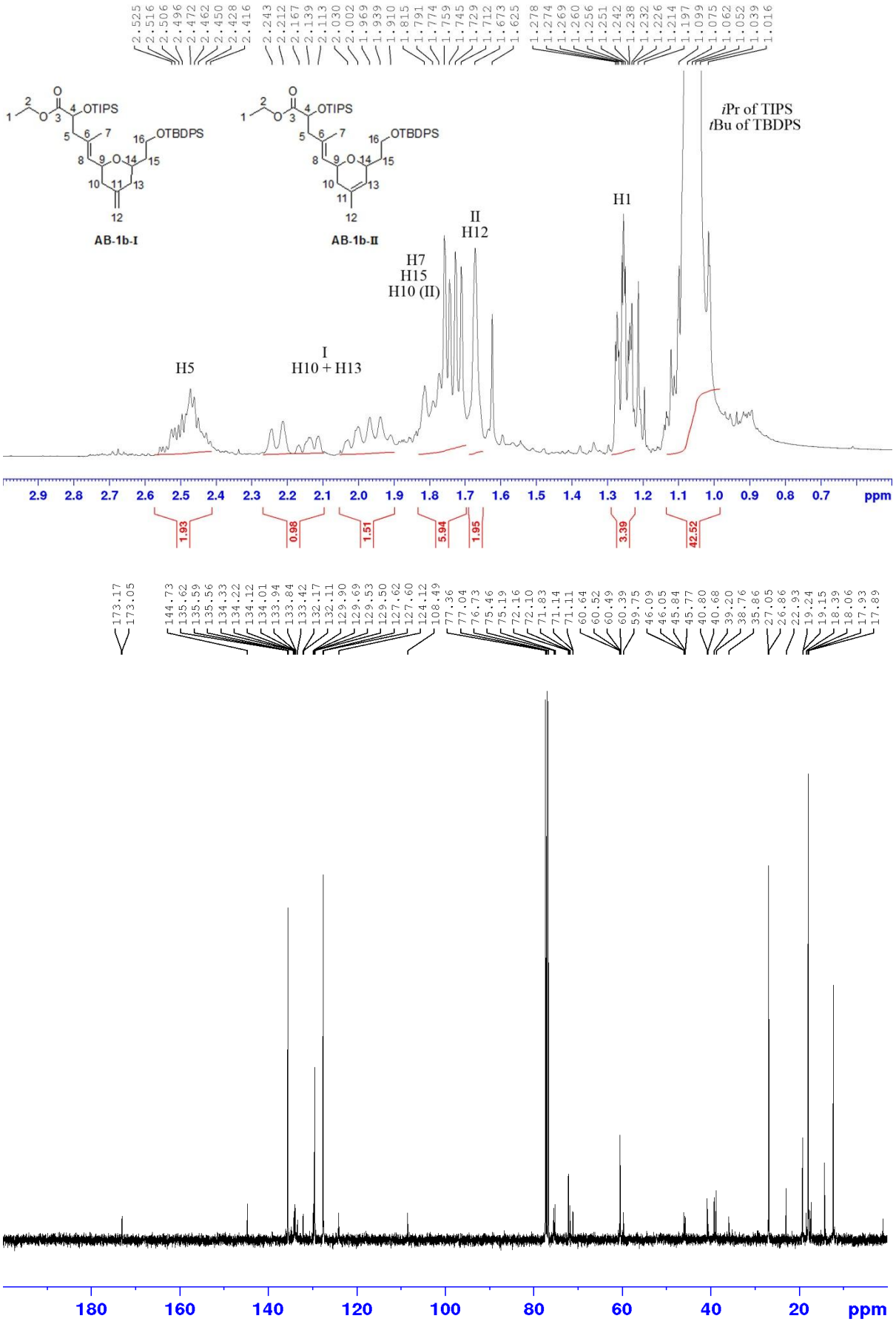
AB-1b-I
AB-1b-II
iPr of TIPS
tBu of TBDPS
H1
II
H12
H7
H15
H10 (II)
I
H10 + H13
H5
ppm
1.93
0.98
1.51
5.94
1.95
3.39
42.52

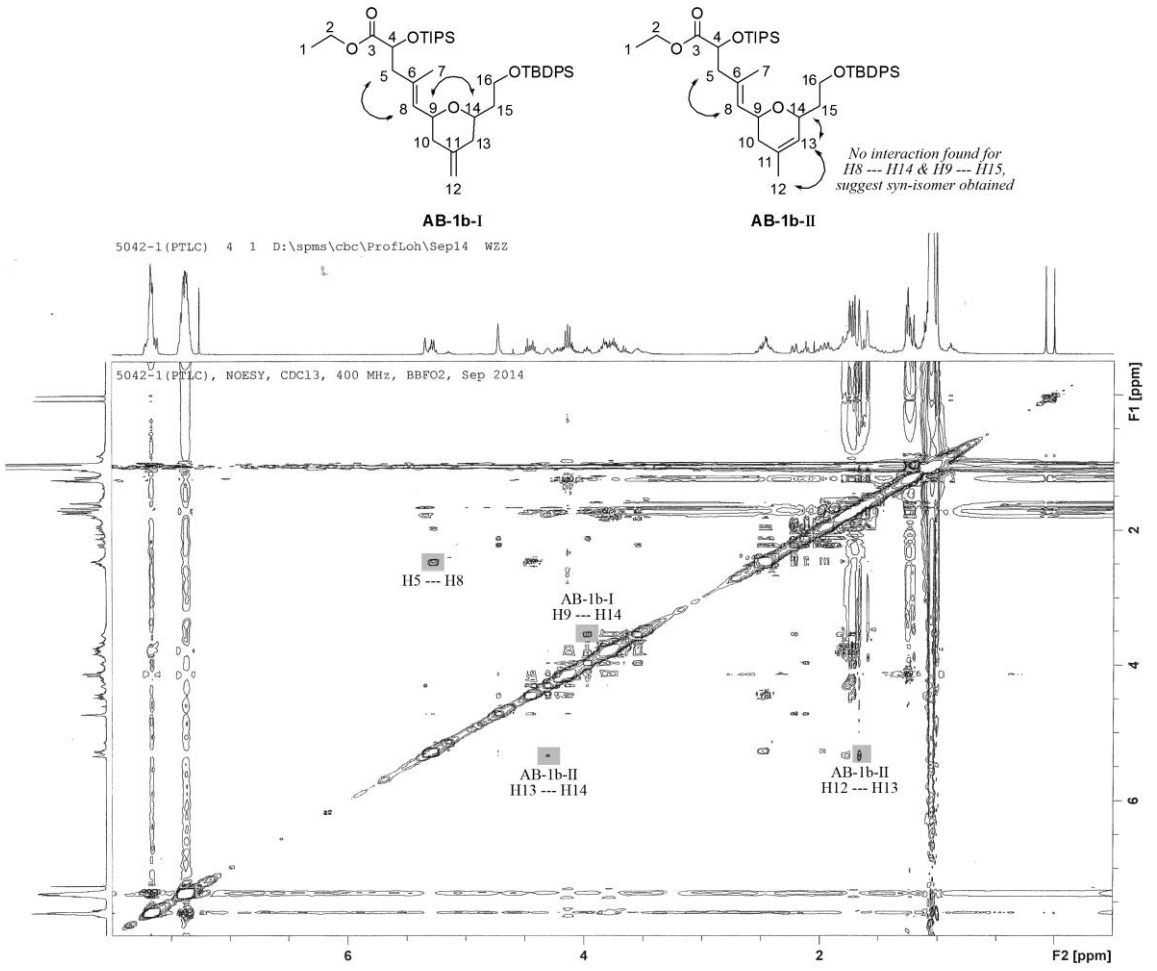
OTIPS
OTBDPS
AB-1b-I
AB-1b-II
No interaction found for H8 --- H14 & H9 --- H15, suggest syn-isomer obtained
5042-1(PTLC) 4 1 D:\spms\cbc\ProfLoh\Sep14 WZZ
5042-1(PTLC), NOESY, CDCl3, 400 MHz, BBFO2, Sep 2014
H5 --- H8
AB-1b-I
H9 --- H14
AB-1b-II
H13 --- H14
AB-1b-II
H12 --- H13
F1 [ppm]
F2 [ppm]

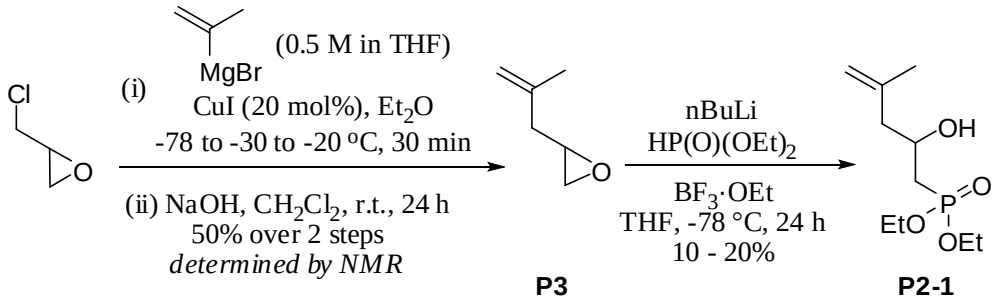

Diethyl 2-hydroxy-4-methylpent-4-enylphosphonate (P2-1):

To a solution of copper iodide (1.14 g, 6.0 mmol) in anhydrous Et_2O (60.0 mL), isopropenylmagenesium bromide solution (66.0 mL, Aldrich 0.5 M in THF, 33.0 mmol) was added at -78 ^oC under N_2 atmosphere. The solution was allowed to stir for 15 mins at -30 ^oC. (±)-Epichlorohydrin (2.35 mL, 30.0 mmol) was then added dropwise and the resulting solution was allowed to warm from -30 ^oC to -20 ^oC. The colour of solution was changed from yellow to black or dark green during the addition. After stirring for 30 min, the reaction was quenched by saturated NH_4Cl aqueous solution (60.0 mL). The mixture was extracted with EtOAc (3 x 60.0 mL) and washed with brine (60.0 mL). The combined organic layer was dried over Na_2SO_4, filtered and concentrated in *vacuo*. The crude residue was subjected to epoxidation without purification.

To a solution of crude residue above in CH_2Cl_2 (30.0 mL), crushed NaOH (2.40 g, 60.0 mmol) was added at room temperature. The solution was allowed to stir for 24 h. $MgSO_4$ was then added into the solution, filtered and concentrated under 450 mmHg at 30 ^oC for 1.5 h to remove CH_2Cl_2. Epoxide **P3** was obtained at a crude yield of 50% (determined by NMR) as colorless liquid.

To a solution of diethylphosphite (5.75 mL, 45.0 mmol) in anhydrous THF (30.0 mL), *n*-butyllithium solution (28.2 mL, Aldrich 1.6 M in hexanes, 45.0 mmol) was added at -78 ^oC under N_2 atmosphere. The solution was allowed to stir for 30 mins. After that, epoxide **P3** obtained above (approx. 15.0 mmol) and $BF_3 \cdot OEt_2$ (5.55 mL, 45.0 mmol) were added subsequently. The reaction mixture was allowed to stir for another 6 h and quenched by saturated $NaHCO_3$ aqueous solution (30.0 mL). The resulting mixture was extracted with EtOAc (3 x 30.0 mL) and washed with brine (30.0 mL). The combined organic layer was dried over Na_2SO_4, filtered and concentrated in *vacuo*. The crude residue was purified by column chromatography (hexane/EtOAc = 1:1 to 100% EtOAc) to afford phosphonate **P2-1** (0.354 – 0.709 g, 1.5 – 3.0 mmol, 10 - 20% yield) as colorless liquid.

Note: Phosphonate **P2-1** could not be visualized *via* UV or $KMnO_4$ or ceric ammonium molybdate. **P2-1** was eluted from column chromatography with EtOAc after diethylphosphite, which was able to be visualized *via* UV, was eluted. Therefore, spectrum of **P2-1** might show impurities or diethyl phosphate.

R_f value (100% EtOAc): < 0.37;

^{1}H NMR (400MHz, $CDCl_3$): δ 4.87 (s, 1H), 4.78 (s, 1H), 4.21 – 4.04 (m, 2 x $CH_3C\underline{\mathbf{H}}_2O$ + $R_2C\underline{\mathbf{H}}OH$), 3.30 (br, 1H), 2.33 (dd, *J* = 7.2, 13.6 Hz, 1H), 2.21 (dd, *J* = 6.0, 13.6 Hz, 1H), 2.06 – 1.82 (m, 2H), 1.76 (s, 3H), 1.37 (t, *J* = 7.2 Hz, 6H) ppm.

^{13}C NMR (100MHz, $CDCl_3$): δ 142.0, 113.7, 64.5, 61.9, 46.5, 33.7 ($R\underline{\mathbf{C}}H_2P$), 32.3 ($R\underline{\mathbf{C}}H_2P$), 22.5, 16.4 ppm.

^{31}P NMR (162MHz, $CDCl_3$): δ 30.4 ppm.

HRMS (ESI): m/z calculated for $C_{10}H_{21}O_4PNa$ $[M+Na]^+$: 259.1075, found: 259.1078.

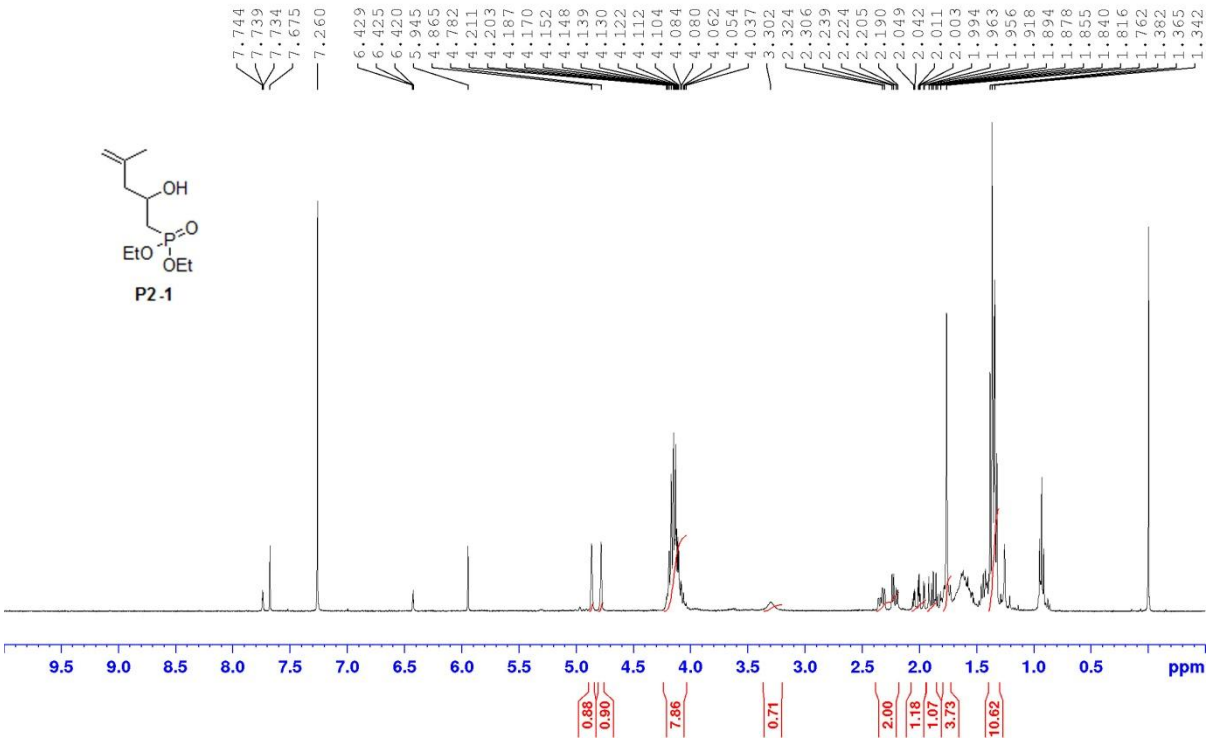
7.744
7.739
7.734
7.675
7.260
6.429
6.425
6.420
5.945
4.865
4.782
4.211
4.203
4.187
4.170
4.152
4.148
4.139
4.130
4.122
4.112
4.104
4.084
4.080
4.062
4.054
4.037
3.302
2.324
2.306
2.239
2.224
2.205
2.190
2.049
2.042
2.011
2.003
1.994
1.963
1.956
1.918
1.894
1.878
1.855
1.840
1.816
1.762
1.382
1.365
1.342
OH
EtO
P
O
OEt
P2-1
9.5
9.0
8.5
8.0
7.5
7.0
6.5
6.0
5.5
5.0
4.5
4.0
3.5
3.0
2.5
2.0
1.5
1.0
0.5
ppm
0.88
0.90
7.86
0.71
2.00
1.18
1.07
3.73
10.62

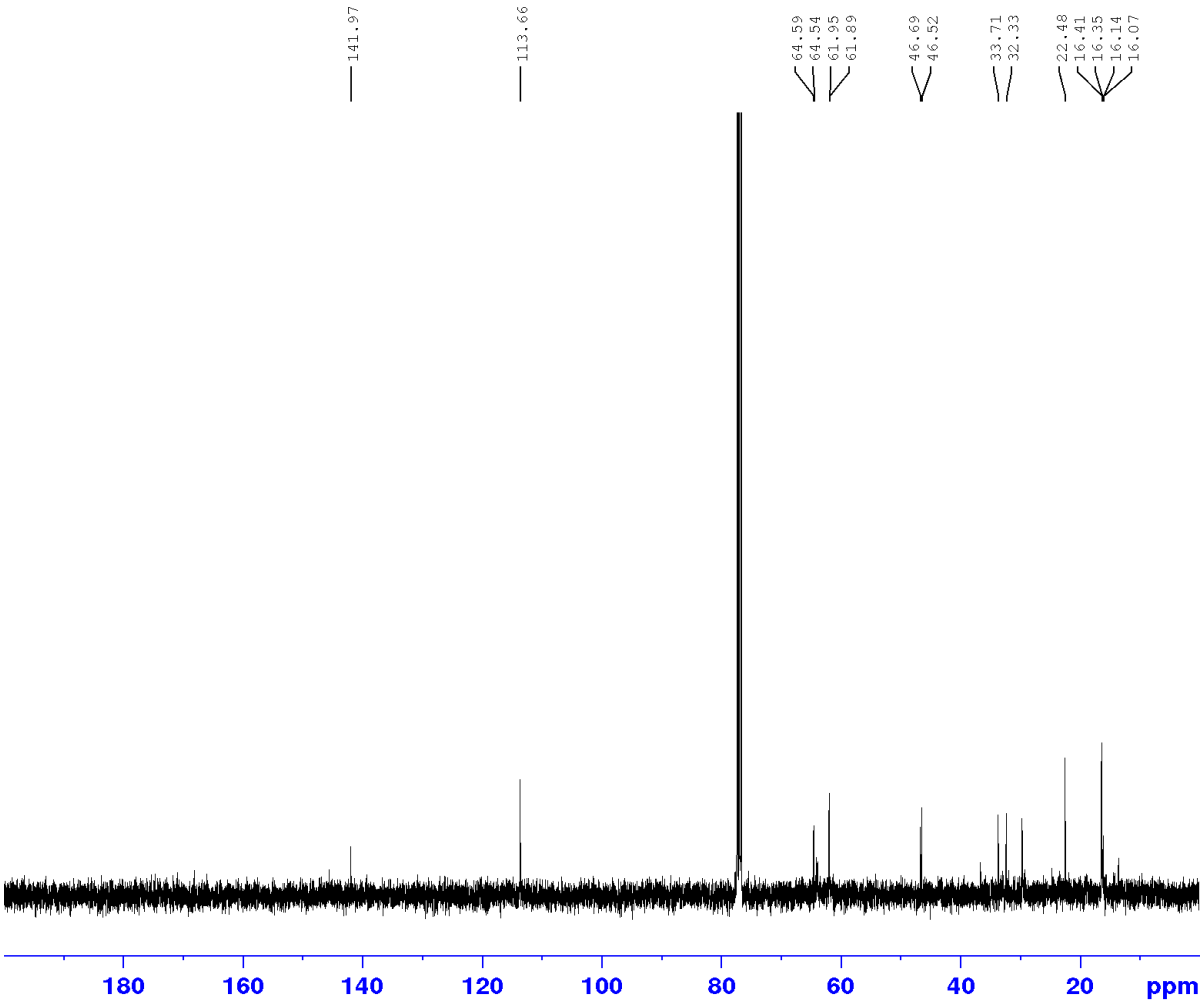
141.97
113.66
64.59
64.54
61.95
61.89
46.69
46.52
33.71
32.33
22.48
16.41
16.35
16.14
16.07
180
160
140
120
100
80
60
40
20
ppm

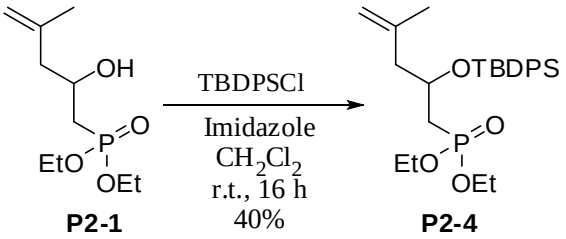

Diethyl 2-(*tert*-butyldiphenylsilyloxy)-4-methylpent-4-enylphosphonate (P2-4):

To a solution of phosphonate **P2-1** (0.172 g, 0.73 mmol) in CH_2Cl_2 (1.4 mL), imidazole (0.099 g, 1.46 mmol) and *tert*-Butyldiphenylsilyl chloride (0.38 mL, 1.46 mmol) were added subsequently at room temperature. The reaction was allowed to stir 16 h. Then, the reaction was quenched by H_2O (5.0 mL), extracted with CH_2Cl_2 (3 x 10 mL) and washed with brine (10 mL). The combined organic extracts were dried over Na_2SO_4, filtered and concentrated in *vacuo*. The crude residue was purified by column chromatography (hexane/EtOAc = 2:1) to afford phosphonate **P2-4** (0.139 g, 0.29 mmol, 40% yield) as colorless liquid.

R_f value (hexane/EtOAc = 1:1): 0.39;

^{1}H NMR (400MHz, $CDCl_3$): δ 7.73 – 7.69 (m, 4H), 7.46 – 7.35 (m, 6H), 4.75 (s,1H), 4.73 (s,1H), 4.28 – 4.19 (m, 1H), 3.98 – 3.87 (m, 4H), 2.39 (dd, *J* = 6.0, 7.6 Hz, 1H), 2.22 (dd, *J* = 5.6, 8.0 Hz, 1H), 2.13 – 1.88 (m, 2H), 1.48 (s, 3H), 1.21 (t, *J* = 7.0 Hz, 6H), 1.05 (s, 9H) ppm.

^{13}C NMR (100 MHz, $CDCl_3$): δ 142.1, 136.0, 133.9, 129.6, 127.6, 114.0, 67.7, 61.3, 46.2, 33.9 (R**C**H_2P), 32.5 (R**C**H_2P), 26.9, 22.6, 19.3, 16.4 ppm.

^{31}P NMR (162MHz, $CDCl_3$): δ 28.2 ppm.

HRMS (ESI): m/z calculated for $C_{26}H_{39}O_4SiPNa$ $[M+Na]^+$: 497.2253, found: 497.2252.

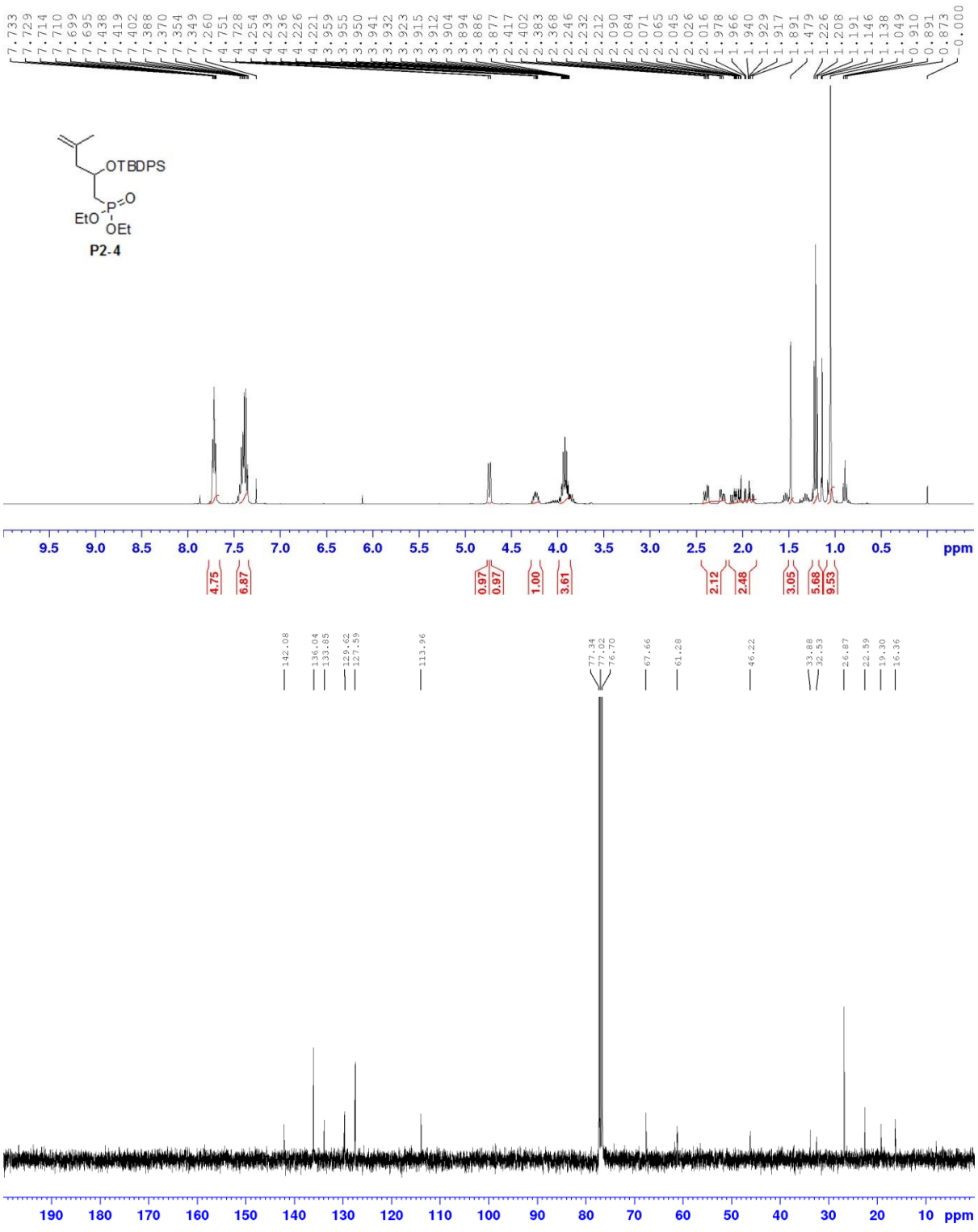
OTBDPS
EtO
P
O
OEt
P2-4
ppm
4.75
6.87
0.97
0.97
1.00
3.61
2.12
2.48
3.05
5.68
9.53
ppm

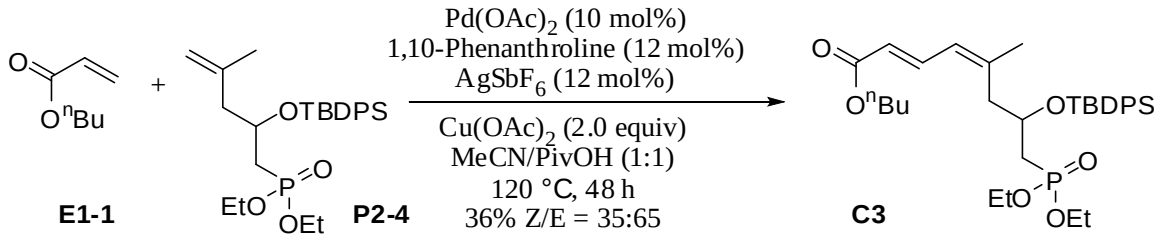

(2*E*,4*Z*)-Butyl 7-(*tert*-butyldiphenylsilyloxy)-8-(diethoxyphosphoryl)-5-methylocta-2,4-dienoate (C3):

Palladium(II) acetate (0.0065 g, 0.029 mmol), 1,10-phenanthroline (0.0063 g, 0.035 mmol), silver hexafluoroantimonate (0.0199 g, 0.058 mmol), copper(II) acetate (0.1053 g, 0.58 mmol), *n*-butyl acrylate **E1-1** (0.17 mL, 1.16 mmol), alkene **P2-4** (0.139 g, 0.29 mmol) were dissolved in MeCN/PivOH (0.58 mL; v/v = 1:1). The mixture was allowed to stir for 48 h at 120 ^{o}C. The resulting mixture was then allowed to cool to r.t., filtered and diluted with ethyl acetate (10.0 mL). After that, the solution was washed with H_2O (3 x 10.0 mL), saturated sodium bicarbonate aqueous solution (3 x 10.0 mL) until organic layer turned into yellow. The combined aqueous layer was extracted with ethyl acetate (3 x 10.0 mL). The organic layer was combined and washed with brine (10.0 mL), dried over Na_2SO_4, filtered and concentrated in vacuo. The crude residue was further purified by column chromatography (eluting with hexane/EtOAc = 2:1) to yield conjugated diene ester **C3** (0.0627 g, 0.10 mmol, 36% yield; *E*/*Z* = 65:35) as yellow liquid.

Note: *E* and *Z* isomers of **C3** could not be separated by column chromatography.

R_f value (hexane/EtOAc = 1:1): 0.29;

^{1}H NMR (400MHz, $CDCl_3$):

E-isomer: δ 7.71 – 7.62 (m, 4H), 7.47 (dd, *J* = 11.2, 15.2 Hz, 1H), 7.44 – 7.35 (m, 6H), 6.01 (d, *J* = 11.2 Hz, 1H), 5.71 (d, *J* = 15.2 Hz, 1H), 4.28 – 4.21 (m,1H), 4.15 (t, *J* = 6.7 Hz, 2H), 3.97 – 3.86 (m, 4H), 2.58 (dd, *J* = 4.7, 13.4 Hz, 1H), 2.32 (dd, *J* = 7.1, 13.5 Hz, 1H), 2.03 – 1.90 (m, 2H), 1.69 – 1.62 (m, 2H), 1.61 (s, 3H), 1.44 – 1.39 (m, 2H), 1.23 – 1.17 (m, 6H), 1.02 (s, 9H), 0.97 – 0.93 (m, 3H) ppm.

Z-isomer: δ 7.71 – 7.62 (m, 5H), 7.44 – 7.35 (m, 6H), 6.03 (d, *J* = 10.0 Hz, 1H), 5.77 (d, *J* = 15.1 Hz, 1H), 4.28 – 4.21 (m,1H), 4.15 (t, *J* = 6.7 Hz, 2H), 3.97 – 3.86 (m, 4H), 2.65 (dd, *J* = 4.5, 13.6 Hz, 1H), 2.60 – 2.56 (m, 1H), 2.03 – 1.90 (m, 2H), 1.69 – 1.62 (m, 2H), 1.61 (s, 3H), 1.44 – 1.39 (m, 2H), 1.23 – 1.17 (m, 6H), 1.02 (s, 9H), 0.97 – 0.93 (m, 3H) ppm.

^{13}C NMR (100 MHz, $CDCl_3$):

E-isomer: δ 167.7, 145.8, 140.5, 136.0, 133.7, 129.8, 127.7, 126.6, 119.5, 67.6, 64.1, 61.4, 48.3, 34.6, 30.8, 26.9, 24.4, 19.2, 17.6, 16.4, 13.7 ppm.

Z-isomer: δ 167.6, 146.1, 140.8, 136.0, 133.4, 129.8, 127.6, 126.7, 119.7, 67.7, 64.0, 61.4, 41.4, 33.2, 26.8, 24.7, 24.4, 19.2, 17.6, 16.3, 13.7 ppm.

^{31}P NMR (162MHz, $CDCl_3$): δ 27.3 ppm.

HRMS (ESI): m/z calculated for $C_{33}H_{50}O_6SiP$ $[M+H]^+$: 601.3114, found: 601.3110.

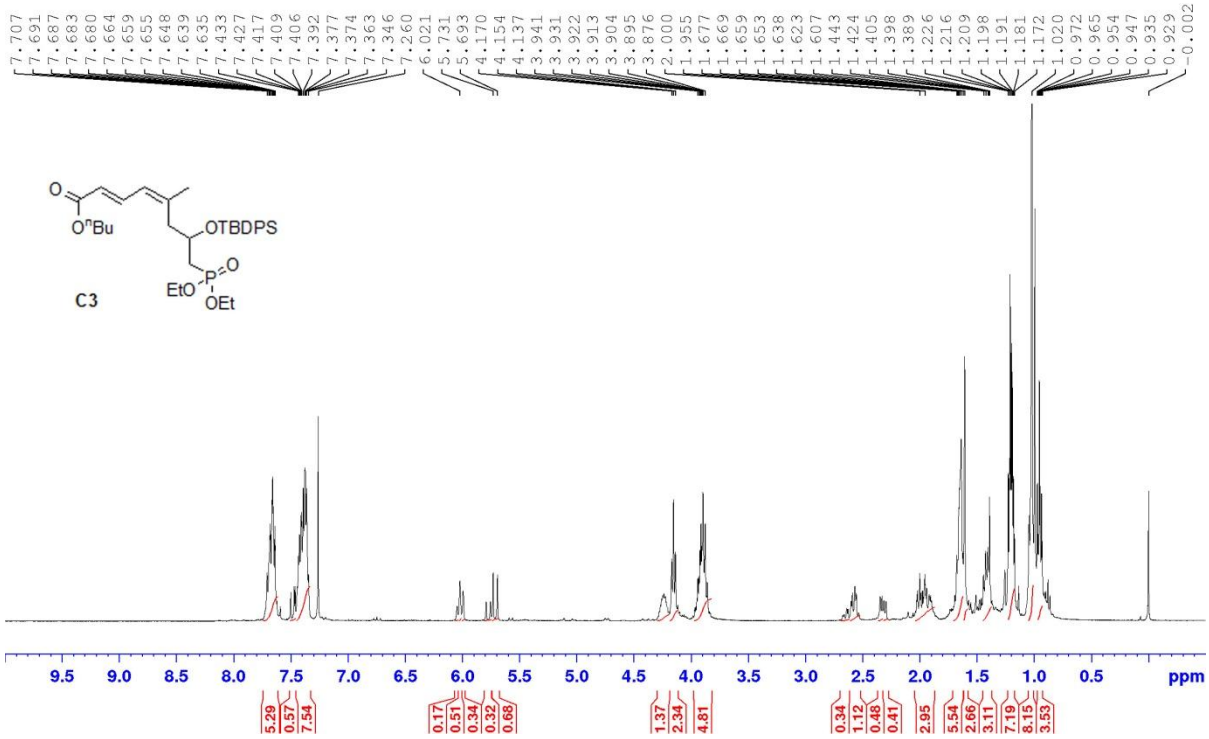
C3
ppm

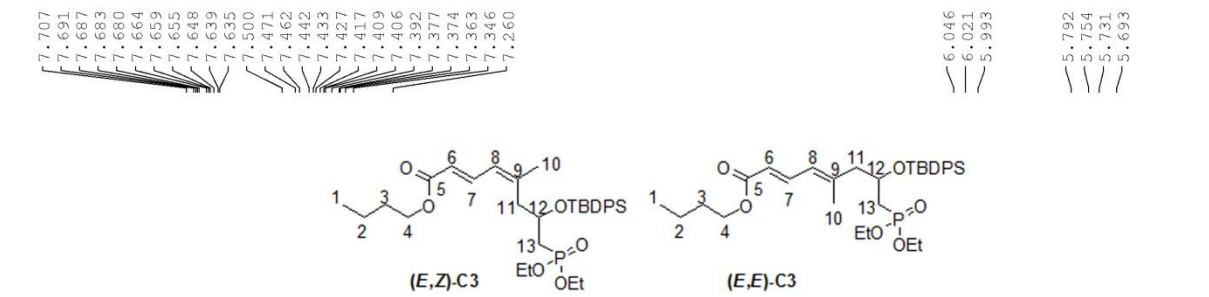
(E,Z)-C3
(E,E)-C3

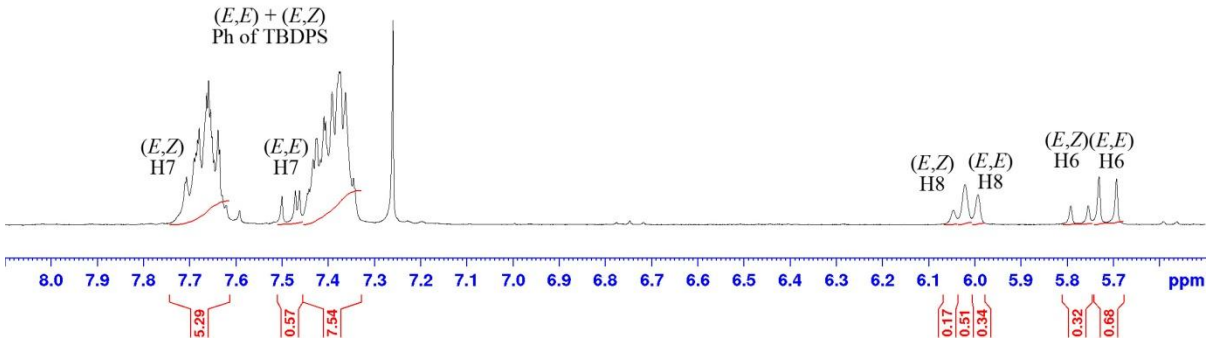
(E,E) + (E,Z)
Ph of TBDPS
(E,Z) H7
(E,E) H7
(E,Z) H8
(E,E) H8
(E,Z)(E,E) H6 H6
ppm

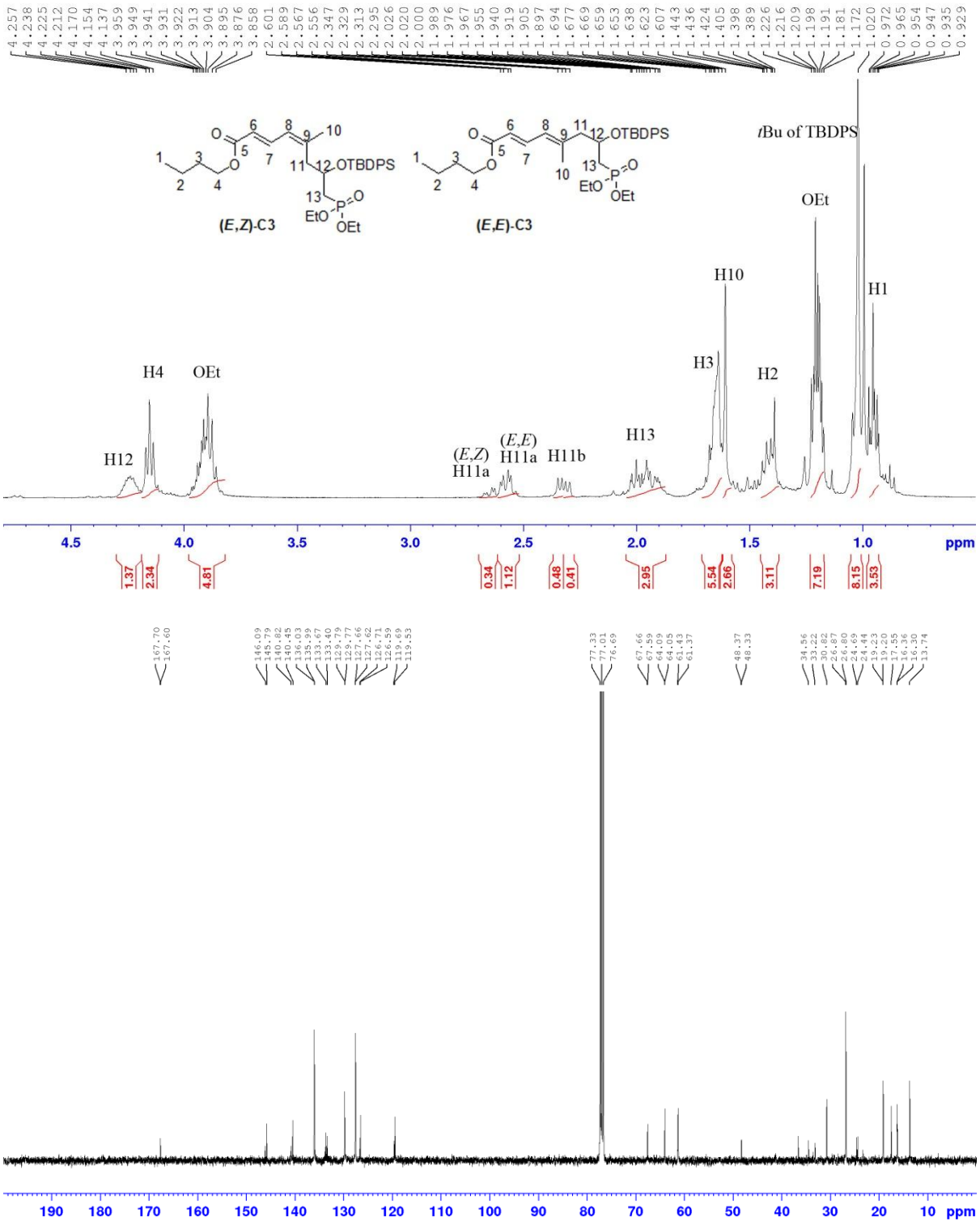
(E,Z)-C3
(E,E)-C3
tBu of TBDPS
OEt
H10
H1
H3
H2
H4
OEt
H12
(E,Z) H11a
(E,E) H11a
H11b
H13
ppm
1.37
2.34
4.81
0.34
1.12
0.48
0.41
2.95
5.54
2.66
3.11
7.19
8.15
3.53
ppm

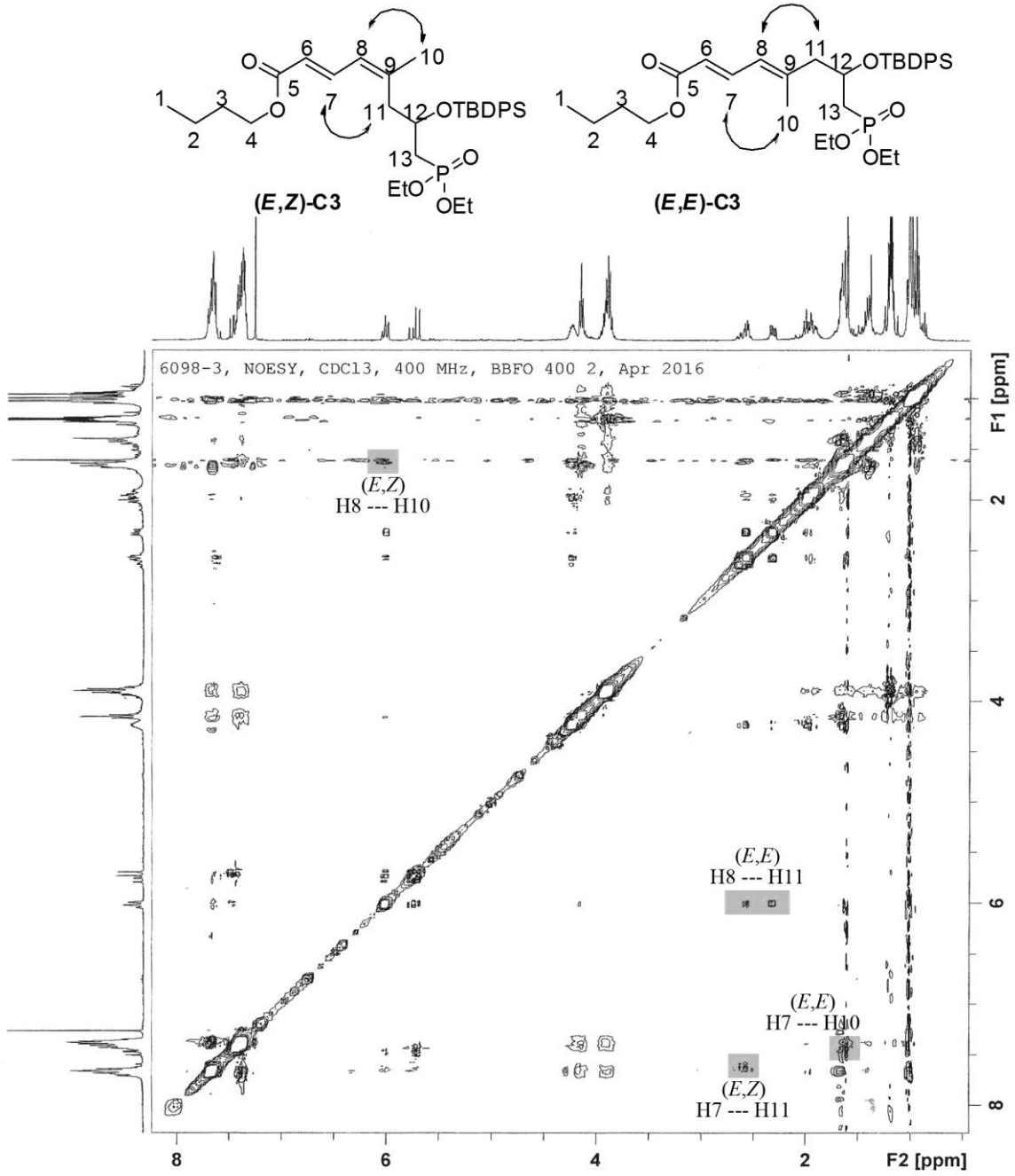
(E,Z)-C3
(E,E)-C3
6098-3, NOESY, CDCl3, 400 MHz, BBFO 400 2, Apr 2016
(E,Z)
H8 --- H10
(E,E)
H8 --- H11
(E,E)
H7 --- H10
(E,Z)
H7 --- H11
F1 [ppm]
F2 [ppm]

4.2.2 Selected compounds synthesized in 1st Generation Synthetic Route[146]

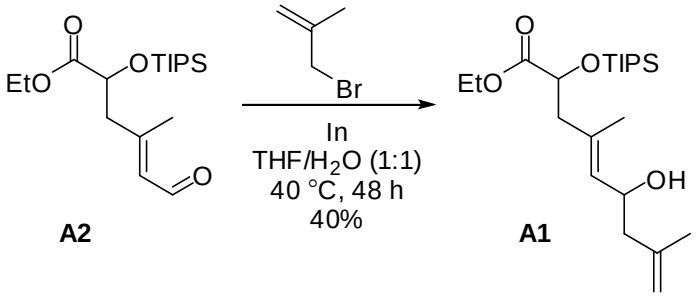

(*E*)-Ethyl 6-hydroxy-4,8-dimethyl-2-(triisopropylsilyloxy)nona-4,8-dienoate (A1):
Indium (0.161 g, 1.4 mmol) and 3-bromo-2-methylpropene (0.14 mL, 1.4 mmol) was added into a mixture of THF (0.9 mL) and H_2O (0.9 mL) at room temperature and allowed to stir for 30 mins. Aldehyde **A2** (0.120 g, 0.35 mmol) was then added into the mixture and stirred for 48 h at 40 ^oC. After that, the reaction mixture was filtered through celite, extracted with Et_2O (3 x 10.0 mL) and washed with brine (10.0 mL). The combined organic extracts were dried over Na_2SO_4, filtered and concentrated in *vacuo*. The crude residue was purified by column chromatography (hexane/EtOAc = 5:1) to afford homoallylic alcohol **A1** (0.056 g, 0.14 mmol, 40% yield) as colorless liquid.

R_f value (hexane/EtOAc = 4:1): 0.36;
^{1}H NMR (400 MHz, $CDCl_3$): δ 5.25 (br s, 1H), 4.85 (s, 1H), 4.78 (s, 1H), 4.44 (q, *J* = 6.4 Hz, 2 H), 4.18-4.08 (m, 2H), 2.49-2.40 (m, 2H), 2.22-2.08 (m, 2H), 1.77 (s, 3H), 1.76 (s, 3H), 1.65 (dd, *J* = 2.4, 6.4 Hz, 1H), 1.26 (t, *J* = 7.2 Hz, 3H), 1.13-1.06 (m, 21H) ppm.
^{13}C NMR (100 MHz, $CDCl_3$): δ 173.0, 142.2, 133.7, 131.1, 113.5, 72.1, 65.7, 60.6, 45.9, 45.7, 22.4, 17.9, 17.1, 14.2, 12.2 ppm.

[146] HRMS of the compounds listed in this section and ^{13}C NMR of compound **B2-1** are not provided.

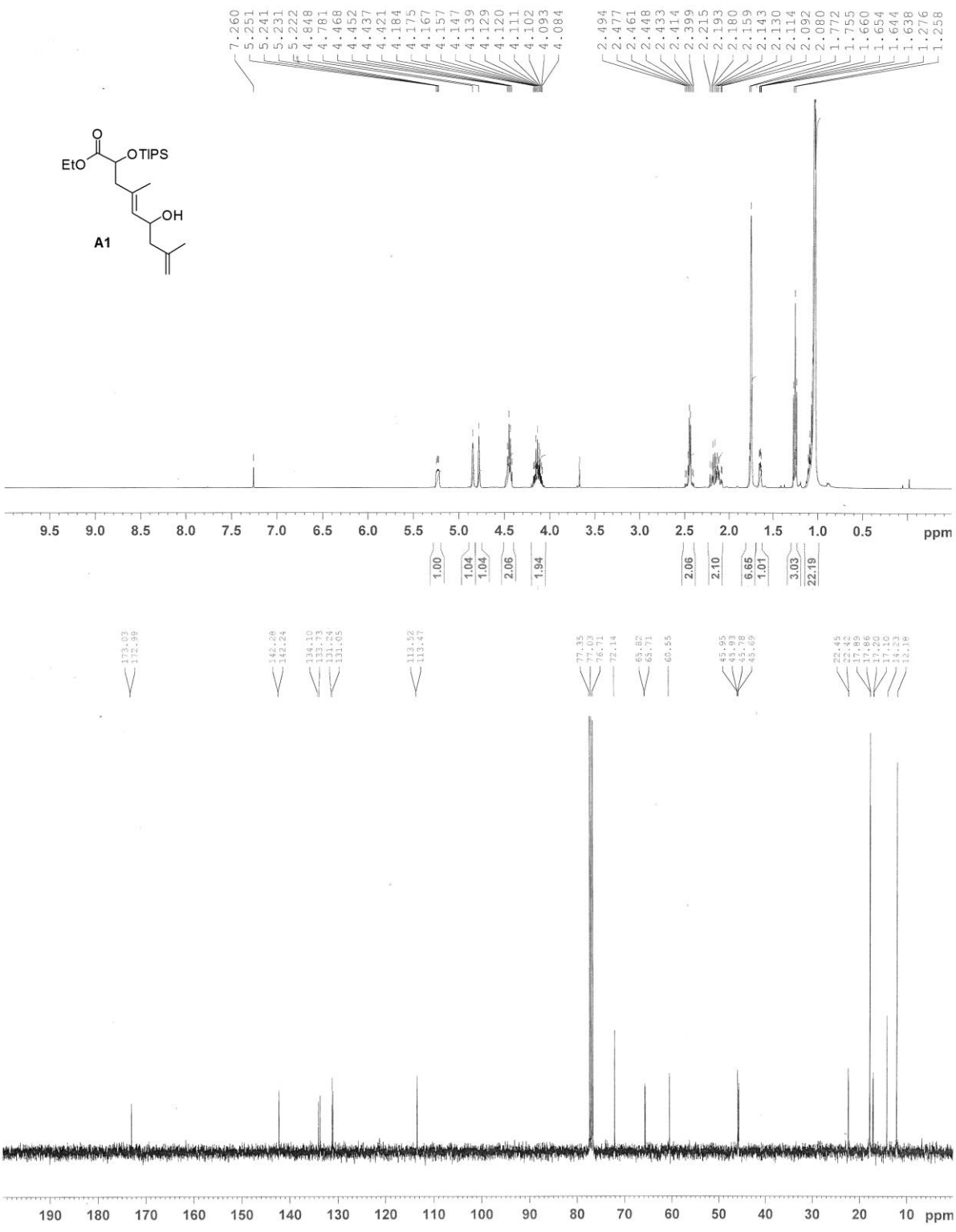
7.260
5.251
5.241
5.231
5.222
4.848
4.781
4.468
4.452
4.437
4.421
4.184
4.175
4.167
4.157
4.147
4.139
4.129
4.120
4.111
4.102
4.093
4.084
2.494
2.477
2.461
2.448
2.433
2.414
2.399
2.215
2.193
2.180
2.159
2.143
2.130
2.114
2.092
2.080
1.772
1.755
1.660
1.654
1.644
1.638
1.276
1.258
EtO
OTIPS
OH
A1
9.5 9.0 8.5 8.0 7.5 7.0 6.5 6.0 5.5 5.0 4.5 4.0 3.5 3.0 2.5 2.0 1.5 1.0 0.5 ppm
1.00
1.04
1.04
2.06
1.94
2.06
2.10
6.65
1.01
3.03
22.19
173.03
172.99
142.28
142.24
134.10
133.73
131.24
131.05
113.52
113.47
77.35
77.03
76.71
72.14
65.82
65.71
60.55
45.95
45.93
45.78
45.69
22.45
22.42
17.89
17.86
17.20
17.10
14.13
13.18
190 180 170 160 150 140 130 120 110 100 90 80 70 60 50 40 30 20 10 ppm

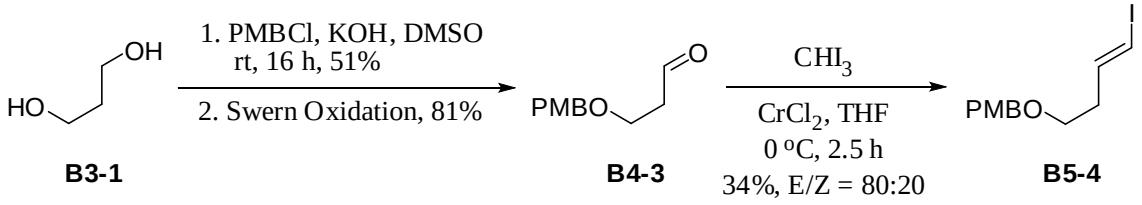

B3-1 **B4-3** **B5-4**

(*E*)-1-((4-Iodobut-3-enyloxy)methyl)-4-methoxybenzene (B5-4):

Potassium hydroxide (1.12 g, 20.0 mmol) was dissolved into a solution of 1,3-propanediol **B3-1** (1.44 mL, 20.0 mmol) in DMSO (6.66 mL) at room temperature. 4-Methoxybenzyl chloride (2.71 mL, 20.0 mmol) was then added into the mixture and allowed to stir for 16 h. After that, the reaction mixture was cooled to 0 ^{o}C, followed by the addition of 6 M HCl (3.34 mL). The mixture was then extracted with EtOAc (3 x 10.0 mL) and washed with brine (10.0 mL). The combined organic layer was dried over Na_2SO_4, filtered and concentrated in *vacuo*. The crude residue was further purified by column chromatography (eluting with hexane/EtOAc = 3:1) to yield 3-(4-methoxybenzyloxy)propan-1-ol (2.00 g, 10.2 mmol, 51% yield) as pale yellow liquid.

Oxalyl chloride (0.47 mL, 5.5 mmol) was added into a solution of DMSO (0.85 mL, 12.0 mmol) in CH_2Cl_2 (5.0 mL) at -60 ^{o}C under N_2 atmosphere and allowed to stir for 10 mins. Then, 3-(4-methoxybenzyloxy)propan-1-ol (0.981 g, 5.0 mmol) was dissolved in CH_2Cl_2 (5.0 mL) and added into the reaction mixture. After stirred for 15 mins, triethylamine (3.49 mL, 25.0 mmol) was added dropwise and the reaction mixture was allowed to stir for 5 mins. Then, the mixture was warmed to room temperature, followed by addition of H_2O (10.0 mL) and stirred for 10 mins. The mixture was extracted with CH_2Cl_2 (3 x 10.0 mL), washed with dilute HCl (10.0 mL), H_2O (10.0 mL), dilute Na_2CO_3 (10.0 mL), H_2O (10.0 mL). The combined organic layer was dried over Na_2SO_4, filtered and concentrated in *vacuo*. The crude residue was further purified by column chromatography (eluting with hexane/EtOAc = 5:1) to yield aldehyde **B4-3** (0.787 g, 4.05 mmol, 81% yield) as yellow liquid.

Chromium(II) chloride (0.246 g, 2.0 mmol) was dissolved in anhydrous THF (2.4 mL) at 0 ^{o}C under N_2 atmosphere. A solution of aldehyde **B4-3** (0.0778 g, 0.4 mmol) and iodoform (0.4725 g, 1.2 mmol) in anhydrous 1,4-dioxane (2.4 mL) was then added into the mixture and allowed to stir for 2.5 h. The reaction mixture was then poured into saturated sodium bicarbonate aqueous solution (5.0 mL) and filtered through celite. The extracts was washed with saturated sodium thiosulfate aqueous solution (3 x 10.0 mL),

extracted with Et_2O (3 x 10.0 mL) and washed with brine (10.0 mL). The combined organic layer was dried over Na_2SO_4, filtered and concentrated in *vacuo*. The crude residue was further purified by column chromatography (eluting with hexane/EtOAc = 10:1) to yield iodide **B5-4** (0.0435 g, 0.137 mmol, 34% yield; *E/Z* = 80:20) as colorless liquid.

R_f value (hexane/EtOAc = 1:1): 0.73;

^{1}H NMR (400MHz, $CDCl_3$):

***E*-isomer:** δ 7.24 (d, *J* = 8.4 Hz, 2H), 6.88 (d, *J* = 8.4 Hz, 2H), 6.54 (dt, *J* = 7.2, 14.4 Hz, 1H), 6.09 (dt, *J* = 1.2, 14.4 Hz, 1H), 4.43 (s, 2H), 3.80 (s, 3H), 3.47 (t, *J* = 6.4 Hz, 2H), 2.34 (ddd, *J* = 1.2, 6.4, 13.6 Hz, 2H) ppm;

***Z*-isomer:** δ 7.26 (d, *J* = 8.4 Hz, 2H), 6.88 (d, *J* = 8.4 Hz, 2H), 6.30-6.25 (m, 2H), 4.45 (s, 2H), 3.80 (s, 3H), 3.53 (t, *J* = 6.6 Hz, 2H), 2.47-2.42 (m, 2H) ppm;

^{13}C NMR (100MHz, $CDCl_3$):

***E*-isomer:** δ 158.2, 142.0, 129.2, 128.3, 112.8, 75.4, 71.6, 67.1, 54.3, 35.3 ppm.

***Z*-isomer:** δ 158.2, 137.2, 129.2, 128.2, 112.8, 82.9, 71.5, 66.8, 54.3, 34.4 ppm.

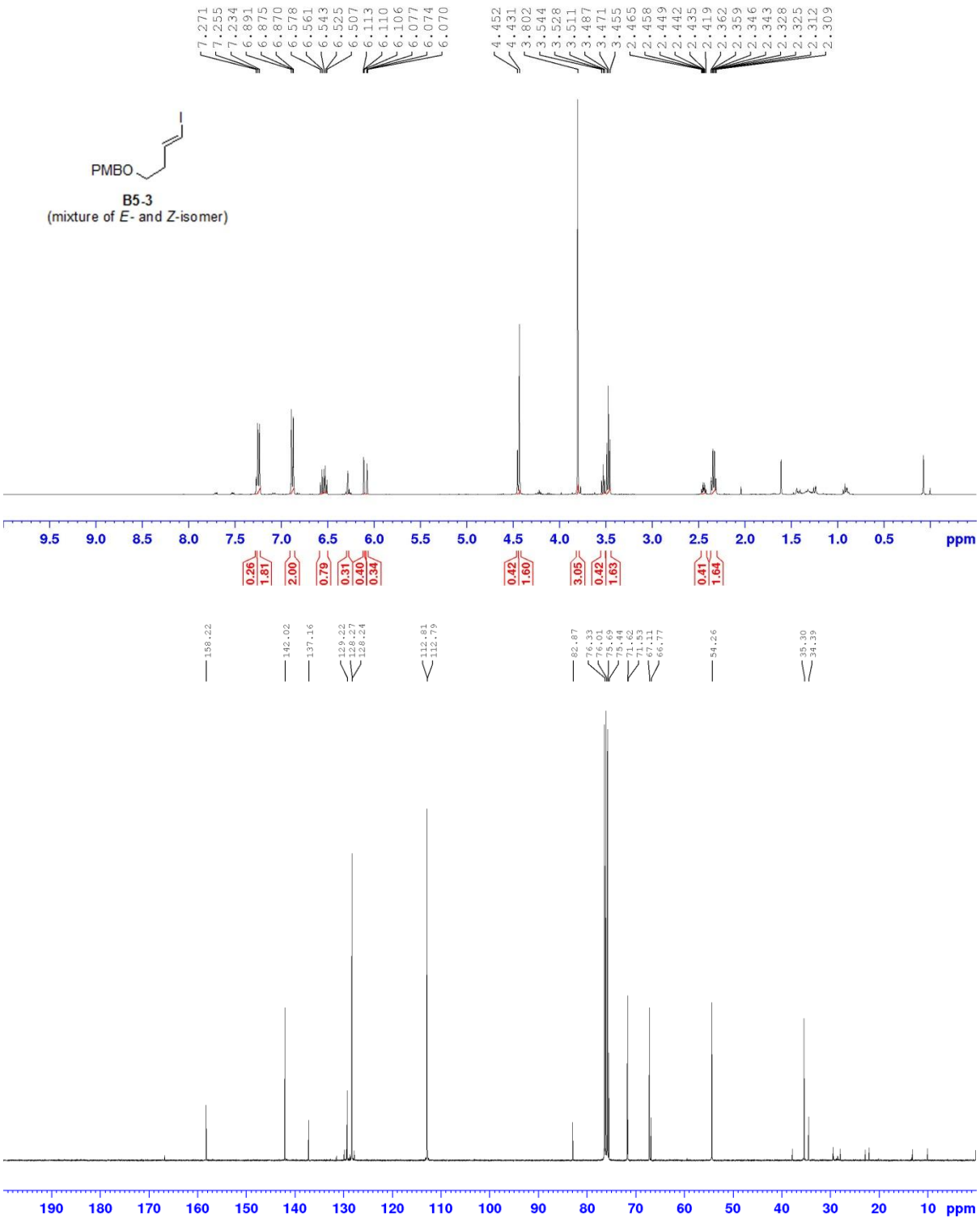
7.271
7.255
7.234
6.891
6.875
6.870
6.578
6.561
6.543
6.525
6.507
6.113
6.110
6.106
6.077
6.074
6.070
4.452
4.431
3.802
3.544
3.528
3.511
3.487
3.471
3.455
2.465
2.458
2.449
2.442
2.435
2.419
2.362
2.359
2.346
2.343
2.328
2.325
2.312
2.309
I
PMBO
B5-3
(mixture of E- and Z-isomer)
9.5 9.0 8.5 8.0 7.5 7.0 6.5 6.0 5.5 5.0 4.5 4.0 3.5 3.0 2.5 2.0 1.5 1.0 0.5 ppm
0.26
1.81
2.00
0.79
0.31
0.40
0.34
0.42
1.60
3.05
0.42
1.63
0.41
1.64
158.22
142.02
137.16
130.22
128.27
128.24
112.81
112.79
82.87
76.33
76.01
75.69
75.44
71.62
71.53
67.11
66.77
54.26
35.30
34.39
190 180 170 160 150 140 130 120 110 100 90 80 70 60 50 40 30 20 10 ppm

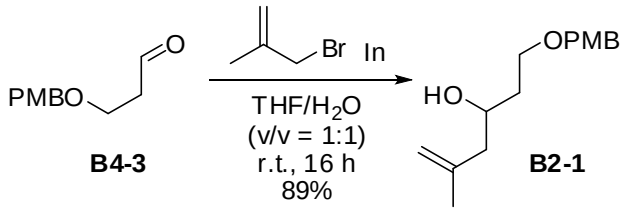

1-(4-Methoxybenzyloxy)-5-methylhex-5-en-3-ol (B2-1):

Indium (0.689 g, 6.0 mmol) and 3-bromo-2-methylpropene (0.60 mL, 6.0 mmol) was added into a mixture of THF (7.5 mL) and H_2O (7.5 mL) at room temperature and allowed to stir for 30 mins. 3-(4-methoxybenzyloxy)propanal **B4-3** (0.583 g, 3.0 mmol) was then added into the mixture and stirred for 16 h. After that, the reaction mixture was filtered through celite, extracted with Et_2O (3 x 30.0 mL) and washed with brine (30.0 mL). The combined organic extracts were dried over Na_2SO_4, filtered and concentrated in *vacuo*. The crude residue was purified by column chromatography (hexane/EtOAc = 5:1) to afford homoallylic alcohol **B2-1** (0.666 g, 2.66 mmol, 89% yield) as colorless liquid.

R_f value (hexane/EtOAc = 1:1): 0.51;

^{1}H NMR (400MHz, $CDCl_3$): δ 7.25 (d, *J* = 7.2 Hz, 2H), 6.89-6.86 (m, 2H), 4.84 (s, 1H), 4.77 (s, 1H), 4.46 (s, 2H), 3.98-3.94 (m, 1H), 3.80 (s, 3H), 3.72-3.59 (m, 2H), 2.72 (s, 1H), 2.23-2.14 (m, 2H), 1.79-1.57 (m, 5H) ppm.

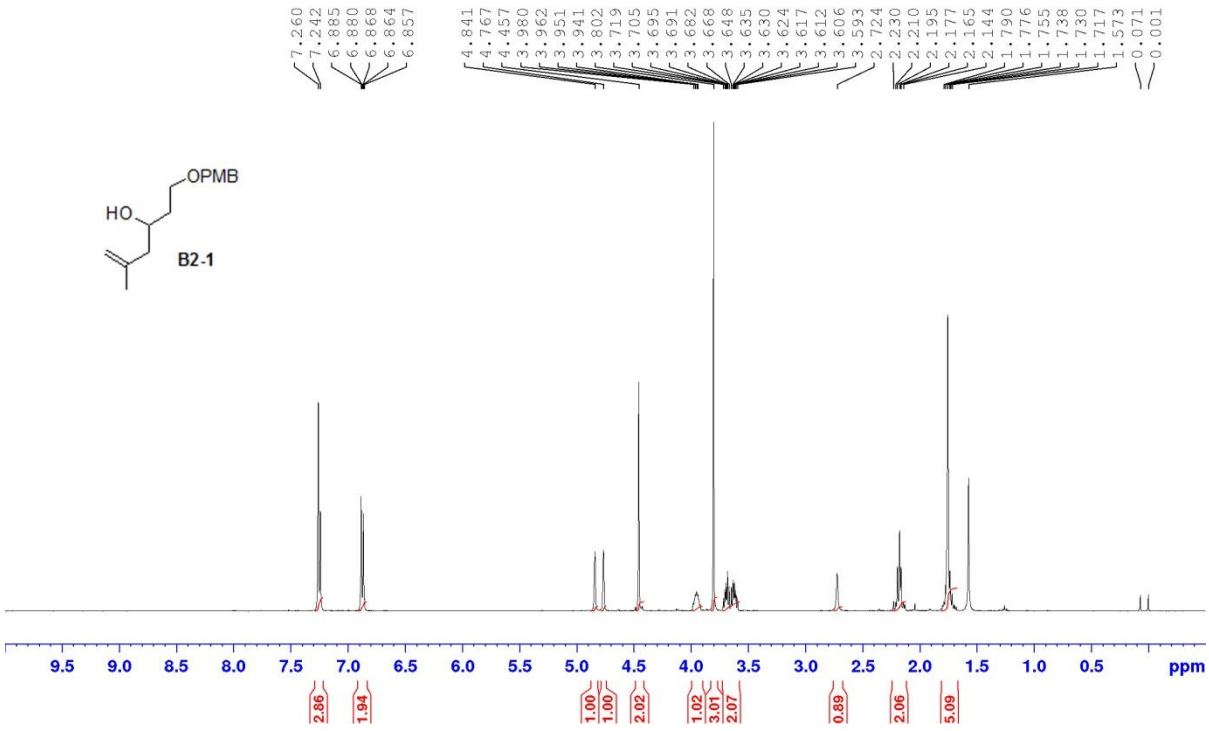

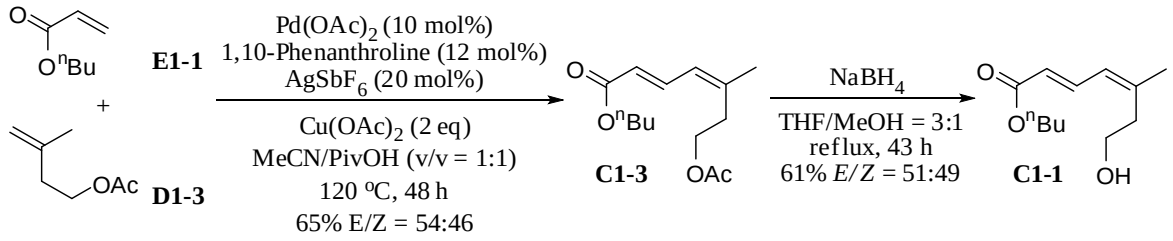

(*2E,4Z*)-Butyl 7-hydroxy-5-methylhepta-2,4-dienoate (C1-1):

Palladium(II) acetate (0.0225 g, 0.1 mmol), 1,10-phenanthroline (0.0216 g, 0.12 mmol), silver hexafluoroantimonate (0.0687 g, 0.2 mmol), copper(II) acetate (0.3633 g, 2.0 mmol), *n*-butyl acrylate **E1-1** (0.29 mL, 2.0 mmol) and alkene **D1-3** (0.128 g, 1.0 mmol) were dissolved in MeCN/PivOH (2.0 mL; v/v = 1:1, mL). The mixture was allowed to stir for 48 h at 120 ^{o}C. The resulting mixture was then allowed to cool to r.t., filtered and diluted with ethyl acetate (20.0 mL). After that, the solution was washed with H_2O (3 x 10.0 mL), saturated sodium bicarbonate aqueous solution (3 x 10.0 mL) until organic layer turned into yellow. The combined aqueous layer was extracted with ethyl acetate (3 x 10.0 mL). The organic layer was combined and washed with brine (10.0 mL), dried over Na_2SO_4, filtered and concentrated in *vacuo*. The crude residue was further purified by column chromatography (eluting with hexane/EtOAc = 5:1) to yield conjugated dienoate **C1-3** (0.166 g, 0.65 mmol, 65% yield; *E*/*Z* = 54:46) as yellow liquid.

E/Z mixture of conjugated diene ester **C1-3** (1.27 g, 5.0 mmol) was dissolved in THF (25.0 mL) at 0 ^{o}C and stirred for 30 mins. $NaBH_4$ (0.378 g, 10.0 mmol) was added in one portion to the solution, followed by dropwise addition of MeOH (8.3 mL). The mixture was allowed to stir for 43 h under reflux. After that, the reaction was quenched by saturated ammonium chloride aqueous solution (10.0 mL). The reaction mixture was then extracted with Et_2O (3 x 30 mL) and washed with brine (50 mL). The combined organic layer was dried over Na_2SO_4, filtered and concentrated in *vacuo*. The crude residue was further purified by column chromatography (eluting with hexane/EtOAc = 2:1) to yield alcohol **C1-1** (0.652 g, 3.07 mmol, 61% yield; *E*/*Z* = 51:49) as yellow liquid.

R_f value (hexane/EtOAc = 1:1): 0.48;

^{1}H NMR (400MHz, $CDCl_3$): δ 7.56 (dd, *J* = 11.6, 15.2 Hz, 1H), 6.13 (d, *J* = 11.6 Hz, 1H), 5.81 (d, *J* = 15.2 Hz, 1H), 4.14 (t, *J* = 6.8 Hz, 2H), 3.76 (t, *J* = 6.2 Hz, 2H), 2.58 (t, *J* = 6.6 Hz, 2H), 1.92 (s, 3H), 1.68-1.61 (m, 2H), 1.43-1.35 (m, 3H), 0.94 (t, *J* = 3.4 Hz, 3H) ppm;

^{13}C NMR (100MHz, $CDCl_3$): δ 167.7 (C), 140.1 (C), 126.3 (CH), 125.4 (CH), 120.0 (CH), 64.2 (CH_2), 60.4 (CH_2), 43.2 (CH_2), 36.0 (CH_2), 24.6 (CH_3), 19.2 (CH_2), 13.7 (CH_3) ppm.

Remarks:

Syntheses of conjugated dienoate **C1-3** and **C1-1** were established through the study shown in Scheme 4.2.1 and 4.2.2 respectively.

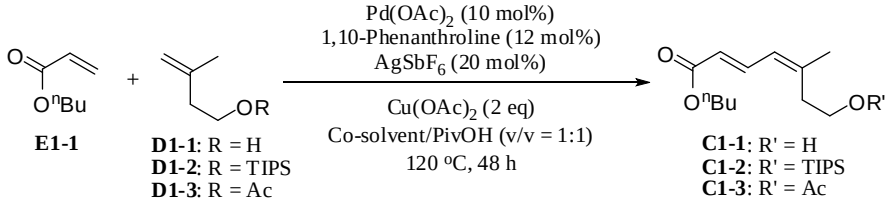

E1-1

D1-1: R = H
D1-2: R = TIPS
D1-3: R = Ac

C1-1: R' = H
C1-2: R' = TIPS
C1-3: R' = Ac

Entry	D1	Co-solvent	Product
1[a]	**D1-2**	NMP	**C1-2** (30% E/Z = 67:33) + **C1-3** (32% E/Z = 67:33)
2	**D1-2**	MeCN	**C1-2** (33% E/Z = 53:47)
3	**D1-1**	MeCN	**C1-3** (26% E/Z = 56:44) + **C1-1** (26% E/Z = 52:48)
4	**D1-3**	MeCN	**C1-3** (65% E/Z = 54:46)

Scheme 4.2.1 Synthesis of dienoate *via* Pd-catalyzed direct cross coupling. [a] Reported result by Wen *et al*.

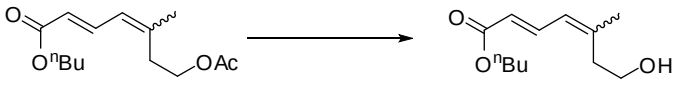

C1-3 **C1-1**

Entry	Condition	Yield (E/E:E/Z)
1	NaOMe, MeOH, reflux	NR
2	2M NH_3 in MeOH, reflux	NR
3	K_2CO_3 (3 eqv.), H_2O/MeOH (v/v = 3:2) r.t., 5 days	37%
4	LiOH (1 eqv.) THF/H_2O/MeOH (v/v = 1:2:2) r.t., 3 h	56% (57:43)
5	$NaBH_4$ (2 eqv.) THF/MeOH = 3:1 reflux, 43 h	61% (51:49)

Scheme 4.2.2 Reduction of acetate **C1-3** to alcohol **C1-1**.

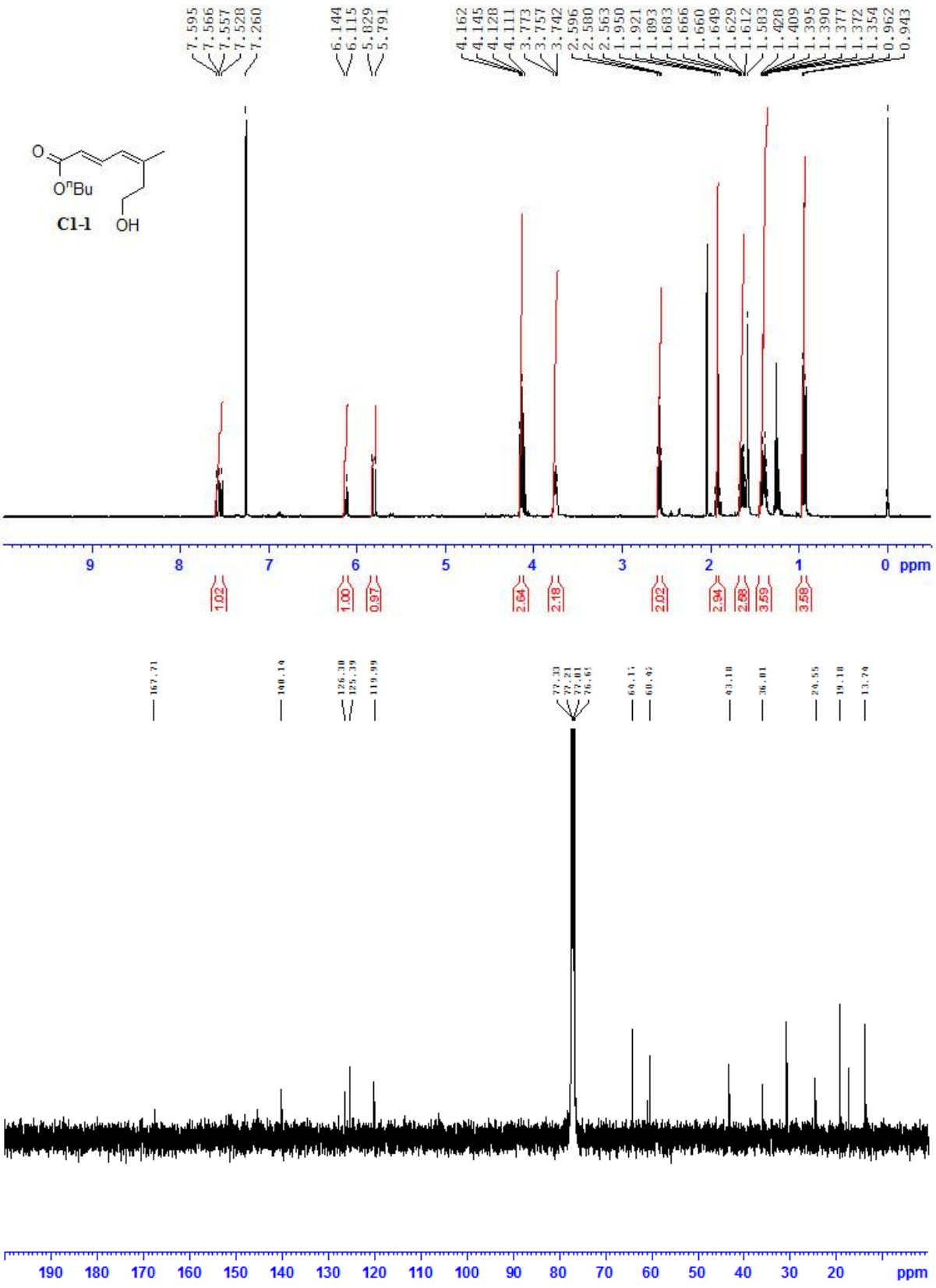
7.595
7.566
7.557
7.528
7.260
6.144
6.115
5.829
5.791
4.162
4.145
4.128
4.111
3.773
3.757
3.742
2.596
2.580
2.563
1.950
1.921
1.893
1.683
1.666
1.660
1.649
1.629
1.612
1.583
1.428
1.409
1.395
1.390
1.377
1.372
1.354
0.962
0.943
O
O^{n}Bu
C1-1
OH
9
8
7
6
5
4
3
2
1
0 ppm
1.02
1.00
0.97
2.64
2.18
2.02
2.94
2.68
3.59
3.58
167.71
140.14
126.30
125.39
119.99
77.33
77.21
77.01
76.65
64.11
60.45
43.18
36.01
24.55
19.18
13.74
190
180
170
160
150
140
130
120
110
100
90
80
70
60
50
40
30
20
ppm

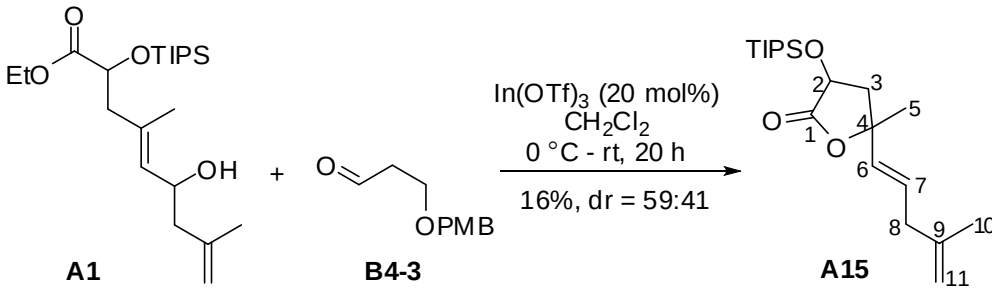

A1 **B4-3** **A15**

(*E*)-5-Methyl-5-(4-methylpenta-1,4-dienyl)-3-(triisopropylsilyloxy)dihydrofuran-2(3*H*)-one (A15):

A solution of aldehyde **A1** (0.109 g, 0.27 mmol) and homoallylic alcohol **B4-3** (0.027 g, 0.14 mmol) in anhydrous CH_2Cl_2 (0.41 mL) was treated with indium trifluormethanesulfonate (0.031 g, 0.055 mmol) at 0 ^oC. The reaction was allowed to warm to room temperature and stir for 20 h. Then, the reaction mixture was diluted with CH_2Cl_2 (10.0 mL), extracted with saturated $NaHCO_3$ aqueous solution (10.0 mL), followed by CH_2Cl_2 (2 x 10.0 mL), and washed with brine (10.0 mL). The combined organic extracts were dried over Na_2SO_4, filtered and concentrated in *vacuo*. The crude residue was purified by column chromatography (hexane/EtOAc = 10:1) to afford dihydrofuranone **A15** (0.016 g, 0.044 mmol, 16% yield; d.r. = 59:41) as colorless liquid.

R_f value (hexane/EtOAc = 4:1): 0.67;

^{1}H NMR (400MHz, $CDCl_3$):

Major isomer: δ 5.69 (dt, *J* = 6.8, 15.6 Hz, 1H, H7), 5.54 (d, *J* = 15.6 Hz, 1H, H6), 4.76 (s, 1H, H11a), 4.66 (s, 1H, H11b), 4.55 (dd, *J* = 7.8, 9.4 Hz, 1H, H2), 2.72 (d, *J* = 7.2 Hz, 2H, H8), 2.54 (dd, *J* = 8.0, 12.4 Hz, 1H, H3a), 2.09 (dd, *J* = 9.6, 12.4 Hz, 1H, H3b), 1.69 (s, 3H, H10), 1.53 (s, 3H, H5), 1.18 – 1.07 (m, 21H, TIPS) ppm.

Minor isomer: δ 5.74-5.71 (m, 2H, H6 & H7), 4.76 (s, 1H, H11a), 4.70 (s, 1H, H11b), 4.65 (t, *J* = 8.2 Hz, 1H, H2), 2.73 (d, *J* = 5.6 Hz, 2H, H8), 2.43 (dd, *J* = 8.0, 12.8 Hz, 1H, H3a), 2.20 (dd, *J* = 8.4, 12.8 Hz, 1H, H3b), 1.71 (s, 3H, H10), 1.47 (s, 3H, H5), 1.18 – 1.07 (m, 21H, TIPS) ppm.

^{13}C NMR:

Major isomer (100MHz, $CDCl_3$): δ 175.2 (C1), 143.7 (C9), 133.7 (C6), 127.5 (C7), 111.2 (C11), 81.3 (C4), 69.4 (C2), 44.0 (C3), 40.4 (C8), 27.8 (C5), 22.3 (C10), 17.8 (**C**H_3 of TIPS), 12.1 (**C**H of TIPS) ppm.

Minor isomer (75MHz, $CDCl_3$): δ 174.8(C1), 143.7 (C9), 134.6 (C6), 128.1 (C7), 111.3 (C11), 81.5 (C4), 69.4 (C2), 44.4 (C3), 40.5 (C8), 26.3 (C5), 22.4 (C10), 17.8 (**C**H_3 of TIPS), 12.1 (**C**H of TIPS) ppm.

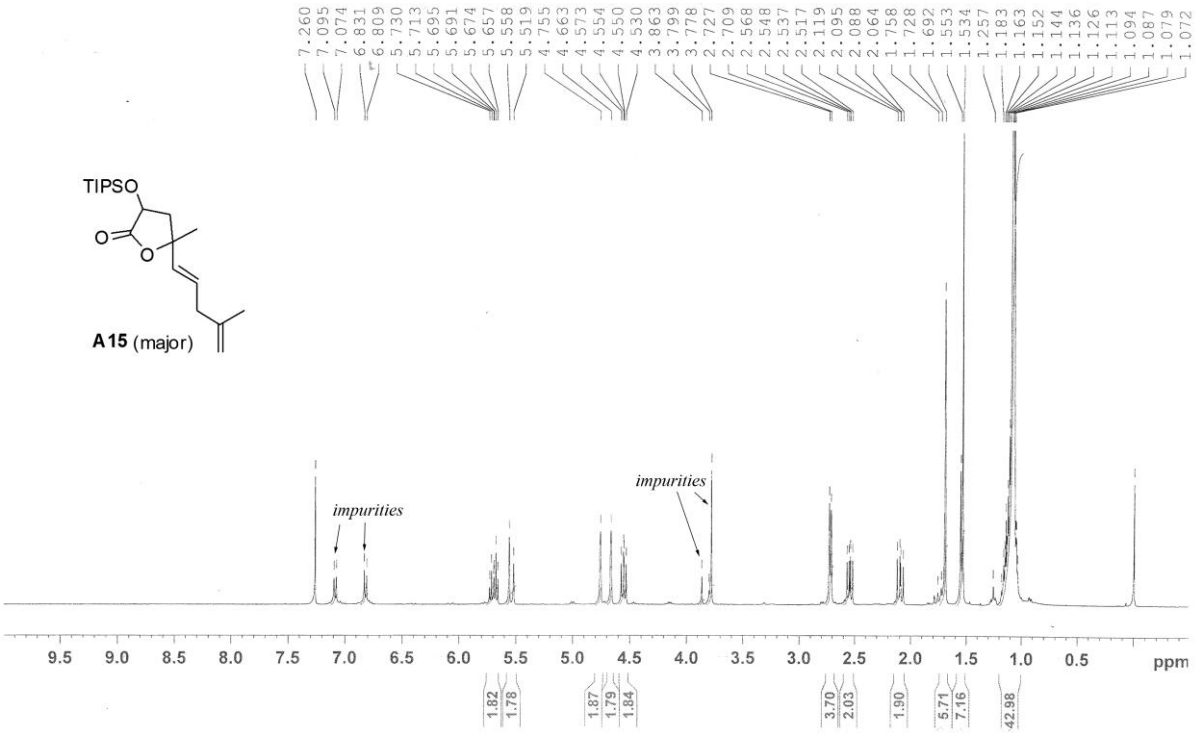
TIPSO
O
O
A15 (major)
impurities
impurities
ppm

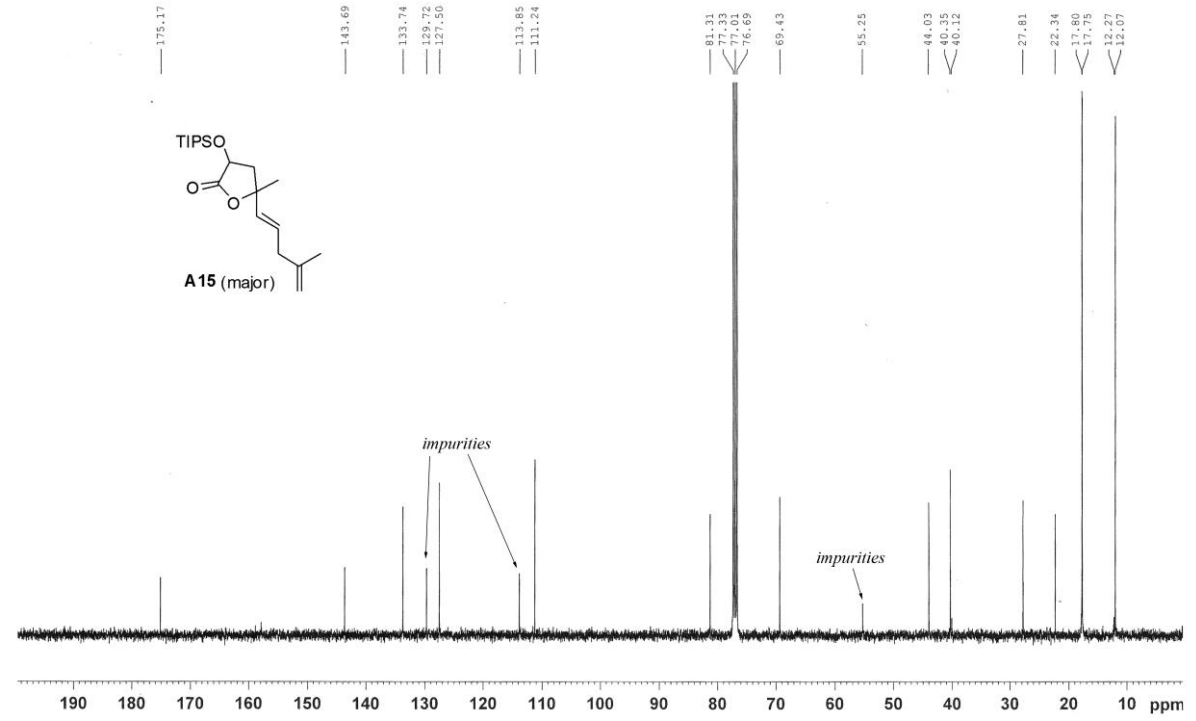
TIPSO
O
O
A15 (major)
impurities
impurities
ppm

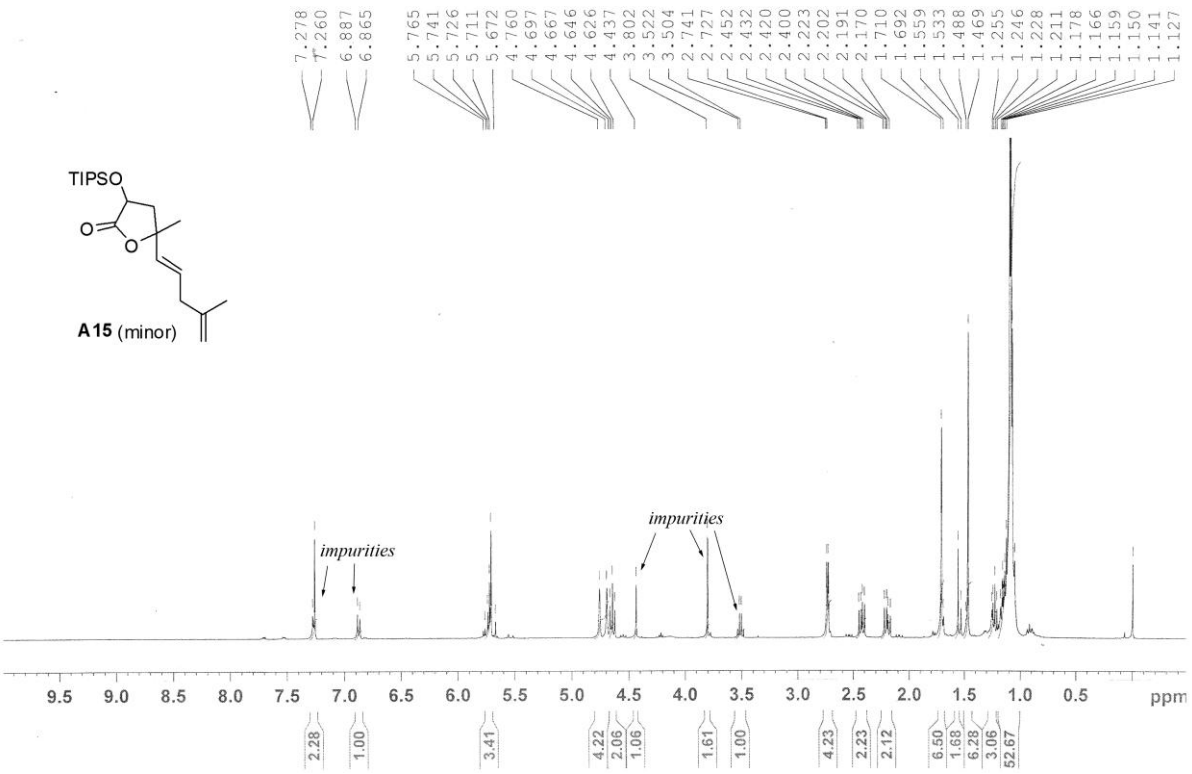
7.278
7.260
6.887
6.865
5.765
5.741
5.726
5.711
5.672
4.760
4.697
4.667
4.646
4.626
4.437
3.802
3.522
3.504
2.741
2.727
2.452
2.432
2.420
2.400
2.223
2.202
2.191
2.170
1.710
1.692
1.559
1.533
1.488
1.469
1.255
1.246
1.228
1.211
1.178
1.166
1.159
1.150
1.141
1.127
TIPSO
O
O
A15 (minor)
impurities
impurities
9.5 9.0 8.5 8.0 7.5 7.0 6.5 6.0 5.5 5.0 4.5 4.0 3.5 3.0 2.5 2.0 1.5 1.0 0.5 ppm
2.28
1.00
3.41
4.22
2.06
1.06
1.61
1.00
4.23
2.23
2.12
6.50
1.68
6.28
3.06
52.67

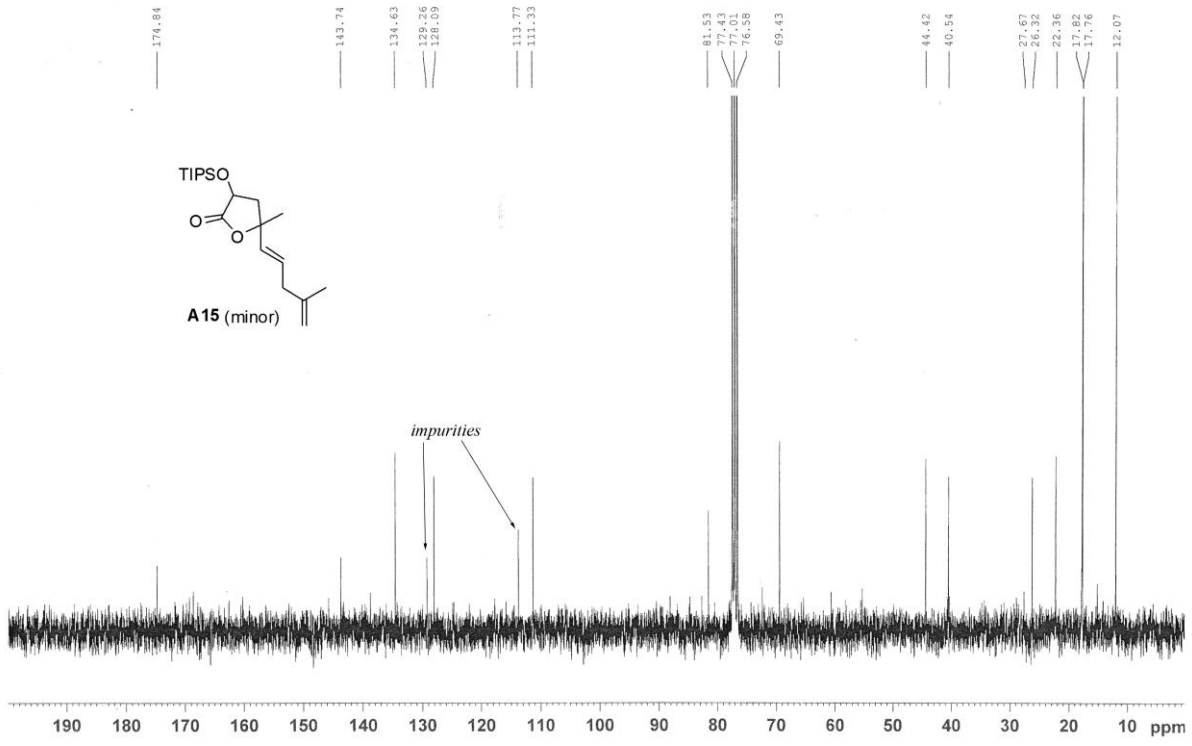
174.84
143.74
134.63
129.26
128.09
113.77
111.33
81.53
77.43
77.01
76.58
69.43
44.42
40.54
27.67
26.32
22.36
17.82
17.76
12.07
TIPSO
O
O
A15 (minor)
impurities
190 180 170 160 150 140 130 120 110 100 90 80 70 60 50 40 30 20 10 ppm

4.2.3 Compounds synthesized in reexamination of synthesis of 2,6-*syn*-4-exomethylene tetrahydropyrans[147]

General procedure of $In(OTf)_3$-catalyzed intramolecular 2,5-oxonium-ene cyclization, please refer to the synthesis of (*E*)-ethyl 5-(6-(2-(*tert*-butyldiphenylsilyloxy)ethyl)-4-methylenetetrahydro-2*H*-pyran-2-yl)-4-methyl-2-(triisopropylsilyloxy)pent-4-enoate (**AB-1b-I**) mentioned in p166.

The compounds that synthesized in the reexamination were as followed:

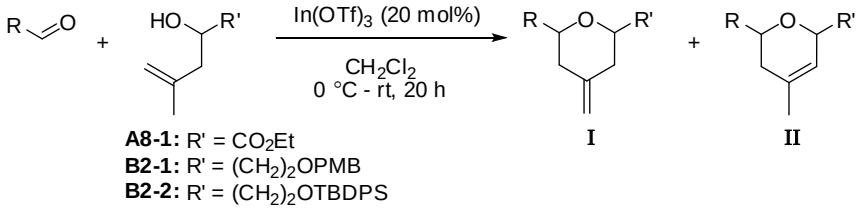

Entry	Aldehyde	Alcohol	Desired Product	Yield of I	Total Yield (I+II)	Ratio of I:II[a]
1	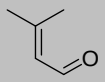 **E2-1**	**B2-1**	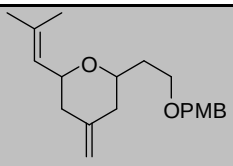 **B6-1-I**	2%	4%	50:50
2	 **E2-1**	**B2-2**	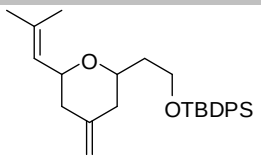 **B6-2-I**	7%	11%	64:36
Ref	(Table 1, Entry 12 reported in *TL*, **2002**, *43*, 7193)			55%, *syn*:*anti* = 75:25		
3	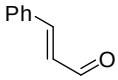 **E2-2**	**B2-2**	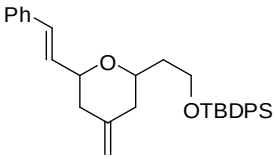 **B6-3-I**	47%	74%[b]	63:37
Ref	(Table 1, Entry 10 reported in *TL*, **2002**, *43*, 7193)			90%, *syn*:*anti* = 75:25		
4	 **E2-3**	**B2-2**	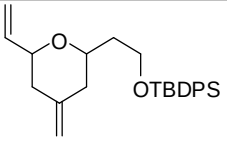 **B6-4-I**	28%	53%	53:47

[147] HRMS of the compounds listed in this section and ^{13}C NMR of compound **B6-1-I/B6-1-II, B6-7a-I/B6-7a-II/B6-7a-III, B6-8-I/B6-8-II** are not provided.

Entry	Aldehyde	Alcohol	Desired Product	Yield of I	Total Yield (I+II)	Ratio of I:II[a]
5		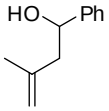	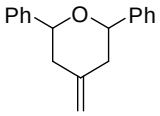 **B6-5**	45%	45%	100:0
Ref	(Table 1, Entry 2 reported in *TL*, **2002**, *43*, 7193)			80%, *syn*:*anti* = 95:5		
6		**A8-1**	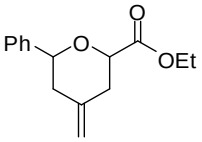 **B6-6-I**	17%	30%	56:44
7	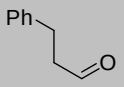	**A8-1**	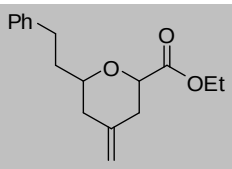 **B6-7a-I**	19%	42%	45:55
8	**B4-3**	**B2-1**	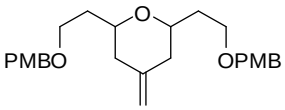 **B6-8-I**	11%	27%	40:60
9		**B2-2**	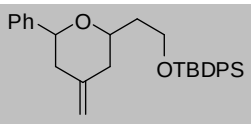 **B6-9-I**	22%	35%	63:37

Table 4.2.1 Reexamination of tetrahydropyran ring synthesis catalyzed by $In(OTf)_3$. Ratio of aldehyde to homoallylic alcohol = 1:2. [a] determined from ^1H NMR; [b] calculated from ^1H NMR with $PhNO_2$ as internal standard.

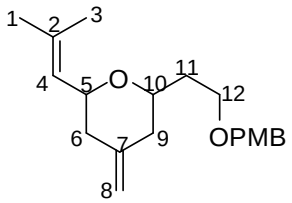

B6-1-I

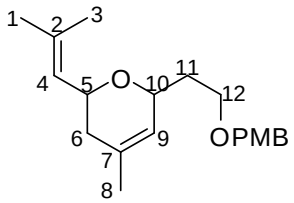

B6-1-II

2-(2-(4-Methoxybenzyloxy)ethyl)-4-methylene-6-(2-methylprop-1-enyl)tetrahydro-2*H*-pyran (B6-1-I)

6-(2-(4-Methoxybenzyloxy)ethyl)-4-methyl-2-(2-methylprop-1-enyl)-3,6-dihydro-2*H*-pyran (B6-1-II)

R_f value (hexane/EtOAc = 4:1): 0.50;

^{1}H NMR (400MHz, $CDCl_3$):

B6-1-I: δ 7.25 (d, *J* = 8.4 Hz, 2H, Ph of PMB), 6.87 (d, *J* = 8.4 Hz, 2H, Ph of PMB), 5.24 – 5.20 (app t, 1H, H4), 4.71 (s, 2H, H8), 4.43 (s, 2H, CH_2 of PMB), 4.00 – 3.95 (m, 1H, H5), 3.80 (s, 3H, CH_3 of PMB), 3.63 – 3.53 (m, 2H, H12), 3.53 – 3.45 (m, 1H, H10), 2.21 – 1.78 (m, 6H, H6, H9 & H11), 1.72 (s, 3H, H1), 1.67 (s, 3H, H3) ppm.

B6-1-II: δ 7.25 (d, *J* = 8.4 Hz, 2H, Ph of PMB), 6.87 (d, *J* = 8.4 Hz, 2H, Ph of PMB), 5.33 (s, 1H, H9), 5.24 – 5.20 (app t, 1H, H4), 4.43 (s, 2H, CH_2 of PMB), 4.25 – 4.22 (m, 2H, H5 & H10), 3.80 (s, 3H, CH_3 of PMB), 3.63 – 3.53 (m, 2H, H12), 2.21 – 1.78 (m, 4H, H6, H11), 1.72 (s, 3H, H1), 1.67 (s, 6H, H3 & H8) ppm.

Remarks:

(a) Peaks assigned to H5 and H10 of both compounds are roughly deduced from ^{1}H NMR compared with ^{1}H NMR of **AB-1b-I** and **AB-1b-II** without further confirmation with 2D NMR.

(b) Peaks assigned to H1 and H3 of both compounds are roughly deduced from ^{1}H NMR without further confirmation with 2D NMR.

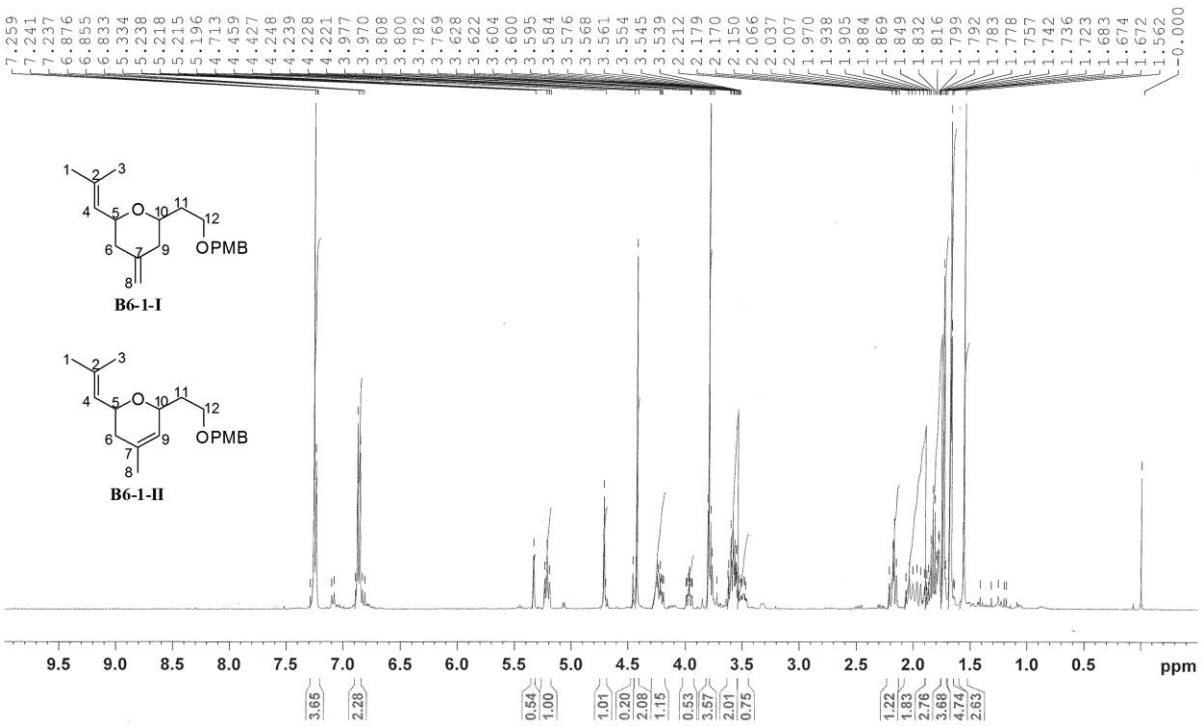

^{1}H NMR spectrum (ratio of **B6-1-I:B6-1-II** = 50:50)

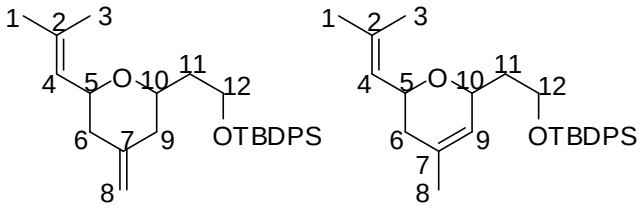

B6-2-I **B6-2-II**

***tert*-Butyl(2-(4-methylene-6-(2-methylprop-1-enyl)tetrahydro-2*H*-pyran-2-yl)ethoxy)diphenylsilane (B6-2-I)**

***tert*-Butyl(2-(4-methyl-6-(2-methylprop-1-enyl)-5,6-dihydro-2*H*-pyran-2-yl)ethoxy)diphenylsilane (B6-2-II)**

R_f value (hexane/EtOAc = 4:1): 0.76;

^{1}H NMR (400MHz, $CDCl_3$):

B6-2-I: δ 7.74 – 7.67 (m, 4H, Ph of TBDPS), 7.42 – 7.37 (m, 6H, Ph of TBDPS), 5.21 (d, *J* = 6.8 Hz, 1H, H4), 4.74 (s, 2H, H8), 4.00 (t, *J* = 9.4 Hz, 1H, H5), 3.88 – 3.72 (m, 2H, H12), 3.61 – 3.58 (m, 1H, H10), 2.26 – 1.73 (m, 6H, H6, H9 & H11), 1.75 (s, 3H, H1), 1.56 (s, 3H, H3), 1.05 (s, 9H, *t*Bu of TBDPS) ppm.

B6-2-II: δ 7.74 – 7.67 (m, 4H, Ph of TBDPS), 7.42 – 7.37 (m, 6H, Ph of TBDPS), 5.37 (s, 1H, H9), 5.23 (d, *J* = 7.6 Hz, 1H, H4), 4.36 (br s, 1H, H10), 4.30 – 4.25 (m, 1H, H5), 3.88 – 3.72 (m, 2H, H12), 2.26 – 1.73 (m, 4H, H6 & H11), 1.75 (s, 3H, H1), 1.57 (s, 3H, H8), 1.56 (s, 3H, H3), 1.05 (s, 9H, *t*Bu of TBDPS) ppm.

^{13}C NMR (100MHz, $CDCl_3$):

B6-2-I: δ 145.0 (C7), 136.0 (Ph), 135.6 (Ph), 134.0 (C2), 129.5 (Ph), 127.4 (Ph), 126.0 (C4), 108.3 (C8), 75.6 (C5), 75.1 (C10), 60.4 (C12), 41.1 & 40.7 (C6 & C9), 39.2 (C11), 26.8 (**C**H_3 of TBDPS), 25.8 (C1), 19.2 (C of TBDPS), 18.5 (C3) ppm.

B6-2-II: δ 136.0 (Ph), 135.6 (Ph), 134.0 (C2), 132.3 (C7), 129.5 (Ph), 127.4 (Ph), 126.2 (C4), 124.1 (C9), 71.8 (C10), 71.3 (C5), 60.4 (C12), 38.7 (C11), 36.2 (C6), 26.8 (**C**H_3 of TBDPS), 25.8 (C1), 22.9 (C8), 19.2 (C of TBDPS), 18.5 (C3) ppm.

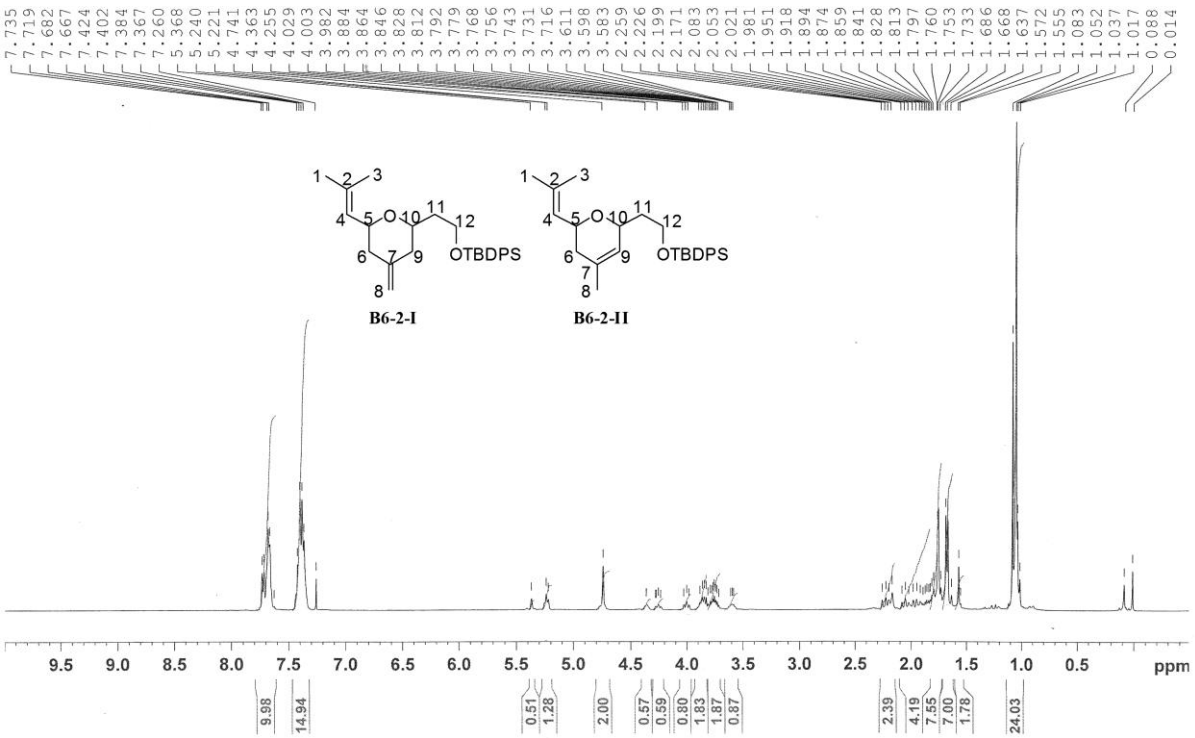

^{1}H NMR spectrum (ratio of **B6-2-I:B6-2-II** = 59:41)

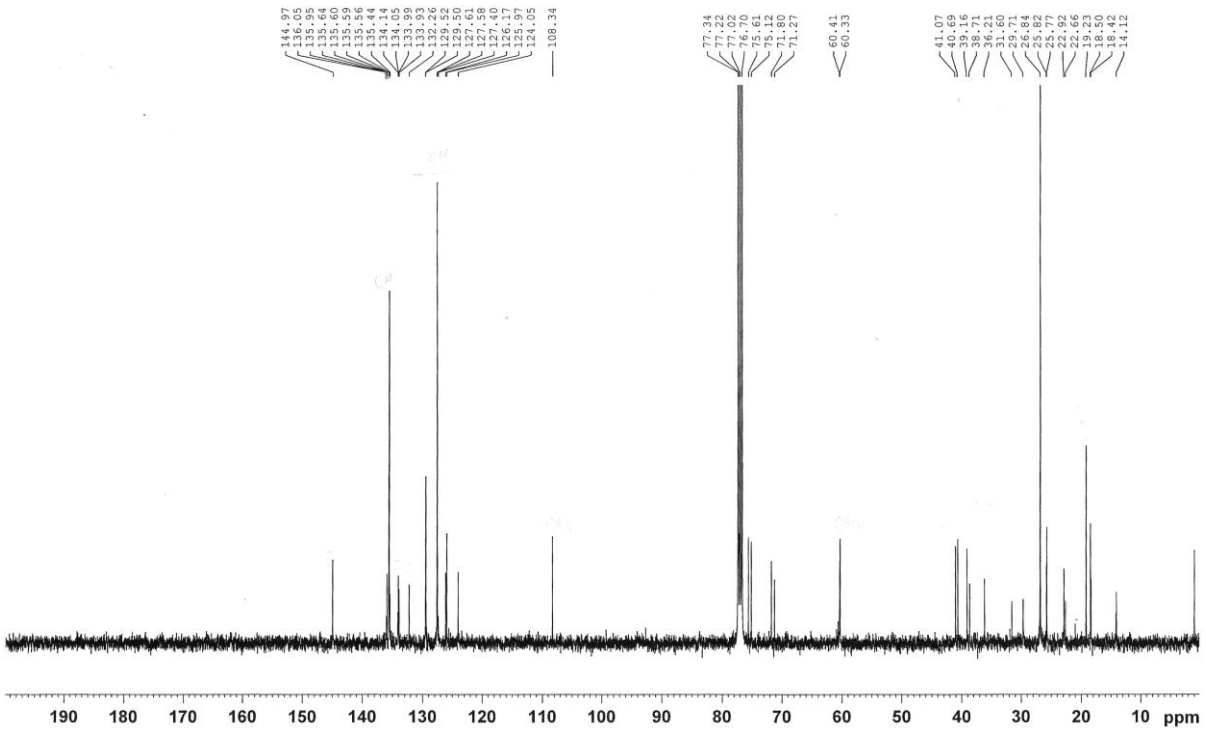

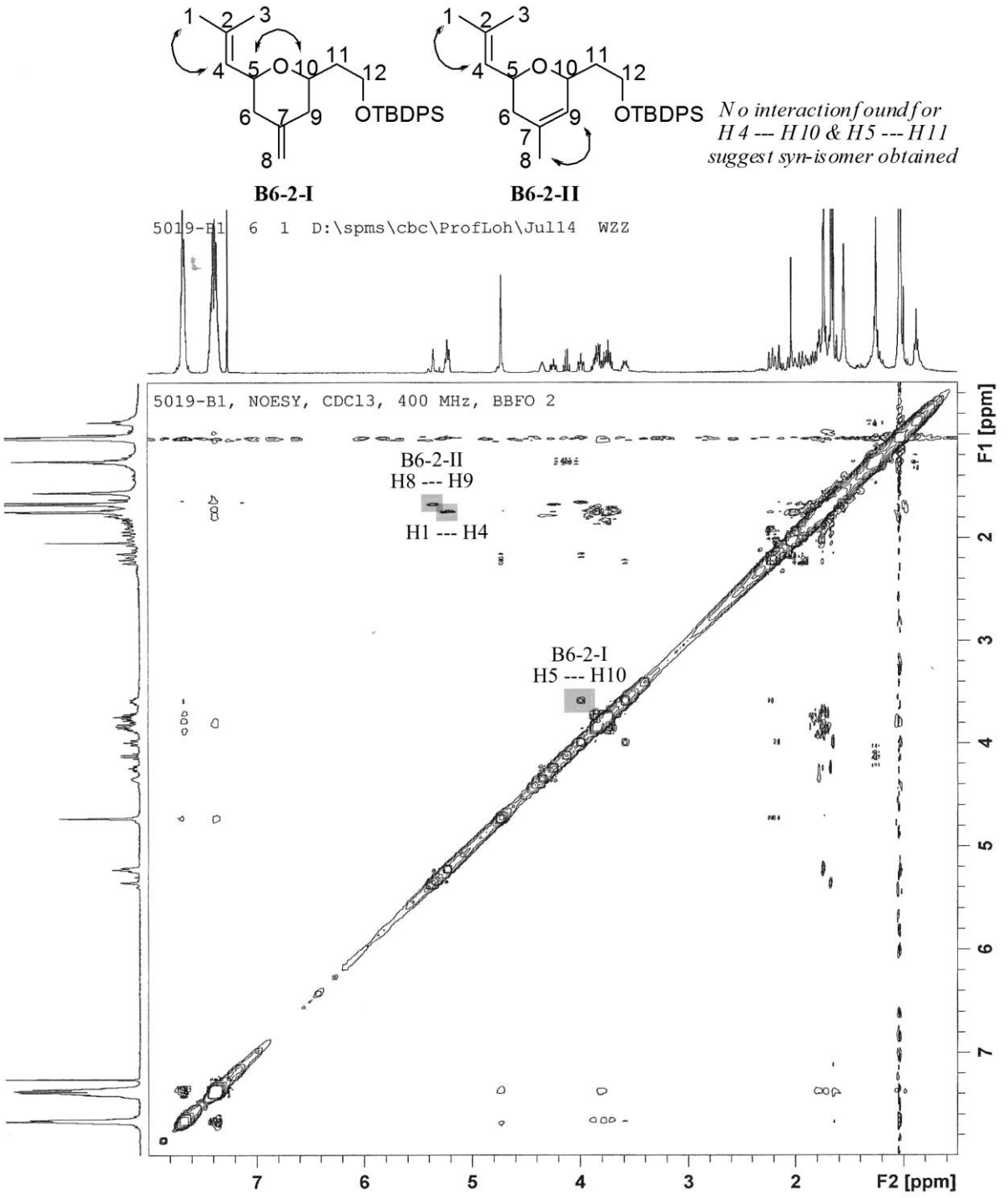
B6-2-I
B6-2-II
No interaction found for
H4 --- H10 & H5 --- H11
suggest syn-isomer obtained
5019-B1 6 1 D:\spms\cbc\ProfLoh\Jul14 WZZ
5019-B1, NOESY, CDCl3, 400 MHz, BBFO 2
B6-2-II
H8 --- H9
H1 --- H4
B6-2-I
H5 --- H10
F1 [ppm]
F2 [ppm]

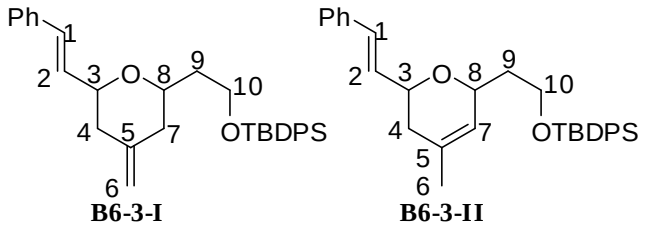

B6-3-I **B6-3-II**

(*E*)-*tert*-Butyl(2-(4-methylene-6-styryltetrahydro-2*H*-pyran-2-yl)ethoxy)diphenylsilane (B6-3-I)[148]

(*E*)-*tert*-Butyl(2-(4-methyl-6-styryl-5,6-dihydro-2*H*-pyran-2-yl)ethoxy)diphenylsilane (B6-3-II)

R_f value (hexane/EtOAc = 4:1): 0.63;

^{1}H NMR (400MHz, $CDCl_3$):

B6-3-I: δ 7.67 – 7.62 (m, 4H, Ph of TBDPS), 7.43 – 7.21 (m, 11H, Ph of TBDPS & Ph-C1), 6.58 (d, *J* = 16.0 Hz, 1H, H1), 6.24 (dd, *J* = 5.6, 16.0 Hz, 1H, H2), 4.78 (s, 2H, H6), 3.98 – 3.62 (m, 4H, H3, H8 & H10), 2.36 (d, *J* = 13.2 Hz, 1H, H4a), 2.27 (d, *J* = 13.2 Hz, 1H, H7a), 2.17 – 1.95 (m, 2H, H4b & H7b), 1.91 – 1.75 (m, 2H, H9), 1.05 (s, 9H, *t*Bu of TBDPS) ppm.

B6-3-II: δ 7.67 – 7.62 (m, 4H, Ph of TBDPS), 7.43 – 7.21 (m, 11H, Ph of TBDPS & Ph-C1), 6.59 (d, *J* = 16.0 Hz, 1H, H1), 6.27 (dd, *J* = 5.6, 16.0 Hz, 1H, H2), 5.39 (s, 1H, H7), 4.40 (br s, 1H, H8), 4.24 – 4.19 (m, 1H, H3), 3.98 – 3.62 (m, 2H, H10), 2.17 – 1.95 (m, 2H, H4), 1.91 – 1.75 (m, 2H, H9), 1.70 (s, 3H, H6), 1.05 (s, 9H, *t*Bu of TBDPS) ppm.

^{13}C NMR (100MHz, $CDCl_3$):

B6-3-I: δ 144.4 (C5), 137.0, 135.6, 134.0, 133.9, 130.4 (C1), 130.2 (C2), 129.6, 128.5, 127.7, 126.5, 108.9 (C6), 78.6 (C3), 75.2 (C8), 60.2 (C10), 41.1 & 40.8 (C4 & C7), 39.1 (C9), 26.8 (**C**H_3 of TBDPS), 19.3 (C of TBDPS) ppm.

B6-3-II: δ 137.0, 136.1 (C5), 135.6, 134.0, 133.9, 130.4 (C1), 130.0 (C2), 129.6, 128.5, 127.7, 126.5, 124.2 (C7), 74.3 (C3), 71.9 (C8), 60.4 (C10), 38.8 (C9), 36.1 (C4), 26.8 (**C**H_3 of TBDPS), 23.0 (C6), 19.2 (C of TBDPS) ppm.

[148] NMR data are referred with the data published for compound 16 in following reference: Ghosh, A. K.; Cheng, X.; Bai, R.; Hamel, E., *Eur. J. Org. Chem.* **2012**, 4130-4139.

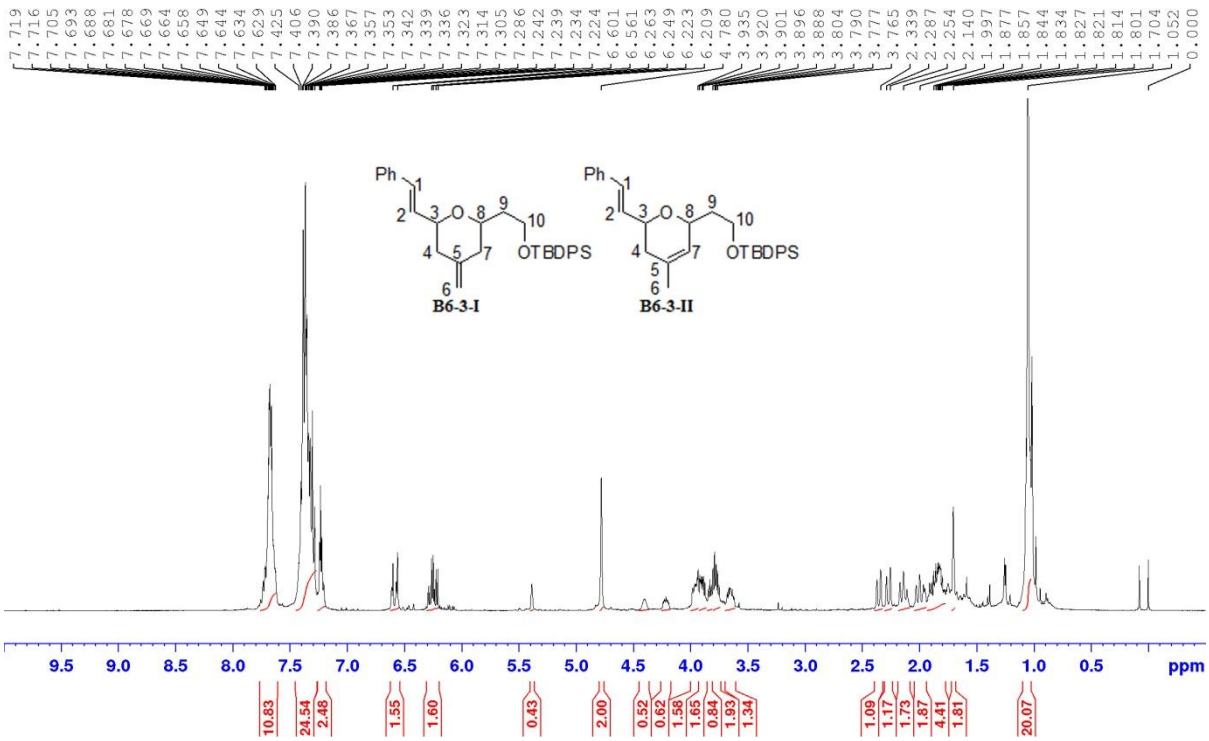

^{1}H NMR spectrum (ratio of **B6-3-I:B6-3-II** = 67:33)

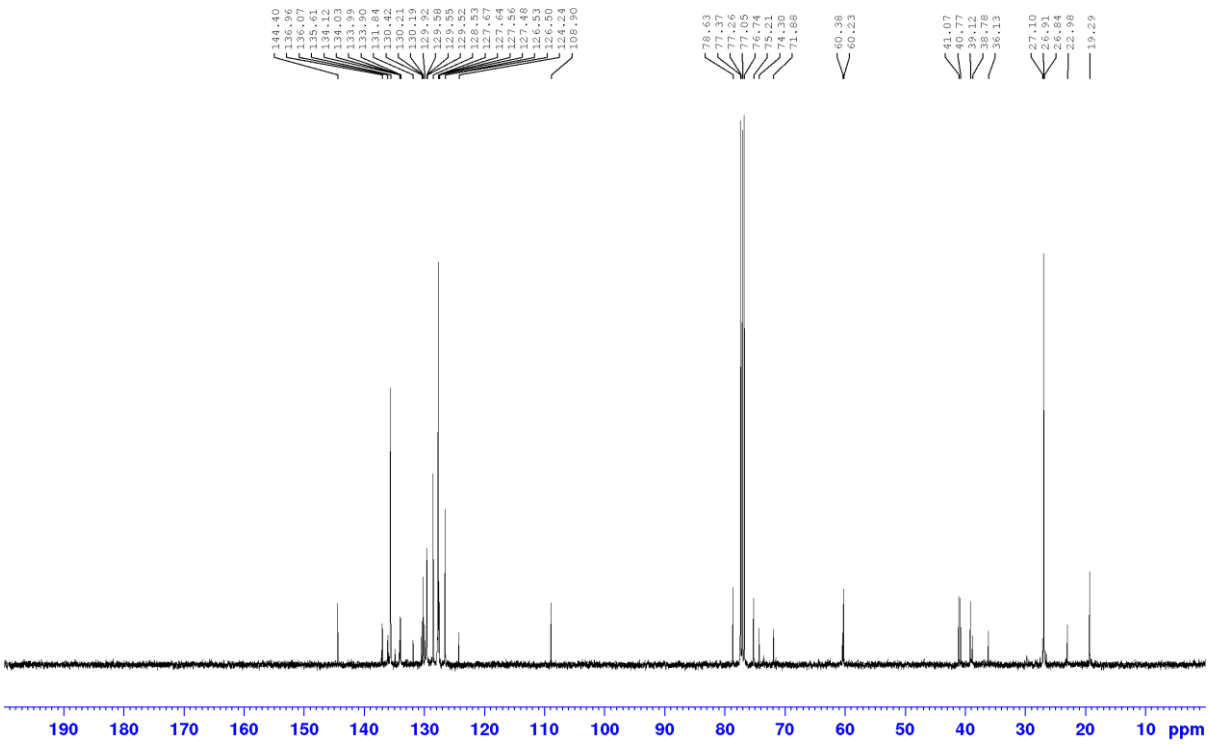

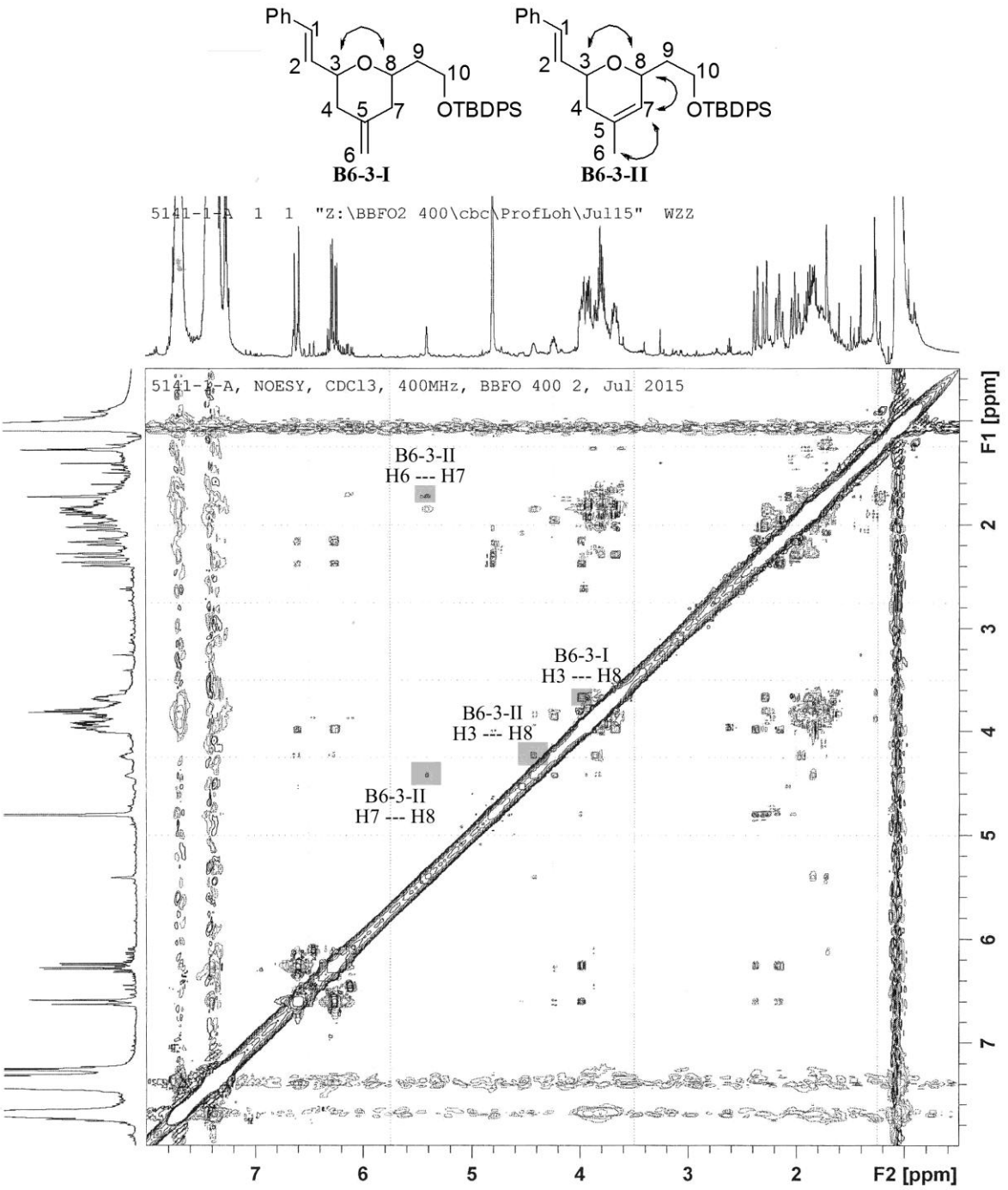
Ph
OTBDPS
B6-3-I
B6-3-II
5141-1-A 1 1 "Z:\BBFO2 400\cbc\ProfLoh\Jul15" WZZ
5141-1-A, NOESY, CDCl3, 400MHz, BBFO 400 2, Jul 2015
B6-3-II
H6 --- H7
B6-3-I
H3 --- H8
B6-3-II
H3 --- H8
B6-3-II
H7 --- H8
F1 [ppm]
F2 [ppm]

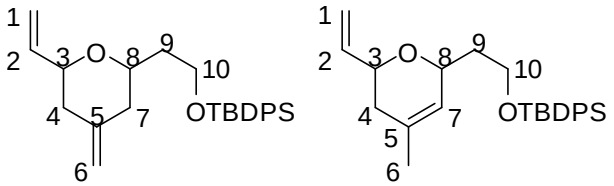

B6-4-I **B6-4-II**

***tert*-Butyl(2-(4-methylene-6-vinyltetrahydro-2*H*-pyran-2-yl)ethoxy)diphenylsilane (B6-4-I)**[149]

***tert*-Butyl(2-(4-methyl-6-vinyl-5,6-dihydro-2*H*-pyran-2-yl)ethoxy)diphenylsilane (B6-4-II)**

R_f value (hexane/EtOAc = 4:1): 0.68;

^{1}H NMR (400MHz, $CDCl_3$):

B6-4-I: δ 7.70 – 7.66 (m, 4H, Ph of TBDPS), 7.44 – 7.36 (m, 6H, Ph of TBDPS), 5.90 (ddd, *J* = 5.2, 10.4, 17.2 Hz, 1H, H2), 5.26 (d, *J* = 17.2 Hz, 1H, H1a), 5.14 (d, *J* = 10.8 Hz, 1H, H1b), 4.77 (s, 2H, H6), 3.95 – 3.74 (m, 3H, H8 & H10), 3.64 – 3.58 (m, 1H, H3), 2.31 – 2.24 (m, 2H, H4a & H7a), 2.08 – 1.94 (m, 2H, H4b & H7b), 1.91 – 1.75 (m, 2H, H9), 1.05 (s, 9H, *t*Bu of TBDPS) ppm.

B6-4-II: δ 7.70 – 7.66 (m, 4H, Ph of TBDPS), 7.44 – 7.36 (m, 6H, Ph of TBDPS), 5.93 (ddd, *J* = 5.6, 10.8, 17.6 Hz, 1H, H2), 5.37 (s, 1H, H7), 5.26 (d, *J* = 17.2 Hz, 1H, H1a), 5.14 (d, *J* = 10.8 Hz, 1H, H1b), 4.36 (br s, 1H, H8), 4.08 – 4.03 (m, 1H, H3), 3.95 – 3.74 (m, 2H, H10), 2.08 – 1.94 (m, 2H, H4), 1.91 – 1.75 (m, 2H, H9), 1.70 (s, 3H, H6), 1.05 (s, 9H, *t*Bu of TBDPS) ppm.

[149] NMR data are referred with the data published for compound 13 in following reference: Ghosh, A. K.; Cheng, X., *Org. Lett.* **2011,** *13*, 4108-4111.

^{13}C NMR (100MHz, $CDCl_3$):

B6-4-I: δ 144.5 (C5), 138.8 (C2), 135.6, 134.0, 129.5, 127.6, 114.9 (C1), 108.7 (C6), 78.7 (C3), 75.1 (C8), 60.2 (C10), 40.8 & 40.6 (C4 & C7), 39.1 (C9), 26.9 (**C**H_3 of TBDPS), 19.3 (C of TBDPS) ppm.

B6-4-II: δ 139.0 (C2), 135.6, 134.0, 129.6, 127.6, 131.8 (C5), 124.2 (C7), 114.6 (C1), 74.4 (C3), 71.7 (C8), 60.4 (C10), 38.7 (C9), 35.7 (C4), 26.9 (**C**H_3 of TBDPS), 22.9 (C6), 19.3 (C of TBDPS) ppm.

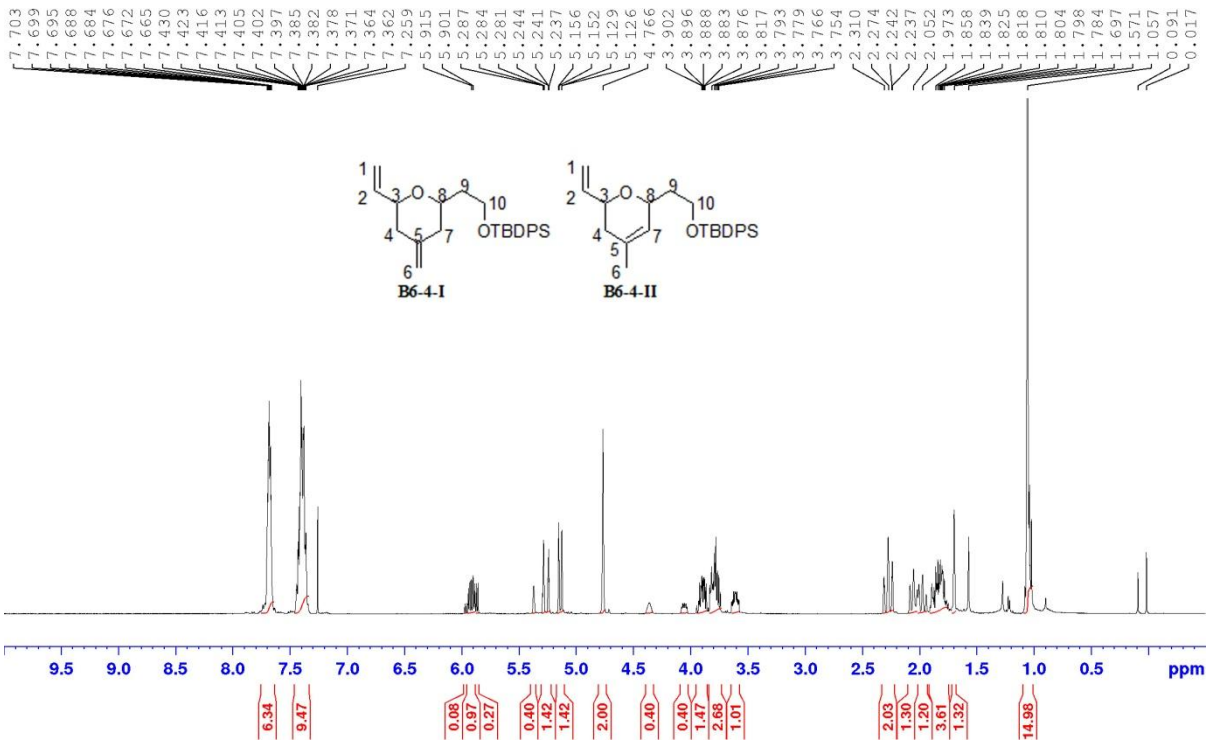

^{1}H NMR spectrum (ratio of **B6-4-I:B6-4-II** = 71:29)

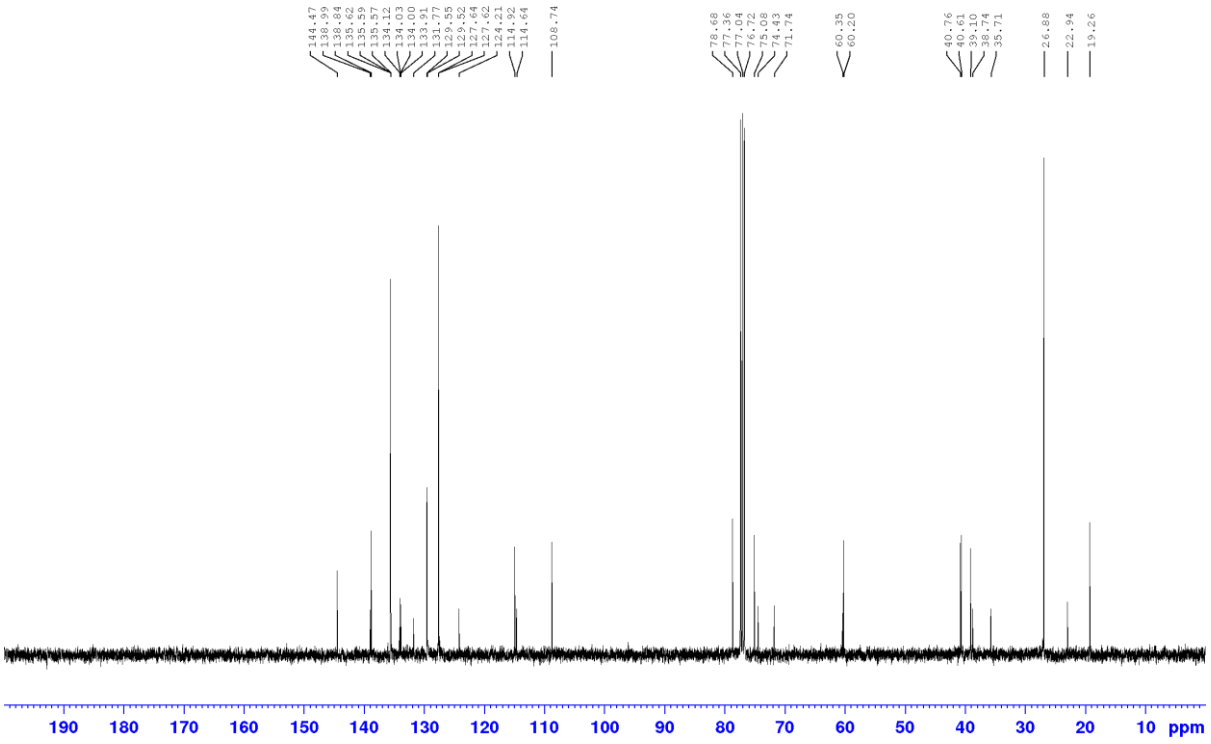

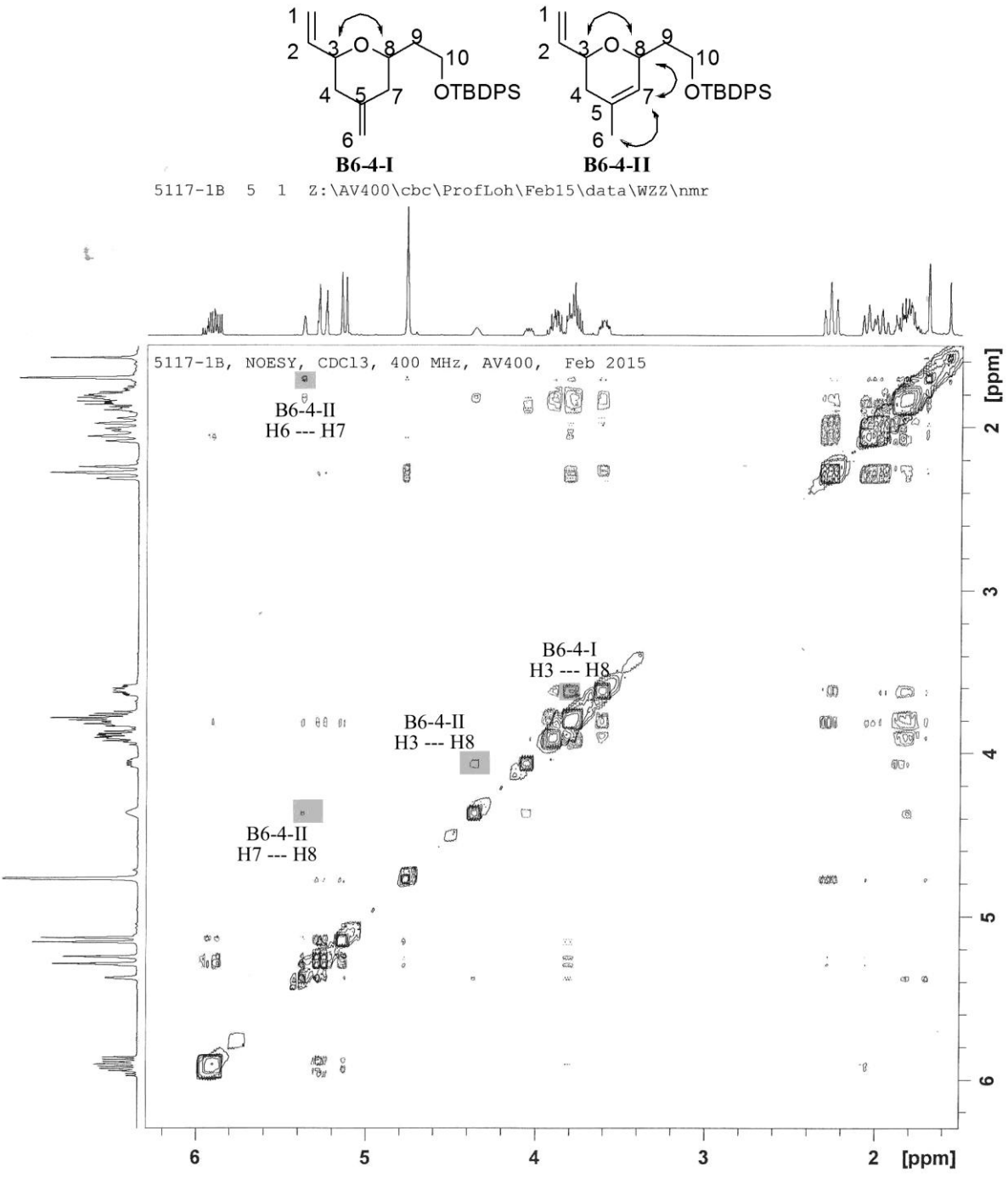
B6-4-I
B6-4-II
5117-1B 5 1 Z:\AV400\cbc\ProfLoh\Feb15\data\WZZ\nmr
5117-1B, NOESY, CDCl3, 400 MHz, AV400, Feb 2015
B6-4-II
H6 --- H7
B6-4-I
H3 --- H8
B6-4-II
H3 --- H8
B6-4-II
H7 --- H8
[ppm]
[ppm]

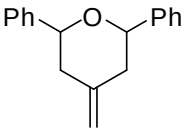

4-Methylene-2,6-diphenyltetrahydro-2*H*-pyran (B6-5):

Please refer to supporting information of Compound 2a published in following reference: Pham, M.; Allatabakhsh, A.; Minehan, T. G. *J. Org. Chem.* **2008**, *73*, 741-744.

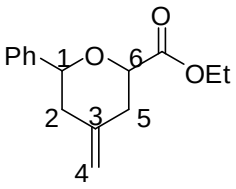

B6-6-I

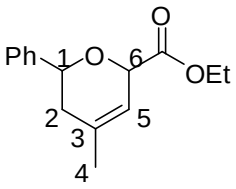

B6-6-II

Ethyl 4-methylene-6-phenyltetrahydro-2*H*-pyran-2-carboxylate (B6-6-I)

Ethyl 4-methyl-6-phenyl-5,6-dihydro-2*H*-pyran-2-carboxylate (B6-6-II)

R_f value (hexane/EtOAc = 4:1): 0.63;

^{1}H NMR (400MHz, $CDCl_3$):

B6-6-I: δ 7.45 – 7.26 (m, 5H, Ph), 4.93 (s, 1H, H4a), 4.90 (s, 1H, H4b), 4.39 (dd, *J* = 2.4, 11.6 Hz, 1H, H1), 4.28 – 4.21 (m, 2H, OC**H$_2$**CH_3), 4.12 (dd, *J* = 2.6, 11.8 Hz, 1H, H6), 2.62 (d, *J* = 13.2 Hz, 1H, H5a), 2.49 (d, *J* = 13.6 Hz, 1H, H2a), 2.44 – 2.30 (m, 2H, H2b & H5b), 1.34 – 1.29 (m, 3H, OCH_2C**H$_3$**) ppm.

B6-6-II: δ 7.45 – 7.26 (m, 5H, Ph), 5.62 (s, 1H, H5), 4.93 (m, 1H, H6), 4.64 (dd, *J* = 3.2, 10.8 Hz, 1H, H1), 4.28 – 4.21 (m, 2H, OC**H$_2$**CH_3), 2.44 – 2.30 (m, 2H, H2), 1.78 (s, 3H, H4), 1.34 – 1.29 (m, 3H, OCH_2C**H$_3$**) ppm.

^{13}C NMR (100MHz, $CDCl_3$):

B6-6-I: δ 170.6 (C=O), 142.5 (C3), 141.5 (Ph(**C**)-C1), 128.4, 127.7, 125.9, 110.5 (C4), 80.5 (C1), 77.3 (C6), 61.1 (O**C**H_2CH_3), 42.5 (C2), 37.3 (C5), 14.2 (OCH_2**C**H_3) ppm.

B6-6-II: δ 170.6 (C=O), 141.5 (Ph(**C**)-C1), 135.5 (C3), 128.4, 127.7, 125.9, 117.9 (C5), 75.7 (C1), 75.5 (C6), 61.2 (O**C**H_2CH_3), 37.5 (C2), 23.0 (C4), 14.2 (OCH_2**C**H_3) ppm.

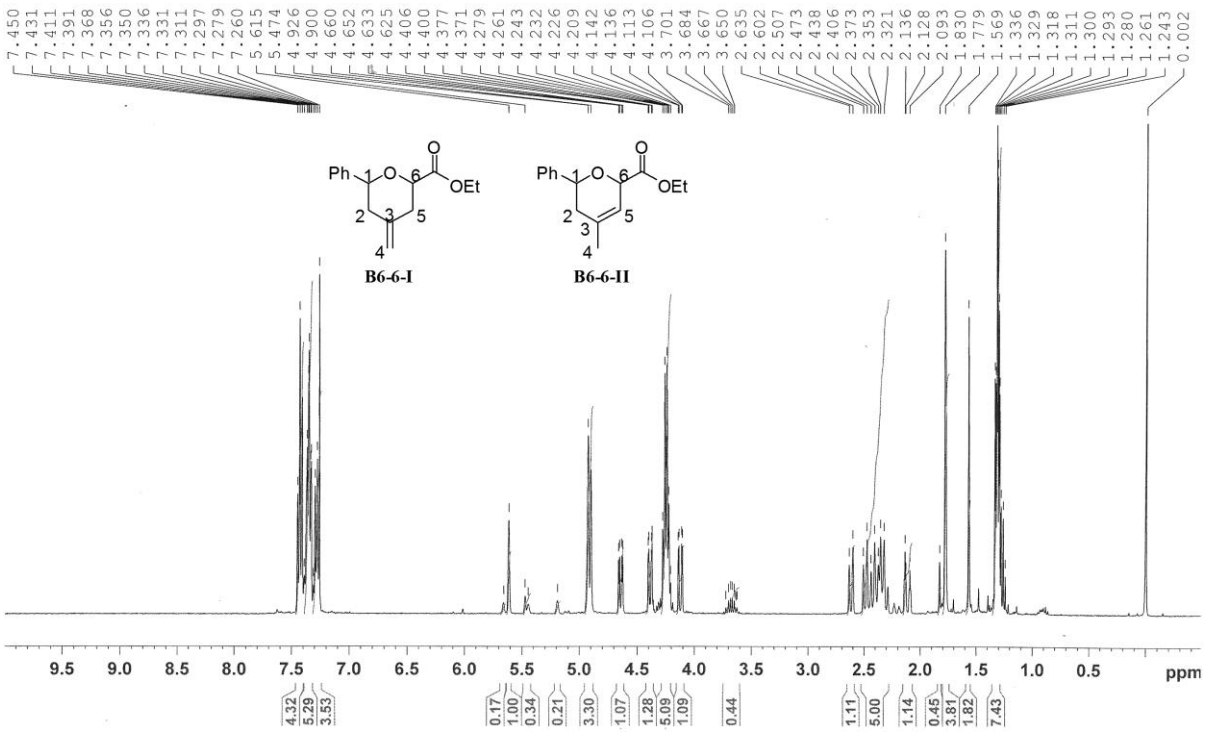

^{1}H NMR spectrum (ratio of **B6-6-I:B6-6-II** = 56:44)

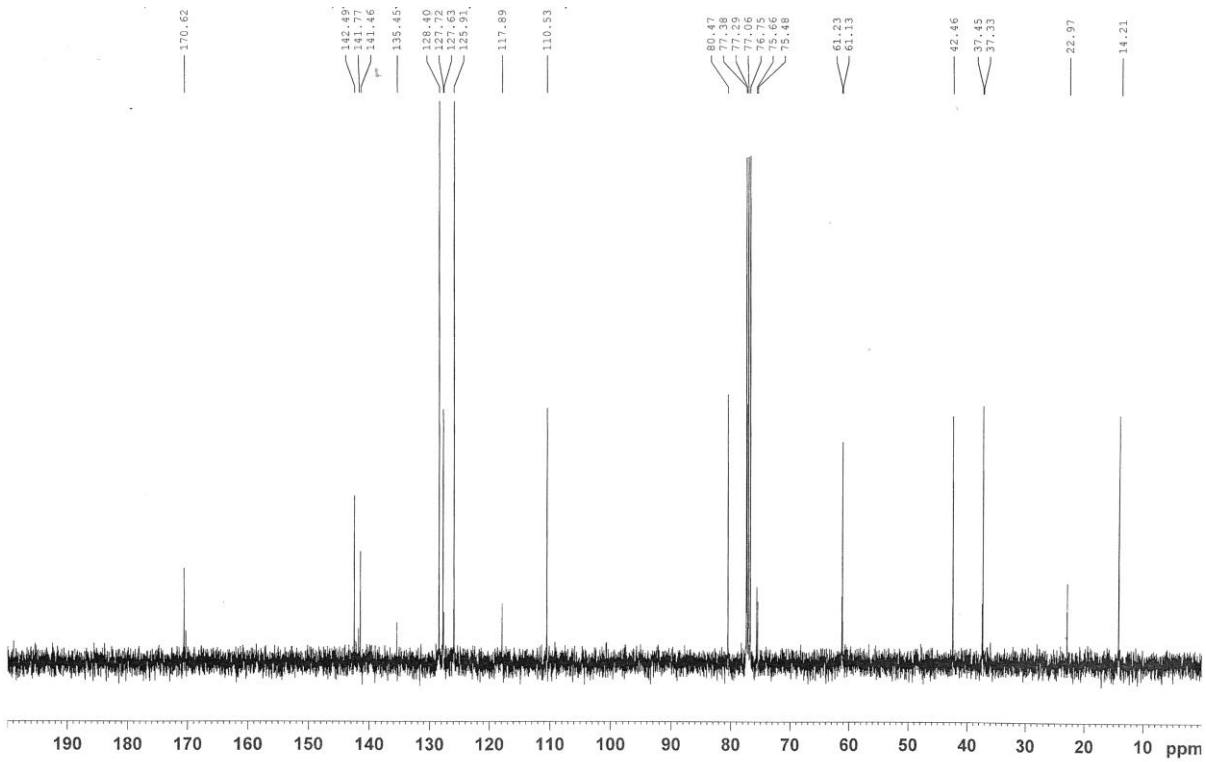

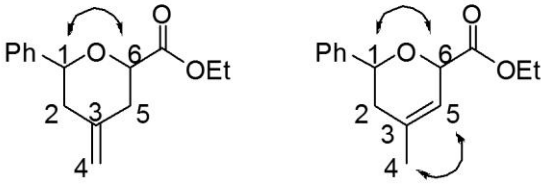

B6-6-I **B6-6-II**

No interaction found for H6 --- Ph

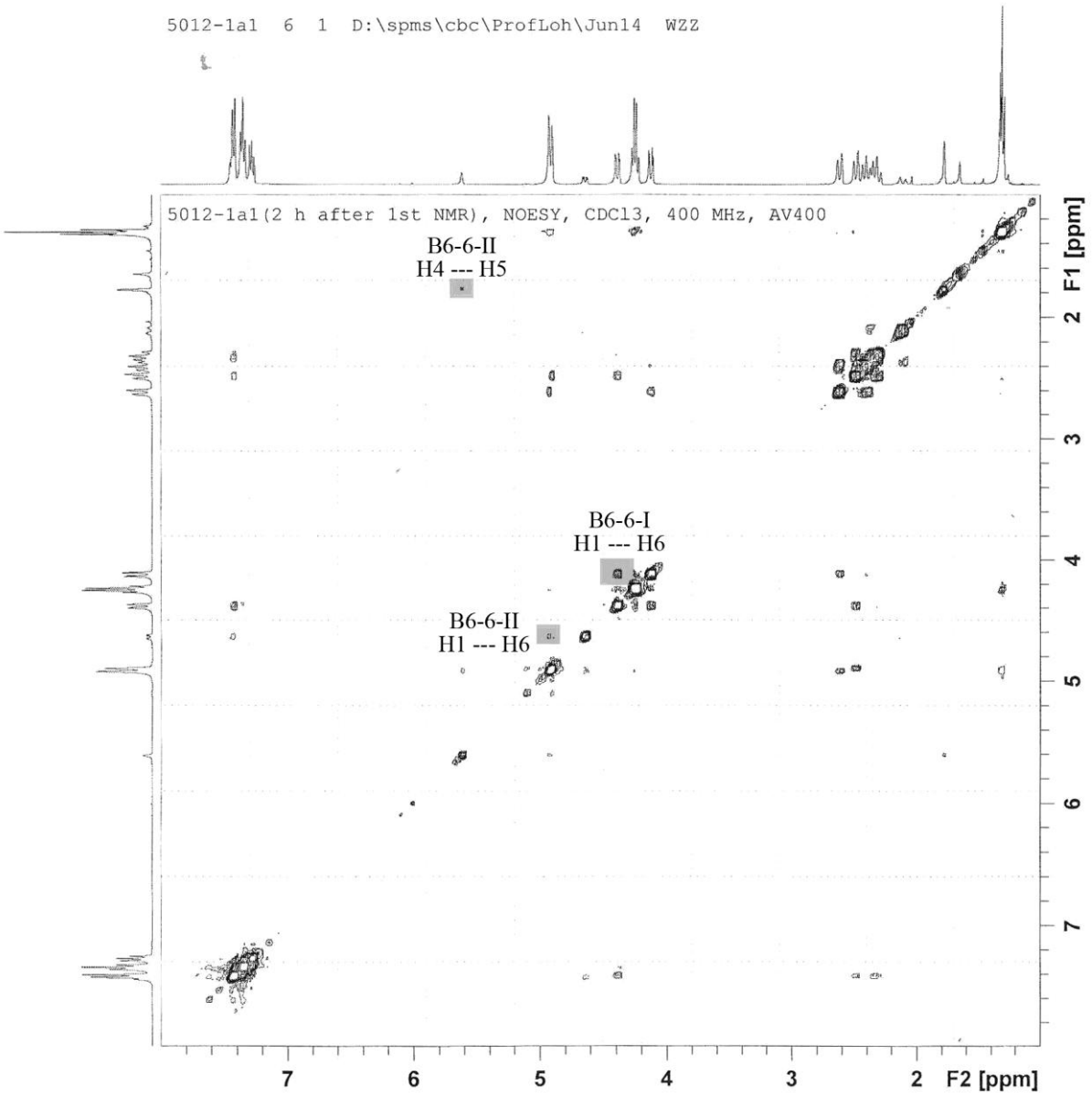

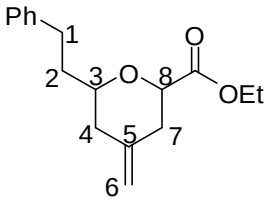

B6-7a-I

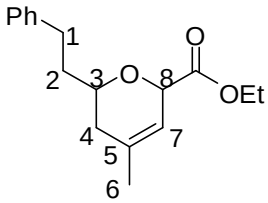

B6-7a-II

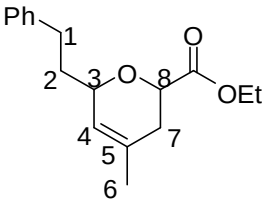

B6-7a-III

Ethyl 4-methylene-6-phenethyltetrahydro-2*H*-pyran-2-carboxylate (B6-7a-I)

Ethyl 4-methyl-6-phenethyl-5,6-dihydro-2*H*-pyran-2-carboxylate (B6-7a-II)

Ethyl 4-methyl-6-phenethyl-3,6-dihydro-2*H*-pyran-2-carboxylate (B6-7a-III)

R_f value (hexane/EtOAc = 4:1): 0.50;

^{1}H NMR (400MHz, $CDCl_3$):

B6-7a-I: δ 7.29 – 7.17 (m, 5H, Ph), 4.81 (s, 1H, H6a), 4.78 (s, 1H, H6b), 4.28 – 4.23 (m, 2H, OC**H**$_2$$CH_3$), 4.19 – 4.15 (m, 1H, H3 or H8), 3.91 (dd, *J* = 1.2, 12.0 Hz, 1H, H3 or H8), 2.84 – 2.69 (m, 2H, H1), 2.55 – 1.78 (m, 6H, H2, H4 & H7), 1.31 (t, *J* = 7.2 Hz, 3H, OCH_2C**H**$_3$) ppm.

B6-7a-II: δ 7.29 – 7.17 (m, 5H, Ph), 5.50 (s, 1H, H7), 4.28 – 4.23 (m, 2H, OC**H**$_2$$CH_3$), 3.55 – 3.50 (m, 1H, H3 or H8), 3.30 – 3.25 (m, 1H, H3 or H8), 2.84 – 2.69 (m, 2H, H1), 2.55 – 1.78 (m, 4H, H2 & H4), 1.71 (s, 3H, H6), 1.31 (t, *J* = 7.2 Hz, 3H, OCH_2C**H**$_3$) ppm.

B6-7a-III: δ 7.29 – 7.17 (m, 5H, Ph), 5.36 (s, 1H, H4), 4.28 – 4.23 (m, 2H, OC**H**$_2$$CH_3$), 4.19 – 4.15 (m, 2H, H3 & H8), 2.84 – 2.69 (m, 2H, H1), 2.55 – 1.78 (m, 4H, H2 & H7), 1.73 (s, 3H, H6), 1.31 (t, *J* = 7.2 Hz, 3H, OCH_2C**H**$_3$) ppm.

Remarks:

(a) Peaks assigned to H3 and H8 of compounds above were roughly deduced from ^{1}H NMR compared with ^{1}H NMR of **B6-7b-I**, **B6-7b-II** and **B6-7b-III** (*vide infra*) without further confirmation with 2D NMR.

(b) **B6-7b-I**, **B6-7b-II** and **B6-7b-III** were obtained *via* DIBAL-H reduction on the mixture of **B6-7a-I**, **B6-7a-II** and **B6-7a-III**.

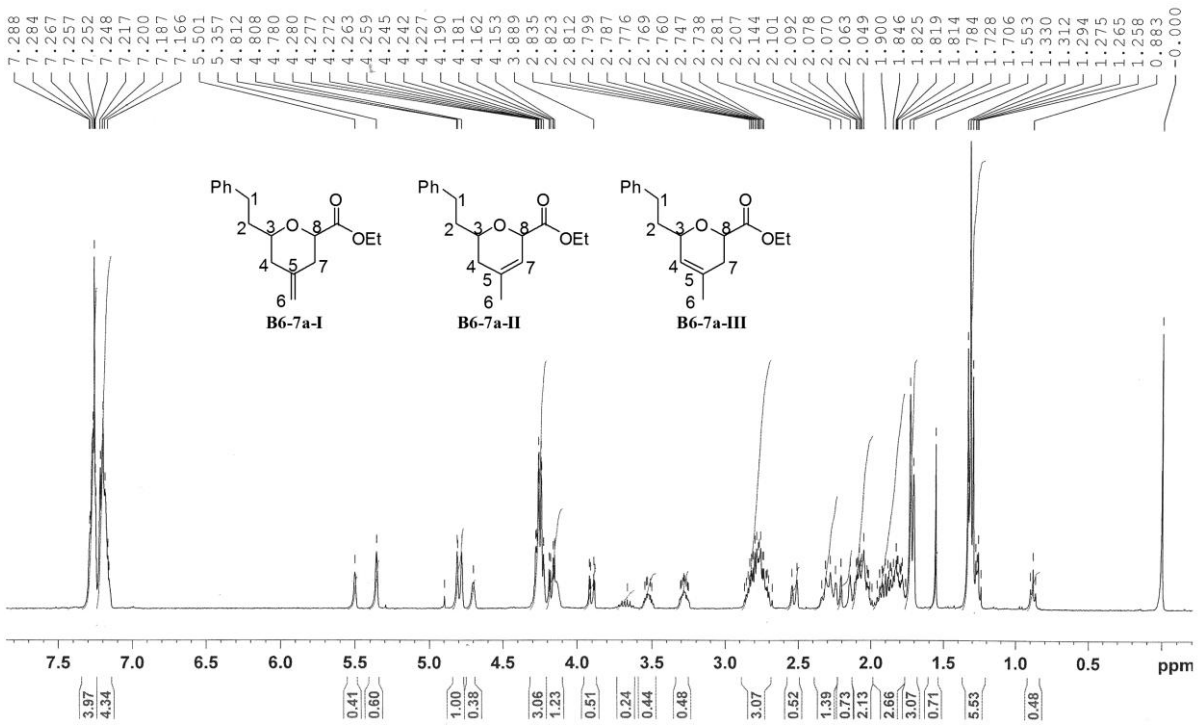

^{1}H NMR spectrum (ratio of **B6-7a-I:B6-7a-II:B6-7a-III** = 33:27:40)

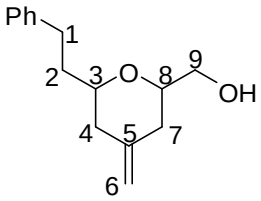

B6-7b-I

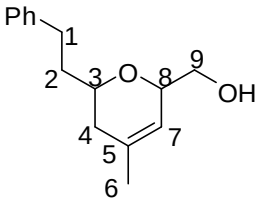

B6-7b-II

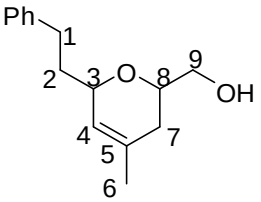

B6-7b-III

(4-Methylene-6-phenethyltetrahydro-2*H*-pyran-2-yl)methanol (B6-7b-I)

(4-Methyl-6-phenethyl-5,6-dihydro-2*H*-pyran-2-yl)methanol (B6-7b-II)

(4-Methyl-6-phenethyl-3,6-dihydro-2*H*-pyran-2-yl)methanol (B6-7b-III)

R_f value (hexane/EtOAc = 4:1): 0.23;

^{1}H NMR (300MHz, $CDCl_3$):

B6-7b-I: δ 7.31 – 7.16 (m, 5H, Ph), 4.73 (s, 2H, H6), 4.16 (br s, 1H, H8), 3.70 – 3.52 (m, 3H, H3 & H9), 2.86 – 2.66 (m, 2H, H1), 2.24 – 1.67 (m, 7H, H2, H4, H7 & OH) ppm.

B6-7b-II: δ 7.31 – 7.16 (m, 5H, Ph), 5.34 (s, 1H, H7), 3.70 – 3.52 (m, 2H, H9), 3.47 – 3.36 (m, 1H, H8), 3.34 – 3.26 (m, 1H, H3), 2.86 – 2.66 (m, 2H, H1), 2.24 – 1.67 (m, 5H, H2, H4 & OH), 1.70 (s, 3H, H6) ppm.

B6-7b-III: δ 7.31 – 7.16 (m, 5H, Ph), 5.25 (s, 1H, H4), 4.11 (br s, 1H, H8), 3.70 – 3.52 (m, 3H, H3 & H9), 2.86 – 2.66 (m, 2H, H1), 2.24 – 1.67 (m, 5H, H2, H7 & OH), 1.70 (s, 3H, H6) ppm.

^{13}C NMR (100MHz, $CDCl_3$):

B6-7b-I: δ 143.8 (C5), 142.3 (Ph(**C**)), 128.4, 128.4, 125.8, 109.2 (C6), 75.5 (C8), 72.9 (C3), 66.1 (C9), 40.8 (C4), 37.3 (C7), 36.4 (C2), 31.9 (C1) ppm.

B6-7b-II: δ 142.3 (Ph(**C**)), 134.9 (C5), 128.4, 128.4, 125.8, 119.9 (C7), 78.4 (C8), 77.6 (C3), 65.9 (C9), 37.7 (C4), 36.4 (C2), 31.8 (C1), 23.0 (C6) ppm.

B6-7b-III: δ 142.3 (Ph(**C**)), 132.1 (C5), 128.4, 128.4, 125.8, 123.8 (C4), 74.3 (C3), 74.0 (C8), 65.8 (C9), 37.3 (C7), 36.4 (C2), 31.4 (C1), 23.0 (C6) ppm.

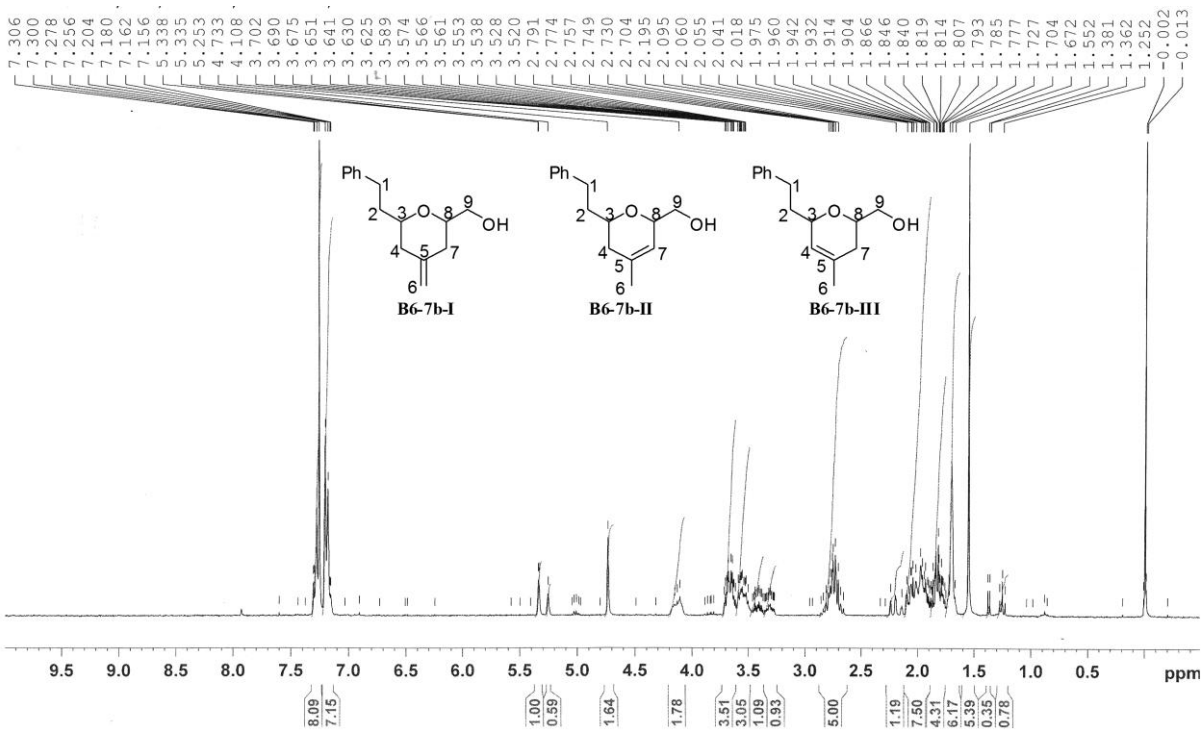

^{1}H NMR spectrum (ratio of **B6-7b-I:B6-7b-II:B6-7b-III** = 33:25:42)

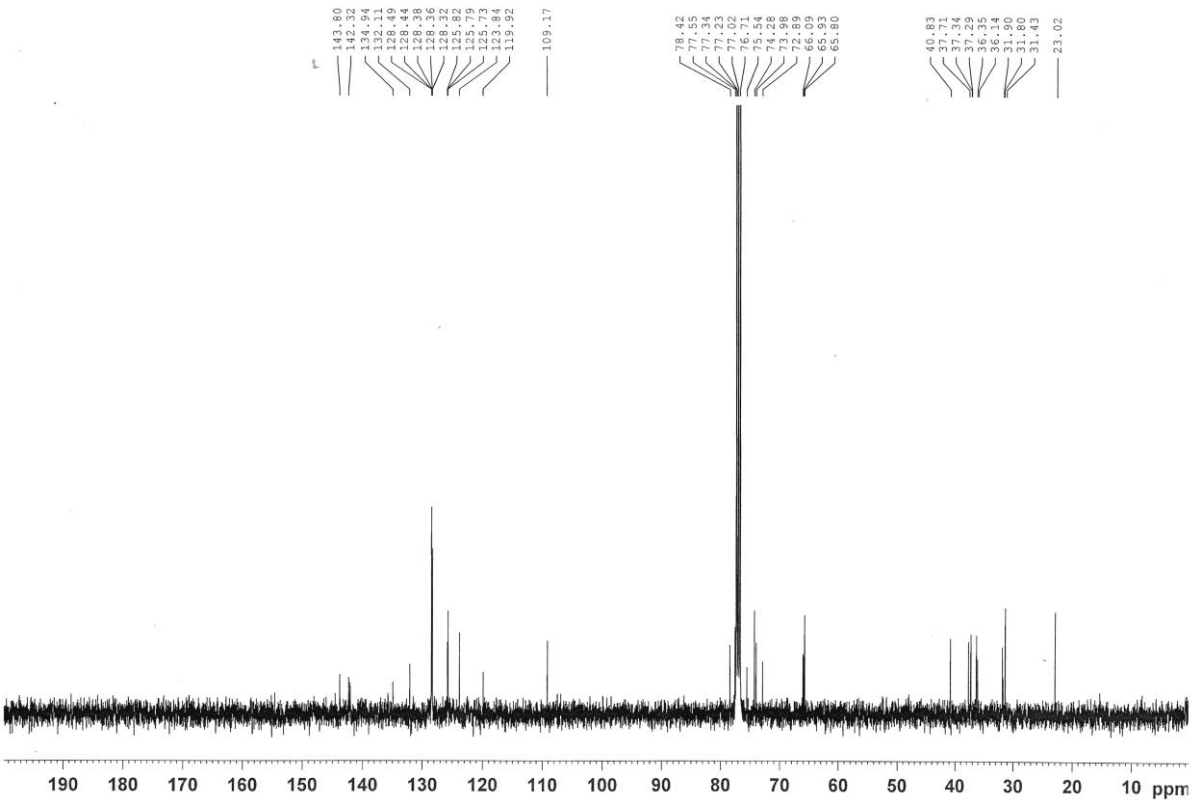

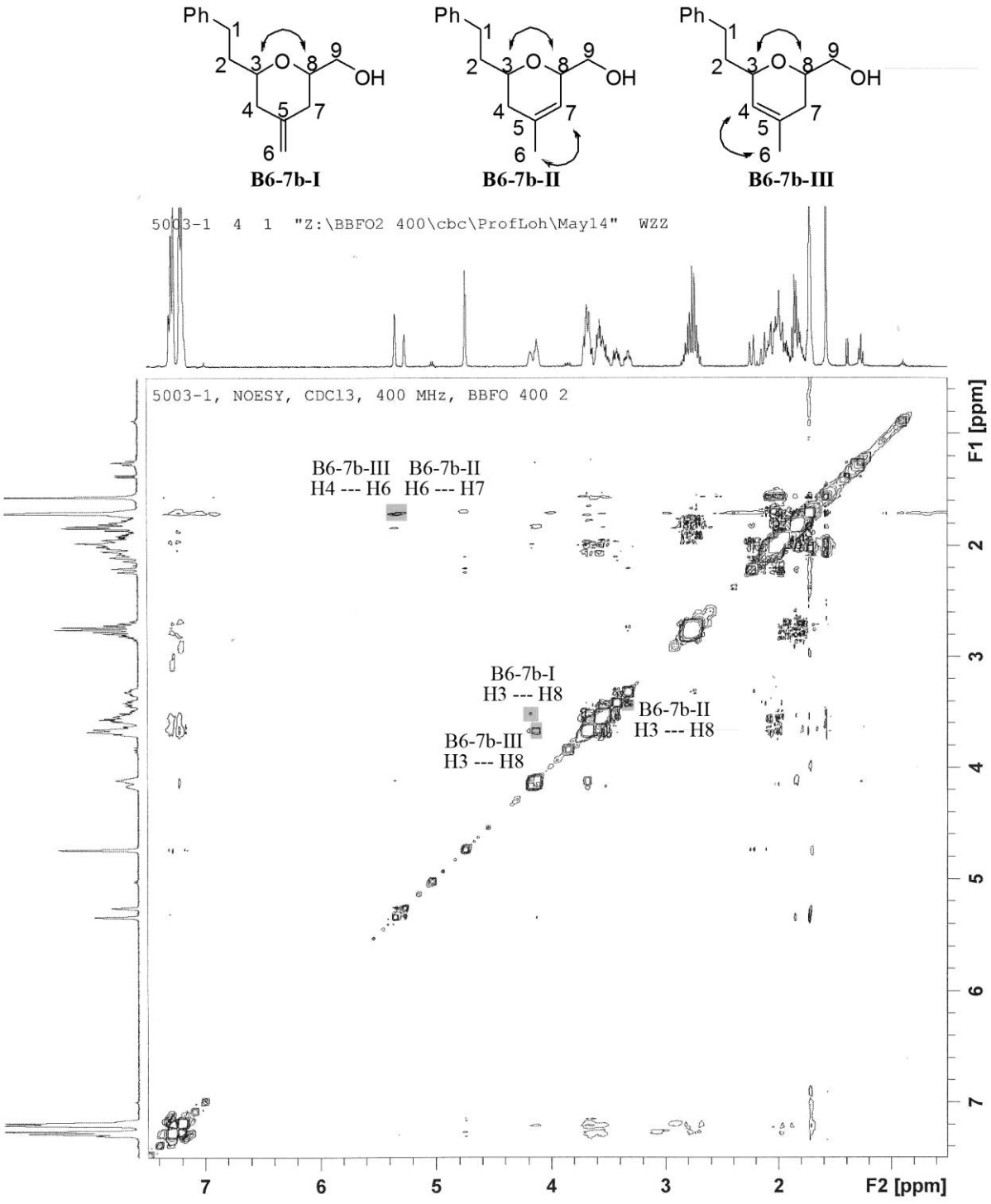
B6-7b-I
B6-7b-II
B6-7b-III
5003-1 4 1 "Z:\BBFO2 400\cbc\ProfLoh\May14" WZZ
5003-1, NOESY, CDCl3, 400 MHz, BBFO 400 2
B6-7b-III H4 --- H6
B6-7b-II H6 --- H7
B6-7b-I H3 --- H8
B6-7b-II H3 --- H8
B6-7b-III H3 --- H8
F1 [ppm]
F2 [ppm]

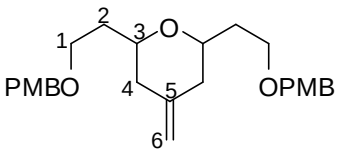

B6-8-I

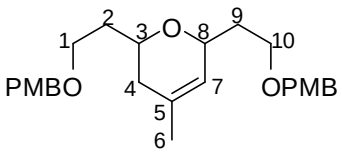

B6-8-II

2,6-Bis(2-(4-methoxybenzyloxy)ethyl)-4-methylenetetrahydro-2*H*-pyran (B6-8-I)

2,6-Bis(2-(4-methoxybenzyloxy)ethyl)-4-methyl-3,6-dihydro-2*H*-pyran (B6-8-II)

R_f value (hexane/EtOAc = 1:1): 0.68;

^{1}H NMR (400MHz, $CDCl_3$):

B6-8-I: δ 7.26 – 7.22 (m, 4H, Ph of PMB), 6.88 – 6.84 (m, 4H, Ph of PMB), 4.69 (s, 2H, H6), 4.42 (s, 4H, CH_2 of PMB), 3.80 – 3.75 (m, 2H, H3), 3.78 (s, 6H, CH_3 of PMB), 3.61 – 3.53 (m, 4H, H1), 1.82 – 1.72 (m, 8H, H2 & H4) ppm.

B6-8-II: δ 7.26 – 7.22 (m, 4H, Ph of PMB), 6.88 – 6.84 (m, 4H, Ph of PMB), 5.31 (s, 1H, H7), 4.42 (s, 4H, CH_2 of PMB), 3.80 – 3.75 (m, 1H, H3 or H8), 3.78 (s, 6H, CH_3 of PMB), 3.61 – 3.53 (m, 5H, H1, H3 or H8, H10), 1.82 – 1.72 (m, 6H, H2, H4 & H9), 1.66 (s, 3H, H6) ppm.

Remarks:

(c) Peaks assigned to H3 and H8 of both compounds were roughly deduced from ^{1}H NMR without further confirmation with 2D NMR.

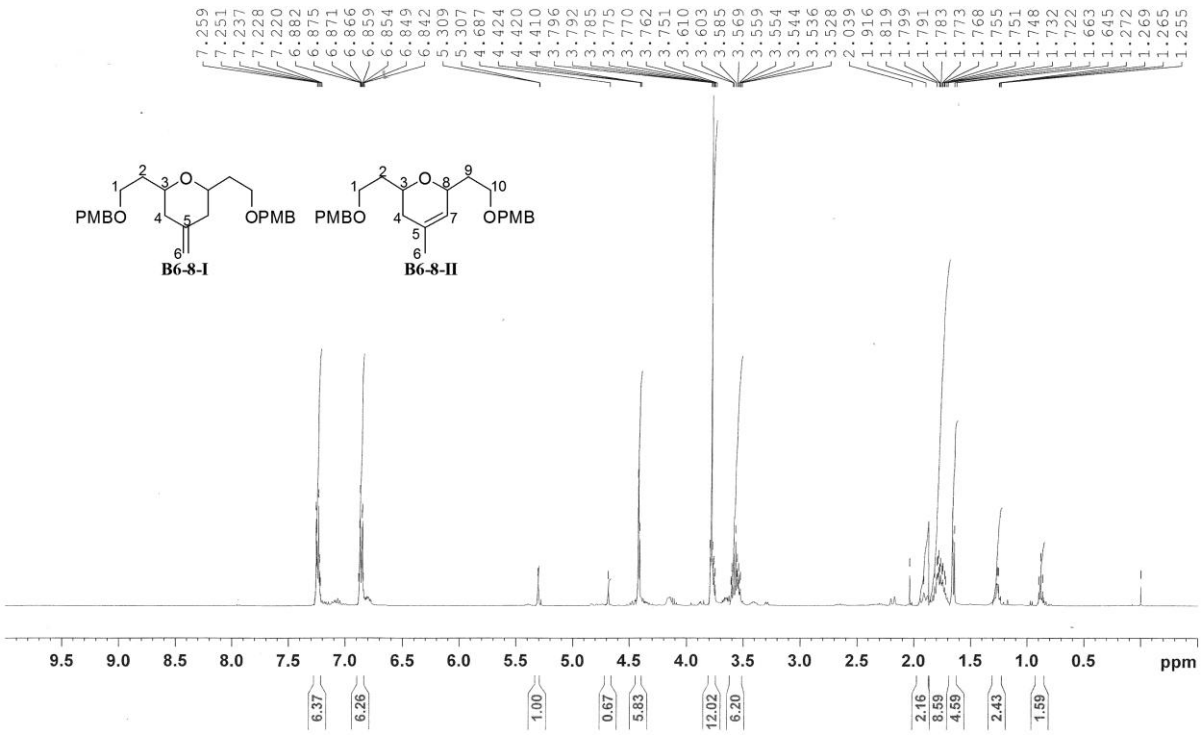

^{1}H NMR spectrum (ratio of **B6-8-I:B6-8-II** = 27:73)

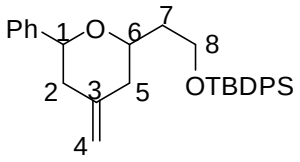

B6-9-I

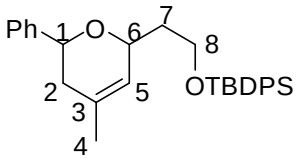

B6-9-II

***tert*-Butyl(2-(4-methylene-6-phenyltetrahydro-2*H*-pyran-2-yl)ethoxy)diphenylsilane (B6-9-I)**

***tert*-Butyl(2-(4-methyl-6-phenyl-5,6-dihydro-2*H*-pyran-2-yl)ethoxy)diphenylsilane (B6-9-II)**

R_f value (hexane/EtOAc = 4:1): 0.75;

^{1}H NMR (400MHz, $CDCl_3$):

B6-9-I: δ 7.69 – 7.62 (m, 4H, Ph of TBDPS), 7.40 – 7.31 (m, 8H, Ph of TBDPS & Ph-C1), 7.28 – 7.21 (m, 3H, Ph-C1), 4.80 (s, 2H, H4), 4.33 (dd, *J* = 2.4, 11.6 Hz, 1H, H1), 3.98 – 3.69 (m, 3H, H6 & H8), 2.48 (d, *J* = 13.2 Hz, 1H, H2a), 2.31 (d, *J* = 13.2 Hz, 1H, H5a), 2.24 – 2.06 (m, 2H, H2b & H5b), 1.91 – 1.83 (m, 2H, H7), 1.04 (s, 9H, *t*Bu of TBDPS) ppm.

B6-9-II: δ 7.69 – 7.62 (m, 4H, Ph of TBDPS), 7.40 – 7.31 (m, 8H, Ph of TBDPS & Ph-C1), 7.28 – 7.21 (m, 3H, Ph-C1), 5.42 (s, 1H, H5), 4.57 (dd, *J* = 4.2, 11.2 Hz, 1H, H1), 4.47 (br s, 1H, H6), 3.98 – 3.77 (m, 2H, H8), 2.24 – 2.06 (m, 2H, H2), 1.91 – 1.83 (m, 2H, H7), 1.71 (s, 3H, H4), 1.04 (s, 9H, *t*Bu of TBDPS) ppm.

^{13}C NMR (100MHz, $CDCl_3$):

B6-9-I: δ 144.9 (C3), 142.8 (Ph(**C**)-C1), 135.6 (Ph of TBDPS), 134.0 (Ph(**C**) of TBDPS), 129.5, 128.3, 127.6, 127.3, 125.8, 108.8 (C4), 80.0 (C1), 75.5 (C6), 60.2 (C8), 43.0 (C2), 40.8 (C5), 39.2 (C7), 26.9 (**C**H_3 of TBDPS), 19.3 (C of TBDPS) ppm.

B6-9-II: δ 143.1 (Ph(**C**)-C1), 135.6 (Ph of TBDPS), 134.0 (Ph(**C**) of TBDPS), 132.2 (C3), 129.5, 128.3, 127.6, 127.2, 125.7, 124.3 (C5), 75.6 (C1), 72.3 (C6), 60.4 (C8), 38.2 (C2), 38.8 (C7), 26.9 (**C**H_3 of TBDPS), 22.9 (C4), 19.3 (C of TBDPS) ppm.

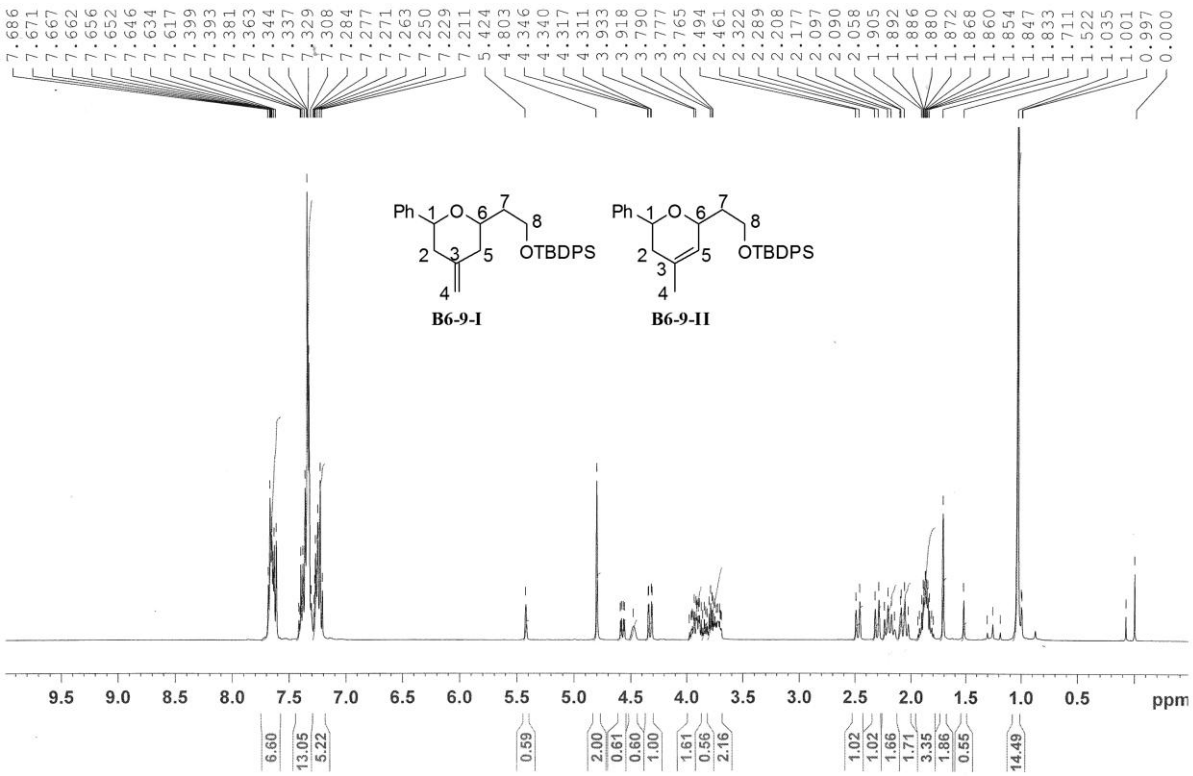

^{1}H NMR spectrum (ratio of **B6-9-I:B6-9-II** = 63:37)

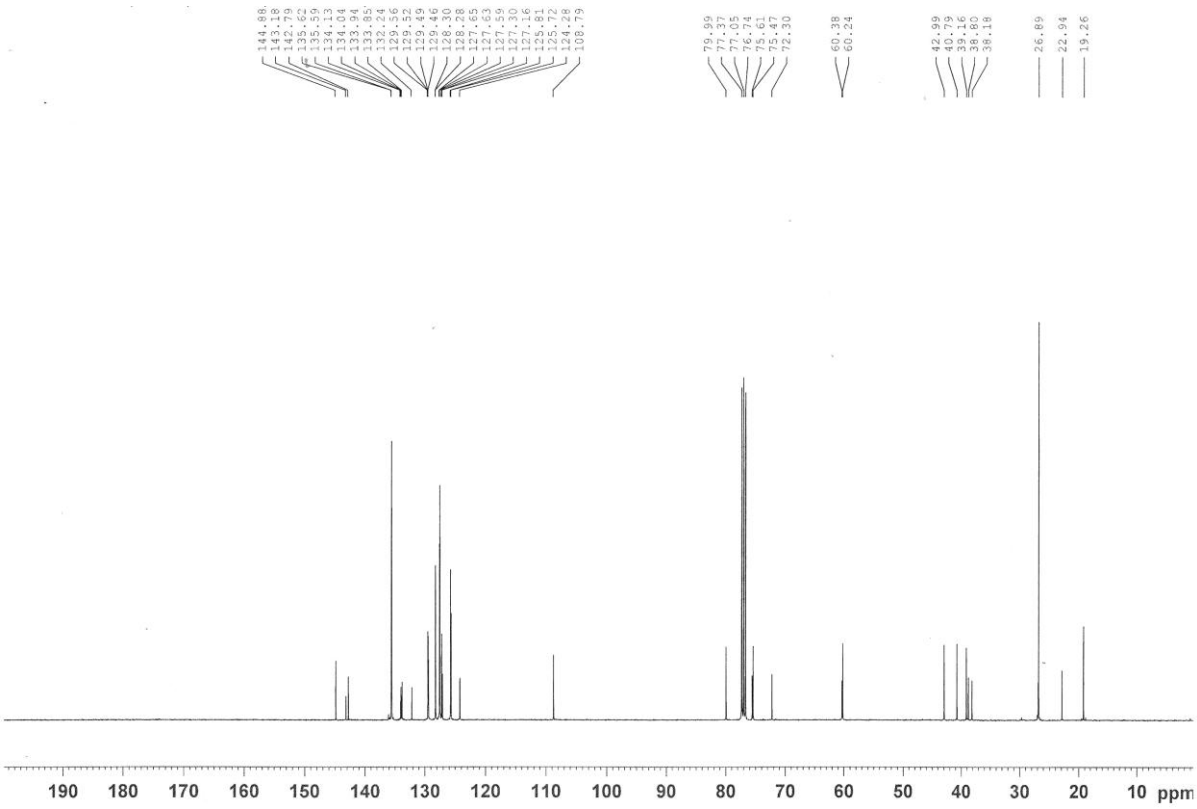

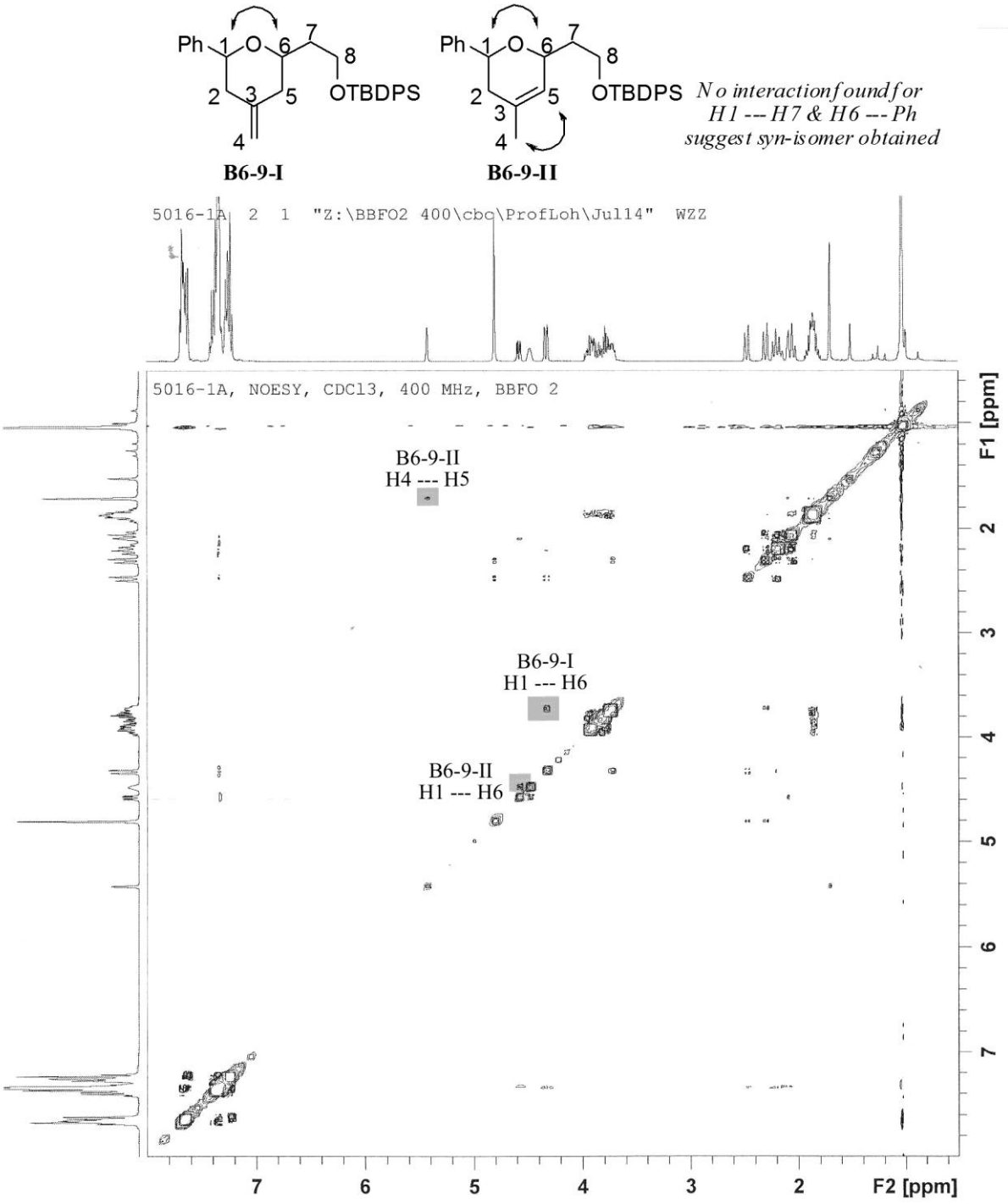
B6-9-I
B6-9-II
No interaction found for
H1 --- H7 & H6 --- Ph
suggest syn-isomer obtained
5016-1A 2 1 "Z:\BBFO2 400\cbc\ProfLoh\Jul14" WZZ
5016-1A, NOESY, CDCl3, 400 MHz, BBFO 2
B6-9-II
H4 --- H5
B6-9-I
H1 --- H6
B6-9-II
H1 --- H6
F1 [ppm]
F2 [ppm]